

2013

# Investigations into alkene hydration and alkene oxidation catalysis

William Schreiter

Louisiana State University and Agricultural and Mechanical College, wschre1@lsu.edu

Follow this and additional works at: [https://digitalcommons.lsu.edu/gradschool\\_dissertations](https://digitalcommons.lsu.edu/gradschool_dissertations)



Part of the [Chemistry Commons](#)

---

## Recommended Citation

Schreiter, William, "Investigations into alkene hydration and alkene oxidation catalysis" (2013). *LSU Doctoral Dissertations*. 473.  
[https://digitalcommons.lsu.edu/gradschool\\_dissertations/473](https://digitalcommons.lsu.edu/gradschool_dissertations/473)

This Dissertation is brought to you for free and open access by the Graduate School at LSU Digital Commons. It has been accepted for inclusion in LSU Doctoral Dissertations by an authorized graduate school editor of LSU Digital Commons. For more information, please contact [gradetd@lsu.edu](mailto:gradetd@lsu.edu).

INVESTIGATIONS INTO ALKENE HYDRATION  
AND ALKENE OXIDATION CATALYSIS

A Dissertation

Submitted to the Graduate Faculty of the  
Louisiana State University and  
Agricultural and Mechanical College  
in partial fulfillment of the  
requirements for the degree of  
Doctor of Philosophy

In

The Department of Chemistry

by  
William James Schreiter  
B. A., Lawrence University, 2004  
May 2013

## TABLE OF CONTENTS

ABSTRACT.....	v
CHAPTER 1. INTRODUCTION .....	1
1.1 Alkene Hydration.....	1
1.2 Alkene Oxidation .....	9
1.3 References.....	20
CHAPTER 2. INVESTIGATION INTO ALKENE HYDRATION CATALYSIS .....	27
2.1 Motivation.....	27
2.2 Attempted Alkene Hydration Catalysis with Ni/Phosphine Complexes .....	29
2.3 Attempted Hydration Catalysis Utilizing Other Metal/Phosphine Complexes .....	33
2.4 The White Solid “Product” – How to Waste a Year in Graduate School and Get Your Advisor Excited (at least initially) .....	36
2.5 Catalytic Screening for Possible Alkene Hydration Catalysis.....	40
2.6 Conclusions.....	45
2.7 References.....	47
CHAPTER 3. INVESTIGATION INTO ALKENE OXIDATION CATALYSIS UTILIZING Ni/PHOSPHINE COMPLEXES.....	49
3.1 Motivation.....	49
3.2 Alkene Oxidative Cleavage via Bimetallic Ni/Phosphine Complexes .....	51
3.3 Identification of the Broad Resonances .....	65
3.4 Monometallic Metal Complexes as Possible Oxidative Cleavage Catalysts.....	72
3.5 Other Oxidizing Agents .....	74
3.6 Mechanistic Possibilities.....	76
3.7 Conclusions.....	83
CHAPTER 4. <sup>1</sup> H AND <sup>31</sup> P{ <sup>1</sup> H} NMR STUDIES OF <i>RAC</i> - AND <i>MESO</i> -Ni <sub>2</sub> Cl <sub>4</sub> ( <i>et</i> , <i>ph</i> -P <sub>4</sub> ), Ni <sub>2</sub> 1R and Ni <sub>2</sub> 1M .....	87
4.1 Introduction.....	87
4.2 Ni <sub>2</sub> Cl <sub>4</sub> ( <i>meso</i> - <i>et</i> , <i>ph</i> -P <sub>4</sub> ), Ni <sub>2</sub> 1M, and Ni <sub>2</sub> Cl <sub>4</sub> ( <i>rac</i> - <i>et</i> , <i>ph</i> -P <sub>4</sub> ), Ni <sub>2</sub> 1R .....	89
4.3 Effect of Water on Ni <sub>2</sub> 1M.....	92
4.4 Effect of the Organic Solvent on the Reaction Between Ni <sub>2</sub> 1M and Water.....	96
4.5 Varying the Concentration of Water .....	104
4.6 Identification of <b>F</b> and Attempts to Synthesize <b>A</b> , <b>B</b> and <b>C</b> .....	107
4.7 Ni <sub>2</sub> 1R and Water.....	112
4.8 Effect of Other Additives on the Reaction (NaCl, O <sub>2</sub> . Inhibitors, Heat) .....	119
4.9 Conclusions and Proposals .....	124
4.10 References.....	134
CHAPTER 5. SYNTHESIS, SEPARATION AND CHARACTERIZATION OF 2R AND 2M AND Ni <sub>2</sub> 2M AND Ni <sub>2</sub> 2R.....	135
5.1 Introduction.....	135
5.2 Synthesis and Characterization of 2R and 2M .....	136
5.3 Synthesis and Separation of Ni <sub>2</sub> 2M and Ni <sub>2</sub> 2R.....	138

5.4 Cyanolysis of <b>Ni<sub>2</sub>2M</b> and <b>Ni<sub>2</sub>2R</b> and Isolation of the Pure Diastereomers .....	141
5.5 Preliminary Investigation into the Solution-State Chemistry and Reactivity of <b>Ni<sub>2</sub>2M</b> and <b>Ni<sub>2</sub>2R</b> .....	146
5.6 Conclusions.....	148
5.7 References.....	150
<b>CHAPTER 6. EXPERIMENTAL PROCEDURES</b> .....	<b>152</b>
6.1 General.....	152
6.2 Attempts at Alkene Hydration Catalysis.....	153
6.2.1 General Comments.....	153
6.2.2 Reaction Types.....	154
6.2.3 Reaction Table .....	155
6.3 Hydration Screening Experiments .....	169
6.3.1 The Ligand Solution .....	169
6.3.2 Reaction Setup .....	169
6.3.3 Reaction Table .....	170
6.4 Oxidative Cleavage Reactions .....	173
6.4.1 Reaction Types.....	173
6.4.2 Reaction Tables.....	173
6.5 NMR Reactions.....	183
6.5.1 Reaction Conditions When Acetone- <i>d</i> <sub>6</sub> was Utilized .....	183
6.5.2 Reaction Conditions When CD <sub>3</sub> CN or DMSO- <i>d</i> <sub>6</sub> was Utilized .....	183
6.5.3 Reaction Table .....	184
6.6 <b>Ni<sub>2</sub>1M</b> Under Balloon Pressure O <sub>2</sub> .....	187
6.6.1 Acetone and Water.....	187
6.6.2 Acetonitrile and Water .....	187
6.6.3 DMSO and Water .....	187
6.6.4 Added Substrate .....	187
6.7 Identification of the Broad Resonances .....	187
6.7.1 Oxidation of <b>1M</b> and <b>1R</b> and the Interaction with Added NiCl <sub>2</sub> .....	187
6.7.2 <b>Ni<sub>2</sub>1M</b> and O <sub>2</sub> .....	188
6.8 Synthesis of [Ni <sub>2</sub> (μ-Cl)( <b>1M</b> ) <sub>2</sub> ][BF <sub>4</sub> ] <sub>3</sub> , <b>F</b> .....	188
6.9 Attempted Synthesis of <b>F-1R</b> .....	189
6.10 Reactions Between <b>Ni<sub>2</sub>1M</b> and AgBF <sub>4</sub> .....	189
6.11 Synthesis of <i>racemic</i> -, <i>meso</i> - <i>et,ph</i> -P <sub>4</sub> -Ph, <b>2R</b> and <b>2M</b> .....	190
6.11.1 Synthesis of bis-(chlorophenylphosphino)methane, <b>4</b> .....	190
6.11.2 Synthesis of 1-(diethylphosphino)-2-iodobenzene, <b>6</b> .....	190
6.11.3 Synthesis of <i>rac</i> -, <i>meso</i> - <i>et,ph</i> -P <sub>4</sub> -Ph, <b>2R</b> and <b>2M</b> .....	191
6.12 Synthesis of <i>rac</i> -, <i>meso</i> -Ni <sub>2</sub> Cl <sub>4</sub> ( <i>et,ph</i> -P <sub>4</sub> -Ph), <b>Ni<sub>2</sub>2R</b> and <b>Ni<sub>2</sub>2M</b> .....	192
6.13 Cyanolysis of <b>Ni<sub>2</sub>2R</b> and <b>Ni<sub>2</sub>2M</b> .....	193
6.13.1 Cyanolysis of <b>Ni<sub>2</sub>2M</b> .....	193
6.13.2 Cyanolysis of <b>Ni<sub>2</sub>2R</b> .....	194
6.13.3 Cyanolysis of mixed <b>Ni<sub>2</sub>2M/Ni<sub>2</sub>2R</b> .....	194
6.14 References.....	195

APPENDIX.....	196
VITA.....	209

## ABSTRACT

Bimetallic Ni complexes **Ni<sub>2</sub>1M** and **Ni<sub>2</sub>1R** and monometallic transition metal complexes were investigated as possible alkene hydration catalysts under a multitude of different reaction conditions. All attempts at performing this catalytic reaction failed to give any alcohol products. Catalytic screening experiments were conducted using a mixture of *racemic*-*et*,*ph*-P4 and *meso*-*et*,*ph*-P4, **1M** and **1R**, and various transition metals. These experiments gave several different products including 1-phenylethanol from styrene.

During the course of the hydration experiments, an aldehyde product was identified from experiments conducted with the bimetallic complexes in air. Experiments have shown that the aldehyde is produced from the oxidative cleavage of the double bond of an alkene. The oxidative cleavage is a non-catalytic reaction and all attempts to produce a catalytic reaction have failed. The evidence collected suggests the oxidative cleavage is coupled with phosphine oxidation and a catalytic reaction will not be possible.

A detailed solution-state investigation of **Ni<sub>2</sub>1M** and **Ni<sub>2</sub>2R** was conducted via <sup>1</sup>H and <sup>31</sup>P{<sup>1</sup>H} NMR spectroscopy in the presence of water. These experiments have shown that a complex reaction occurs between the bimetallic complexes and water which ultimately leads to the formation of bimetallic Ni complexes with two tetraphosphine ligands bound. The reaction that occurs is dependent on several variables. One of these bimetallic complexes, [Ni<sub>2</sub>(μ-Cl)(**1M**)<sub>2</sub>][BF<sub>4</sub>]<sub>3</sub>, has been independently synthesized and characterized via X-ray crystallography. The NMR experiments have allowed us to propose a reaction scheme in which phosphine dissociation from one of the complexes formed in solution ultimately leads to the formation of the double ligand species.

The synthesis, separation and characterization of *racemic*- and *meso*-(Et<sub>2</sub>P-1,2-C<sub>6</sub>H<sub>4</sub>)PCH<sub>2</sub>P(1,2-C<sub>6</sub>H<sub>4</sub>-PEt<sub>2</sub>), **2R** and **2M** has been successfully achieved. A successful synthesis of the bimetallic Ni complexes has been developed which allows for clean separation of both diastereomers. Cyanolysis of the two bimetallic complexes has allowed us to isolate each diastereomer of the ligand in greater than 95% purity. Unfortunately the cyanolysis suffers from low yields of the free ligand and is not a practical means for isolating the pure diastereomers. Two monometallic Ni cyanide complexes isolated from the cyanolysis experiments have been characterized via X-ray crystallography.

# CHAPTER 1: INTRODUCTION

## 1.1 Alkene Hydration

The synthesis of alcohols is a very important area for chemical industry. Many of the simpler alcohols (ethanol, 2-propanol, 2-methyl-2-propanol, 1-butanol, etc.) are common laboratory solvents. Other alcohols are further reacted to produce detergents, plasticizers, surfactants and other important chemicals that are used in many aspects of people's lives.<sup>1-3</sup> The fine chemicals and pharmaceutical industries also synthesize alcohol functionalities as part of more complex molecules.<sup>1-3</sup> Unfortunately, several different synthetic strategies have to be utilized to produce alcohols and many of them suffer from major drawbacks, including multi-step processes, large amounts of waste, not to mention corrosive and toxic reagents. There is a great need for a one-step, cheap and atom-economical synthesis that is amenable to many different types of alcohols.

Alkene hydration<sup>4</sup> is a catalytic process that involves the addition of water across the double bond of an alkene to produce an alcohol (Figure 1.1). This is the most direct and atom-economical approach to the synthesis of alcohols. Acid-catalyzed alkene hydration<sup>4</sup> is the most well-known hydration process. This process is used industrially with several different acidic species as the catalyst, including zeolites, oxides, solid phosphoric acid and sulfuric acid.<sup>1-3,5-6</sup> There are several major drawbacks with this catalytic process. The first drawback is the acidic environment which is very corrosive and can lead to degradation of reactors or the need to use specially engineered and expensive reactors to resist the acidic conditions. Another drawback is the acidic environment required for hydration is not suitable for alkenes with acid-sensitive functional groups. Thus, this process is typically only used with simple alkenes such as ethylene, propylene and butenes. The final and biggest drawback is the selectivity of the reaction. Acid-



catalyzed hydration follows Markovnikov's rule which states that the proton will add to the carbon with the most hydrogens attached to it. Therefore, starting with propylene, acid-catalyzed hydration will always be selective for internal alcohols (secondary or tertiary). Except for ethanol, primary alcohols cannot be synthesized by acid-catalyzed hydration. Generally, primary alcohols are the more valuable commodity industrially. Therefore, different synthetic strategies have to be invented for the synthesis of primary alcohols.

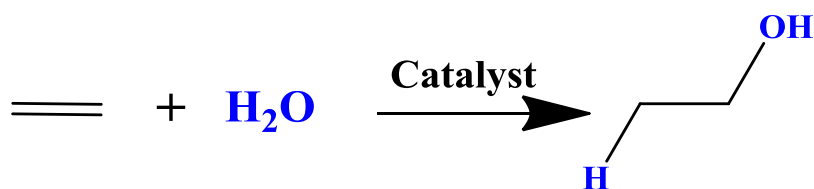


**Figure 1.1** Hydration of ethylene

One such process that was developed is known as hydroboration/oxidation.<sup>4</sup> This is a two-step process (Figure 1.2) in which a boron reagent reacts with an alkene and transfers one hydrogen to produce an alkylborane. When  $\text{BH}_3 \cdot \text{THF}$  is used as the boron reagent, this occurs three times to produce a trialkylborane. The trialkylborane is then oxidized with hydrogen peroxide and leads to the formation of a primary alcohol. Formally, this reaction is the addition of water across a double bond to form an alcohol with anti-Markovnikov selectivity. The reason for this is because of the first step of the reaction. For acid-catalyzed hydration, the proton that attacks the double bond is the electrophile and adds to the carbon atom with the most hydrogen atoms attached. This leads to the most stable carbocation intermediate (secondary or tertiary). For hydroboration, the boron atom is the electrophile and not hydrogen. Therefore, in accord with Markovnikov's rule, the boron atom adds to the carbon with the most hydrogen atoms attached to it and, after the oxidation step, a primary alcohol will always be produced from a terminal alkene. The major drawback for this reaction is the boron-containing waste that is

generated. The borate waste is difficult to recycle and severely limits the use of this reaction on an industrial scale.

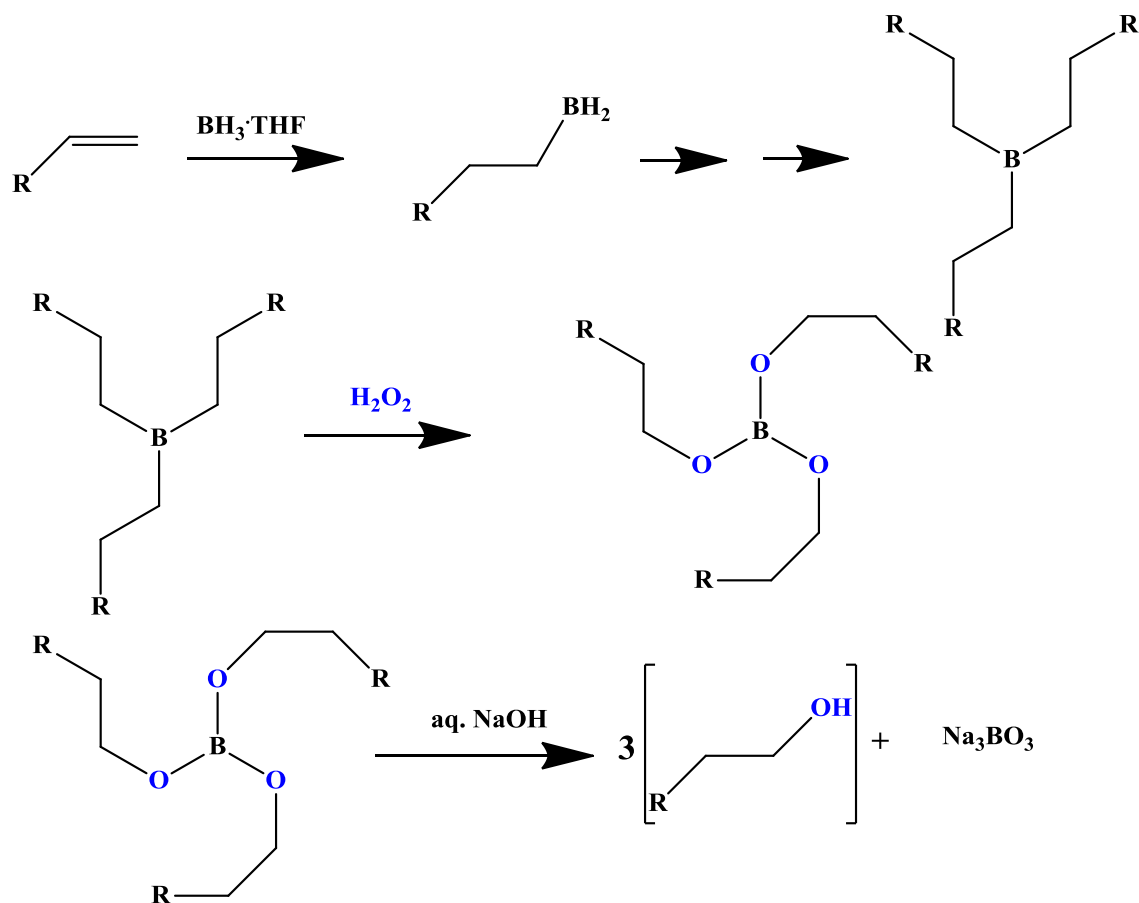


**Figure 1.2** Hydroboration-oxidation process to produce primary alcohols

Another process that was developed is known as the Ziegler process<sup>1-3</sup> (Figure 1.3).

Triethylaluminum is reacted with high-pressure ethylene gas. Ethylene is oligomerized via insertion into the Al-C bond producing trialkylaluminum compounds with varying chain lengths. The trialkylaluminum species are then oxidized with molecular oxygen to give aluminum alkoxides which are then subjected to hydrolysis producing primary alcohols. This process produces a mixture of alcohols with an even number of carbon atoms. Fractional distillation is performed to separate the individual alcohols. This is a very energy-intensive process. This is the current technology that Sasol North American uses at its Lake Charles, Louisiana facility.

Al(OH)<sub>3</sub> is generated as a byproduct of this process. Sasol has developed proprietary technologies to produce a high-grade alumina from the Al(OH)<sub>3</sub> that it sells commercially, turning a potential waste product into a useful material. One major drawback of this technology is that it is a multi-step process and each step must be carefully controlled to get the required alcohol products. The second major drawback is the fact that a mixture of alcohols is produced and has to be separated. Fractional distillation must be performed and must be carefully controlled to ensure each pure alcohol is obtained. Another drawback is that only even-numbered carbon chains are produced during this process and thus only primary alcohols with an even number of carbons can be obtained. Finally, the large amount of Al(OH)<sub>3</sub> must be either converted to a useful commodity or recycled or the process would not be economically feasible.

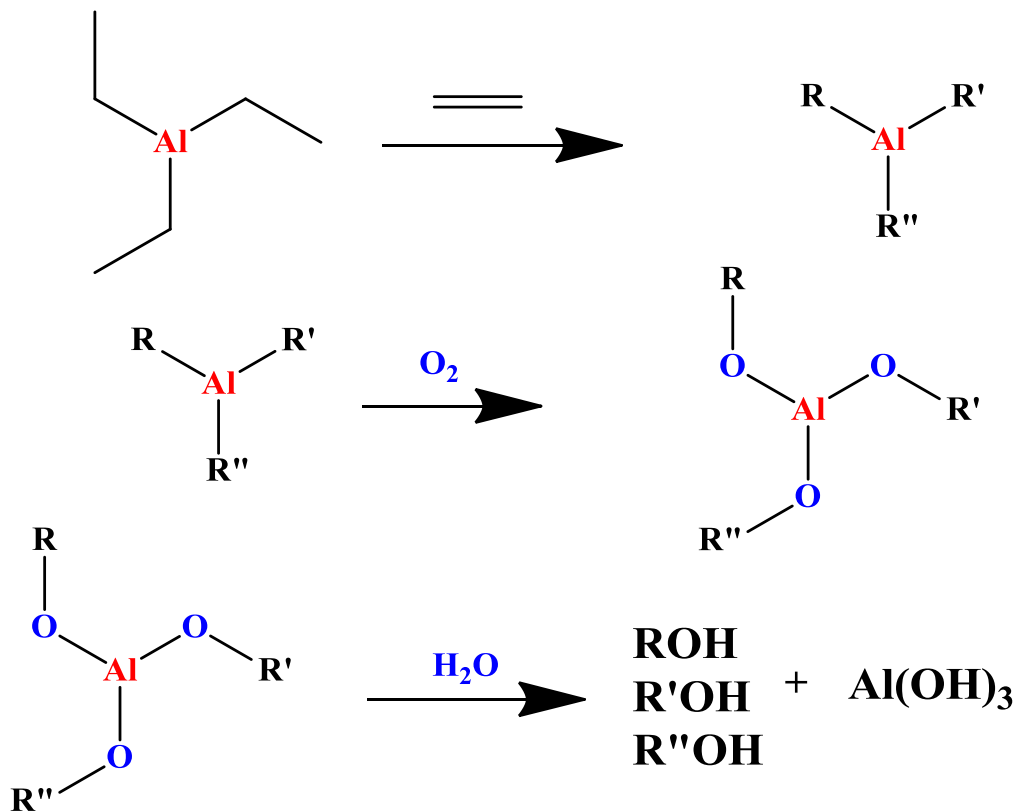


**Figure 1.3** The Ziegler process for the production of primary alcohols

Another method for the production of primary alcohols involves the coupling of two known catalytic processes, hydroformylation and hydrogenation.<sup>1-3</sup> In the first stage of the

process an alkene is reacted with a mixture of H<sub>2</sub> and CO gas in the presence of a Co or Rh catalyst at high temperatures and pressures to produce a mixture of linear and branched aldehydes via hydroformylation. The linear aldehydes are then separated from the reaction mixture and purified and further reacted with H<sub>2</sub> gas at high pressure in the presence of a solid metal catalyst to produce the alcohol via hydrogenation. If the starting alkene contains an even number of carbons (e. g. 1-hexene), the final alcohol would contain an odd numbered carbon chain (e. g. 1-heptanol). One drawback of this process is that it is a multi-step process which can utilize very expensive noble metal catalysts for each step.

As can be seen from the reactions above, the synthesis of primary alcohols is a very challenging endeavor. Several elegant synthetic routes have been developed for the production of primary alcohols. However, they all suffer from major drawbacks. Thus, there is a great desire to develop a transition metal catalyzed route to synthesize primary alcohols via the addition of water to an alkene. Dr. James Roth, a well-known industrial catalyst scientist, identified the anti-Markovnikov addition of water to an alkene to produce a primary alcohol as one of the ten “challenges of industrial catalysis” in 1993-94.<sup>7</sup> A large amount of academic and industrial research has been devoted to solving this challenge.

In 1986 Jensen and Trogler reported on a Pt complex, *trans*-PtHCl(PMe<sub>3</sub>)<sub>2</sub> (Figure 1.4), that they claimed was capable of producing 1-hexanol from 1-hexene.<sup>8</sup> The catalytic reaction was carried out in a biphasic mixture of aqueous NaOH and alkene with a phase-transfer catalyst and gave excellent selectivity for primary alcohols. Unfortunately, this work has been shown to be irreproducible. Ramprasad *et al.*<sup>9</sup> attempted to reproduce the results of Jensen and Trogler but all of their attempts failed. They found that the only reaction *trans*-PtHCl(PMe<sub>3</sub>)<sub>2</sub> was capable of performing under the conditions reported by Jensen and Trogler was isomerization of an alkene.

In an article<sup>10</sup> concerning the reactivity of hydridobis(phosphine) Platinum complexes, Trogler himself stated that “the reaction has proved erratic in its reproducibility”. Since then, nothing has been published concerning this complex’s ability to perform alkene hydration.

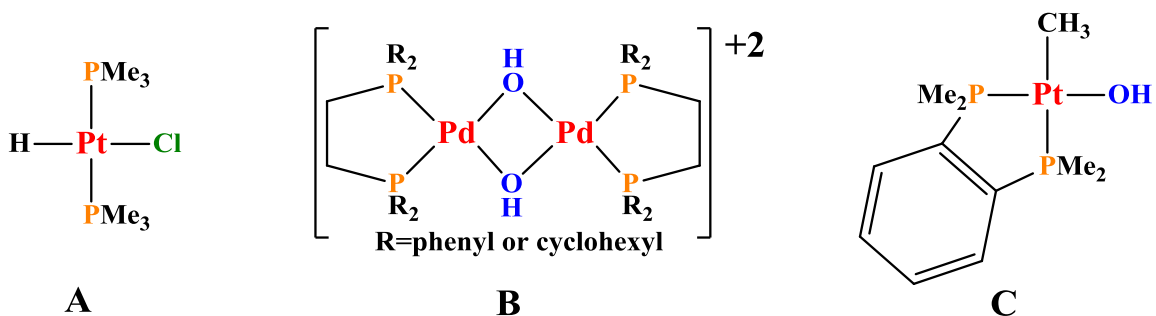


**Figure 1.4** Metal complexes tested for alkene hydration reactivity. **A** – *trans*-PtHCl(PMe<sub>3</sub>)<sub>2</sub> used by Jensen and Trogler. **B** – [Pd(μ-OH)(bisphosphine)]<sub>2</sub> tested for the catalytic hydration of diethyl maleate. **C** – Pt(CH<sub>3</sub>)(OH)[*o*-phenylenebis(dimethylphosphine)] tested for the stoichiometric hydration of dimethyl maleate.

Very few other reports appear in the literature concerning a transition metal catalyst capable of performing alkene hydration. The majority of the reports center on activated alkenes containing electron-withdrawing functionalities. One early example<sup>11</sup> involves the catalytic hydration of 1,1-difluoroethylene and vinyl fluoride via chlororuthenate(II) to produce acetic acid and acetaldehyde. The authors propose that the reaction involves the insertion of the alkene into a Ru-OH bond. Another example<sup>12</sup> involves the catalytic hydration of diethyl maleate via a hydroxide-bridged bimetallic Pd/bisphosphine complex (Figure 1.4) to produce diethyl malate. The reaction suffers from low conversions to the alcohol and no alcohol production occurs with unactivated alkenes such as 1-octene. A non-catalytic reaction between dimethyl maleate and several Pt(OH)CH<sub>3</sub>(L<sub>2</sub>) [L<sub>2</sub> = 2 PPh<sub>3</sub>, 1,2-bis-(diphenylphosphino)ethane or *o*-phenylenebis(dimethylphosphine)] (Figure 1.4) complexes was reported by Bennett *et al.*<sup>13</sup> They showed that dimethyl maleate inserted into the Pt-OH bond over the course of several days. The addition of a small amount of acid (HBF<sub>4</sub> or HPF<sub>6</sub>) gave the alcohol, dimethyl malate, in ~80% yield.

A related report by Bergman *et al.*<sup>14-15</sup> involves the insertion of ethylene into an Ir-OH bond (Figure 1.5) to produce a hydroxyethyl ligand attached to the Ir(III) center. Their work showed that this was a tandem reaction between two Ir complexes. One of the Ir centers contains a bound ethylene and the other contains the hydroxide ligand. These two species come together and lead to the insertion product. No alcohol product was produced from this reaction because the hydroxyethyl ligand further reacts to give a formylmethyl ligand. Bergman *et al.*<sup>16</sup> also reported on a transition metal-free catalytic hydration of activated alkenes to give alcohols. They found that trimethylphosphine could be used as a catalyst to produce  $\beta$ -hydroxy ketones from enones and water. The reaction proceeded with excellent selectivity and activity. However, it was limited to activated alkenes such as enones.

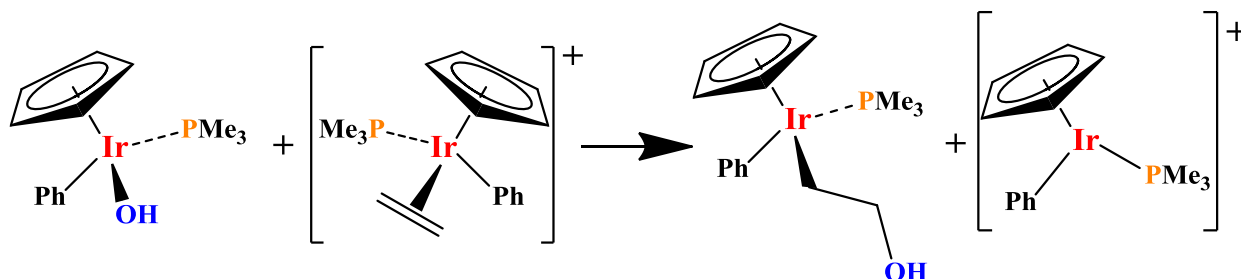


**Figure 1.5** The reaction between two Ir centers reported by Bergman *et al.* showing the insertion of ethylene into the Ir-OH bond.

Two more recent examples involve tandem catalytic processes to produce primary alcohols. The first was reported in 2010 by Nozaki *et al.*<sup>17</sup> They reported on a tandem hydroformylation/hydrogenation process to produce primary alcohols from alkenes and H<sub>2</sub>/CO gas. Their process is a one-pot process in which two different catalysts are mixed together in the presence of the alkene and H<sub>2</sub>/CO gas to produce the alcohols. As mentioned earlier, this tandem catalytic process is currently used industrially. However, it is a multi-step process and not a simple one-pot process. The two catalysts utilized by Nozaki *et al.* are the Rh/Xantphos catalyst for hydroformylation and Shvo's catalyst (Figure 1.6) for the hydrogenation. It is well known

that the Rh/Xantphos catalyst gives very high selectivities for the linear aldehyde which, after hydrogenation, leads to the more valuable primary alcohol and Shvo's catalyst is known to be more selective for the hydrogenation of the aldehyde over the alkene. After optimization of the reaction conditions, they reported a percent yield of 90.1% for the primary alcohol. They state that the yield "is the highest among reported values to date for the one-pot process".

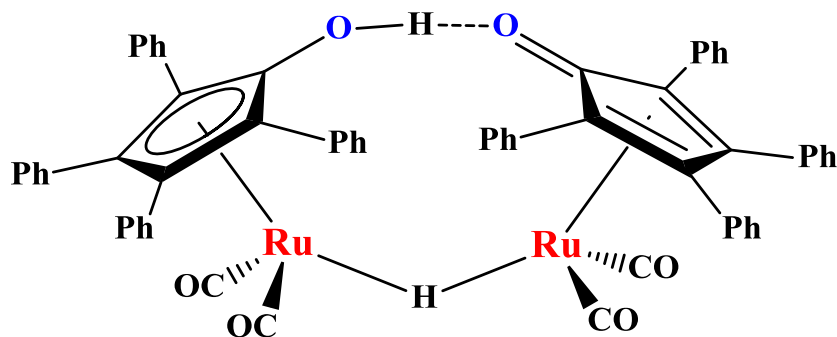


**Figure 1.6** Shvo's Catalyst

The second tandem catalytic process was reported by Grubbs *et al.* in 2011.<sup>18</sup> They dubbed it a triple-relay catalytic process, which formally produces primary alcohols from alkenes and water. They coupled together two known catalytic processes: Pd-catalyzed oxidation (Wacker oxidation) and Ru-catalyzed transfer hydrogenation. Generally, the Wacker oxidation is selective for the production of methyl ketones. Hydrogenation of the ketones would lead to secondary alcohols which are not the desired product. However, the use of 2-methyl-2-propanol as a solvent and chloride ligands has been shown to increase the selectivity for aldehydes. Grubbs and coworkers utilized both of these ideas for the oxidation of the alkene to selectively produce the aldehydes. For the transfer hydrogenation, they selected a combination of 2-propanol and Shvo's catalyst to produce the primary alcohol as the final product. It is dubbed a triple relay catalytic process because in the first stage of the reaction, the alkene is converted via Pd-catalyzed oxidation to the *t*-butyl vinyl ether. Some acid (HCl) is generated during this process and the ether, in the presence of water, is converted to the aldehyde via acid-catalyzed

hydrolysis. The third process involves the transfer-hydrogenation of the aldehyde via Shvo's catalyst and 2-propanol to give the primary alcohol and acetone. This system gave very good selectivities for the primary alcohol (greater than 20:1 primary to secondary) for styrene and substituted styrenes and also worked for aliphatic alkenes (1-octene). However, with 1-octene, the catalytic system gave higher amounts of secondary alcohol (1:1.9 primary to secondary). This system suffers from several major problems including high catalyst loadings (10 mol%  $\text{PdCl}_2(\text{CH}_3\text{CN})_2$ , 10 mol% Shvo's catalyst, 20 mol%  $\text{CuCl}_2$  and 80 mol% benzoquinone) and very low turnover numbers (8.4 turnovers being the best).

The production of primary alcohols from alkenes has proven to be an extremely difficult process. Several different strategies have been developed to produce these important commodities industrially. However, they all suffer from major issues. A lot of research has gone into the catalytic anti-Markovnikov hydration of terminal alkenes to produce primary alcohols and some progress has been made. However, no group to date has been able to achieve this challenging endeavor. Clearly, this area of research is extremely important and is waiting for someone to develop this catalytic process.

## **1.2 Alkene Oxidation**

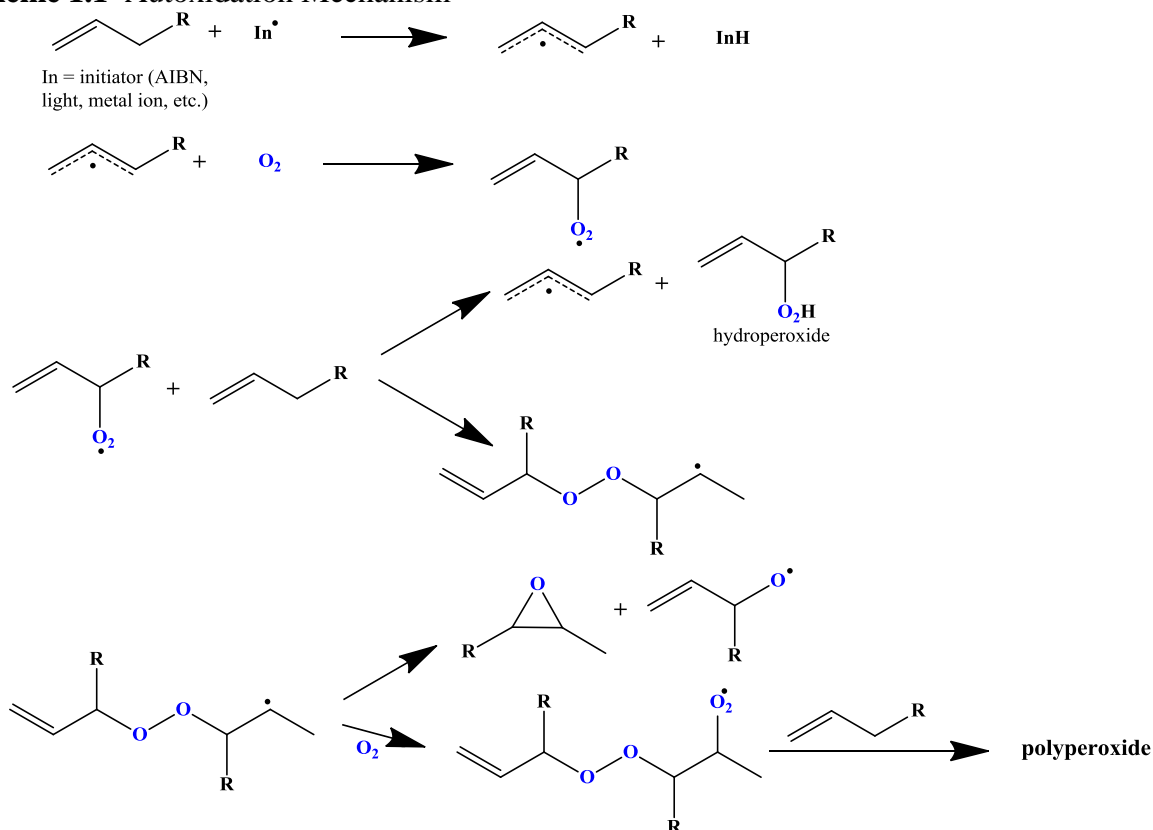
The oxidation of organic compounds is a vast, vast area of chemical research that spans a few hundred years. The area of transition metal catalyzed alkene oxidation also encompasses a large area of research. Nearly every transition metal on the periodic table has been investigated for alkene oxidation. Thus, a comprehensive review of the metal-catalyzed oxidations is not possible in this document. An excellent book by Sheldon and Kochi covers the material up to 1980<sup>19</sup> and there are many review articles<sup>20-30</sup> covering the important discoveries up to the present day.



Several different reactions are possible during any oxidation process. These reactions include free-radical autoxidation, oxidative cleavage of the double bond, epoxidation, dihydroxylation, and Wacker-type oxidations to name a few. One general problem with oxidation catalysis is that different reactions can give rise to the same product and it is highly important to determine what reaction pathway is occurring during any catalyzed oxidation reaction. Autoxidation is one of the most studied and well-known reaction pathways.<sup>31-40</sup> The reaction is a naturally-occurring process for organic compounds when they are exposed to air for prolonged periods of time. It was identified many years ago that the spoilage of oils, rubbers and other compounds was caused by the uptake of oxygen by these compounds. Initially, studies were conducted to try and stop the process from happening. It was discovered that certain molecules (ethers and alkenes) were more susceptible to this reaction. It was realized that known radical inhibitors (BHT – butylated hydroxytoluene and MEHQ – hydroquinone monomethyl ether or 4-methoxyphenol) could greatly hinder or stop this reaction completely. It has been studied extensively to determine the exact course of the reaction with different types of compounds (alkanes, alkenes, ethers, etc.). This work led to the proposal of a radical-chain mechanism that is now the accepted mechanism for this reaction.

Scheme 1.1 shows the steps that occur during the autoxidation of a typical alkene. The reaction can be initiated by several different species (AIBN – azobisisobutyronitrile, a typical radical initiator, UV light, metal ions, etc.). These species all cause the formation of a carbon-centered radical via the homolytic cleavage of a carbon-hydrogen bond. When oxygen is present, the carbon radical will trap a molecule of oxygen to form an oxygen-centered radical.

### Scheme 1.1 Autoxidation Mechanism

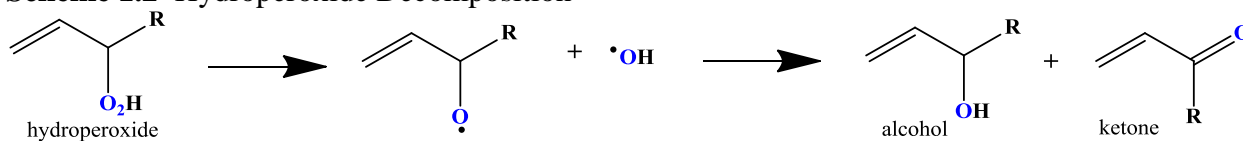


There are two possible reactions that can occur with this species. It can abstract a proton from another molecule of the alkene to produce a new carbon radical and an allylic hydroperoxide species. For the majority of alkenes the hydroperoxide is the major product of autoxidation. However, it is typically not isolated because hydroperoxides can be very unstable. There are examples of stable hydroperoxides (*tert*butyl hydroperoxide) that can be isolated in high yield. The other possible reaction is the addition of this oxygen-centered radical to the double bond of another alkene molecule. This species has two possible reactions as well. It can decompose to give a molecule of epoxide and another oxygen-centered radical or it can continue to add oxygen and alkene in an alternating fashion to give a polymer product called a polyperoxide. If the oxygen concentration is not high enough and the alkene concentration is fairly high, a typical alkene polymer can also be formed. The three main products from this

reaction are typically the hydroperoxide, epoxide and polyperoxide. The ratio of the three products depends on the structure of the alkene and the reaction conditions.

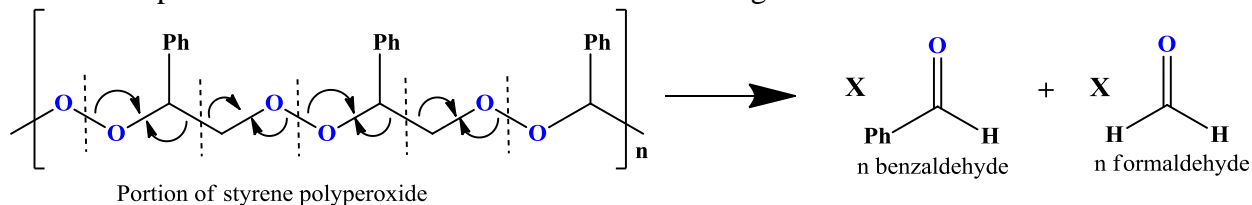
The hydroperoxide and the polyperoxide typically undergo further reactions to give other products. The hydroperoxide can homolytically cleave at the O-O bond to give hydroxyl radicals and an oxygen-centered radical on the alkene. These can react to give alcohol and ketone products (Scheme 1.2).

**Scheme 1.2** Hydroperoxide Decomposition



The polyperoxide can decompose via cleavage of the O-O bond and an adjacent C-C bond to give the products of oxidative cleavage, aldehydes or ketones (Scheme 1.3). The aldehydes from this reaction can also be further oxidized to carboxylic acids and peracids. Thus, from this simple radical-chain reaction, there is the possibility for the formation of hydroperoxides, epoxides, aldehydes, ketones, alcohols, carboxylic acids, carboxylic peracids, polyperoxides and polymer. Autoxidation represents one of the great challenges of oxidation catalysis. Because it is a radical-chain reaction, once this process becomes initiated it can very quickly become the dominant oxidation pathway and lead to a large product distribution.

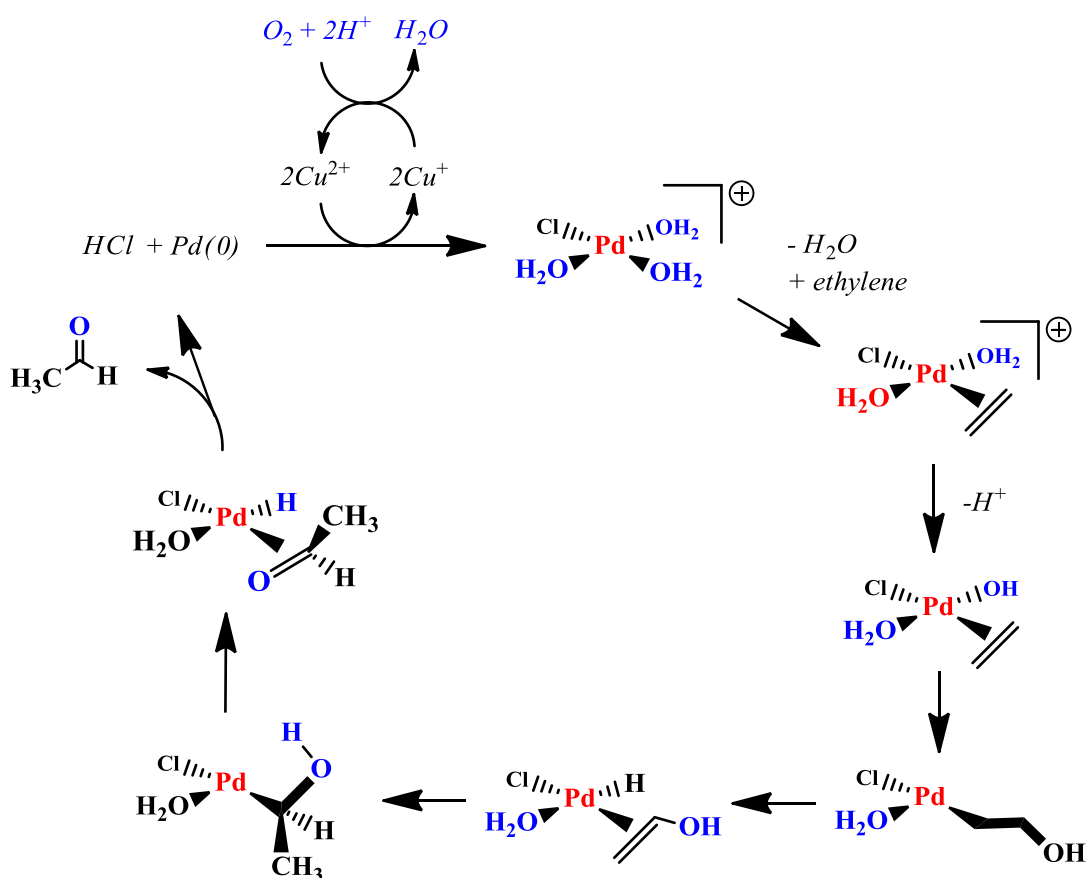
**Scheme 1.3** Polyperoxide Decomposition – The decomposition of styrene polyperoxide is shown as the example. This reaction leads to the oxidative cleavage of the double bond.



The other oxidation reactions mentioned are generally very selective for a specific type of product. The Wacker oxidation<sup>41-64</sup> is one example of such a reaction shown in Scheme 1.4.

This process utilizes late transition metal salts, both Pd(+2) and Cu(+2), water and molecular oxygen to perform this catalytic reaction. The process is an important industrial process for the oxidation of ethylene to produce acetaldehyde. For this reaction water reacts with ethylene, either via nucleophilic attack or by migratory insertion of a hydroxyl ligand formed via hydrolysis of the Pd-Cl bond, to form a  $\beta$ -hydroxyalkyl group. Scheme 1.4 shows the generally accepted migratory insertion mechanism for the Wacker oxidation.

**Scheme 1.4** Migratory Insertion Mechanism for Wacker Oxidation Catalysis



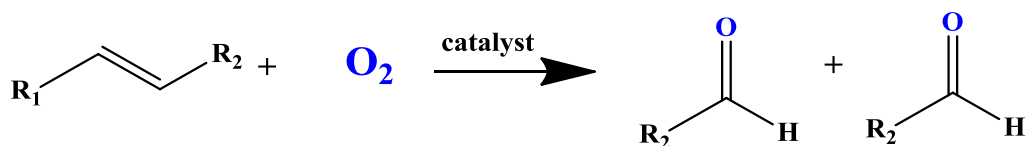
Both modes of attack have been shown to occur, experimentally and computationally, and it is believed that the exact mechanism is completely dependent on the exact reaction conditions utilized. After formation of the  $\beta$ -hydroxyalkyl group, the remaining steps include  $\beta$ -hydride elimination, rearrangement and reductive elimination to produce acetaldehyde, Pd(0) and

HCl. A co-catalyst is required to oxidize the Pd(0) back to Pd(+2) to maintain the catalytic cycle. Industrially, a Cu(+2) salt is usually the co-catalyst utilized and air or O<sub>2</sub> is used to oxidize the Cu(+1) back to Cu(+2) but other oxidants are used including hydroquinone. When alkenes larger than ethylene are subjected to this catalytic process, the methyl ketone is typically the major product. However, there are many examples of catalytic mixtures that selectively produce the aldehyde.

A related catalytic process has been reported utilizing Rh/phosphine complexes.<sup>65-72</sup> This oxidation also gives high selectivity for the methyl ketone like the Wacker oxidation. The biggest different between these two processes is that the Rh system does not require water. In fact studies have shown that water inhibits this catalytic oxidation. During the course of the Rh oxidation, one molecule of alkene is converted to the methyl ketone and one molecule of a phosphine ligand is oxidized to the phosphine oxide. Some reports on this catalytic process do not require the use of excess phosphine ligands. Cu salts are used as co-catalysts instead. The proposed mechanism involves a direct interaction between the Rh complex and molecular oxygen. One atom of O<sub>2</sub> is transferred to the alkene forming the methyl ketone and the other atom is transferred to a phosphine forming the phosphine oxide. The Rh/Cu systems operate under a slightly different mechanism but still give rise to the methyl ketone selectively. This is very different from the Wacker oxidation which does not involve any direct interaction between the Pd centers and molecular oxygen.

The selective oxidative cleavage of carbon-carbon double bonds is another desired process if it is the only oxidation pathway. During this reaction, the carbon-carbon double bond of the alkene is cleaved giving rise to aldehyde, ketone or carboxylic acid products depending on the substitution about the double bond and the specific reaction conditions (Scheme 1.5).

**Scheme 1.5** Oxidative Cleavage of an Internal Alkene



In nature, specific enzymes have been identified that catalyze this reaction to produce signaling compounds as well as for the synthesis of vitamins and other biologically important compounds.<sup>73-76</sup> One of the biggest drawbacks can be the selectivity for the cleavage product. Typically oxidation reactions do not show selectivity for the oxidative cleavage and many reports on transition metal-catalyzed oxidations consider the oxidative cleavage to be an overoxidation product and not the desired product. However, there are examples of selective oxidative cleavage reactions.

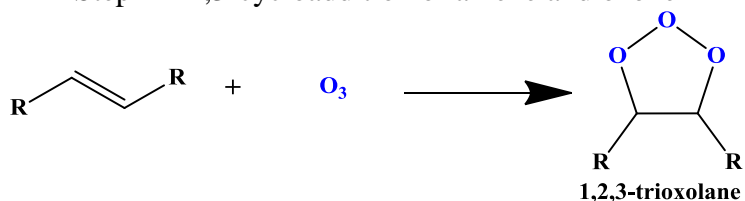
Ozonolysis is one of the most well-studied oxidative cleavage reactions.<sup>77-80</sup> The reaction has been known for over a century. It is a multi-step reaction that cleaves the carbon-carbon double bond of alkenes to produce aldehydes, ketones or carboxylic acids. In the majority of reactions, the alkene is quantitatively cleaved under extremely mild conditions. The products produced depend on the substitution of the double bond and the conditions used during the reaction, especially the solvent utilized and the workup of the products. The major drawback of this synthetic methodology is safety concerns. There have been reports of serious accidents and explosions. The reaction has been employed to synthesize specific products as well as to help identify unknown compounds containing a carbon-carbon double bond by breaking the molecule at the double bond to form more easily identified species.

The commonly accepted mechanism for this transformation was proposed by Criegee. The proposed steps involve several 1,3-dipolar cycloadditions or cycloreversions followed by

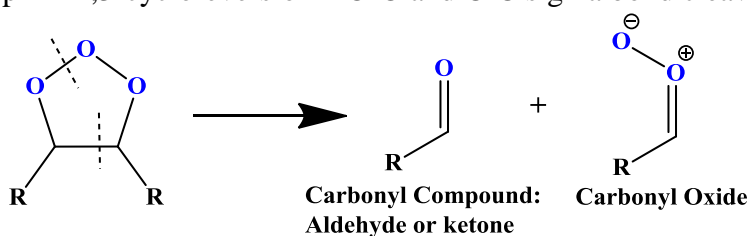
workup of the secondary ozonide to give you the products. The reaction steps are outlined in Scheme 1.6.

### Scheme 1.6 Ozonolysis Mechanism

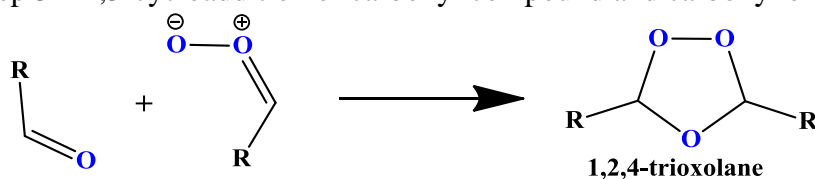
Step 1 – 1,3-cycloaddition of alkene and ozone



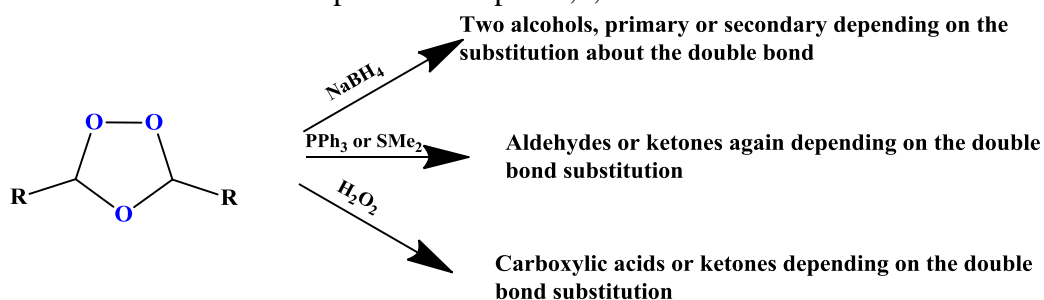
Step 2 – 1,3-cycloreversion – O-O and C-C sigma bond cleavage



Step 3 – 1,3-cycloaddition of carbonyl compound and carbonyl oxide



Step 4 – Workup of 1,2,4-trioxolane



The first step involves the addition of ozone to the double bond of the alkene. This forms the primary ozonide (1,2,3-trioxolane). The primary ozonide then undergoes a 1,3-dipolar cycloreversion to give a carbonyl compound (aldehyde or ketone depending on the substituents) and a carbonyl oxide. These two species react again via a cycloaddition to give the secondary ozonide (1,2,4-trioxolane). Once the secondary ozonide is formed, the workup for this species

will give you your products. The ozonide is susceptible to hydrolysis which would give you either aldehydes or ketones. However, the aldehydes would be subject to further oxidation to give carboxylic acids.  $\text{PPh}_3$  or  $\text{SMe}_2$  typically are used if aldehydes are the desired product. If it is reacted with  $\text{NaBH}_4$ , primary or secondary alcohols can be produced. If the ozonide is allowed to react with  $\text{H}_2\text{O}_2$ , carboxylic acids and ketones will be produced. If polar, protic solvents, such as alcohols, are used, the solvent can intervene and different products can be isolated.

Almost no transition metal complexes are reported in the literature that are selective for the oxidative cleavage of double bonds as shown in Scheme 1.5. The best example comes from a report by Drago *et al.*<sup>81</sup> They reported on a Co complex (Figure 1.7) that was selective for the oxidative cleavage of isoeugenol, 2-methoxy-4-propenyl-phenol. The oxidative cleavage led to the formation of vanillin and acetaldehyde. This was the only substrate investigated in this communication and no other reports on this complex's ability to perform the oxidative cleavage have appeared since this original publication in 1986. The complex showed activity at room temperature as well as elevated temperatures. Only one other product, a dimer of isoeugenol, was identified during the course of the reaction. High turnover numbers of between 530 and 560 were reported for this complex. This report is the best example of a selective homogeneous oxidative cleavage catalyst that has been found in the literature.

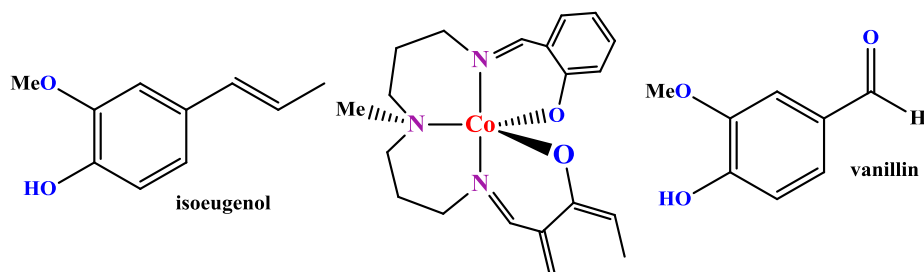


**Figure 1.7** Co catalyst for the selective oxidative cleavage of isoeugenol to produce vanillin and acetaldehyde (not shown).



There are countless reports in the literature concerning the oxidation of alkenes in which some oxidative cleavage occurs with many different transition metal complexes. The remaining discussion will center on the reports concerning Ni complexes as catalysts.<sup>82-120</sup> A wide range of ligands have been tested with Ni as possible oxidation catalysts. These include Schiff base/salen, cyclam, 1,3- $\beta$ -diketone, porphyrin, chelating amines and chelating phosphines (Figure 1.8).

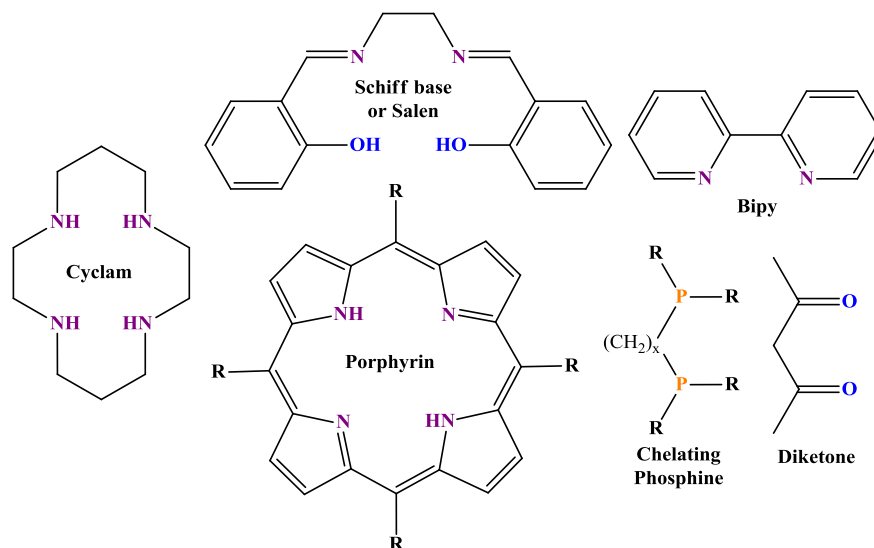


**Figure 1.8** Several different classes of ligands test for alkene oxidation catalysis with Ni

Several different oxidants have also been tested including molecular oxygen,  $O_2$ /aldehydes (Mukaiyama epoxidation),  $H_2O_2$ , TBHP, sodium hypochlorite and iodosylbenzene. The majority of these reports investigated the complexes as possible epoxidation catalysts. Some were found to be selective for the epoxidation but other products were always observed. Many of the proposed mechanisms involve a Ni(IV)-oxo complex as the active species when iodosylbenzene and sodium hypochlorite are the oxidants. This is usually inferred from indirect evidence including  $^{18}O$  labeling studies. They propose the oxidant reacts with the starting Ni(II) complex and oxidizes it to a Ni(IV) species and transfers the oxygen atom forming the Ni=O structure. However, a group utilized Zn and Al complexes with iodosylbenzene and found nearly identical reactivity as that observed with several Ni complexes.<sup>121</sup> These metals are redox

inactive and thus cannot form a metal-oxo species. Also, their labeling studies showed similar results to what other groups had observed. This careful study called into question much of the work in which a high-valent metal-oxo species was believed to be the active species without direct evidence for the formation of this species. This work also showed that  $^{18}\text{O}$  incorporation into the product is not evidence for the formation of a metal-oxo species.

Some of the best Ni oxidation catalysts were found using the Mukaiyama epoxidation conditions.<sup>113-118</sup> For these reactions molecular oxygen is the oxidant with an aldehyde as the co-reductant. This system was developed by Mukaiyama *et al.* Their initial investigations focused on Ni complexes with  $\beta$ -diketone ligands with either alcohols or aldehydes as the reductant. They found that the aldehydes, specifically aliphatic aldehydes and branched aldehydes, gave the best catalytic activity. Several other ligand classes, including cyclam, salen and porphyrin ligands, have been shown to be active using their conditions. Several mechanistic studies have been conducted on this system. The reactivity is not caused by the oxidation of the aldehydes to the peracids, which are powerful epoxidation agents, but via the formation of an acylperoxy radical which reacts with the metal complex and transfers one oxygen atom to the alkene forming the epoxide. This epoxidation reaction is one of the best examples of a Ni complex catalyzed oxidation reaction.

There are very few reports concerning the oxidation reactivity of Ni/ phosphine complexes. One reason these species have not been investigated is because phosphines are easily oxidized species and this could hinder the reactivity towards alkenes. One report utilized  $\text{H}_2\text{O}_2$  as the oxidant with styrene as the substrate.<sup>119</sup> They investigated Ni, Pd and Pt complexes with different chelating phosphines. This reaction led to the formation of several different products and in some cases the oxidative cleavage products were formed the most. The report

did not mention how stable the complexes themselves were towards the oxidant. Based on the product distribution, this is most-likely a case of metal-assisted autoxidation. Kochi *et al*<sup>120</sup> also investigated a few Ni/phosphine complexes for possible epoxidation reactivity with iodosylbenzene as the oxidant. Very little reactivity was observed for these complexes and no mention of the stability of the complexes towards the oxidant was made.

Transition metal-catalyzed alkene oxidation chemistry is a vast and very complex area of chemical research. There are several different oxidants that can be investigated and several different reaction pathways are possible. Almost all transition metals, complexes and simple salts, have been investigated for possible oxidation reactivity and many of them have been reported to be active for some type of oxidation catalysis. However, the majority suffer from poor turnover numbers and very poor product selectivity. Ni complexes have received considerable attention from many groups. The best example of Ni catalyzed oxidation comes from the studies utilizing the Mukaiyama epoxidation conditions. These examples showed high turnovers and good selectivity for the epoxides. Ni/phosphine complexes have been sparsely investigated because of the reactivity of the phosphine towards oxidation. The use of Ni/phosphine complexes as possible oxidation catalysts has the possibility to show high reactivity as long as stable complexes are formed that do not oxidize the phosphine. Strong oxidants like iodosylbenzene or sodium hypochlorite would not be well-suited for this class of compounds. However, the use of O<sub>2</sub>, TBHP or the Mukaiyama conditions could produce a selective oxidation catalyst (epoxidation, oxidative cleavage, etc.) without oxidizing the phosphine ligands.

### 1.3 References

1. Wiseman, P. *An Introduction to Industrial Organic Chemistry*; Applied Science: London, 1979.

2. Falbe, J.; Bahrmann, H.; Lipps, W.; Mayer, D.; Frey, G. D. Alcohols, Aliphatic In *Ullmann's Encyclopedia of Industrial Catalysis*, Wiley-VCH: Weinheim, Germany, 2013.
3. Weissermel, K.; Arpe, H.-J. *Industrial Organic Chemistry*, 3<sup>rd</sup> edition; translated by Lindley, C. R. Wiley-VCH: New York, 1997.
4. Smith, M. B.; March, J. *March's Advanced Organic Chemistry*, 5<sup>th</sup> edition; Wiley: New York, 2001.
5. Nowland, V. J.; Tidwell, T. T. *Acc. Chem. Res.* **1977**, 10, 252-258.
6. Eguchi, K.; Tokiai, T.; Arai, H. *Appl. Catal.* **1987**, 34, 275-287.
7. Haggin, J. *Chem. Eng. News* **1993**, 22, 23-27.
8. Jensen, C. M.; Trogler, W. C. *Science* **1986**, 233, 1069-1071.
9. Ramprasad, D.; Yue, H. J.; Marsella, J. A. *Inorg. Chem.* **1988**, 27, 3151-3155.
10. Trogler, W. C. *J. Chem. Ed.* **1988**, 65, 294-297.
11. James, B. R.; Louie, J. *Inorganica Chimica Acta* **1969**, 3, 568-574.
12. Ganguly, S.; Roundhill, D. M. *Organometallics* **1993**, 12, 4825-4832.
13. Bennett, M. A.; Jin, H.; Li, S.; Rendina, L. M.; Willis, A. C. *J. Am. Chem. Soc.* **1995**, 117, 8335-8340.
14. Woerpel, K. A.; Bergman, R. G. *J. Am. Chem. Soc.* **1993**, 115, 7888-7889.
15. Ritter, J. C. M.; Bergman, R. G. *J. Am. Chem. Soc.* **1997**, 119, 2580-2581.
16. Stewart, I. C.; Bergman, R. G.; Toste, F. D. *J. Am. Chem. Soc.* **2003**, 125, 8696-8697.
17. Takahashi, K.; Yamashita, M.; Ichihara, T.; Nakano, K.; Nozaki, K. *Angew. Chem. Int. Ed.* **2010**, 49, 4488-4490.
18. Dong, G.; Teo, P.; Wickens, Z. K.; Grubbs, R. H. *Science* **2011**, 333, 1609-1612.
19. Sheldon, R. A.; Kochi, J. K. *Metal-Catalyzed Oxidations of Organic Compounds*; Academic Press: New York, 1981.
20. Mukaiyama, T.; Yamada, T. *Bull. Chem. Soc. Jpn.* **1995**, 68, 17-35.
21. Kolb, H. C.; VanNieuwenhze, M. S.; Sharpless, K. B. *Chem. Rev.* B1994, **94**, 2483-2547.
22. Jørgensen, K. A. *Chem. Rev.* **1989**, 89, 431-458.

23. Punniyamurthy, T.; Velusamy, S.; Iqbal, J. *Chem. Rev.* **2005**, 105, 2329-2363.
24. Mimoun, H. *Pure & Appl. Chem.* **1981**, 53, 2389-2399.
25. Gupta, K. C.; Sutar, A. K.; Lin, C-C. *Coord. Chem. Rev.* **2009**, 253, 1926-1946.
26. Piera, J.; Bäckvall, J.-E. *Angew. Chem. Int. Ed.* **2008**, 47, 3506-3523.
27. Gunay, A.; Theopold, K. H. *Chem. Rev.* **2010**, 110, 1060-1081.
28. Shilov, A. E.; Shul'pin, G. B. *Chem. Rev.* **1997**, 97, 2879-2932.
29. Lambert, R. M.; Williams, F. J.; Copley, R. L.; Palermo, A. *J. Mol. Catal. A: Chem.* **2005**, 27-33.
30. Costas, M.; Mehn, M. P.; Jensen, M. P.; Que Jr., L. *Chem. Rev.* **2004**, 104, 939-986.
31. Howard, J. A. *Can. J. Chem.* **1972**, 50, 2298-2304. – rate constants for auto.
32. Ingold, K. U. *Acc. Chem. Res.* **1969**, 2, 1-9.
33. Milas, N. A. *Chem. Rev.* **1932**, 10, 295-364.
34. Moureu, C. *Chem. Rev.* **1926**, 3, 113-162.
35. Frank, C. E. *Chem. Rev.* **1950**, 46, 155-169.
36. Ingold, K. U. *Chem. Rev.* **1961**, 61, 563-589.
37. Bawn, C. E. H.; Pennington, A. A.; Tipper, C. F. H. *J. Chem. Soc.* **1945**, 498, 282-291.
38. Van Sickle, D. E.; Mayo, F. R.; Arluck, R. M. *J. Am. Chem. Soc.* **1965**, 87, 4824-4832.
39. Van Sickle, D. E.; Mayo, F. R.; Arluck, R. M. *J. Am. Chem. Soc.* **1965**, 87, 4832-4837.
40. Van Sickle, D. E.; Mayo, F. R.; Arluck, R. M.; Syz, M. G. *J. Am. Chem. Soc.* **1967**, 89, 967-977.
41. Van Sickle, D. E.; Mayo, F. R.; Gould, E. S.; Arluck, R. M. *J. Am. Chem. Soc.* **1967**, 89, 977-984.
42. Boardman, H.; Selwood, P. W. *J. Am. Chem. Soc.* **1970**, 72, 1372-1377.
43. Mayo, F. R. *J. Am. Chem. Soc.* **1958**, 80, 2465-2480.
44. Mayo, F. R. *J. Am. Chem. Soc.* **1958**, 80, 2497-2500.

45. Mayo, F. R. *J. Am. Chem. Soc.* **1958**, 80, 2500-2507.
46. Miller, A. A.; Mayo, F. R. *J. Am. Chem. Soc.* **1978**, 78, 1017-1023.
47. Mayo, F. R.; Miller, A. A. *J. Am. Chem. Soc.* **1978**, 78, 1023-1034.
48. Howard, J. A.; Ingold, K. U. *J. Am. Chem. Soc.* **1965**, 43, 2729-2736.
49. Smidt, J.; Hafner, W.; Jira, R.; Sedlmeier, J.; Sieber, R.; Ruttinger, R.; Kojer, H. *Angew. Chem., Int. Ed.* **1959**, 71, 176.
50. Henry, P. M. *J. Am. Chem. Soc.* **1964**, 86, 3246-3250.
51. Henry, P. M. *J. Am. Chem. Soc.* **1966**, 88, 1595-1597.
52. Bäckvall, J. E.; Åkermark, B.; Ljunggren, S. O. *J. Am. Chem. Soc.* **1979**, 101, 2411-2416.
53. Wan, W. K.; Zaw, K.; Henry, P. M. *J. Mol. Catal.* **1982**, 81-87.
54. Åkermark, B. C. S. B. *Organometallics* **1987**, 6, 2608-2610.
55. Keith, J. A.; Nielsen, R. J.; Oxgaard, J.; Goddard, III, W. A. *J. Am. Chem. Soc.* **2007**, 129, 12342-12343.
56. Keith, J. A.; Oxgaard, J.; Goddard, III, W. A. *J. Am. Chem. Soc.* **2006**, 128, 3132-3133.
57. Miller, D. G.; Wayner, D. D. M. *J. Org. Chem.* **1990**, 55, 2924-2927.
58. Wenzel, T. T. *J. Chem. Soc., Chem. Comm.* **1993**, 862-865.
59. Feringa, B. L. *J. Chem. Soc., Chem. Comm.* **1986**, 909-910.
60. Takacs, J. M.; Jiang, X.-T. *Curr. Org. Chem.* **2003**, 369-396.
61. Sharma, G. V. M.; Krishna, P. R. *Curr. Org. Chem.* **2004**, 8, 1187-1209.
62. Nelson, D. J.; Li, R.; Brammer, C. J. *J. Am. Chem. Soc.* **2001**, 123, 1564-1568.
63. Cornell, C. N.; Sigman, M. S. *J. Am. Chem. Soc.* **2005**, 127, 2796-2797.
64. Muzart, J. *Tetrahedron* **2007**, 63, 7505-7521.
65. Dudley, C. W.; Read, G.; Walker, P. J. C. *J. Chem. Soc., Dalton Trans.* **1974**, 1926-1931.
66. Read, G.; Walker, P. J. C. *J. Chem. Soc., Dalton Trans.* **1977**, 883-888.
67. Igersheim, F.; Mimoun, H. *J. Chem. Soc., Chem. Comm.* **1978**, 559-560.
68. Read, G. *J. Mol. Catal.* **1978**, 4, 83-84.

69. Dudley, C.; Read, G. *Tetrahedron Lett.* **1972**, 52, 5273-5276.
70. Tang, R.; Mares, F.; Neary, N.; Smith, D. E. *J. Chem. Soc., Chem. Comm.* **1979**, 274-275.
71. Mimoun, H.; Machirant, M. M. P.; Sérée de Roch, I. *J. Am. Chem. Soc.* **1978**, 100, 5437-5444.
72. Drago, R. S.; Zuzich, A.; Nyberg, E. D. *J. Am. Chem. Soc.* **1985**, 107, 2898-2903.
73. Hu, K.-Q.; Liu, C.; Ernst, H.; Kinsky, N. I.; Russell, R. M.; Wang, X.-D. *J. Biol. Chem.* **2006**, 281, 19327-19338.
74. Schmidt, H.; Kurtzer, R.; Eisenreich, W.; Schwab, W. *J. Biol. Chem.* **2006**, 281, 9845-9851.
75. Braaz, R.; Fischer, P.; Jendrossek, D. *Appl. Envir. Microbiol.* **2004**, 70, 7388-7395.
76. Lara, M.; Mutti, F. G.; Glueck, S. M.; Kroutil, W. *J. Am. Chem. Soc.* **2009**, 131, 5368-5369.
77. Criegee, R. *Angew. Chem., Int. Ed.* **1975**, 14, 745-752.
78. Williamson, D. G.; Cvetanovic, R. J. *J. Am. Chem. Soc.* **1968**, 90, 3668-3672.
79. Whitworth, A. J.; Ayoub, R.; Rousseau, Y.; Fliszár, S. *J. Am. Chem. Soc.* **1969**, 91, 7128-7131.
80. Choi, H.-S.; Kuczkowski, R. L. *J. Org. Chem.* **1985**, 50, 901-902.
81. Drago, R. S.; Corden, B. B.; Barnes, C. W. *J. Am. Chem. Soc.* **1986**, 108, 2453-2454.
82. Kinneary, J. F.; Wagler, T. R.; Burrows, C. J. *Tetrahedron Lett.* **1988**, 29, 877-880.
83. Lee, D.; Bang, H.; S, M. P. *J. Mol Catal. A: Chem.* **2000**, 151, 71-78.
84. Yamazaki, S.; Yamazaki, Y. *Bull. Chem. Soc. Jpn.* **1991**, 64, 3185-3187.
85. Wagler, T. R.; Burrows, C. J. *Tetrahedron Lett.* **1988**, 29, 5091-5094.
86. Chatterjee, D.; Mukherjee, S.; Mitra, A. *J. Mol. Catal. A: Chem.* **2000**, 154, 5-8.
87. Wagler, T. R.; Fang, Y.; Burrows, C. J. *J. Org. Chem.* **1989**, 54, 1584-1589.
88. Yoon, H.; Burrows, C. J. *J. Am. Chem. Soc.* **1988**, 110, 4087-4089.
89. Irie, R.; Ito, Y.; Katsuki, T. *Tetrahedron Lett.* **1991**, 32, 6891-6894.
90. Goldcamp, M. J.; Robison, S. E.; Krause Bauer, J. A.; Baldwin, M. J. *Inorg. Chem.* **2002**, 41, 2307-2309.

91. Singh, J.; Hundal, G.; Gupta, R. *Eur. J. Inorg. Chem.* **2008**, 2052-2063.
92. Fernandez, I.; Pedro, J. R.; Rosello, A. L.; Ruiz, R.; Ottenwaelder, X.; Journaux, Y. *Tetrahedron Lett.* **1998**, 39, 2869-2872.
93. Mirkhani, V.; Moghadam, M.; Tangestaninejad, S.; Mohammadpoor-Baltork, I.; Shams, E.; rasouli, N. *Appl. Catal. A: Gen.* **2008**, 334, 106-111.
94. Ferreira, R.; Garcia, H.; de Castro, B.; Freire, C. *Eur. J. Inorg. Chem.* **2005**, 4272-4279.
95. Yoon, H.; Wagler, T. R.; O'Connor, K. J.; Burrows, C. J. *J. Am. Chem. Soc.* **1990**, 112, 4568-4570.
96. Yamada, M.; Ochi, S.; Suzuki, H.; Hisazumi, A.; Kuroda, S.; Shimao, I.; Araki, K. *J. Mol. Catal.* **1994**, 87, 195-202.
97. Ramakrishna, D.; Bhat, B. R.; Karvembu, R. *Catal. Commun.* **2010**, 11, 498-501.
98. Kinneary, J. F.; Albert, J. S.; Burrows, C. J. *J. Am. Chem. Soc.* **1988**, 110, 6124-6129.
99. Rispens, M. T.; Gelling, O. J.; de Vries, A. H. M.; Meetsma, A.; van Bolhuis, f.; Feringa, B. L. *Tetrahedron.* **1996**, 52, 3521-3546.
100. Sohrabi, H.; Esmaeeli, M.; Farzaneh, F.; Ghandi, M. *J. Inclusion Phenom. Macrocyclic Chem.* **2006**, 54, 23-28.
101. Nagataki, T.; Ishii, K.; Tachi, Y.; Itoh, S. *Dalton Trans.* **2007**, 1120-1128.
102. Dangel, B.; Clarke, M.; Haley, J.; Sames, D.; Polt, R. *J. Am. Chem. Soc.* **1997**, 119, 10865-10866.
103. Gerbeleu, N. V.; Palanciuc, S. S.; Simonov, Y. A.; Dvorkin, A. A.; Bourosh, P. N.; Reetz, M. T.; Arion, V. B.; Tollner, K. *Polyhedron.* **1995**, 14, 521-527.
104. Park, Y. C.; Kim, S. S. *Bull. Korean Chem. Soc.* **1992**, 13, 458-459.
105. Larsen, E.; Jorgensen, K. A.; *Acta Chemica Scandinavica.* **1989**, 43, 259-263.
106. Choudhary, V. R.; Jha, R.; Jana, P. *Catal. Commun.* **2008**, 10, 205-207.
107. Maldhure, A. K.; Aswar, A. S. *J. Indian Chem. Soc.* **2009**, 86, 697-702.
108. Bansod, A. D.; Aswar, A. S. *Pol. J. Chem.* **2006**, 80, 1615-1622.
109. Sen, R.; Bhunia, S.; Mal, D.; Koner, S.; Miyashita, Y.; Okamoto, K.-I. *Langmuir.* **2009**, 25, 13667-13672.
110. Gupta, K. C.; Sutar, A. K. *Journal of Macromolecular Science.* **2007**, 44, 1171-1185.



111. Rao, C. R. K.; Aneetha, H.; Srinivas, B.; Zacharias, P. S. *Polyhedron*. **1994**, 13, 2659-2664.
112. Diaz, D. D.; Gupta, S. S.; Kuzelka, J.; Cymborowski, M.; Sabat, M.; Finn, M. G. *Eur. J. Inorg. Chem.* **2006**, 4489-4493.
113. Yamada, T.; Takai, T.; Rhode, O.; Mukaiyama, T. *Bull. Chem. Soc. Jpn.* **1991**, 64, 2109-2117.
114. Mukaiyama, T.; Takai, T.; Yamada, T.; Rhode, O. *Chem. Lett.* **1990**, 1661-1664.
115. Yamada, T.; Takai, T.; Rhode, O.; Mukaiyama, T. *Chem. Lett.* **1991**, 1-4.
116. Nishida, Y.; Tanaka, N.; Okazaki, M. *Polyhedron*. **1994**, 13, 2245-2249.
117. Wentzel, B. B.; Gosling, P. A.; Feiters, M. C.; Nolte, J. M. *J. Chem. Soc., Dalton Trans.* **1998**, 2241-2246.
118. Wentzel, B. B.; Alsters, P. L.; Feiters, M. C.; Nolte, R. J. M. *J. Org. Chem.* **2004**, 69, 3453-3464.
119. Cho, Y.-J.; Lee, D.-C.; Lee, H.-J.; Kim, K.-C.; Park, Y.-C. *Bull. Korean Chem. Soc.* **1997**, 18, 334-336.
120. Koola, J. D.; Kochi, J. K. *Inorg. Chem.* **1987**, 26, 908-916.
121. Nam, W.; Valentine, J. S. *J. Am. Chem. Soc.* **1990**, 112, 4977-4979.

## CHAPTER 2: INVESTIGATION INTO ALKENE HYDRATION CATALYSIS

### 2.1 Motivation

Our group has been interested in the synthesis and applications of linear tetratertiary phosphine ligands *meso*- and *racemic*-(Et<sub>2</sub>PCH<sub>2</sub>CH<sub>2</sub>)(Ph)PCH<sub>2</sub>P(Ph)(CH<sub>2</sub>CH<sub>2</sub>PEt<sub>2</sub>) (*et,ph*-P4, **1M** and **1R**) (Figure 2.1). These ligands were designed to bridge and chelate two metal centers within close proximity to one another and possibly allow for bimetallic cooperativity.<sup>1,2</sup> The main goal was to test these bimetallic complexes for homogeneous catalytic processes and determine whether the two metal centers can show bimetallic cooperativity during a catalytic cycle. This goal was realized with the synthesis of [*rac*-Rh<sub>2</sub>(nbd)<sub>2</sub>(*et,ph*-P4)][BF<sub>4</sub>] (nbd = norbornadiene) (Figure 2.1), which has been shown to be a precursor to a very active and regioselective hydroformylation catalyst and is one of the best examples of bimetallic cooperativity during a catalytic cycle.<sup>3-5</sup> Spectroscopic studies on the bimetallic Rh system have shown that these complexes can readily fall apart, even under fairly mild conditions, and form inactive monometallic and bimetallic systems (Figure 2.2).<sup>4,6-8</sup>

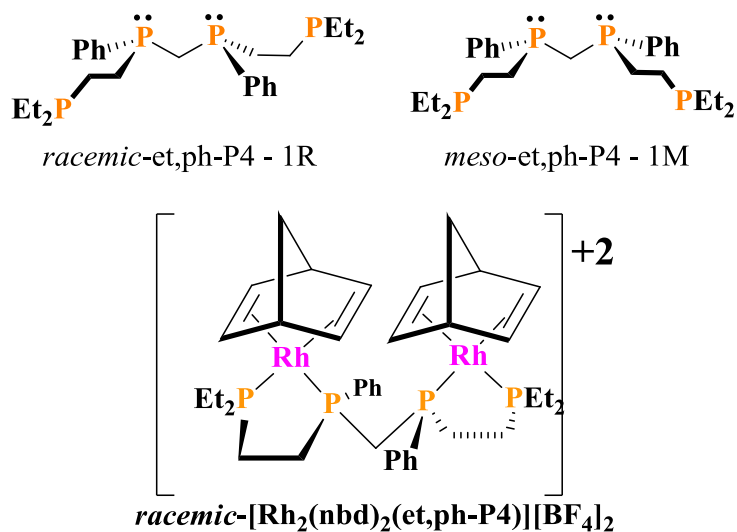


**Figure 2.1** Phosphine ligands **1R** and **1M** and the bimetallic Rh complex active for hydroformylation.

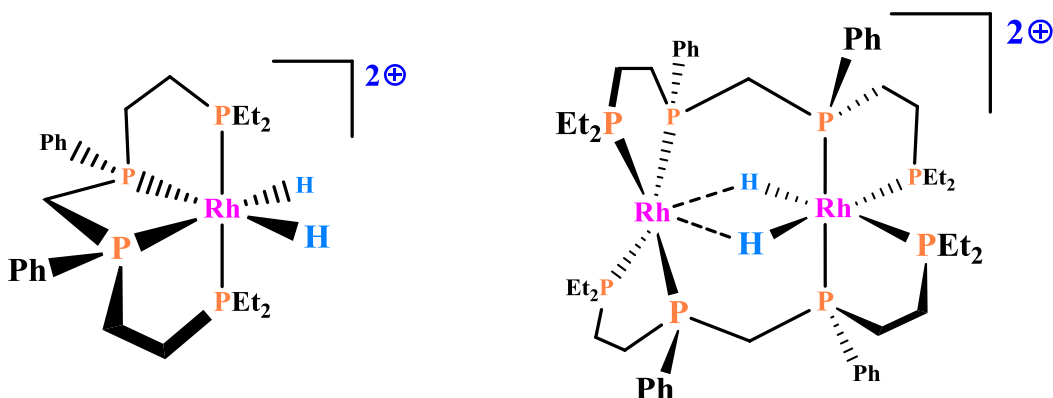


**Figure 2.2** Two inactive Rh species believed to be formed during the hydroformylation of alkenes.

The next goal was to synthesize new linear tetratertiary phosphine ligands, *rac,meso*-(Et<sub>2</sub>P-1,2-C<sub>6</sub>H<sub>4</sub>)PCH<sub>2</sub>P(1,2-C<sub>6</sub>H<sub>4</sub>-PEt<sub>2</sub>) (**2R** and **2M**) (Figure 2.3), in which the ethylene ligand of **1R** and **1M** was replaced with a phenylene linkage. The hope was that the phenylene linkage would give rise to a stronger chelate effect and not allow the bimetallic complexes to fall apart and form inactive species. Dr. Alex Monteil successfully synthesized these new ligands.<sup>9</sup>

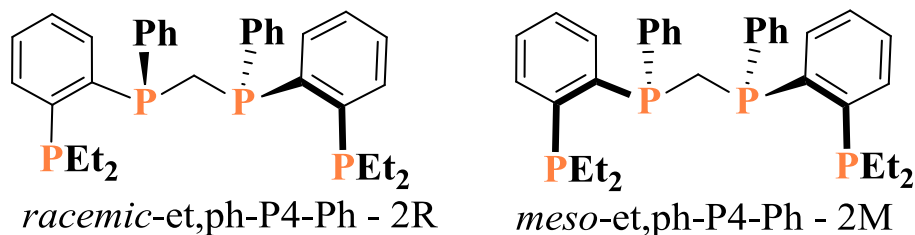


**Figure 2.3** The new, stronger chelating phosphine ligands **2R** and **2M**

Definitive proof of the successful synthesis of the new ligands came from two crystal structures solved by Dr. Frank Fronczek of two different bimetallic Ni complexes. The first structure was for the compound Ni<sub>2</sub>Cl<sub>4</sub>(**2M**), Ni<sub>2</sub>**2M**. The other structure was an unexpected bimetallic Ni complex, [Ni<sub>2</sub>(μ-OH)Cl<sub>2</sub>(**2M**)]<sup>+</sup> (Figure 2.4). This was the first example of a bridging hydroxide complex from our group.

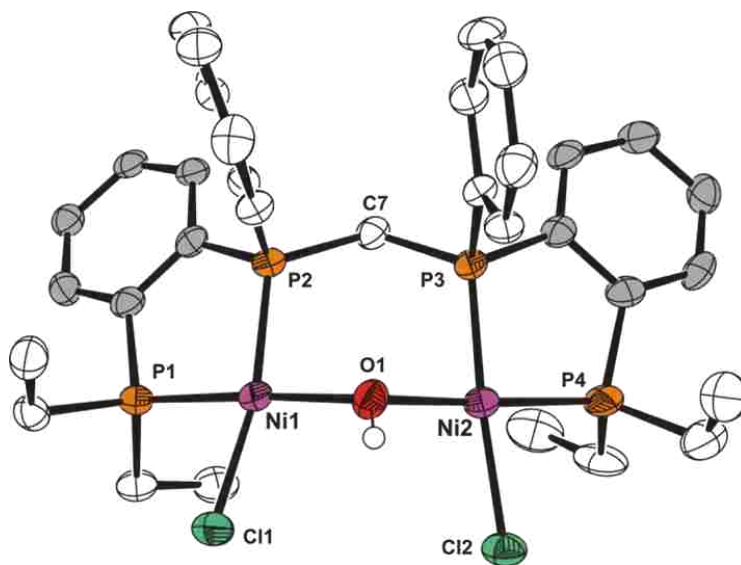


**Figure 2.4** ORTEP plot of  $[\text{Ni}_2(\mu\text{-OH})\text{Cl}_2(2\text{M})]^+$

With this new structural motif identified and characterized, Dr. Stanley began to wonder about the possible reactivity of this complex. Since it is evident that the starting tetrachloro complex could react with water to form a bridging hydroxide, could it be possible for the hydroxide ligand to react and participate in a new catalytic process. One of the most important catalytic reactions to investigate that would involve a hydroxide ligand is alkene hydration. With these ideas, Dr. Stanley proposed the investigation into alkene hydration catalysis utilizing the bimetallic Ni complexes.

## 2.2 Attempted Alkene Hydration Catalysis with Ni/Phosphine Complexes

At the commencement of the project, the synthesis of **2M** and **2R** was still being optimized and there was not a detailed synthetic strategy for the bimetallic Ni complexes. Therefore, initial focus was placed on the bimetallic Ni complexes formed from **1M** and **1R** (Figure 2.5). Because the *meso* diastereomer formed the bridging hydroxide complex, the initial experiments focused on *meso*- $\text{Ni}_2\text{Cl}_4(\text{et,ph-P4})$  (**Ni<sub>2</sub>1M**). All of the early experiments were conducted under an inert atmosphere of  $\text{N}_2$ . For these experiments, 10 mM of **Ni<sub>2</sub>1M** was dissolved in 20 mL of a 30% water/acetone solvent mixture and 4 equivalents of  $\text{AgBF}_4$  were

added. This solution was allowed to stir and AgCl precipitated out of solution. The solution was then filtered through a frit funnel to remove the AgCl solid. Ag was utilized to remove the chloride ligands from the complex for two reasons. The first reason was in order for the formation of a bridging hydroxide complex to occur, some chloride dissociation would have to take place. The addition of Ag would speed up this process and hopefully lead to stable Ni-OH complexes. The second reason was to form cationic or multi-cationic complexes. When the alkene binds to these cationic complexes the positive charge and fairly high electronegativity of nickel (for a transition metal) would help to draw electron density away from the alkene and make it more susceptible to nucleophilic attack by water or migratory insertion of a hydroxide ligand.

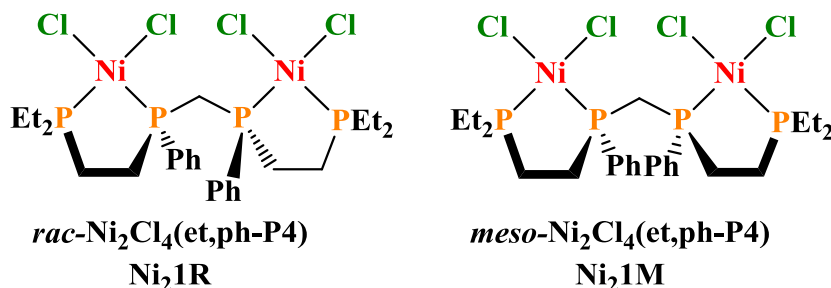


**Figure 2.5** Bimetallic Ni complexes studied for possible alkene hydration catalysis.

After removal of the AgCl, 100 equivalents of 1-hexene were added to the yellow-orange acetone/water solution. Because of the amount of water present, the 1-hexene was not miscible with the acetone/water layer and a biphasic system was observed throughout the experiment. This occurred anytime the water was 30% (by volume) of the solvent system. The mixture was then heated to 90°C and allowed to stir and heat overnight under an N<sub>2</sub> atmosphere. The next day, the reaction mixture was cooled to room temperature and opened to air. A sample was collected and analyzed via GC/MS. No products were identified.

Several more similar experiments were conducted with everything being the same except the amount of  $\text{AgBF}_4$ , which was varied from 1 to 4 equivalents. Again, no products were identified via GC/MS. Also, without any  $\text{AgBF}_4$  added, no products formed. While preparing GC samples from a couple of these initial experiments, a white solid was observed that crashed out of solution after the addition of acetone. The acetone was added for the GC samples to first dilute the solution and to form a homogenous solution between the two layers. It was assumed that this solid was either some  $\text{AgCl}$  or phosphine oxide.

After these failed initial attempts, several different conditions were attempted. The first was trying to oxidize the Ni complex to the +3 oxidation state. It was believed that the higher oxidation state would also help to activate the 1-hexene upon coordination with the Ni centers and make it more susceptible to nucleophilic attack or migratory insertion. Several different oxidizing agents were tested including  $\text{I}_2$ ,  $\text{FeCl}_3$ , Ferrocenium tetrafluoroborate, excess  $\text{Ag}^+$  and  $\text{NaClO}$ . No direct evidence could be obtained that any oxidation of the Ni centers occurred and when  $\text{NaClO}$  was utilized, decomposition of the starting complex was observed.

The next series of experiments involved the addition of acids or bases to the reaction mixture in an attempt to get some reactivity. When 10 equivalents or more of strong base ( $\text{KOH}$  or  $\text{NaOH}$ ) was added, decomposition of the starting complex occurred. Also, when acetone was used as a solvent, the bases reacted with acetone and led to the dimerization of acetone. Weak bases (triethyl amine and  $\text{CaCO}_3$ ) did not cause any reaction to occur. The addition of any acid ( $\text{HCl}$ ,  $\text{HBF}_4$ ,  $\text{H}_2\text{SO}_4$  and  $\text{NH}_4\text{Cl}$ ) also did not produce any reaction.

The amount of water was also varied from 5% (by volume) to 30%. Again, no reactivity was observed. The organic solvent was also varied and included THF, acetonitrile, methanol and DMF. Again, no reactivity was observed. Other phosphine ligands, including

triphenylphosphine (PPh<sub>3</sub>) and tricyclohexylphosphine (PCy<sub>3</sub>), were added to the bimetallic complex but they also did not promote any reactivity. All attempts with **Ni<sub>2</sub>1M** failed to show any reactivity towards the substrate and in no case was an alcohol product observed.

Many of the reaction conditions were also attempted with *racemic*-Ni<sub>2</sub>Cl<sub>4</sub>(et,ph-P4) (**Ni<sub>2</sub>1R**). They included the addition of AgBF<sub>4</sub>, strong bases, strong acids and oxidizing agents. As with the *meso* complex, no alcohol products were observed with the *racemic* complex. The only difference that was observed was **Ni<sub>2</sub>1R** led to a small amount of isomerization of 1-hexene to internal alkenes (2- and 3-hexenes). This was only observed with the *racemic* complex.

Several monometallic Ni/phosphine complexes were also tested for possible alkene hydration catalysis. The complexes included NiCl<sub>2</sub>(PPh<sub>3</sub>)<sub>2</sub>, NiCl<sub>2</sub>(PCy<sub>3</sub>)<sub>2</sub>, NiCl<sub>2</sub>dppe (dppe=1,2-bis(diphenylphosphino)ethane), NiCl<sub>2</sub>dcpe (dcpe=1,2-bis(dicyclohexylphosphino)ethane), NiCl<sub>2</sub>dppp (dppp=1,3-bis(diphenylphosphino)propane) and NiCl<sub>2</sub>dppb (dppb=1,4-bis(diphenylphosphino)butane) (Figure 2.6).

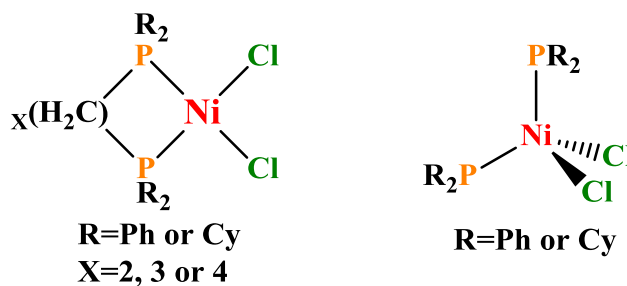


**Figure 2.6** Monometallic Ni/phosphine complexes tested for possible alkene hydration catalysis. For dppe, R=Ph and X=2, for dcpe R=Cy and X=2, for dppp R=Ph and X=3, for dppb R=Ph and X=4.

In most cases the complexes themselves were independently synthesized via literature methods.<sup>10-14</sup> However, in some cases NiCl<sub>2</sub>·6H<sub>2</sub>O was added to the water/organic solvent solution followed by the ligand (1 equivalent for the chelating phosphines and 2 equivalents for the monophosphines) to form the Ni complexes *in situ*. Again many different reaction conditions were attempted including the addition of AgBF<sub>4</sub>, different organic solvents (acetone

and THF), varying amounts of water (15% or 30%), acids and bases (HCl and KOH) and oxidizing agents (I<sub>2</sub> and excess Ag<sup>+</sup>). None of these reactions showed any alcohol products and there was no reaction between any of the complexes and the substrate.

### 2.3 Attempted Hydration Catalysis Utilizing Other Metal/Phosphine Complexes

With all of the Ni/phosphine complexes tested showing no signs of any alkene hydration catalysis, different monometallic transition metal/phosphine complexes were then tested to see if any reactivity would occur. The metals tested include Rh(+1), Rh(+3), Pd(+2), Pt(+2), Co(+2), Cu(+2) and Fe(+2). In some instances metal complexes themselves were added to the reaction mixture as possible catalysts. The complexes tested include *trans*-PdCl<sub>2</sub>(PPh<sub>3</sub>)<sub>2</sub>, *cis*-PtCl<sub>2</sub>(PEt<sub>3</sub>)<sub>2</sub> and RhCl(PPh<sub>3</sub>)<sub>3</sub> (Figure 2.7).

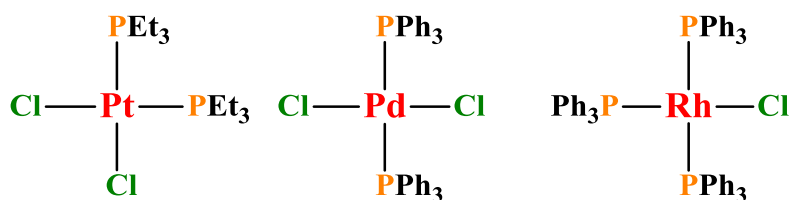


**Figure 2.7** Monometallic transition metal/phosphine complexes tested for alkene hydration.

For other experiments a metal precursor/salt was added followed by 1 to 3 equivalents of a phosphine ligand (dppe, PCy<sub>3</sub> and PPh<sub>3</sub>). The precursor/salts used were Rh(acac)(CO)<sub>2</sub>, RhCl<sub>3</sub>, CoCl<sub>2</sub>, CuSO<sub>4</sub> and FeCl<sub>2</sub>. The reactions were conducted in a similar fashion to the Ni studies. The metal complex or metal/ligand was dissolved in a water/organic solvent mixture and 100 equivalents of 1-hexene were added and the solutions were allowed to stir overnight. The majority were heated to 90°C. Most were conducted under an N<sub>2</sub> atmosphere. The organic solvents utilized were acetone, acetonitrile, THF and methanol along with 30% water (by volume). The experiments utilizing Co and Cu as the metal did not show any signs of reactivity. The experiments with Fe showed a small amount of isomerization to internal alkenes but no



other products were detected via GC/MS. Experiments with  $\text{PtCl}_2(\text{PEt}_3)_2$  also showed some isomerization but no other reactivity was detected.

When  $\text{PdCl}_2(\text{PPh}_3)_2$  was utilized as a possible catalyst, some reactivity was observed. The solubility of this complex was very poor in the water/organic solvent systems. Two experiments were conducted in which the water was decreased to 5% and 5 mL of dichloromethane were added with 14 mL of acetone to dissolve the complex. The complex still did not completely dissolve. Therefore, a homogeneous solution was never observed for these experiments. Also, during every one of the experiments, some decomposition of the starting complex occurred and led to the formation of Pd metal as small black particles suspended in the solution. Again, even with the decomposition, the starting yellow complex did not completely dissolve even after heating overnight.

There were two different types of reactivity that was observed with this complex. The first and most common was the isomerization of 1-hexene to 2- and 3-hexenes. This was observed for every reaction with the Pd complex. The isomerization was most likely caused by the insertion of 1-hexene into a Pd-H that formed in solution followed by  $\beta$ -hydride elimination from the newly formed alkyl ligand which would reform the Pd-H and release an internal alkene (Figure 2.8). However, there are other possible mechanisms that could lead to the formation of internal alkenes including an allylic mechanism. Also, the Pd metal formed from the decomposition of the starting complex could be responsible for the isomerization.

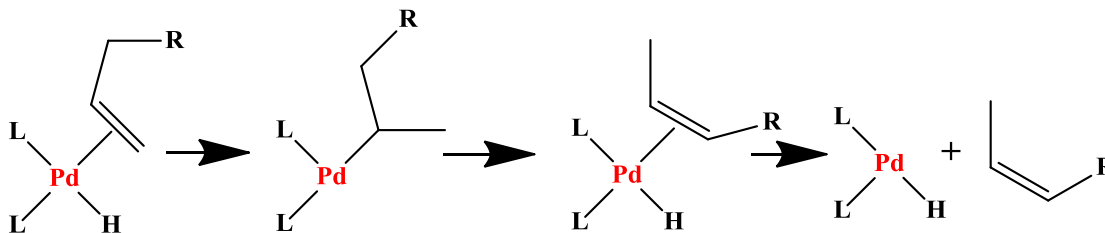


**Figure 2.8** The mechanism for the formation of internal alkenes via a metal hydride is depicted. Pd is shown as the metal but the mechanism is the same for all other transition metals.

The other mode of reactivity that was observed was the formation of a small amount of 2-hexanone. This product comes about from the Wacker oxidation process discussed in Chapter 1. The amount of 2-hexanone observed for these reactions was quite small. Even when  $\text{CuSO}_4$  was added, there was not a significant increase in the amount of product observed. Also, running the reaction in air did not increase the amount of 2-hexanone in a significant way.

The experiments with both  $\text{Rh}(+1)$  and  $\text{Rh}(+3)$  showed some reactivity. The major reaction was again isomerization of 1-hexene. In several instances there was complete isomerization and only internal alkenes were observed via GC/MS. The addition of a large amount of  $\text{KOH}$  (100 equivalents relative to the metal) completely inhibited the isomerization and no reaction occurred. The internal alkenes are most likely produced via the same mechanism as with  $\text{Pd}$ . Again, some decomposition was observed with these complexes and the possibility that the  $\text{Rh}$  metal caused the isomerization cannot be ruled out. The other product that was observed was also 2-hexanone. However, this product does not arise via a Wacker type mechanism.

2-Hexanone was formed when the reaction was conducted in air, unlike the reactions with the  $\text{Pd}$  complex, which gave 2-hexanone even under an atmosphere of  $\text{N}_2$ . As mentioned in Chapter 1,  $\text{Rh}$  complexes are known to oxidize alkenes to produce a methyl ketone. The oxidation of the alkene can be coupled with the oxidation of a phosphine to a phosphine oxide. It has also been shown that water can severely inhibit this reaction. Both 2-hexanone and triphenylphosphine oxide were identified via GC/MS. The amount of 2-hexanone was again quite small. However, the reason for this is that the amount of water (30%) was inhibiting the oxidation process.

All of these reactions with different metal/phosphine complexes showed no signs of alcohol production. They either showed no reaction, like **Ni<sub>2</sub>1M** and the monometallic Ni/phosphine complexes, alkene isomerization, like **Ni<sub>2</sub>1R**, or they showed some expected reactivity (Wacker oxidation with Pd and oxidation with Rh) but in very small amounts.

#### **2.4 The White Solid “Product” – How to Waste a Year in Graduate School and Get Your Advisor Excited (at least initially).**

It was mentioned in Section 2.2 that while preparing a few GC samples from the reactions with **Ni<sub>2</sub>1M** a white solid was observed that precipitated out of solution upon the addition of acetone. Initially it was believed that this was either some AgCl that had remained in solution or some phosphine oxide that formed during the reaction. Neither of these explanations seemed satisfactory. It should be noted that these initial reactions that showed this solid were conducted in a Schlenk flask that was connected to a condenser.

After many reactions which failed to give any product, a lot of reaction conditions were changed in an attempt to get some reactivity. One of the changes that was attempted was slowly adding the water via cannula to the solution as it was heated. The idea was that the water concentration was too high at the beginning of the reaction and was inhibiting the alkene from binding with the metal. Because the water was to be added dropwise via cannula, different glassware had to be utilized. Instead of a Schlenk flask, a 3-neck flask was chosen as the reaction vessel. The vessel was charged with the Ni complex, organic solvent and substrate. The vessel was then connected to a condenser attached to a Schlenk line. The other two necks of the flask were sealed with Suba-Seal<sup>®</sup> septa.

The vessel was then heated to 90°C with rapid stirring and the water was added dropwise. Once all the water was added, the reaction mixture was heated and stirred overnight. The next day, a sample was collected and prepared for GC/MS analysis. Upon the addition of acetone, a

white solid precipitated out of solution. It was not a large quantity but it did appear to be much more than observed previously. Several more experiments were conducted and eventually it was observed that whatever this solid was remained soluble in the 1-hexene layer during the reaction. When the GC sample was prepared, the addition of acetone led to the two layers becoming miscible and precipitated out this solid. Several reactions were conducted and all showed the white solid product.

Blank experiments were conducted in which the Ni complex was not added and everything else remained the same. They were conducted in Schlenk flasks and in the 3-neck flasks. Upon workup, the white solid was observed in the blank reactions using the 3-neck flasks but not in the reactions with Schlenk flasks. New 3-neck flasks were then purchased from Chemglass and more blank experiments were conducted using these new flasks. In all cases (8 total in the two new flasks and two in a Schlenk flask) with the new 3-neck flasks, no white solid was observed! This led us to assume that some reaction was going on between the Ni complex and the 1-hexene and the reason we saw this “product” from the blanks conducted in the old flasks was because of tiny amounts of metal deposits on the glass.

After these blank experiments, it appeared that a real reaction was occurring. Experiments were then conducted to identify the “product”, determine how it was being formed and optimize the reaction conditions. The best means of isolating the white solid was extracting the reaction mixture with hexane, evaporating the hexane solution to dryness, redissolving the yellow/white residue in a minimum quantity of hot ethyl acetate and cooling this concentrated solution in the freezer. A fluffy, white solid precipitated out of solution and can be collected via filtration. The solid was found to be soluble in chloroform and allowed for analysis by NMR. The  $^1\text{H}$  and  $^{13}\text{C}\{^1\text{H}\}$  NMR spectra from one sample of the solid is shown in Figure 2.9 (top red

spectra). The spectra are quite simple and are what is expected of a linear alkane of some chain length. The NMR spectra of a linear alkane ( $C_{36}H_{74}$ ) are shown in Figure 2.9 (bottom black spectra) for comparison. These two sets of spectra clearly show that the white solid is composed mainly of linear alkanes of some chain length. FT-IR and GPC (gel permeation chromatography) analysis was conducted on several different samples. The IR results again showed the white solid to match extremely well with a linear alkane. The GPC data showed the white solid to be a mixture of alkanes with the molecular weight distributions being between 700 and 1000 g/mol for the main fraction.

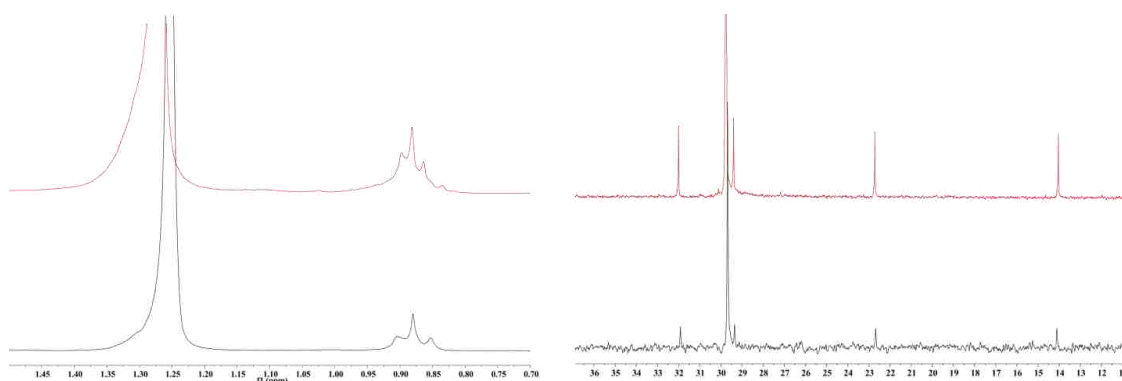


**Figure 2.9**  $^1H$  and  $^{13}C$  NMR spectra of the white solid (top red spectra) and of a linear alkane ( $C_{36}H_{74}$ ) (bottom black spectra).

Subsequent experiments clearly showed that water was required in order to obtain the alkanes. Without water, no reaction occurred and no white solid was observed in any of the reaction mixtures without the presence of water. Other experiments with other metals (Rh, Co, Pd, Pt) also did not show any alkanes. These experiments were conducted in exactly the same manner as the ones with the bimetallic Ni complex in the exact same 3-neck flasks with Suba-Seal<sup>®</sup> septa. All of this evidence pointed to the fact that we had discovered a new way of oligomerizing alkenes and that somehow water was a key component of the reaction.

We began investigating other alkenes to test the scope of the reaction and to try and optimize the reaction conditions. Other alkenes tested included 1-octene, styrene and allyl

alcohol. It was during these tests that major questions began to arise. When styrene and allyl alcohol were utilized as substrate, white solid was again observed, collected and analyzed. NMR analysis revealed the white solid had the exact same structure as the solid collected from 1-hexene or 1-octene. This should not occur unless the hydroxyl group from allyl alcohol was somehow removed along with the phenyl group from styrene. These scenarios seem chemically impossible under these reaction conditions. Also, for every reaction in which the white solid was collected, only a very small portion of solid was obtained. Typically it was less than 100 mg. As more reactions were conducted it became increasingly clear that this newly discovered reaction was not what we thought it was.

After careful experimentation by me and Katerina Kalachnikova, we could come to only one conclusion. The white solid “product” we thought we were making was actually being extracted from the Suba-Seal<sup>®</sup> septa! These septa are composed of natural rubber and are a registered trademark of Sigma-Aldrich. These septa contain a lot of extractable material and are not rated for very high temperatures (maximum of 85°C). This was the only logic conclusion after looking at all of the evidence and experiments conducted. However, several things still do not make sense. Why were no alkanes extracted when water was not present? Why did reactions conducted with other metal/phosphine complexes not show the alkanes? Why did a few reactions conducted in Schlenk flasks without septa show the alkanes? Why did multiple blank experiments using 3-neck flasks and septa not show any alkanes? These questions will, unfortunately, never be answered. Prof. Stanley has proposed that different batches or ages of the Suba-Seal<sup>®</sup> Septa could lead to different (or no) extractable alkane product, thus accounting for the variable results with blank samples.

## 2.5 Catalytic Screening for Possible Alkene Hydration Catalysis

After wasting more than a year tracking down the nature of the white solid alkanes and with the continued failed attempts at observing any alkene hydration catalysis with Ni/phosphine (mono- and bimetallic) complexes and other monometallic metal/phosphine complexes, a series of catalytic screening experiments were conducted utilizing the tetratertiary phosphine ligands **1R** and **1M** and several different transition metal sources. The main reason for doing this was to test several different bimetallic metal complexes for possible catalysis without going through the somewhat difficult process of synthesizing the complexes and separating and purifying the individual diastereomers. This would allow us to identify possible catalytically active complexes and concentrate on synthesizing those complexes. The other reason for these experiments was to test mixed metal systems as possible catalysts. Synthesizing heterobimetallic complexes can be a very challenging and time-consuming endeavor and doing these screening experiments would allow us to identify combinations of metals that show interesting reactivity and focus on synthesizing these heterobimetallic complexes.

Several different late transition metals were selected for these experiments. The metals include: Ir(+1), Ir(+3), Rh(+1), Rh(+3), Ni(0), Ni(+2), Pd(+2), Pt(+2), Ru(+2), Co(+2), Cu(+2) and Fe(+2). The metals (either salts or metal complexes) were added to a pressure vessel inside the glovebox followed by the organic solvent (THF, acetone, acetonitrile, 2-propanol, 2-methyl-2-propanol). 200  $\mu\text{L}$  of a 1 M diethyl ether solution of 75% **1R**/25% **1M** (based on  $^{31}\text{P}$ ) was then added via syringe. The vessel was sealed and the resulting mixture was allowed to stir and heat to form a homogeneous solution, then cooled to room temperature and brought back into the glovebox. Once inside, 100 equivalents of alkene (1-hexene or styrene) was added to the flask followed by the appropriate amount of water bringing the total volume of the solution to 20 mL.

These solutions had a tetrphosphine concentration of 10 mM and a metal concentration of 20 mM. The flask was then sealed, removed from the glovebox and heated to 90°C with rapid stirring. The reactions were allowed to proceed in many cases overnight unless complete decomposition was observed. They were analyzed via GC/MS to identify any products and a few were analyzed via  $^1\text{H}$  and  $^{31}\text{P}$  NMR.

The analysis from many of the reactions allowed us to identify several different products. One product that occurred with several different metal combinations was ethylbenzene when styrene was the alkene. It comes about from the hydrogenation of styrene. It was a common product for most of the reactions when Ir(+1) was part of the metal component. It also appeared when Ni(0), Pd(+2), Rh(+1) and Ru(+2) were used as well. The identification of this product points to the idea that metal-hydride bonds were formed and are responsible for the hydrogenation. However, it is interesting to note that when 1-hexene was the alkene no hexane could be identified. The amount of ethylbenzene was never large and no attempt was made to quantify how much was being produced.

Another common reactivity that occurred was dimerization of acetone. Several reactions were conducted utilizing acetone as the organic solvent. In the majority of these reactions acetone dimerization occurred to produce 4-hydroxy-4-methyl-2-pentanone, 4-methyl-3-penten-2-one and methyl isobutyl ketone (Figure 2.10). In one reaction with Cu(+2) and Rh(+1) as the mixed metal system large quantities of these products were observed. After this observation, the use of acetone as a solvent for any further catalytic reactions was abandoned. Acetone had been utilized as a solvent for many of the previous reactions with Ni/phosphine complexes as possible catalysts. However, these products were never observed in large quantities unless a strong acid or base was added.



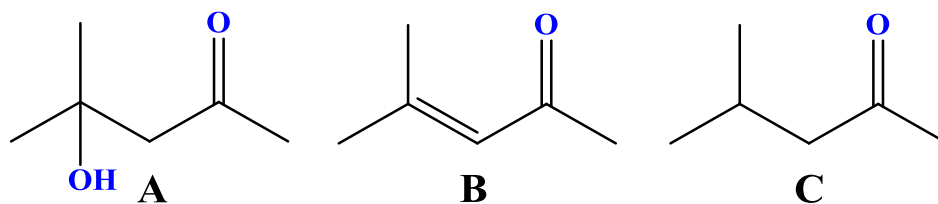


**Figure 2.10** The products formed from the dimerization of acetone and subsequent reactions. **A** – 4-hydroxy-4-methyl-2-pentanone is formed from the dimerization, **B** – 4-methyl-3-penten-2-one is formed from the dehydration of A, **C** – methyl isobutyl ketone is formed from the hydrogenation of B.

When Ir(+3) was utilized, either by itself or in combination with another metal, dimerization of the alkene occurred in the majority of the reactions. This led to a very complex mixture of alkenes identified via GC/MS. When 1-hexene was the substrate, a mixture of methyl-undecenes and dodecenes were obtained. The GC was able to identify upwards of 10-15 distinct peaks for some of these reactions. Differences in the position of the double bond and the methyl group led to the formation of this complex mixture of products. When styrene was the substrate, another complex mixture of products occurred containing diphenyl-substituted butenes. The position of the phenyl rings and double bond varied giving rise to this complex mixture. This reactivity was not unprecedented for Ir(+3) compounds. Several examples were found in the literature.<sup>15-16</sup> Since this reactivity had been reported previously and because the dimerization was not selective, no attempts were made to quantify the amounts or pursue this reactivity.

Another common product observed for several reactions involved the formation of Wacker oxidation products, 2-hexanone when 1-hexene was the substrate and acetophenone and phenylacetaldehyde with styrene. The majority of these products were produced when Pd(+2) was utilized. These were expected products and had been observed previously when other Pd(+2) complexes were tested. As mentioned previously, this oxidation usually affords the methyl ketone selectively. For 1-hexene, 2-hexanone was the only oxidation product observed.

However, for styrene a mixture of acetophenone and phenylacetaldehyde was observed and in some cases the aldehyde was produced in larger amounts (based on GC analysis). The difference between the two products was never extremely large and it did not occur every time. Some 2-hexanone and acetophenone was also produced with other metals and metal combination.

Pt(+2) and Ir(+3), Pt(+2) and Rh(+3) and Ir(+1) by themselves all showed a small amount of methyl ketone. These reactions were conducted in an inert atmosphere of N<sub>2</sub>. Because there was no O<sub>2</sub> present, it seems that these products do not come about from the O<sub>2</sub> mediated oxidation of alkenes via Rh complexes discussed in Chapter 1. They could come about from a Wacker type mechanism. Pd(+2) is not the only metal to catalyze the Wacker oxidation. Other metals, including Pt(+2), Rh and Ir, are known to perform this catalysis. However, they are not as efficient as Pd(+2).

The final and most interesting product that was observed during these catalytic screening experiments was the formation of 1-phenylethanol from styrene. This was the first observed alcohol product for any of the catalytic reactions conducted. Unfortunately, the product was produced in small quantities for every reaction that produced it and it is a secondary alcohol. The metal combinations that produced the secondary alcohol include: Rh/Fe, Rh/Fe/Cu, Ir/Fe, Ir/Fe/Cu, Pd/Ru/Cu, Ir/Cu, Pt/Rh, Pt/Cu, Ir, Ir/Pd and Pd/Ru. In the cases where 3 metals are listed, the third metal (Cu) was added with the substrate and water after the first two metals were allowed to heat and stir in solution with the tetraphosphine ligand. The Cu was added as a redox active metal to help oxidize reduced metal species. When these same metal combinations were combined with 1-hexene, no secondary alcohol was produced.

Inspection of this list reveals one thing; no one metal is common in any of the reactions. Also, different solvents (THF, methanol, acetonitrile, 2-propanol and 2-methyl-2-propanol) were

used for the different reactions. There are only two things that are common throughout all of these reactions. The first is obviously that each reaction contained the tetrakisphosphine ligand and the second is that every metal species contained at least one chloride ligand. In fact, every metal precursor used for all of the alkene hydration studies (starting with the bimetallic Ni complexes) contained at least one chloride ligand except when  $\text{Ni}(\text{COD})_2$  (COD=1,5-cyclooctadiene) and  $\text{Ni}(\text{BF}_4)_2$  were used. Reactions conducted with just the phosphine ligands by themselves gave no products.

The formation of the secondary alcohol could come about from simple acid-catalyzed hydration. It is well-known and well understood that dissolving transition metal salts in an aqueous environment leads to the formation of an acidic solution. Water molecules bind to a positively-charged metal ion in solution via its lone-pair electrons. Because of the positive charge on the metal, electron density is pulled away from the oxygen atom and can lead to the dissociation of  $\text{H}^+$  and formation of  $\text{M-OH}$ . The acidity depends on the charge on the metal cation as well as the size of the cation and the properties of the other ligands bound to the metal (if there are any other ligands present). Because all of the solutions would range from slightly to moderately acidic, the secondary alcohol could be formed via simple acid-catalyzed hydration. The  $\text{H}^+$  ions present in solution would add to styrene to form a benzylic cation, a resonance-stabilized cation, which would then react with water or  $\text{OH}^-$  to form the secondary alcohol.

One problem with this hypothesis is since all of these solutions are acidic, why is secondary alcohol formation not observed for every reaction with styrene. When **Ni<sub>2</sub>1M**, **Ni<sub>2</sub>1R**, monometallic Ni/phosphine complexes (Section 2.2) and other metal/phosphine complexes (Section 2.3) were tested for alkene hydration, they all were run with styrene as the substrate. Not one of these reactions showed the formation of 1-phenylethanol. Also, many of the

screening experiments were run with styrene as the substrate and the only times 1-phenylethanol were produced was for the metal combinations listed. These observations seem to point to the fact that the secondary alcohol could have been produced via other mechanisms. One possible mechanism (Figure 2.11) would involve styrene binding to the metal followed by either migratory insertion of a hydroxyl group to styrene or nucleophilic attack by water. Protonation of the hydroxyalkyl group would give rise to the secondary alcohol. Steric effects from the tetraphosphine ligand could favor the formation of the secondary alcohol vs. the primary alcohol. This is only one possible mechanism and many others could be devised for the formation of this product including ones involving bimetallic complexes.

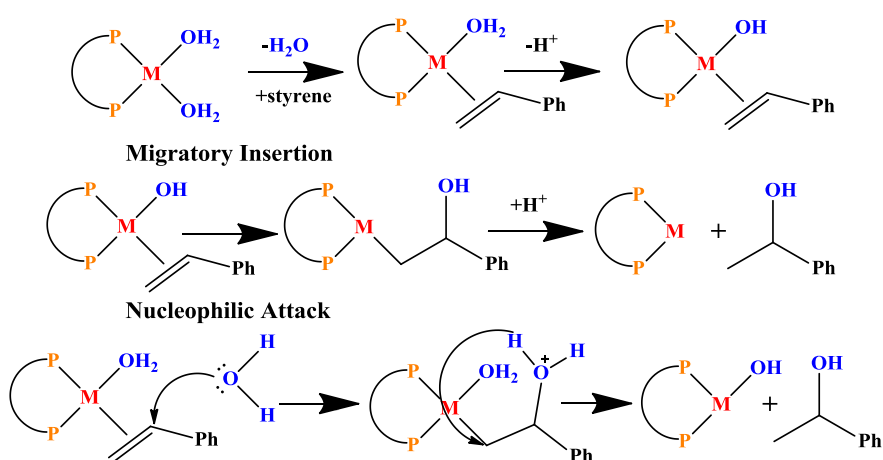


**Figure 2.11** A reaction scheme showing two possible mechanisms for the formation of 1-phenylethanol from styrene.

## 2.6 Conclusions

A multitude of different transition metal/phosphine complexes were tested for possible alkene hydration catalysis. They included **Ni<sub>2</sub>1M** and **Ni<sub>2</sub>1R**, monometallic Ni/phosphine complexes, monometallic metal/phosphine complexes (Rh, Pd, Pt, Co, Cu and Fe). All of these reactions failed to produce any alcohol products. In fact, very little reactivity was observed besides alkene isomerization and alkene oxidation. Catalytic screening experiments were also conducted utilizing a mixture of **1R** and **1M** in combination with several different transition

metals. During these screening experiments, several different metals and metal combination showed some interesting reactivity. The reactivity observed included dimerization of 1-hexene and styrene, hydrogenation of styrene and oxidation of both 1-hexene and styrene.

It was during the course of these experiments that a secondary alcohol product was produced. Future experiments should focus on determining exactly what was causing the formation of the secondary alcohol – acid catalyzed hydration or some type of metal mediated reaction. If it can be determined that the metals themselves or metal complexes formed during the course of the reaction are responsible for this reactivity, then great efforts should go into determining what bimetallic complexes are responsible and attempt to synthesize these complexes and test them for alkene hydration.

Also, there are many more metal combinations that could be utilized for further screening experiments. From all of the experiments conducted for alkene hydration, the results show that Ni/phosphine complexes (mono- or bimetallic) are not active for this type of chemistry. The mixed metal systems gave the most reactivity toward the substrate and much more effort should go into determining what combinations show the most reactivity and attempts to synthesize and purify these heterobimetallic systems should be made.

During the course of these hydration studies, a white solid was observed and isolated. It was characterized via  $^1\text{H}$  and  $^{13}\text{C}$  NMR, FT-IR and GPC and was shown to be a mixture of linear alkanes ranging in molecular weight from 700-1000 g/mol. We had very strong evidence that a new catalytic oligomerization reaction had been discovered. As we continued to investigate these reactions, a lot of conflicting results were obtained and led to the conclusion that these linear alkanes were being extracted from the Suba-Seal<sup>®</sup> septa used to seal the reaction flasks. This conclusion did not coincide with all of the data collected but it explained most of the results.

These experiments serve as a valuable lesson for any chemist to know the exact physical and chemical properties of everything that can possibly come into contact with your reaction flasks. Also, for any chemist working with catalytic reactions, the importance of blank experiments cannot be overlooked. Multiple blank experiments were conducted and in some cases showed the alkane and in some cases did not. I believe that if more blank experiments would have been conducted by me initially, the nature of the alkanes would have been discovered much sooner and more than a year would not have been wasted on this “product”. But, as the saying goes, hindsight is 20/20. However, the experiments were not completely wasted. Almost every experiment conducted trying to optimize the formation of the white solid was analyzed for alkene hydration reactivity before workup began to isolate the alkanes. Also, NMR experiments conducted during this time led us to discover some interesting oxidation chemistry which will be discussed in the next chapter.

## 2.7 References

1. Laneman, S. A.; Fronczek, F. R.; Stanley, G. G. *J. Am Chem. Soc.* 1988, 110, 5585-5586.
2. Laneman, S. A.; Fronczek, F. R.; Stanley, G. G. *Inorg. Chem.* 1989, 28, 1872-1878.
3. Broussard, M. E.; Juma, B.; Train, S. G., Peng, W.-J.; Laneman, S. A.; Stanley, G. G. *Science* 1993, 260, 1784-1788.
4. Matthews, R. C.; Howell, D. K.; Peng, W.-J.; Train, S. G.; Treleaven, W. D.; Stanley, G. *G. Angew. Chem., Int. Ed.* 1996, 35, 2253-2256.
5. Aubry, D. A.; Bridges, N. N.; Ezell, K.; Stanley, G. G. *J. Am Chem. Soc.* 2003, 125, 11180-11181.
6. Matthews, R. C. *Ph. D. Dissertation, Louisiana State University, 1999.*
7. Gueorguieva, P. G. *Ph. D. Dissertation, Louisiana State University, 2004.*
8. Polakova, D. *Ph. D. Dissertation, Louisiana State University, 2012.*
9. Monteil, A. *Ph. D. Dissertation, Louisiana State University, 2006.*
10. Van Hecke, G. R.; Horrocks, Jr., W. D. *Inorg. Chem.* 1966, 5, 1968-1974.

11. Venanzi, L. M. *J. Chem. Soc.* **1958**, 719-724.
12. Browning, M. C.; Davies, R. F. B.; Morgan, D. J.; Sutton, L. E.; Venanzi, L. M. *J. Chem. Soc.* **1961**, 4816-4823.
13. Booth, G.; Chatt, J. *J. Chem. Soc.* **1965**, 3238-3241.
14. Angulo, I. M.; Bouwman, E.; van Gorkum, R.; Lok, S. M.; Lutz, M.; Spek, A. L. *J. Mol. Catal. A: Chem.* **2003**, 202, 97-106.
15. Osborn, J. A.; Schrock, R. R. *J. Am. Chem. Soc.* **1971**, 93, 3089-3091.
16. Pillai, S. M.; Ravindranathan, M.; Sivaram. S. *Chem. Rev.* **1986**, 86, 353-399.

## CHAPTER 3: INVESTIGATION INTO ALKENE OXIDATION CATALYSIS UTILIZING Ni/PHOSPHINE COMPLEXES

### 3.1 Motivation

During the course of the white solid oligomerization/alkene hydration experiments an NMR scale reaction was conducted to try and characterize the oligomerization reaction via  $^1\text{H}$  and  $^{31}\text{P}$  NMR. For this experiment a vial was charged with 14 mg of  $\text{Ni}_2\text{IM}$ , 1.7 mL acetone- $d_6$  and 0.3 mL  $\text{D}_2\text{O}$  in air. The mixture was heated and stirred until the complex completely dissolved. The vial was then cooled and 100 equivalents of 1-hexene were added via syringe. Part of this solution was transferred to a high-pressure NMR tube. The tube was sealed and placed into an oil bath and heated to  $90^\circ\text{C}$  overnight. The remaining solution was left inside the vial overnight. During the course of the night, both solutions lightened in color with the solution remaining in the vial being a lighter shade of yellow.

$^1\text{H}$  NMR analysis of both solutions revealed a peak at 9.72 ppm (Figure 3.1). This region of the spectrum is typically where aldehyde protons resonate. The close-ups of the two aldehyde peaks are shown for each spectrum. From the top spectrum, you can clearly see splitting in this peak that resembles a triplet. The bottom close-up is not as well resolved as the top spectrum but there are two shoulders on either side of this broadened peak suggesting this is also a triplet. A triplet pattern is what is expected for an aliphatic aldehyde like hexanal (or pentanal) caused by equivalent coupling from the two protons attached to the carbon next to the carbonyl. We initially proposed that this aldehyde, which we believed was hexanal, was produced during the alkene oligomerization reaction. However, GC analysis of the remaining solution inside the vial and on other experiments conducted in a similar manner revealed the aldehyde to be pentanal and not hexanal. Once it was shown that the oligomerization reaction was not occurring, we set out to determine how this aldehyde was being formed.



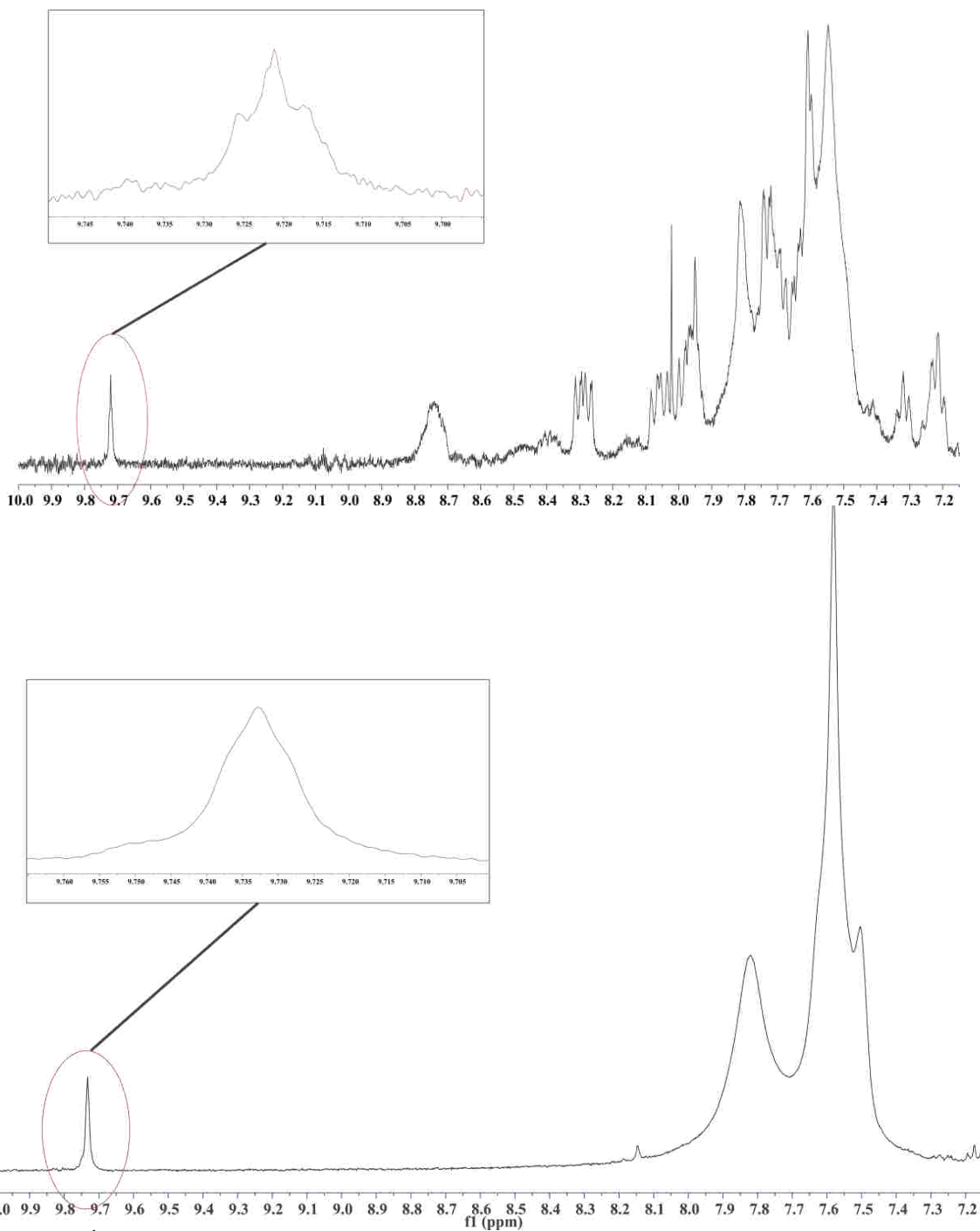


**Figure 3.1**  $^1\text{H}$  NMR spectra showing the aldehyde peak observed during the reaction. The top spectrum was recorded after 2 hours. The bottom spectrum was recorded after 3 days. The inserts are a close-up of the aldehyde peak observed for both spectra.

Another experiment was conducted to determine what factor caused the formation of the aldehyde. The previous NMR experiment was both exposed to air and heated. Therefore, the previous experimental conditions (14 mg  $\text{Ni}_2\text{IM}$ , 1.7 mL acetone- $d_6$ , 0.3 mL  $\text{D}_2\text{O}$ , 100

equivalents 1-hexene) were repeated with the only difference being that everything was loaded into the vial under an inert atmosphere. Once the complex was dissolved, three different samples were placed into NMR tubes under an inert atmosphere. The first sample was placed inside a high-pressure NMR tube and heated to 90°C. The second tube was kept inside the glovebox at room temperature. The third tube was removed from the glovebox and was exposed to air and allowed to sit at room temperature. The NMR tubes were all monitored periodically via  $^1\text{H}$  and  $^{31}\text{P}$  NMR.

A series of  $^1\text{H}$  NMR spectra are shown in Figure 3.2 that summarizes the results of this experiment. The black spectrum was the initial  $^1\text{H}$  NMR spectrum taken before any heat or air was introduced to any of the samples. The red spectrum was recorded after heating the high pressure NMR tube for 3 days and 20 hours in an oil bath at 90°C. The green spectrum was recorded after the second NMR tube sat inside the glovebox for 3 days and 22 hours. The blue spectrum was recorded after the third NMR tube was exposed to air and sat for almost 4 days at room temperature. The only spectrum that shows the aldehyde peak at 9.72 ppm was recorded from the sample that was exposed to air. This experiment clearly demonstrates that the introduction of air leads to the formation of pentanal from 1-hexene. Based on these results, when air is added to the atmosphere, the oxidative cleavage of 1-hexene occurs and leads to the formation of pentanal. Based on stoichiometry, another aldehyde, formaldehyde, should also be formed in equal amounts. We were unable to identify formaldehyde via NMR or GC/MS analysis.

### **3.2 Alkene Oxidative Cleavage via Bimetallic Ni/Phosphine Complexes**

Following these initial experiments, our first goal was to establish that the Ni complex was playing a role in the reaction. Several different blank experiments were conducted, both on

an NMR scale and on the bench-top. For the NMR experiments a 15% D<sub>2</sub>O/acetone-*d*<sub>6</sub> solvent system was utilized. NMR tubes were charged with this solvent system in air and the alkene was then added. These tubes were allowed to sit at room temperature for several weeks and were periodically opened and flushed with air. <sup>1</sup>H NMR spectra were recorded over the course of the experiment and in no case was an aldehyde peak observed. The same experiments were conducted on a larger scale on the bench-top. For some of these blank reactions, the reaction mixture was purged with air and then sealed and allowed to stir overnight. GC/MS analysis revealed no products. Other experiments were also conducted in which a balloon was attached to a Schlenk flask containing the reaction mixture. The balloon was then filled with pure O<sub>2</sub> gas and the solution was allowed to stir overnight. No products were identified via GC/MS and NMR analysis. All of these blank experiments were repeated several times and none of them revealed any products via NMR and GC/MS.

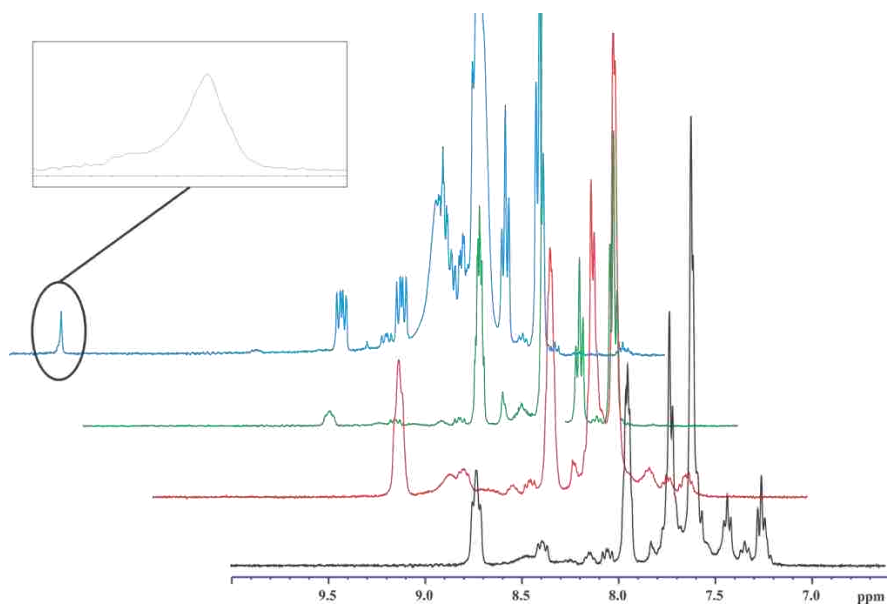


**Figure 3.2** A series of <sup>1</sup>H NMR spectra is depicted. The black spectrum is the initial spectrum. The red spectrum was recorded after heating a high pressure tube for 3 days and 20 hours. The green spectrum was recorded after a sample sat under N<sub>2</sub> for 3 days and 22 hours. The blue spectrum was recorded after a sample was exposed to air and sat for almost 4 days. The insert is a close-up of the peak at 9.72 ppm on the blue spectrum. The spectra are all the same ppm scale but offset in order to better show the spectra.

Once we established the importance of the Ni complex for the formation of the aldehyde, we then set out to try and understand how the aldehyde was being formed. The first experiments investigated whether water was required for the reaction to occur. For these experiments, the complex was dissolved in a pure solvent (DCM, acetone and acetonitrile) and the substrate was then added. For NMR scale reactions, the NMR tubes were prepared in air and then purged with air and followed for several days. For the bench-top reactions, the reaction mixtures were either purged with air and sealed and stirred or placed under a balloon atmosphere of O<sub>2</sub> and stirred. In all of these experiments, no products were observed via NMR and GC/MS. These experiments established that the presence of water is required for the reaction to occur when acetone or acetonitrile are utilized as organic solvents.

We then set out to determine how much water was required for the reaction to occur in these two solvents. A series of experiments were conducted on the bench-top in which the amount of added water was varied from 0% to 15%. We found that when no water is added, no aldehyde is formed. We also found that the addition of small amounts of water (less than 5%) does not lead to the formation of the aldehyde. 5% or more of water is required for the formation of the aldehyde to occur in acetone or acetonitrile. Subsequent NMR experiments (Chapter 4) have established that the addition of 5% or more of water to these solvents causes the formation of new species identified via <sup>1</sup>H and <sup>31</sup>P NMR spectroscopy. Over time the reaction with water leads to the formation of one species (Chapter 4). We theorized that it was one of these new complexes that form during the reaction with water that is responsible for the oxidative cleavage reaction.

To test the scope of this reaction, several different alkene substrates were tested. The alkenes tested include 1-hexene, 1-octene, styrene, *trans*-stilbene,  $\alpha$ -methylstyrene, *trans*- $\beta$ -

methylstyrene, cyclopentene, cyclohexene and *trans*-5-decene (Figure 3.3). All of the substrates gave rise to an aldehyde via the cleavage of the carbon-carbon double bond (Figure 3.3). The products were identified via both GC/MS and NMR analysis.

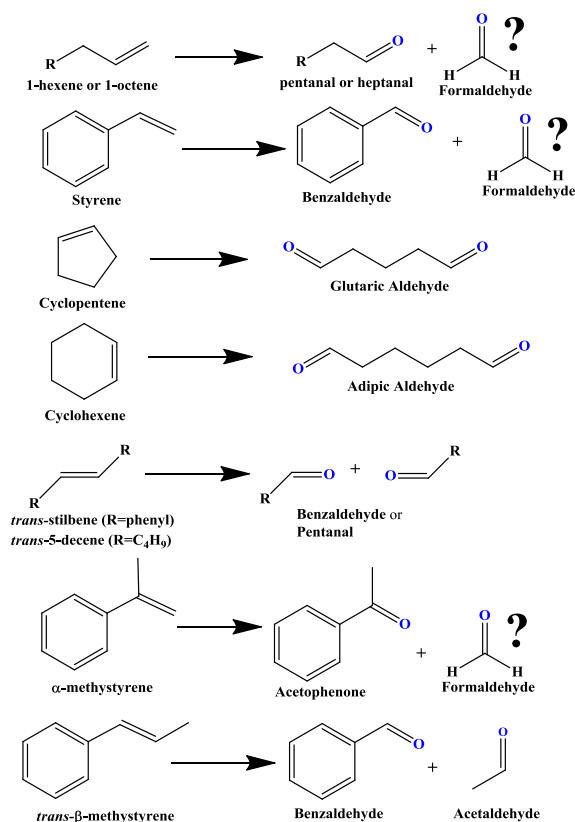


**Figure 3.3** List showing the alkenes tested and products formed during the oxidative cleavage reaction.

For all substrates tested, a very small amount of aldehyde was produced. The only product that was not identified was formaldehyde. Based on the stoichiometry of the reaction, one equivalent of formaldehyde has to be produced for every equivalent of aldehyde. When an unsymmetrical alkene, *trans*- $\beta$ -methylstyrene, was tested for the oxidative cleavage, NMR analysis revealed the <sup>1</sup>H spectrum depicted in Figure 3.4.

Two distinct aldehyde resonances can be identified. The first peak appears as a singlet at 9.98 ppm. This peak corresponds to the aldehyde proton of benzaldehyde, which was also identified via GC/MS. The other aldehyde signal is a quartet centered at 9.68 ppm. The splitting

comes from the coupling between the aldehyde proton and three equivalent protons. This is what is expected for acetaldehyde since the three protons of the methyl group would be equivalent and couple to the aldehyde proton giving rise to a quartet. Experiments conducting with this unsymmetrical alkene show that the oxidative cleavage reaction gives rise to two different aldehydes that have been identified and is convincing evidence for the formation of formaldehyde when terminal alkenes are subjected to the oxidative cleavage reaction.

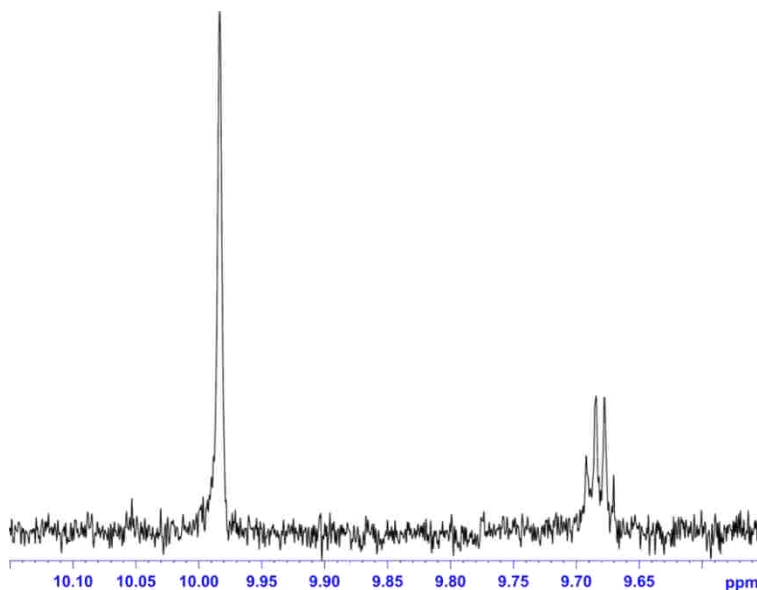


**Figure 3.4**  $^1\text{H}$  NMR spectrum showing the two aldehydes (benzaldehyde and acetaldehyde) during the oxidative cleavage reaction.

When the two cyclic alkenes were tested, reproducibility was a major problem. The first 2 or 3 times these substrates were tested, the dialdehyde products (adipic aldehyde and glutaric aldehyde) were identified via GC/MS. However, besides these first 2 to 3 experiments, the dialdehyde products were not identified via GC/MS when these cyclic alkenes were tested. Both alkenes were rerun several times and in all cases we were unable to reproduce the results of the first 2 or 3 experiments. We currently do not have any explanation for these results. Some allylic oxidation was observed with cyclohexene and produced alcohol and ketone products.

After these experiments were conducted, we then set out to try and optimize the reaction and produce a catalytic reaction. From the NMR and GC analyses the amount of aldehyde was always very small but it was the only identifiable product. This suggests that the reaction is very clean but for some reason it was not turning over and producing a catalytic reaction. The hope was that adjusting the reaction conditions would lead to a catalytic reaction that cleanly performed the oxidative cleavage reaction.

Three main reaction types were conducted for these experiments. The first involved purging the solution with air and then sealing the flask with a glass stopper and allowing it to stir overnight or longer at room temperature. The flasks were opened to air each day and a GC sample was collected. The flasks were then purged with air before being resealed and allowed to stir. These experiments showed a small increase in the aldehyde product from the first day to the second but after that there was no change in the amount of product.

The second involved running the reaction under a balloon atmosphere of pure O<sub>2</sub>. The balloon was filled with the gas from a gas regulator set to 30 psig. These reactions were typically allowed to stir overnight. After one night, the O<sub>2</sub> gas was released and samples were collected for analysis (GC and NMR samples). The third type involved higher pressure reactions. These were conducted either in a high pressure NMR tube or a stainless steel autoclave. The pressures for these reactions were between 50 and 100 psig. In many instances these reactions were also heated since they were pressurized in a closed system. When heating was employed the amount of aldehyde plateaued after 1 to 2 hours and there was no increase in the amount of product beyond 2 hours. In all three reaction setups the amount of aldehyde produced was almost identical. The major difference was the amount of time required to achieve the amount of product with the high pressure and high temperature reactions being the fastest

and the purged reactions being the slowest. Using these three different setups, a multitude of different reaction conditions were tested to try and produce a catalytic oxidative cleavage reaction.

The first variable changed was the organic solvent. Since it was already established that water was required for the oxidative cleavage reaction to occur, we set out to determine what, if any, effect the organic solvent has on the reaction. Three main solvents (acetone, acetonitrile, DMSO) were tested. Other solvents were also tested, including methanol, ethanol, THF and DMF. The results in acetone and acetonitrile were very similar to one another. When 1-hexene, 1-octene or styrene were utilized as substrates, the only product identified was the aldehyde produced from the cleavage of the carbon-carbon double bond (pentanal, heptanal and benzaldehyde). The amounts produced in these two solvents were the same and in very small amounts. Based on GC/MS analysis, the amount of aldehyde produced during the reaction was at the very most around 5 mM, which would not even amount to a stoichiometric reaction because the complex concentration was always 10 mM.

The only differences observed between these two solvents were the final color of many of the reactions and the  $^{31}\text{P}$  NMR spectra recorded after the reactions were stopped. With acetone as a solvent, the solution was always very light yellow in color. This color was observed for the purged solutions, the solutions stirred under balloon pressure and the solutions exposed to high pressures. The purged solutions took several days to reach this color but the other two types only required at the most one night to reach this color. NMR analysis of these solutions revealed the spectrum shown in Figure 3.5.A.

These broad resonances are the only peaks present. This spectrum was always observed at the end of the reaction when acetone was the organic solvent. With acetonitrile as the organic



solvent, subtle color differences were observed compared to the acetone reactions. For the purged solutions, the color remained orange/yellow or yellow/orange for several days and the majority of the reactions never achieved the light yellow color observed for the acetone reactions even after a week or longer. NMR analysis of these solutions did reveal the presence of the broad resonances but there are also sharp resonances present which overlap with the broad resonances (Figure 3.5.B). Under a balloon pressure, the solutions turned a lighter yellow/orange color compared to the purged solutions but they were not as light in color as the acetone reactions. NMR analysis showed sharp resonances overlapping with the broad resonances but the intensity of the sharp resonances decreased significantly compared to the purged reactions (Figure 3.5.C). Under elevated pressures, the broad resonances are the only resonances observed for both solvent systems.

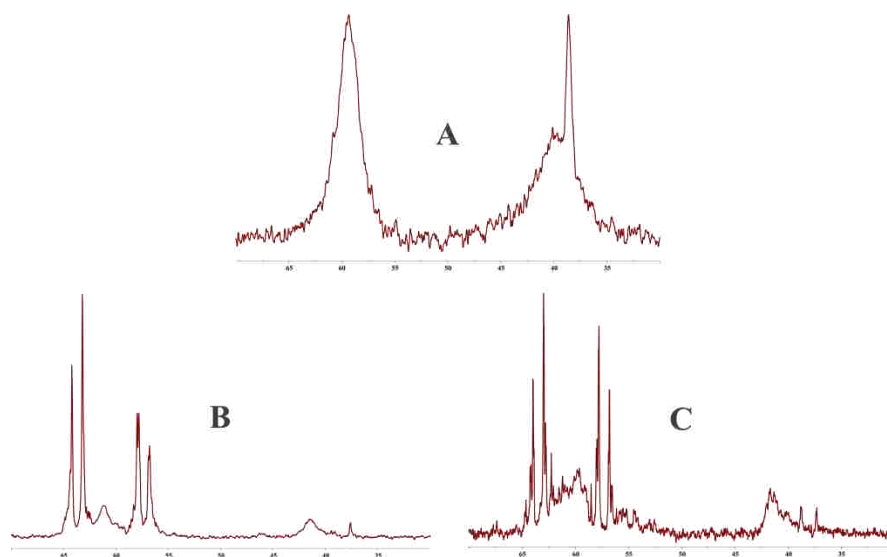


**Figure 3.5**  $^{31}\text{P}$  NMR spectra recorded after  $\text{Ni}_2\text{1M}$  was stirred under air/ $\text{O}_2$ . **A** – A balloon pressure solution with 15% water/acetone as the solvent after 3 days. **B** – A purged solution with 15% water/acetonitrile as the solvent after 3 days. **C** – A balloon pressure solution with 15% water/acetonitrile as the solvent after 1 night.

After observing these broad resonances, we set out to determine if the appearance of these resonances result from the oxidative cleavage reaction or if they come about simply from dissolving  $\text{Ni}_2\text{1M}$  in a water/organic solvent solution and exposed it to  $\text{O}_2$ . Balloon atmosphere

experiments were conducted in which **Ni<sub>2</sub>IM** was dissolved in 15% water/acetone or 15% water/acetonitrile and allowed to stir overnight for 1 or 2 days. After stirring the balloon pressure was vented and samples were collected for NMR analysis. The <sup>31</sup>P NMR spectrum when water/acetone was utilized was exactly what was observed in Figure 3.5.A. The color was also light yellow as observed with substrate present.

With water/acetonitrile as the solvent system, the <sup>31</sup>P NMR spectrum almost exactly matched what was observed in Figure 3.5.B. This was observed after 1 or 2 days of stirring under the balloon pressure. Clearly acetonitrile helps to limit or slow down the formation of these broad resonances. However, once substrate is present the broad resonances become the major species present on the <sup>31</sup>P NMR spectra. This suggests that the broad resonances are related to the oxidative cleavage reaction. Once these resonances become the dominant species, oxidative cleavage stops. If substrate is added after the broad resonances become the dominant species no oxidative cleavage occurs. These results suggest that one reason why a catalytic oxidative cleavage reaction does not occur is because of the formation of these broad resonances.

When DMSO and DMSO/water are used as solvents some differences were observed. When these solvents were used for bench-top reactions under a balloon atmosphere of O<sub>2</sub>, the aldehyde was not the only product identified. There were several reactions that showed some oxidation of DMSO to dimethyl sulfone. Also, when styrene was used as substrate, benzaldehyde and acetophenone were produced. Acetophenone was only observed when DMSO or DMSO/water was the solvent. These results could suggest a different reaction mechanism for the oxidation reaction when it is conducted in DMSO.

No reaction conducted in acetone or acetonitrile with O<sub>2</sub> as the oxidant showed the formation of acetophenone. This product was only observed in DMSO or when other oxidants

were tested (Section 3.5). The colors of these bench-top reactions were also always darker compared to water/acetone and water/acetonitrile solutions. NMR analysis revealed a small amount of the broad resonances with many sharp resonances present (very similar to Figure 3.5.B). When these balloon pressure reactions were repeated with no substrate present, the broad resonances were not observed. When DMSO was used for NMR scale reactions, an aldehyde peak was not observed on the  $^1\text{H}$  NMR spectrum. This occurred at atmospheric pressures as well as at elevated pressures and temperatures. Also, the broad resonances were not observed with these NMR reactions despite the fact that substrate was present. We believe this is because of the viscosity of the solvent, especially at room temperature. Without any way to stir the NMR reaction mixtures, air or  $\text{O}_2$  cannot effectively dissolve into the solvent and cause the oxidative cleavage of the substrate or the formation of the broad resonances.

When methanol and ethanol were used as solvents, the results matched what was observed with acetone. THF showed some slightly different reactivity. The aldehyde product was observed via GC/MS and NMR analysis but the light yellow color and broad resonances appeared much faster in this solvent system than with any other solvent system tested. This comes about because of the sensitivity of this solvent to air oxidation and the formation of hydroperoxides. This reactivity is accelerated when a metal complex is present and occurred in purged solutions within 1 to 2 hours. When DMF was utilized as a solvent, no oxidative cleavage occurred. This was observed with or without the addition of water. NMR analysis of these reaction mixtures showed  $^{31}\text{P}$  NMR spectra that nearly matched what was observed with DMSO. We currently do not have an explanation for why DMF is not a suitable solvent for the oxidative cleavage reaction.

One of the first additives to be tested was radical inhibitors. During the course of many oxidation processes, such as autoxidation, free-radicals are present during the course of the reaction. The addition of radical inhibitors can slow down or completely suppress many of these radical-based oxidation processes. Radical inhibitors tested include TEMPO, BHT and MEHQ (Figure 3.6). When 1 to 4 equivalents (relative to the complex) were added, the formation of the aldehyde was slowed down but it was not completely inhibited. The formation of the broad resonances was also slowed down.

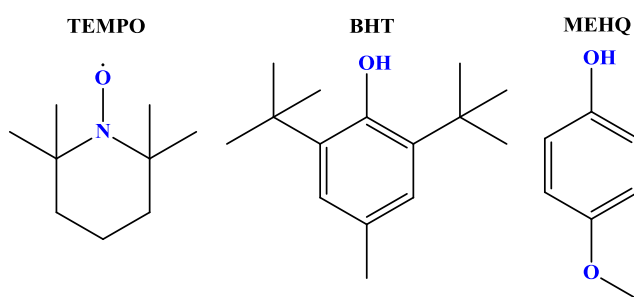


**Figure 3.6** Radical inhibitors utilized during the alkene oxidative cleavage reactions. TEMPO – 2,2,6,6-tetramethylpiperidine-1-oxyl, BHT – butylated hydroxytoluene or 2,6-*tert*-butyl-4-methylphenol, MEHQ – 4-methoxyphenol.

When 10 or more equivalents of the inhibitor were added, the reaction was completely suppressed and no products were formed. The large excess of radical inhibitor also suppressed the formation of the broad resonances. These results point to the fact that the reaction mechanism has to have some radical character. When the NMR reactions were conducted with the radical inhibitors present under an atmosphere of N<sub>2</sub>, no differences were observed via <sup>1</sup>H and <sup>31</sup>P NMR. This indicates that the radical inhibitors do not directly interact with the metal complex during the reaction with water. The inhibitors appear to only interact during the oxidation reaction.

Another additive that was tested was NaCl. We have established that in order for the oxidative cleavage to occur, 5% or more of water must be present for the majority of the solvents tested. This amount (or more) of water reacts with the complex and begins forming new species

(Chapter 4) and it is during this time that the aldehyde is formed. We proposed that the reactivity between the starting complex and water involves some chloride ligand dissociation. The addition of NaCl should slow down this reaction and hopefully would lead to the formation of more aldehyde.

We have found that the addition of 10 equivalents of NaCl or more will suppress the oxidative cleavage. When smaller amounts of NaCl (1-4 equivalents) are added, the formation of the aldehyde is slowed down but the product is still produced. Also, the addition of other sources of chloride, such as other metal salts, also slows down or completely suppresses the formation of the aldehyde product. Unfortunately, the amount of product did not increase over time and remained the same as that produced without the addition of NaCl and the addition of NaCl caused longer reaction times to form the same amount of aldehyde.

These results are strong evidence that chloride dissociation is an important reaction step when the starting complex reacts with water. The addition of more chloride slows this dissociation reaction and also slows down the formation of new species. Since this reaction is slowed down and it is during this reaction that the aldehyde is produced, then it makes sense that the formation of the aldehyde is also slowed down. The addition of 10 equivalents or more of chloride suppresses chloride dissociation from the complex. Because this process is suppressed, the reaction between the complex and water does not occur and therefore the formation of the aldehyde is not observed.

With the effects of added chloride known, the next additive tested was  $\text{AgBF}_4$ . We believed that the removal of chloride via the precipitation of AgCl should allow for the reaction to take place without the addition of water. This hypothesis was tested using 1, 2, and 4 equivalents in acetone. What we discovered was that the oxidative cleavage reaction did not

occur. No products were identified via GC/MS or NMR analysis. This was a very surprising result. Also, the addition of water to these solutions after removing the precipitated AgCl did not produce any aldehyde products. Based on these results, chloride dissociation is not the only important factor leading to the oxidative cleavage reaction. If the dissociation was the main factor leading to the cleavage, the addition of Ag should have allowed for the reaction to occur without the need for water.

The results suggest that chloride dissociation needs to occur with water present in order for the oxidative cleavage to occur. The only problem with this hypothesis is the fact that DMSO does not require the addition of water in order to see this reactivity. One explanation for this discrepancy could be the hygroscopic nature of DMSO. The DMSO used for these reactions was degassed and stored over molecular sieves and under a N<sub>2</sub> atmosphere. All of the reactions were loaded in air and DMSO could have pulled water from the air into solution. Since DMSO alone showed some new species being formed without the addition of water, the small amount of water pulled from the air could be enough to cause the water reactivity to continue and lead to the oxidative cleavage. Another possibility could be a different reaction mechanism occurs in DMSO because both benzaldehyde and acetophenone are produced when styrene is the substrate.

Several other additives were also tested to try and achieve a catalytic reaction. The agents include acids, bases, reducing agents, phosphine ligands and metal salts. The acids tested include acetic, ascorbic and malonic acid. These compounds are not only weak acids but they also can be possible reducing agents. 10 equivalents of acetic acid and malonic acid had no effect on the reaction. 10 equivalents of ascorbic acid completely retarded the reaction. The bases tested include CsOH and K<sub>2</sub>CO<sub>3</sub>. With the addition of either of these additives the oxidative cleavage did not occur. When 4 equivalents or more of CsOH were added, the starting

complex decomposed into phosphine oxide and Ni salts (either chloride or hydroxide salts). Other metal salts, including CuCl, Fe(BF<sub>4</sub>)<sub>2</sub> and CoCl<sub>2</sub>, were also tested. The chloride salts slowed down or completely retarded the reaction and the Fe<sup>+2</sup> showed no major effect on the oxidative cleavage.

Several different reducing agents were tested for the reaction. We initially believed the broad resonances on the <sup>31</sup>P NMR were caused by paramagnetic Ni complexes formed during the oxidation reaction. We theorized that the reason a catalytic reaction was not being achieved was because there was nothing to reduce the oxidized complex back to the active species. Alcohols (ethanol, 2-propanol and 1-butanol), aldehydes (propanal and isobutyraldehyde), ascorbic acid, malonic acid and potassium oxalate (K<sub>2</sub>C<sub>2</sub>O<sub>4</sub>) were all tested. The addition of any amount of alcohol caused no change in the reaction. The addition of an aldehyde (1 equivalent relative to the substrate or lower) also had no effect on the oxidative cleavage. A larger amount of aldehyde led to the formation of other products via a different reaction mechanism (Mukaiyama epoxidation). As discussed in Chapter 1 the Mukaiyama epoxidation has been shown to be a selective epoxidation protocol with many different metal complexes. Unfortunately no selective epoxidation was observed with any complex tested. The addition of 10 equivalents of K<sub>2</sub>C<sub>2</sub>O<sub>4</sub> led to the decomposition of the starting complex. No reaction showed an increase in the amount of aldehyde produced.

The addition of other phosphine ligands, including PPh<sub>3</sub> and dppe, was also tested to see if an increase in aldehyde product could be achieved. As much as ten equivalents of the phosphine ligand were added to the reaction mixture. There was no observed increase in the amount of aldehyde produced and in a few instances the reaction was completely retarded.

Many of these reaction conditions were attempted using **Ni<sub>2</sub>1R**. It was found that this complex has the same reactivity as **Ni<sub>2</sub>1M**. Aldehyde products were identified using this complex as a possible catalyst via GC/MS and NMR analysis. Again the amount of product was very small and at most about 5 mM of aldehyde was formed. The addition of water was required for this complex to show activity. The additives tested, including NaCl, AgBF<sub>4</sub>, acids, bases and phosphine ligands, showed the same pattern as with **Ni<sub>2</sub>1M**. The additives did not affect the reaction, slowed it down or completely retarded the reaction. In every instance the reactivity observed for **Ni<sub>2</sub>1R** exactly matched the reactivity observed for the *meso* complex.

### **3.3 Identification of the Broad Resonances**

During the oxidative cleavage studies using **Ni<sub>2</sub>1M**, these broad resonances (Figure 3.5) always appeared on the NMR spectra. One major goal was to identify what compound or compounds were giving rise to these resonances. From the experiments, we knew that they only appeared in the presence of both water and O<sub>2</sub>. Also, as these resonances grew in intensity the amount of aldehyde increased as well. These observations indicate that the broad resonances are linked with the oxidative cleavage reaction.

Our first hypothesis was that these resonances were caused by paramagnetic Ni<sup>+3</sup> complexes being formed upon exposure to air. Experiments with reducing agents did not show any signs of being able to reduce these hypothetical complexes back to diamagnetic (Ni<sup>+2</sup>) species. EPR (Electron Paramagnetic Resonance) spectroscopy was conducted on several different samples to determine whether any paramagnetic species were present. EPR spectroscopy is a technique for studying systems with unpaired electrons. The principles of EPR are analogous to NMR spectroscopy except that EPR deals with electron spins and NMR deals with nuclear spins. Dr. Rupnik analyzed several different samples of these broad resonances at



room temperature and low temperatures and in no case was a signal detected. This was very convincing evidence that paramagnetic species were not present in the reaction mixture.

We also proposed that some type of dynamic exchange reaction was occurring in solution. The exchange process is an intermediate exchange process on the NMR timescale at room temperature and leads to the broad resonances. Generally, when an exchange process is fast on the NMR timescale, a sharp resonance is observed that is the average between the two exchanging states. When the process is slow, two separate sharp signals are observed for the two states. An intermediate process leads to broadened resonances. Changes in the linewidths and peaks as the temperature is changed can allow you to calculate kinetic and thermodynamic data about the exchange process.

To investigate this hypothesis variable temperature NMR experiments were conducted. Figure 3.7 shows the results from two different variable temperature NMR experiments. The two experiments were both conducted in 15% D<sub>2</sub>O/acetone-*d*<sub>6</sub>. One experiment (top three spectra) was conducted in air and the other experiment (bottom two spectra) was conducted at 100 psig O<sub>2</sub>. Both had substrate present. The two black spectra were recorded at room temperature. The top spectrum contains sharp resonances overlapping with the broad resonances while the bottom spectrum contains just the broad resonances. The red spectra were recorded after heating the samples to 50°C (top) and 100°C (bottom).

The broad resonances completely disappear and all that is left is the sharp resonances that overlapped with these resonances. The sharp resonances appear to be unaffected by heating. At no point between 50 and 100°C do any other sharp resonances appear. The green spectrum was recorded at -15°C. The broad resonances are beginning to sharpen. As you go lower in temperature these resonances continue to sharpen. The lowest temperature attempted was -30°C.

Lower temperatures were not possible because the added water would begin to freeze out of solution and the spectral resolution would become compromised. The disappearance and sharpening of these broad resonances is completely reversible. These NMR experiments were conducted several times and this process was observed each time.

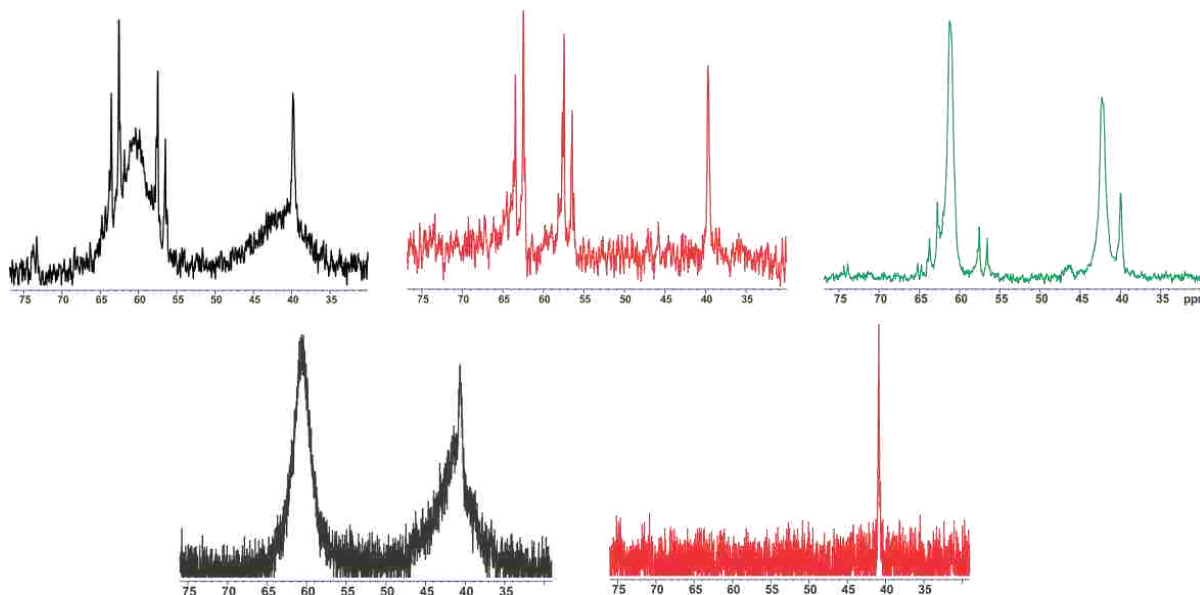


**Figure 3.7**  $^{31}\text{P}$  NMR spectra illustrating the effect of temperature on the broad resonances. The black spectra were recorded at 25°C. The red spectra were recorded at higher temperatures (50°C and 100°C). The green spectrum was recorded at -15°C.

These results did not seem consistent with a typical dynamic exchange process.

Typically, when an intermediate exchange process is occurring, heating the sample should increase the rate of the process and eventually lead to the appearance of one sharp signal which would be an average between the two possible states. This was never observed via NMR. Once the broad resonances disappeared, no other resonance appeared at every temperature attempted. However, the temperature required to reach this point might have been higher than 100°C and this was the highest temperature attempted. The increase in resolution as the samples were cooled is consistent with slowing down the exchange process. However, due to the temperature limits of the solvent system, the broad resonances were never fully resolved.

Several discussions with Dr. Dale Treleaven and Dr. Thomas Weldeghiorghis led to several different possible proposals. The one that made the most sense based on the observed NMR spectra was an exchange process between a diamagnetic and paramagnetic species. At room temperature there was an equilibrium mixture of both diamagnetic and paramagnetic species which would lead to broadened lines. When the temperature is increased the equilibrium would be shifted completely to the paramagnetic species and completely wipe out the signals. When the temperature is lowered, the equilibrium would favor the diamagnetic species and cause an increase in resolution as more of the diamagnetic species is formed. However, if this process was occurring, room temperature EPR experiments should have given a signal for the paramagnetic species but no signal was observed. Unfortunately, high temperature EPR experiments are not typically conducted and we were unable to record an EPR spectrum at temperatures above room temperature to definitely prove or disprove this hypothesis.

Several attempts were made to try and crystallize out species from these reaction mixtures. The addition of counteranions such as  $\text{BF}_4$  or  $\text{BPh}_4$  did not produce any crystals. Cooling the solutions for days or weeks in a freezer also failed to produce any precipitate. Vapor diffusion was also attempted but nothing precipitated out of solution. Several reaction mixtures were also evaporated to dryness under vacuum to try and isolate what species remained in solution. As mentioned previously, these solutions were all yellow or light yellow in color. When the solutions were completely stripped of all volatile materials, a green powder was all that remained. It was found that this powder was highly soluble in water and allowed for NMR analysis. Figure 3.8 shows the  $^{31}\text{P}$  NMR spectrum obtained in  $\text{D}_2\text{O}$ .

There are two main resonances, one centered at 64.9 ppm and the other centered at 43.3 ppm. A  $^{31}\text{P}$ - $^{31}\text{P}$  COSY (Correlation Spectroscopy) experiment established that these two

resonances are correlated to each other meaning they are from different phosphorus nuclei on the same species. The broad doublets observed are near where the broad resonances appear in water/acetone or water/acetonitrile. Attempts to crystallize out any species from these D<sub>2</sub>O solutions failed to produce any single crystals.

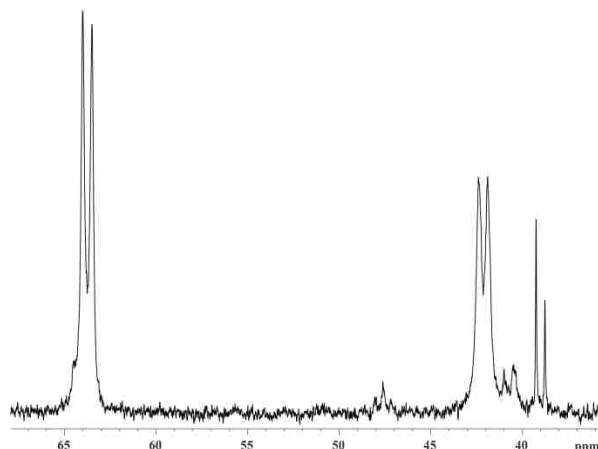


**Figure 3.8** <sup>31</sup>P NMR spectrum in D<sub>2</sub>O of the green solid after stirring **Ni<sub>2</sub>1M** under a balloon atmosphere of O<sub>2</sub> and removing all volatile materials

With these results in mind, an experiment was conducted to try and determine what was giving rise to these resonances. Figures 3.9 and 3.10 show the NMR spectra obtained from this series of experiments. A mixture of 63% **1M**/37% **1R** was dissolved in 15% D<sub>2</sub>O/acetone-*d*<sub>6</sub>. An NMR spectrum of this solution was then recorded (Figure 3.9.A). The solution was then subjected to an excess of 35% aqueous H<sub>2</sub>O<sub>2</sub> and allowed to stir in air for 30 minutes. A sample of this solution was collected and analyzed via <sup>31</sup>P NMR (Figure 3.9.B).

**1M** and **1R** were completely and quantitatively oxidized to their corresponding tetraphosphine oxides. The remaining solution was then evaporated to dryness under vacuum and redissolved in 50% D<sub>2</sub>O/acetone-*d*<sub>6</sub> with 30 mg of NiCl<sub>2</sub>·6H<sub>2</sub>O added. A sample was collected and analyzed via NMR (Figure 3.9.C). Comparison of 3.9.B and 3.9.C clearly show a significant amount of broadening upon the addition of NiCl<sub>2</sub>. This suggests that the broad resonances are caused by an interaction between the tetraphosphine oxide and NiCl<sub>2</sub>. To prove

this was correct, the remaining solution was evacuated to dryness under vacuum and the residue was redissolved in D<sub>2</sub>O. A sample was collected and analyzed via NMR (Figure 3.9.D). The NMR spectrum obtained was then compared to the green solid obtained after Ni<sub>2</sub>1M was stirred under a balloon pressure of 15% water/acetone overnight and evacuated to dryness under vacuum (Figure 3.10).

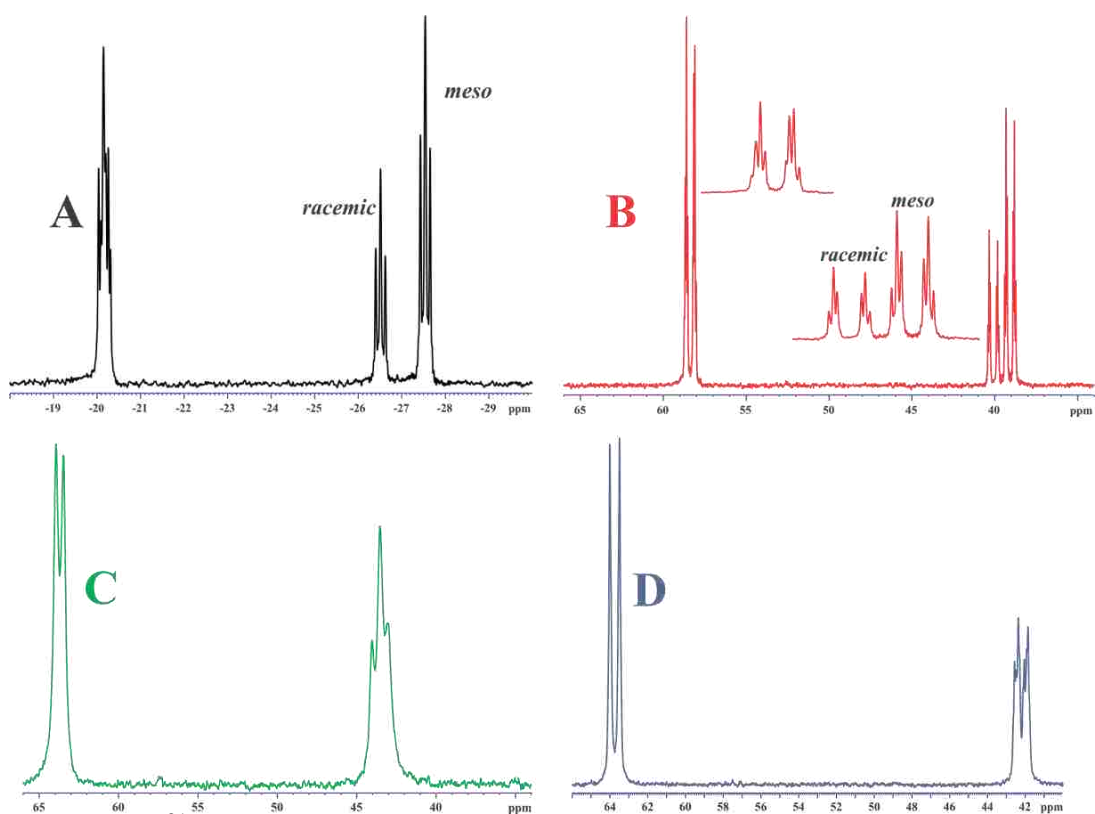


**Figure 3.9** **A** – <sup>31</sup>P NMR spectrum of **1M** and **1R** dissolved in 15% D<sub>2</sub>O/acetone-*d*<sub>6</sub>. **B** – <sup>31</sup>P NMR spectrum of **1M** and **1R** after reacting with H<sub>2</sub>O<sub>2</sub>. **C** – <sup>31</sup>P NMR spectrum of the tetraphosphine oxides with NiCl<sub>2</sub> present in 50% D<sub>2</sub>O/acetone-*d*<sub>6</sub>. **D** – <sup>31</sup>P NMR spectrum of the phosphine oxides/NiCl<sub>2</sub> in D<sub>2</sub>O.

The spectra matched exactly besides the peaks present for the oxide of **1R** which are not present in the green solid. This proves that the broad resonances are caused by an interaction between the tetraphosphine oxide and NiCl<sub>2</sub> and when they are dissolved in water a stable species is formed that gives rise to the sharp resonances observed upon dissolving the green solid

in water. This is the major reason why a catalytic oxidative cleavage reaction has not been realized. During the course of the reaction, the phosphine becomes completely oxidized and forms inactive species.

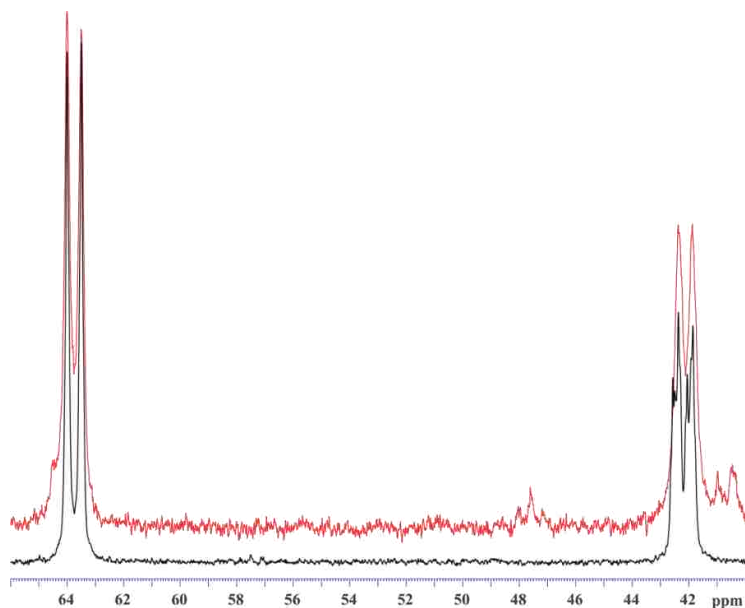


**Figure 3.10** A comparison between the tetraphosphine oxide/ $\text{NiCl}_2$  dissolved in  $\text{D}_2\text{O}$  (black spectrum) and the green solid (red spectrum) dissolved in  $\text{D}_2\text{O}$

The complete oxidation of the phosphine also occurs without the addition of substrate. Stirring the complexes under a balloon pressure of  $\text{O}_2$  in water/acetone and water/acetonitrile gives rise to the tetraphosphine oxide. In acetone the complete oxidation occurs within one to two days. In acetonitrile this reaction is partially inhibited and even stirring the complex for several days will not completely oxidize the phosphine. When DMSO is used as a solvent without added substrate, this process is also inhibited. After stirring these solutions for several days, there is almost no noticeable phosphine oxidation. This could be because of acetonitrile and DMSO's ability to coordinate to the metal center. Solvent coordination could compete with coordination of  $\text{O}_2$  and not allow the reaction to take place that leads to the oxidation of the phosphine ligand. DMSO is the strongest coordinating solvent among these three and would compete with  $\text{O}_2$  binding the strongest and would inhibit ligand oxidation the most. Acetone has

a much weaker coordinating ability and would not be able to effectively compete with O<sub>2</sub> coordination.

### 3.4 Monometallic Metal Complexes as Possible Oxidative Cleavage Catalysts

As studies were ongoing with the bimetallic Ni complexes, several other monometallic metal complexes were also tested for their possible utilization as oxidative cleavage catalysts. The first series of complexes tested were monometallic Ni/phosphine complexes. The complexes tested were some of the same ones tested during the alkene hydration studies [NiCl<sub>2</sub>(dppe), NiCl<sub>2</sub>(dppp), NiCl<sub>2</sub>(PPh<sub>3</sub>), NiCl<sub>2</sub>(dcpe)]. The phosphine ligands were also tested with Ni(BF<sub>4</sub>)<sub>2</sub> as the Ni source. For these reactions 10 mM of Ni(BF<sub>4</sub>)<sub>2</sub> was added followed by 1 or 2 equivalents of dppe, dppp or dcpe to form the monometallic complexes *in situ*. Other chelating phosphine ligands, including BISBI, NAPHOS and XANTPHOS (Figure 3.11), were also tested in this manner. The reactions were conducted at elevated pressures of O<sub>2</sub> (balloon pressure or high pressure NMR tube).

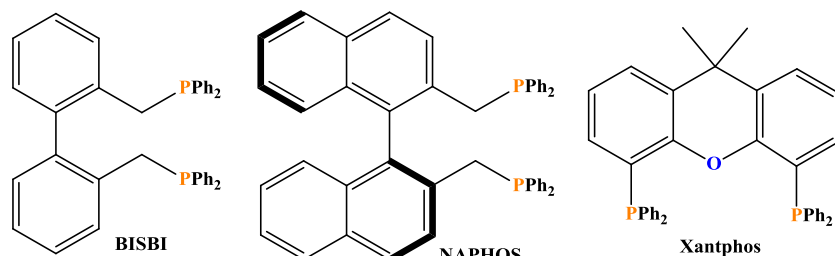


**Figure 3.11** Large bite angle chelating phosphines tested for the oxidative cleavage of alkenes.

The only complex that did not show any reactivity was NiCl<sub>2</sub>(PPh<sub>3</sub>). No reaction occurred in acetonitrile, acetonitrile/water and DMSO. All other complexes tested gave some aldehyde product. The amount of product was always smaller than the amounts observed with the bimetallic Ni complexes. In several cases it was very difficult to identify whether any product was formed via GC/MS or NMR analysis.

This led to some difficulty in assigning activity to each complex in different solvent systems. DMSO was the solvent that showed the most activity for these complexes. Nearly every complex tested showed the aldehyde product when DMSO was utilized. Water was not required for the reactivity to occur with the ligand dppe. Complexes formed from dppe showed activity in acetonitrile by itself, acetonitrile/water and DMSO. Complexes formed from dppp showed activity only in DMSO. Because of the small amount of product observed, even under 100 psig O<sub>2</sub> and elevated temperatures, none of the complexes were tested with other additives to try and increase the amount of aldehyde produced.

Other chelating ligands besides phosphines were also tested with Ni salts to test whether these complexes were active for the oxidative cleavage. The four ligands, TMEDA, 1,10-phenanthroline, 1,2-benzenediamine and dimethylglyoxime, tested are depicted in Figure 3.12. 10 mM of NiCl<sub>2</sub> and Ni(BF<sub>4</sub>)<sub>2</sub> were tested with each ligand. 2 equivalents of the ligand were added for each reaction. The solvent systems tested for these complexes include 15% water/acetone, 15% water/acetonitrile, DMSO and 15% water/DMSO. These four solvent systems were tested for each ligand and each Ni salt. All of the reactions were conducted under a balloon atmosphere of O<sub>2</sub> and were allowed to stir overnight before analysis.

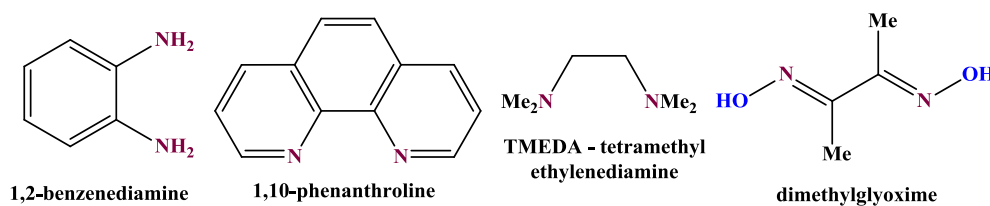


**Figure 3.12** Nitrogen-based chelating ligands tested for the oxidative cleavage of alkenes.

None of these complexes showed any reactivity for the oxidative cleavage. No product could be identified via GC/MS or NMR analysis. Mixed ligand systems containing 1 equivalent of a nitrogen-based ligand and 1 equivalent of dppe were also tested. These also did not show any products via GC/MS and NMR analysis. Dppe was chosen as the phosphine ligand because



the complexes formed with this chelating ligand showed the most activity for the oxidative cleavage. No other phosphine ligands were tested for these mixed ligand systems.

Other transition metal/phosphine complexes were also tested for possible oxidative cleavage reactivity. The complexes tested include *trans*-PdCl<sub>2</sub>(PPh<sub>3</sub>)<sub>2</sub>, *cis*-PtCl<sub>2</sub>(PEt<sub>3</sub>)<sub>2</sub> and RhCl(PPh<sub>3</sub>)<sub>3</sub> (Figure 2.6). Besides these premade complexes, mixtures of a transition metal salt with dppe were also tested. The metal salts investigated include CoCl<sub>2</sub>, Fe(BF<sub>4</sub>)<sub>2</sub>, CuSO<sub>4</sub> and RhCl<sub>3</sub>. The salts were tested with both 1 and 2 equivalents of dppe. Different solvent systems were tested including acetonitrile, DMSO, 15% water/acetonitrile and 15% water/DMSO. These experiments were all conducted under a balloon atmosphere of O<sub>2</sub> and allowed to stir overnight before analysis via GC/MS and NMR. None of these reactions produced any oxidative cleavage products.

Ni salts [NiCl<sub>2</sub>, Ni(BF<sub>4</sub>)<sub>2</sub> and Ni(acac)<sub>2</sub>] and phosphine ligands (PPh<sub>3</sub>, PCy<sub>3</sub> and dppe) were also tested by themselves to see if any oxidative cleavage occurred. 10 mM of the salts or the phosphines were stirred under a balloon pressure of O<sub>2</sub> in several different solvent systems (15% water/acetone, 15% water/acetonitrile, acetone, acetonitrile) overnight. NMR and GC/MS analysis of these solutions revealed no products were formed.

### 3.5 Other Oxidizing Agents

With the continued failed attempts to promote a catalytic oxidative cleavage reaction, other oxidizing agents were also tested with the bimetallic and monometallic Ni/phosphine complexes and the monometallic Ni/nitrogen ligand complexes. The oxidizing agents tested were 35% aqueous hydrogen peroxide (H<sub>2</sub>O<sub>2</sub>), 70% aqueous *tert*-butyl hydroperoxide (TBHP) and more than 2 equivalents (relative to the substrate) of propanal or isobutyraldehyde under a

balloon pressure of O<sub>2</sub> (Mukaiyama epoxidation conditions). Both H<sub>2</sub>O<sub>2</sub> and TBHP were tested under an inert atmosphere of N<sub>2</sub> and under air.

The complexes tested include **Ni<sub>2</sub>1M**, **Ni<sub>2</sub>1R**, NiCl<sub>2</sub>(PPh<sub>3</sub>), NiCl<sub>2</sub>(dppe), NiCl<sub>2</sub>(dcpe), NiCl<sub>2</sub>(dppp) and NiCl<sub>2</sub> + N-based ligands (Figure 3.12). Also tested were the salts NiCl<sub>2</sub>, Ni(BF<sub>4</sub>)<sub>2</sub> and Ni(acac)<sub>2</sub>. Solvent systems tested include DCM, acetone, acetonitrile, DMSO, biphasic DCM/water, acetone/water, acetonitrile/water and DMSO/water. Because H<sub>2</sub>O<sub>2</sub> and TBHP were purchased as aqueous solutions, reactions conducted with these oxidants had to have water present. Oxidation reactions utilizing the aldehydes and O<sub>2</sub> were run with and without water added. All of the reactions were run with styrene as the substrate.

Several different products were identified during the course of these reactions. The products (Figure 3.13) include benzaldehyde, styrene oxide, phenylacetaldehyde, benzoic acid, phenylacetic acid and dimethyl sulfone when DMSO was used as a solvent. No definitive trends could be observed during these reactions. All complexes gave a mixture of benzaldehyde, styrene oxide and phenylacetaldehyde. For some reactions other products, including dimethyl sulfone and unidentified compounds, were also formed. No trends were observed for the formation of these products and longer reaction times led to the formation of the organic acids. No major differences were observed when the reactions were conducted in air or under an inert atmosphere.

The only common feature of these reactions involved the decomposition of the complexes when H<sub>2</sub>O<sub>2</sub> or TBHP were utilized as the oxidant. Every complex decomposed when either of these oxidants was tested. The decomposition occurred between 5 minutes and several hours. When the reactions were conducted under an inert atmosphere, the decomposition reaction took longer but did occur. The Ni salts tested also all showed the products identified

when the complexes were tested. Because the salts themselves gave products and because there was always a multitude of products, these reactions come about from a radical chain mechanism (autoxidation). Further proof of the radical chain mechanism was shown when 2 reactions with  $\text{H}_2\text{O}_2$  and TBHP were tested with the radical inhibitor BHT. No products were identified during these two reactions.

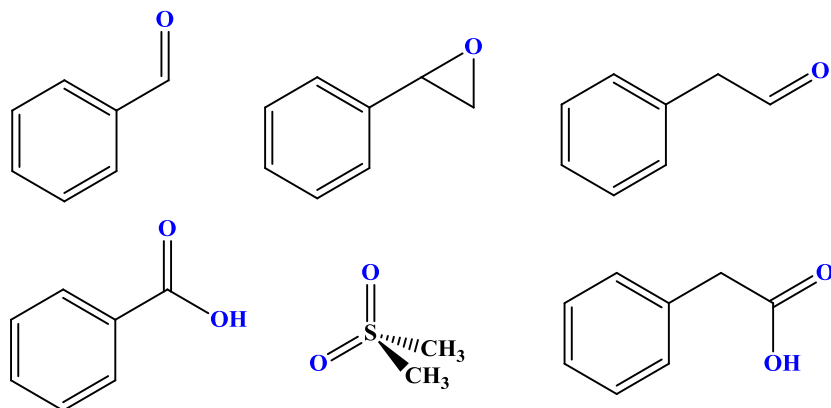


**Figure 3.13** The products identified via GC/MS during the oxidation reactions with other oxidants.

### 3.6 Mechanistic Possibilities

With the identification of the selective but non-catalytic alkene oxidative cleavage reaction mediated by the bimetallic complexes **Ni<sub>2</sub>1M** and **Ni<sub>2</sub>1R** along with some monometallic Ni/phosphine complexes, a lot of experimentation and thought has gone into trying to understand the reaction mechanism. Several facts are known. The first and most important is that water must be present in acetone or acetonitrile in order for this reaction to occur. Without the addition of 5% or more (by volume) of water, no oxidative cleavage occurs and also no phosphine oxidation occurs.

Another important fact is that radical inhibitors will completely inhibit the reaction when they are added in a large excess. Smaller amounts will slow down the reaction but the aldehyde products are still produced. The radical inhibitors also slow down or completely suppress the

phosphine oxidation when they are added. We also know that the addition of excess chloride can slow down or completely inhibit the oxidative cleavage and phosphine oxidation process. The experimental evidence hints at the fact that the oxidative cleavage reaction and phosphine oxidation process are coupled together. When the oxidative cleavage occurs, phosphine oxidation occurs. However, the phosphine oxidation can occur without substrate present.

The first question that needs to be answered is what role does the water play? We know from  $^1\text{H}$  and  $^{31}\text{P}$  NMR studies that the addition of 5% of water or more leads to the formation of new complexes. Since water has to be added to see the oxidative cleavage and phosphine oxidation, a logical assumption is that the water reacts with the complex in the presence of  $\text{O}_2$  and forms a small amount of an active species that is responsible for the oxidative cleavage. Dr. Stanley has proposed one such reaction for  $\text{Ni}_2\mathbf{1M}$ , shown in Figure 3.14.

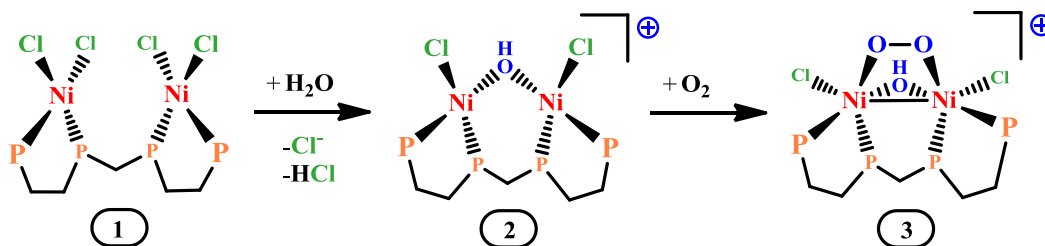


**Figure 3.14** A proposed reaction scheme which shows the formation of a possible active species in the oxidative cleavage reaction.

Hydrolysis of one of the Ni-Cl bonds and chloride dissociation could lead to the formation of the cationic, bridging hydroxide complex (**2**). The addition of  $\text{O}_2$  could lead to the formation of **3** via the oxidation of each Ni center to a +3 oxidation state and the formation of a bridging peroxide ligand and a Ni-Ni bond. This proposal is in line with the experimental evidence obtained thus far. The addition of excess chloride would inhibit the formation of **2** which would suppress the oxidative cleavage. **2** would also not be formed without the addition of water. The oxidation of the Ni centers followed by the formation of a Ni-Ni bond would form a diamagnetic species and not give rise to a signal via EPR. DFT calculations have been

performed by Dr. Stanley on **3** and this peroxy-bridged complex converges well, indicating a relatively stable structure. He has subsequently proposed **3** as one possible active species for the oxidative cleavage reaction.

Following this proposal, Dr. Stanley proposed two different possible reaction mechanisms for the oxidative cleavage reaction. The first proposed mechanism is shown in Figure 3.15. Chloride dissociation from **3** would open up a coordination site and allow the alkene to bind and lead to the formation of **A**. Migratory insertion of the bridging peroxy ligand to the alkene would form **B**. This would be followed by several different electron transfers and rearrangements involving the bridging alkylperoxy ligand, the bridging hydroxide ligand and the Ni centers to give you the two aldehyde products and **2** after chloride addition. **2** would then react with another molecule of O<sub>2</sub> and reform **3** and continue the catalytic cycle.

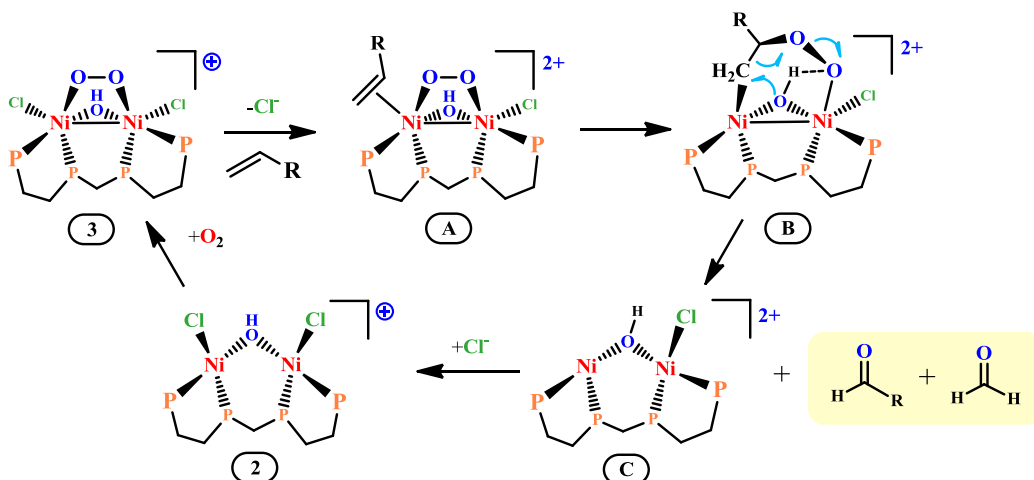


**Figure 3.15** The first proposed reaction mechanism for the oxidative cleavage.

The second proposed mechanism is shown in Figure 3.16. This proposed mechanism is based off of the DFT calculations performed on **3**. The calculated HOMO and 3<sup>rd</sup> highest occupied molecular orbital are shown in Figure 3.17. These filled molecular orbitals contain  $\pi^*$  anti-bonding interactions between the two oxygen atoms of the bridging peroxide ligand. These anti-bonding interactions are of the right symmetry to interact with the empty  $\pi^*$  anti-bonding

orbitals of a double bond. The proposed mechanism involves an alkene reacting directly with the bridging peroxide ligand via a cycloaddition to form a dioxetane molecule. Rearrangement of the dioxetane would release the two aldehydes and reform **2** which could react with  $O_2$  to form **3** and continue the catalytic cycle.

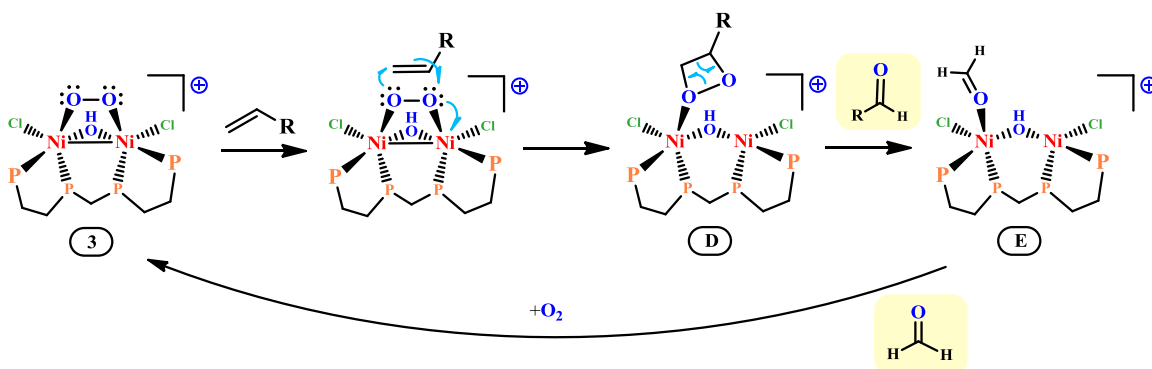


**Figure 3.16** The second proposed mechanism for the oxidative cleavage.

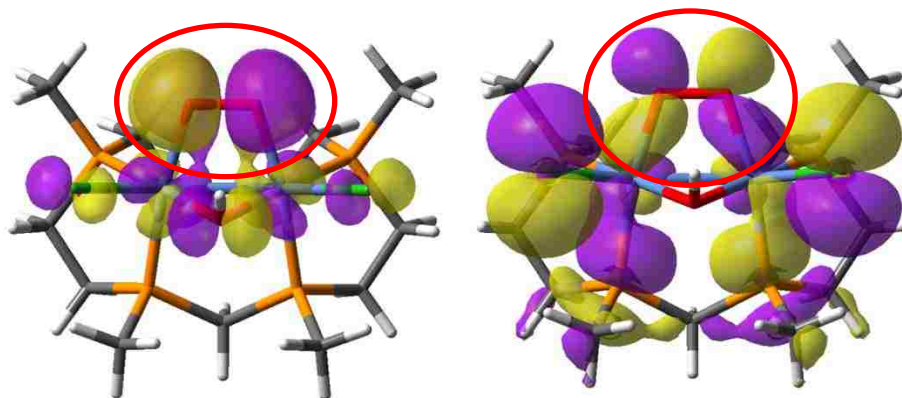


**Figure 3.17** Molecular orbitals of **3** calculated via DFT. The red circles highlight the  $\pi^*$  anti-bonding interactions between the two oxygen atoms.

Both of these proposed mechanisms are not supported by any spectroscopic evidence. Also, there is no spectroscopic evidence that **3** forms in solution and is the active species. Dr. Stanley made these three proposals based on his chemical intuition. One of the biggest differences between the two proposed mechanisms is the first proposal involves alkene coordination to one of the Ni centers while the second mechanism does not involve any direct interaction between the Ni centers and the alkene.

This is an important fact when considering the substrate scope. Several different alkenes have shown reactivity including terminal alkenes (1-hexene, 1-octene), internal alkenes (5-decene and *trans*-stilbene) and styrene. There were no observed differences in the amount of time it took for all of these different alkenes to react. One would expect that if substrate binding was an important step in the reaction mechanism, all of these alkenes should not show the same reactivity due to steric interactions between the alkene and the complex upon binding. The internal alkenes (especially *trans*-stilbene) should have a more difficult time binding to the metal centers due to the larger steric bulk of these alkenes. There also should be differences between 1-hexene and styrene because styrene would be a bulkier terminal alkene. However, none of these differences have manifested themselves in any way. The time required for the reaction to be finished was the same for all alkenes and only depended on the reaction setup. Because of this I believe the first mechanism is highly unlikely to be occurring.

The second proposed mechanism is more favorable when considering the substrate scope found for this reaction. It does not involve any direct binding between the Ni and alkene. Therefore, the alkenes tested should all react in about the same manner. There could still be some repulsive steric interactions between the alkene and the ethyl groups of the ligand. However, these interactions would not be as severe as substrate binding to the Ni centers. Because of this, all of the substrates tested should all show very similar reactivities.

Neither of these mechanisms support all of the experimental evidence collected. They do not address why a radical inhibitor would slow down or completely inhibit the reaction. The first mechanism could involve some radical character during the electron transfer and rearrangement steps which could be inhibited by the radical scavengers. The second mechanism would not involve any radical species. The cycloaddition would more than likely be a concerted electron

transfer process as would the decomposition of the dioxetane molecule to produce the two aldehyde products. Therefore, radical inhibitors should have no effect on this mechanism.

The mechanisms also do not have an explanation for the oxidation of the phosphine ligands. We know that during the oxidative cleavage reaction the phosphine ligand is completely oxidized. We also know that this occurs without substrate being present. Phosphines are generally considered to be air sensitive and easily oxidized species. Therefore, the active species formed in solution, such as **3**, could react with the phosphines bound to the metal and oxidize them or it could interact with free phosphine in solution (observed via NMR, Chapter 4) and oxidize the free phosphine. The addition of a large excess of substrate could lead to some oxidative cleavage but because the phosphines are more easily oxidized, they would be consumed and lead to the end of any oxidation chemistry. We have observed that radical inhibitors slow down or completely inhibit the phosphine oxidation as well. Because both phosphine oxidation and oxidative cleavage are inhibited by the radical scavengers, it seems likely the two processes are operating under similar mechanisms. These observations suggest that the two proposed mechanisms are not occurring.

Another problem with the two proposed mechanisms is the fact that they are only for **Ni<sub>2</sub>1M**. Almost identical reactivity was observed with **Ni<sub>2</sub>1R**. Because these two complexes would form different bridging complexes, it seems unlikely that a structure similar to **3** would occur with **Ni<sub>2</sub>1R**. No calculations have been performed on similar structures using **1R** to determine the stability of these bimetallic Ni complexes. Because of the differences between the two ligands and their ability to form bridging structures, you would not expect them to show almost the same reactivity. This seems to suggest that another mechanism is responsible for both the oxidation of the phosphine ligands and the oxidative cleavage of the alkenes.



We have shown that the addition of water is required for this reactivity to occur. We also know that this leads to free phosphine in solution (Chapter 4). Both of the oxidative processes occur when substrate is present. Without substrate present, phosphine oxidation still occurs. Both **Ni<sub>2</sub>1M** and **Ni<sub>2</sub>1R** show nearly the same reactivity and both complexes give the same amount of product. Radical inhibitors slow down or completely suppress both oxidation reactions. This suggests the reaction mechanism has some radical character. A wide range of substrates all show activity for the oxidative cleavage. This suggests that substrate binding directly to the Ni centers is not occurring. When phosphine ligands are not present the oxidative cleavage does not occur.

Taking all of this evidence into consideration seems to point to one possible reaction mechanism. The mechanism would begin via oxidation of the phosphine ligand upon dissolving the complex in a water/polar organic solvent system and exposing it to O<sub>2</sub>. Once the phosphine oxidation begins, this reaction would produce a species (free radical?) that would perform the oxidative cleavage when substrate is present. Without substrate, the phosphine would continue to be oxidized until completely consumed. The phosphine oxidation and substrate oxidative cleavage would continue until the phosphine is completely consumed which would bring an end to the oxidative cleavage reaction.

The oxidation process would have to possess some radical character but it would not be a simple radical chain mechanism (autoxidation) because this would not lead to a selective oxidative cleavage reaction. Autoxidation would lead to several different products (especially allylic oxidation) and would not stop once the phosphine oxidation was complete. The presence of the Ni atoms would be responsible for the selective oxidation process and also be responsible for the complete oxidation of the phosphine ligands.

One experiment that supports part of this mechanistic idea comes from an experiment in which a sample of a mixture of **1M** and **1R** was stirred under a balloon atmosphere of O<sub>2</sub> dissolved in 15% water/acetone. After one night of stirring, a sample was collected for analysis via NMR. The <sup>31</sup>P NMR revealed a mess of more than 30 peaks on the spectrum. The ligands were not completely oxidized and longer reaction times did not lead to the complete oxidation of the ligands. These results suggest that the presence of Ni, either some complex or Ni ions themselves, plays a role in the complete oxidation of the tetraphosphine ligands.

One piece of evidence that does not support this mechanistic idea comes from the experiments conducted with **Ni<sub>2</sub>1M** and added phosphine ligand. These reactions did not show any increase in the amount of aldehyde produced. If the phosphine oxidation leads to the oxidative cleavage of the alkene, one would expect the addition of more phosphine ligand to lead to more alkene oxidative cleavage. However, this was not observed even with 10 equivalents of dppe added (20 equivalents of phosphine total). It appears that the reaction mechanism is very complex and would require more experimentation to elucidate exactly what is occurring during both the phosphine oxidation and oxidative cleavage reaction.

### 3.7 Conclusions

During the course of the alkene hydration/oligomerization experiments NMR experiments were conducted which led to the identification of an aldehyde being produced. GC/MS analysis revealed the aldehyde to be pentanal when 1-hexene was the substrate and benzaldehyde when styrene was the substrate. Subsequent NMR and bench top experiments have proven that the oxidative cleavage reaction comes about when **Ni<sub>2</sub>1M**, **Ni<sub>2</sub>1R** and other monometallic Ni/phosphine complexes are dissolved in a water/polar organic solvent system and exposed to air. Water is required for this reactivity to occur when **Ni<sub>2</sub>1M** and **Ni<sub>2</sub>1R** are utilized.

Without at least 5% (by volume) of water added, no reactivity occurs between the complex and substrate and between the complex and O<sub>2</sub>. Several different substrates, including 1-hexene, 1-octene, styrene, *trans*- $\beta$ -methylstyrene,  $\alpha$ -methylstyrene, *trans*-stilbene and *trans*-5-decene, have been tested and all show the formation of the aldehyde product. When terminal alkenes are used, one equivalent of formaldehyde is formed for every equivalent of aldehyde. This is inferred from stoichiometry and from the identification of both benzaldehyde and acetaldehyde from reactions with *trans*- $\beta$ -methylstyrene. A large number of blank reactions have been conducted and established that the complexes are responsible for this oxidative cleavage reaction.

The oxidative cleavage reaction is not catalytic! At most around 5 mM of aldehyde is produced for each reaction. The amount of product is about the same for every reaction tested with **Ni<sub>2</sub>1M** and **Ni<sub>2</sub>1R**. The major difference comes about from the time it takes to reach this amount of product. The time is completely dependent on the reaction conditions. When the reaction solutions are exposed to air and purged, several days are required for the reaction to be completed. When a balloon atmosphere of O<sub>2</sub> is used, the reaction is complete after stirring for one night. When higher pressures are used, reaction completion can take a few hours. If heat is applied, the reaction finishes within 1 to 2 hours. No additive tested (reducing agents, acids, bases, AgBF<sub>4</sub>, NaCl, other metal salts, phosphine ligands) increases the amount of product formed. They either do nothing to the reaction, slow it down, or completely inhibit product formation.

Some monometallic Ni/phosphine complexes were also tested for the oxidative cleavage reaction. Some of these complexes, especially NiCl<sub>2</sub>(dppe), showed some oxidative cleavage reactivity. The amount of aldehyde produced was always smaller with the monometallic complexes than with the bimetallic complexes. Other monometallic Ni complexes with N-based

ligands were not active under all conditions tested. Also, other transition metal/phosphine complexes tested were not active for the oxidative cleavage. Other oxidants ( $\text{H}_2\text{O}_2$ , TBHP, Mukaiyama epoxidation conditions) have been tested with the bimetallic and monometallic Ni complexes. A multitude of different products were formed and none of these reactions were selective for the oxidative cleavage reaction or any other oxidation process (epoxidation).

The major reason a catalytic reaction has not been realized is because during the course of the oxidative cleavage reaction, the tetrakisphosphine ligands are completely oxidized to the tetrakisphosphine oxide. The phosphine oxides give rise to two broad resonances (around 60 and 40 ppm) on the  $^{31}\text{P}$  NMR spectra. The broad resonances are caused by an interaction between the phosphine oxide and  $\text{NiCl}_2$ . This has been proven experimentally. Efforts to determine exactly what species is formed (such as a bimetallic Ni tetrakisphosphine oxide complex, polymeric structure containing chains of the oxide and Ni, exchange process between tetrahedral and square planar complexes) have failed.

Based on all of the evidence collected, the mechanism responsible for the oxidation of the phosphine ligand and alkene oxidative cleavage is a very complex reaction. Dr. Stanley has proposed two main mechanisms for the oxidative cleavage reaction based on the experimental evidence and DFT calculations. Unfortunately, neither of these mechanisms completely explains all experimental observations. The experimental evidence points to the idea that both oxidative processes are coupled together and alkene oxidation cannot occur without phosphine oxidation. The addition of water leads to free phosphine in solution.

This free phosphine is oxidized via a Ni species and this process then leads to the oxidative cleavage of the alkene. Once the phosphine is completely oxidized, the oxidative cleavage reaction stops. More experimentation would be required to elucidate the exact

mechanism for this transformation. However, because this is not a catalytic reaction and all efforts have failed to produce a catalytic reaction or increase the amount of product formed, care should be taken not to waste too much time on a reaction that does not appear likely to produce a viable and economical catalytic process. At best, this oxidative cleavage reaction would amount to a stoichiometric oxidative cleavage coupled with the complete oxidation of the phosphine ligands to phosphine oxides.

## CHAPTER 4: $^1\text{H}$ AND $^{31}\text{P}\{^1\text{H}\}$ NMR STUDIES OF *RAC*- AND *MESO*- $\text{Ni}_2\text{Cl}_4(\text{et},\text{ph-P4})$ , $\text{Ni}_2\text{1R}$ AND $\text{Ni}_2\text{1M}$

### 4.1 Introduction

Nuclear Magnetic Resonances (NMR) spectroscopy is one of the most powerful spectroscopic techniques for the identification and characterization of organic and organometallic complexes.<sup>1-3</sup> This technique can tell you valuable information concerning the size of the molecule (integration), the functional groups within the molecule (chemical shift) and the connectivity of the molecule (coupling constants). Any synthetic chemist involved in the synthesis of diamagnetic compounds will routinely utilize this technique to help identify and characterize any new compound.

Some of the most important nuclei investigated with NMR include  $^1\text{H}$ ,  $^{13}\text{C}$ ,  $^{19}\text{F}$  and  $^{31}\text{P}$ . These nuclei all possess a spin quantum number of  $\frac{1}{2}$  and give rise to sharp, well-resolved signals on the NMR spectra.  $^{31}\text{P}$  NMR plays a special role with transition metal chemists involved in the synthesis and characterization of diamagnetic transition metal phosphine complexes. Because of the prevalence of metal phosphine complexes in homogeneous catalysis, important information can be gathered concerning the structure of the catalyst in solution, other complexes formed during the catalytic cycle and decomposition pathways occurring during the catalytic cycle.<sup>3</sup>

Some important trends and observations have been made concerning the effects of a tertiary phosphine ligand bonding to a metal center.<sup>3-4</sup> Generally, the chemical shift of a phosphine is shifted downfield (positive ppm) upon complexing to a metal center. The magnitude of the shift depends on the donating ability of the phosphine and the nature of the metal center (electron density and oxidation state).<sup>3</sup> This can be an important trend when

investigating a reaction mixture via  $^{31}\text{P}$  NMR. This trend can make it possible to identify coordinated and non-coordinated phosphines from the observed chemical shifts.

The presence of chelate rings between the phosphines can also have a large effect on the chemical shift.<sup>4</sup> 4 and 6-membered chelate rings will show an upfield shift while the presence of a 5-membered ring will show a downfield shift. These shifts can be important when different size chelate rings are possible (like **1M** and **1R**). The 4- and 5-membered rings show the largest shifts. When a phosphine is part of two different size chelate rings, the effects are additive and can be cancelled out (e. g. one phosphine in both a 4- and 5-membered ring).

Measured coupling constants can also provide some valuable data concerning the structure of a metal complex.<sup>3</sup> Large differences are observed between phosphines oriented *cis* or *trans* to one another. The measured coupling constants between two inequivalent *trans* phosphines are usually quite large (more than 100 Hz and sometimes much larger) while the coupling constants between *cis* phosphines are much small (near 50 Hz). These differences can aid in the identification of the configuration of square planar and octahedral complexes. These trends and observations become especially important when coupled with 2-dimensional NMR techniques which allow for the identification of individual compounds present in reaction mixtures.

$^{31}\text{P}$  NMR spectroscopy has become an invaluable tool for all organometallic chemists studying diamagnetic metal phosphine complexes. This technique is an important tool for the identification of specific compounds exactly like  $^1\text{H}$  and  $^{13}\text{C}$ . The trends and observations concerning the chemical shift and coupling constants along with 2-dimensional NMR techniques make structural assignments possible when investigating reaction mixtures and can allow for very detailed reaction mechanisms to be proposed.

## 4.2 Ni<sub>2</sub>Cl<sub>4</sub>(*meso*-*et*,*ph*-P4), Ni<sub>2</sub>1M, and Ni<sub>2</sub>Cl<sub>4</sub>(*rac*-*et*,*ph*-P4), Ni<sub>2</sub>1R.

When Ni<sub>2</sub>1M or Ni<sub>2</sub>1R is dissolved in any organic solvent, an orange solution is formed. Upon the addition of water, there are very subtle color changes. The solution becomes much redder in color and darkens. This was especially evident when water was added drop-wise during the course of some alkene hydration experiments (Chapter 2). The starting orange solution immediately started becoming redder upon the addition of water and as the addition continued the solution darkened and became red/orange. NMR samples collected from some of these solutions and after an overnight experiment revealed a complex mixture of resonances that did not resemble the starting complex (Figure 4.1). This suggested that the addition of water causes several different species to form. This prompted us to begin a detailed solution-state study of both Ni<sub>2</sub>(1M) and Ni<sub>2</sub>(1R) via <sup>1</sup>H and <sup>31</sup>P{<sup>1</sup>H} NMR spectroscopy.

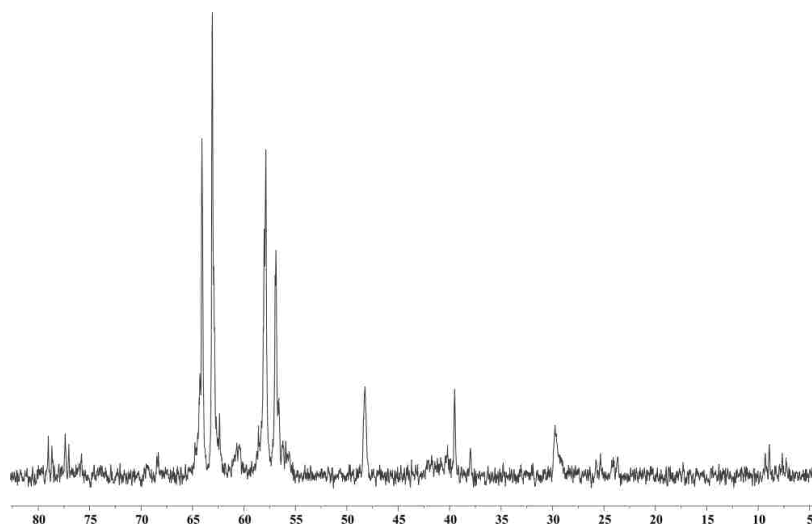


**Figure 4.1** <sup>31</sup>P NMR spectrum showing the new resonances observed when water was present.

Both Ni<sub>2</sub>1M and Ni<sub>2</sub>1R have previously been synthesized and characterized, both spectroscopically and structurally, by the group.<sup>5</sup> The <sup>31</sup>P{<sup>1</sup>H} NMR data, as reported previously, is given in Table 4.1. The group reported that both internal and external phosphine signals give rise to a doublet of triplet pattern with the coupling constants reported in Table 4.1.



The large coupling is between the internal and external phosphines *cis* to each other. The smaller coupling was explained via virtual coupling.

**Table 4.1**  $^{31}\text{P}\{^1\text{H}\}$  NMR Data for **Ni<sub>2</sub>1M** and **Ni<sub>2</sub>1R** reported.<sup>5</sup> Chemical shifts are referenced externally to 85% H<sub>3</sub>PO<sub>4</sub> and were recorded on a Bruker AC-100 with CD<sub>2</sub>Cl<sub>2</sub> as solvent. dt – doublet of triplets

		chemical shifts, ppm	coupling constants, Hz
<b>Ni<sub>2</sub>(1M)</b>	external	74.28 (dt)	72.8, 10.8
	internal	58.32 (dt)	
<b>Ni<sub>2</sub>(1R)</b>	external	75.41 (dt)	69.0, 3.9
	internal	57.97 (dt)	

**Table 4.2**  $^{31}\text{P}\{^1\text{H}\}$  NMR Data for **Ni<sub>2</sub>1M** and **Ni<sub>2</sub>1R**. Chemical shifts are referenced externally to 85% H<sub>3</sub>PO<sub>4</sub> and were recorded on Bruker DPX-250 and DPX-400 spectrometers.

		chemical shifts, ppm	splittings, Hz
<b>Ni<sub>2</sub>1M</b>	external	73.0	72.6, 10.0, 11.7
	internal	57.0	
<b>Ni<sub>2</sub>1R</b>	external	74.0	CD <sub>3</sub> CN – 69.6, 2.9 Acetone- <i>d</i> <sub>6</sub> – 73.1
	internal	56.7	CD <sub>2</sub> Cl <sub>2</sub> – 75.1

When complexes **Ni<sub>2</sub>1M** and **Ni<sub>2</sub>1R** were synthesized and characterized during the course of this work, some surprising results were obtained. Figure 4.2 shows the  $^{31}\text{P}\{^1\text{H}\}$  NMR spectra for **Ni<sub>2</sub>1M** and **Ni<sub>2</sub>1R** and Figure 4.3 depicts the  $^1\text{H}$  NMR spectra (aromatic region). Each complex gives rise to two distinct overlapping multiplets in the aromatic region with a slight difference in chemical shift between the two diastereomers. Both complexes also give rise to two sets of multiplets on the  $^{31}\text{P}$  NMR spectra that again only differ slightly in chemical shift (Table 4.2).

Initially, when looking at the  $^{31}\text{P}$  NMR spectrum for **Ni<sub>2</sub>1M**, the signals appear to be simple doublets of triplets. However, a detailed analysis of the splitting pattern has revealed that these signals are not doublets of triplets. Measurements of multiple spectra in three different solvents (acetone-*d*<sub>6</sub>, CD<sub>3</sub>CN and CD<sub>2</sub>Cl<sub>2</sub>) on two different spectrometers have revealed that this splitting is not symmetrical (Table 4.2). One of the splittings in the “triplet” pattern is 1.7 Hertz

smaller than the other. Also, as can be observed on the spectrum, there is a distinct slanting of the signals towards the center of each multiplet. This suggests that this is not a simple first order doublet of triplets but rather a second order pattern.

Inspection of the  $^{31}\text{P}$  for **Ni<sub>2</sub>1R** also reveals something surprising. The spectrum appears as two doublets with no other splitting resolved. These results were obtained in all solvents and on both spectrometers. When the spectroscopic data for this complex was initially reported, the  $^{31}\text{P}$  NMR spectrum was recorded on a 100 MHz spectrometer. The spectra obtained here were on 250 and 400 MHz spectrometers and in no case was the complete doublet of triplet pattern observed. This is most likely caused by CSA (chemical shift anisotropy) relaxation effects. For  $^{31}\text{P}$  NMR, as you go to higher field instruments these CSA effects broaden the signals observed. Depending on the size and structure of your molecule, these effects can cause you to lose valuable coupling data even with modest field strength increases. Because the reported splitting was only 3.9 Hz, the CSA relaxation effects broadened the signals enough on the spectrometers and did not allow us to observe the doublet of triplet pattern obtained on a 100 MHz machine.

On two occasions, one half of the doublet of triplet pattern was resolved. This required special data sets using a very small spectral window (for phosphorus) and very high digital resolution in order to resolve some of the splitting. But the entire doublet of triplet pattern could never be completely resolved. The measured splitting from these two experiments gave a value of 2.9 Hz. The splitting was symmetrical for this complex compared to the *meso* complex. But, the measured splitting was 1 Hz smaller than reported previously.

Another surprising aspect of this complex is the variability of the large splitting depending on solvent. For the *meso* complex, the large splitting showed no variability from solvent to solvent and gave a value of 72.6 Hz, which is in agreement with the previously

reported value of 72.8 Hz. For the *racemic* complex, the large splitting varied 2-3 Hertz from solvent to solvent (Table 4.2). Generally, coupling constants do not vary with solvent.

However, the three solvents utilized for these measurements all vary in polarity and coordination ability.

These differences could lead to different stable rotational conformations of the same complex in each solvent. Coupling constants are dependent on both the proximity between the coupled nuclei and the conformation of the molecule. Therefore, these splitting values could represent true coupling constants and the variability between the different solvents is caused by the different conformation adopted by the complex. If these splitting values are true coupling constants and the variability is caused by different stable conformations in each solvent, then these results could represent a significant challenge in the solution-state NMR study. Measured coupling constants could vary from solvent to solvent even though they are for the same complex in solution. This could lead to missed assignments and makes direct comparisons between solvent systems somewhat difficult.

### 4.3 Effect of Water on Ni<sub>2</sub>1M

As mentioned previously, during the course of the alkene hydration and oxidation experiments, samples of the reaction mixtures containing either Ni<sub>2</sub>1M or Ni<sub>2</sub>1R were collected and analyzed via <sup>1</sup>H and <sup>31</sup>P NMR. The <sup>31</sup>P NMR spectra revealed a complex mixture of resonances that did not resemble the starting complex. Experiments were conducted to first prove that water was the cause of these new signals. The only other possible causes for these new species being formed would be the substrate reacting with the complexes or the presence of air or heating the complex causing new species to form. First, both complexes were dissolved in CD<sub>3</sub>CN in air and allowed to sit for several weeks at room temperature and monitored

periodically via NMR. The spectra remained unchanged after two weeks. These experiments were repeated except that 1-hexene was added to the solution. Again, the spectra remained unchanged after two weeks. Also, heating the complex to 90°C overnight did not lead to any new resonances.

After eliminating the possibility that the substrate, air or heat was causing these changes to occur, we then set out to prove that water was the source of these changes. For this experiment **Ni<sub>2</sub>1M** was dissolved in acetone-*d*<sub>6</sub> under N<sub>2</sub>. Part of this solution was transferred to an NMR tube and the <sup>1</sup>H and <sup>31</sup>P{<sup>1</sup>H} NMR spectra were recorded. The tube was then opened to air and three drops of D<sub>2</sub>O were added. The tube was sealed and shaken and <sup>1</sup>H NMR spectra were recorded over the course of 3 hours. Figure 4.2 shows three different <sup>1</sup>H NMR spectra from this experiment. The bottom black spectrum is the bimetallic complex dissolved in only acetone-*d*<sub>6</sub> under N<sub>2</sub>. The starred peaks are residual **Ni<sub>2</sub>1R** present in the *meso* (~1%) sample used for this experiment. The red spectrum was recorded after the addition of the D<sub>2</sub>O. The top magenta spectrum was recorded 3 hours after the addition of D<sub>2</sub>O.

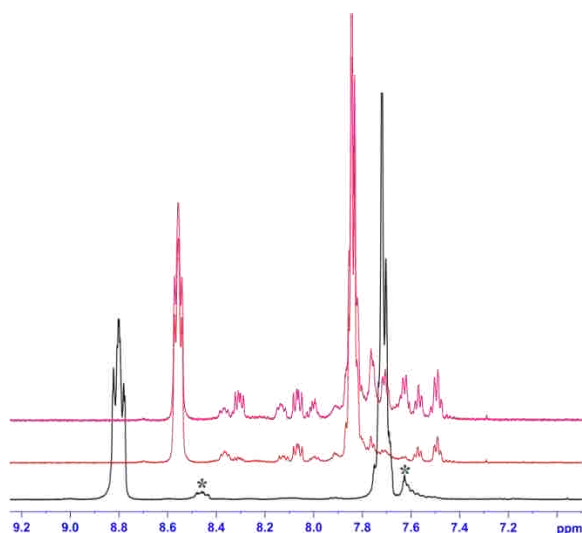


**Figure 4.2** <sup>1</sup>H NMR spectra from 6.9 ppm to 9.2 ppm. The black spectrum is **Ni<sub>2</sub>1M** dissolved in acetone-*d*<sub>6</sub>. The starred peaks are from a small amount of **Ni<sub>2</sub>1R**. The red spectrum was recorded after the tube was exposed to air and 3 drops of D<sub>2</sub>O were added from a syringe. The magenta spectrum is the same sample after 3 hours.

Clearly it is evident that several new signals begin to appear immediately and grow in intensity over time. Also evident from the comparison is the shift in the initial signals upon the addition of D<sub>2</sub>O. One shifts slightly downfield and the other shifts upfield. These shifts are caused by the addition of D<sub>2</sub>O and represent a solvent effect. Chemical shifts are solvent dependent and even the addition of a small amount of a different solvent (especially water) can cause changes in the chemical shifts.

Figure 4.3 is the <sup>31</sup>P{<sup>1</sup>H} NMR spectrum of the sample 2 hours after the addition of D<sub>2</sub>O. Again you can clearly see new species forming. Also, from this spectrum, you can see upfield resonances around -21 ppm. This indicates the presence of phosphines not coordinated to Ni. The presence of these “dangling” phosphine resonances indicate that the reaction between the complex and water leads to some phosphine dissociation from the starting Ni complex. This experiment, coupled with the fact that the addition of substrate, air and heat do not cause any change in the initial complex, clearly demonstrated that the addition of water reacts with the initial bimetallic complex to begin forming new species. These new species grow in intensity over time as the signals for the initial complex decrease in intensity.

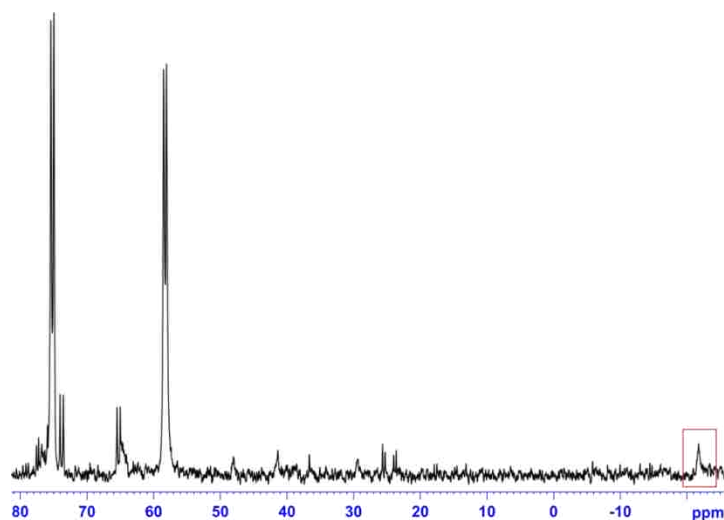


**Figure 4.3** <sup>31</sup>P{<sup>1</sup>H} NMR spectrum of Ni<sub>2</sub>1M in acetone-*d*<sub>6</sub> 2 hours after the addition of D<sub>2</sub>O. The upfield resonance indicating dangling phosphines are highlighted.

After it was shown that water was reacting with the initial bimetallic complex to create new species, an investigation was begun to better understand this reactivity. Three different organic solvents (acetone- $d_6$ ,  $CD_3CN$  and  $DMSO-d_6$ ) were selected and investigated extensively in order to determine what role the organic solvent plays in this reaction. Regular 1-dimensional and 2-dimensional ( $^{31}P$ - $^{31}P$  COSY) NMR techniques were utilized to try and better understand the reactivity with water and to characterize any of the new species. We also were interested in the effect of varying the amount of water. Different water concentrations, from 5% to 30% (by volume), were tested to see if any differences occurred during the course of the reaction. Also, some synthetic work was utilized to try and synthesize any new complexes that we believed were present during the reaction.

The NMR experiments were all conducted in the same manner. 10 mM concentrations were used for almost all experiments. This is the highest concentration that is possible in acetone/water and was utilized for almost all solvent systems. This concentration gave satisfactory signal to noise ratios on the spectra and made it possible to observe species formed in small concentrations. A few experiments conducted in acetonitrile/water were run at 20 mM concentrations but the main reason for this was to reduce the data collection time for each spectrum but maintain satisfactory signal to noise ratios. All experiments were prepared under an inert atmosphere of  $N_2$ .

Typically, 1 or 2 mL solutions were prepared and 1-3 NMR tubes were loaded using the same solution. This allowed for conditions to be changed (e.g. exposing to air, adding substrate, etc.) in one or two samples while maintaining a “standard” sample of just the complex in the solvent system under inert atmosphere to allow for direct comparisons. NMR spectra were recorded on Bruker DPX-250, DPX-400 and Varian 500 MHz spectrometers. All overnight

experiments were conducted on the DPX-400 or Varian 500 MHz machines. Both  $^1\text{H}$  and  $^{31}\text{P}$  spectra were recorded for each sample except during overnight experiments. For each  $^{31}\text{P}$  NMR spectrum recorded on the DPX-400, 512 scans were recorded which means one spectrum required almost 22 minutes to collect the data. When the Varian 500 MHz spectrometer was utilized, each spectrum required 1024 scans for sufficient signal to noise ratios. This means each spectrum required almost 45 minutes to collect the data.

#### **4.4 Effect of the Organic Solvent on the Reaction Between $\text{Ni}_2\text{1M}$ and Water**

The first experiments conducted utilized a 15% water/organic solvent system. The main reason for this was to eliminate a biphasic system when substrate was added. It was observed during the alkene hydration experiments that higher concentrations of water (30%) led to the formation of a biphasic system. The substrate still had some solubility in the water/acetone layer (observed via NMR and GC/MS) but biphasic systems are not suitable for NMR analysis so it was decided to use 15%. The three organic solvents utilized for these experiments were acetone- $d_6$ ,  $\text{CD}_3\text{CN}$  and  $\text{DMSO-}d_6$ . Two different experiments were used. The first involved preparing the NMR samples and then recording an initial spectrum. The samples were then allowed to sit for a certain period of time (2, 12, 24 hours, etc.) and then another spectrum was recorded. Spectra were recorded over the course of several days in this manner. The other experiment involved recording spectra successively over the course of a certain time period (12-24 hours). The first type produced snapshots of the reaction over longer periods of time and the second type showed the entire course of the reaction during a certain time period.

The results of these experiments are shown in Figures 4.4, 4.5 and 4.6. The spectrum on the left in each figure is the initial spectrum. The spectrum on the right is the spectrum recorded after ~24 hours. Surprisingly, all three solvent systems give rise to the same complex multiplet

after at least 24 hours of sitting at room temperature under an inert atmosphere. A close-up of this multiplet is shown in Figure 4.7. This multiplet becomes the dominant species in all three solvent systems after 24-48 hours. As the samples sit longer, this complex multiplet becomes the only species present via  $^{31}\text{P}$  NMR and remains unchanged for more than a week under an inert atmosphere. A  $^{31}\text{P}$ - $^{31}\text{P}$  COSY experiment proved that this complex multiplet is for one species. This complex will be labeled **F**, the final species. The time required for **F** to become the only species present varies between the three solvents. DMSO requires the least amount of time, followed by  $\text{CD}_3\text{CN}$  and then acetone.

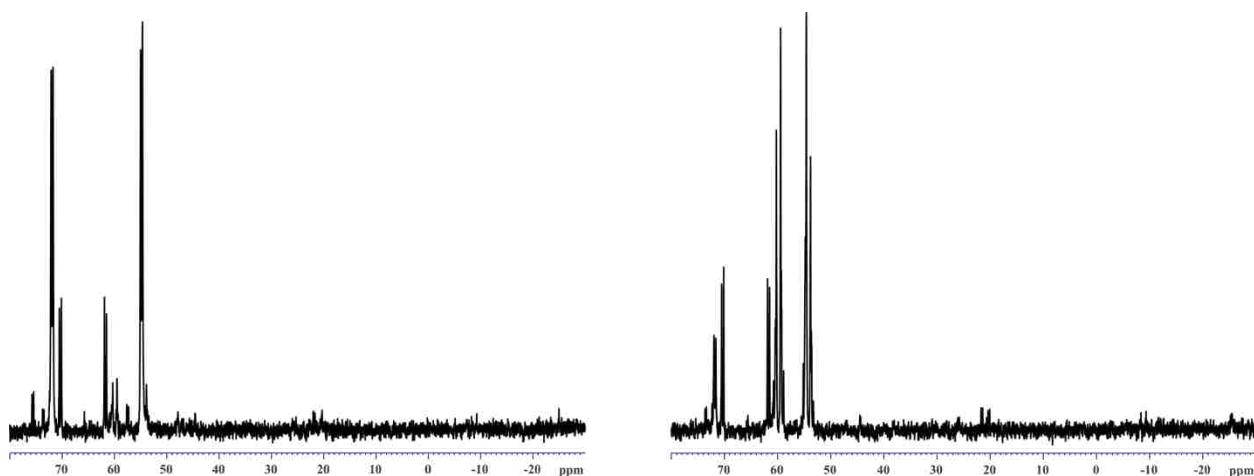


**Figure 4.4**  $^{31}\text{P}$  NMR spectra of  $\text{Ni}_21\text{M}$  in 15% water/acetone- $d_6$ .

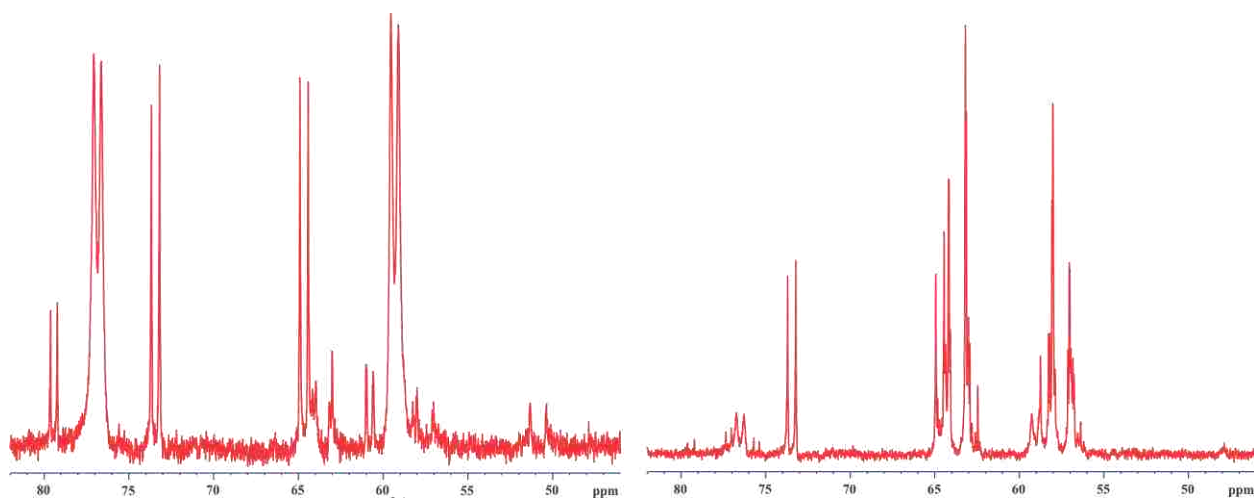


**Figure 4.5**  $^{31}\text{P}$  NMR spectra of  $\text{Ni}_21\text{M}$  in 15% water/ $\text{CD}_3\text{CN}$ .



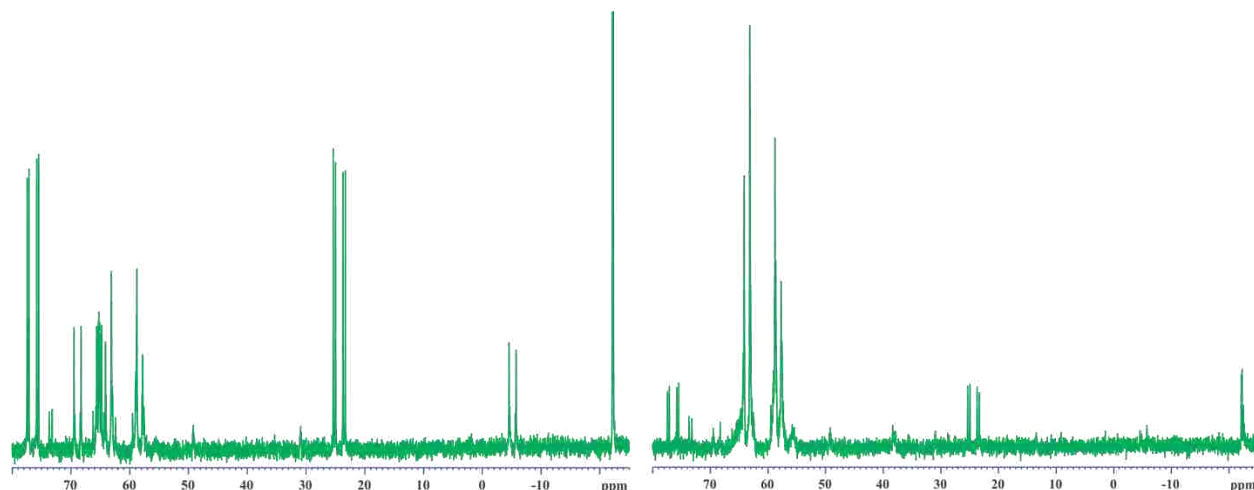


**Figure 4.6**  $^{31}\text{P}$  NMR spectra of  $\text{Ni}_21\text{M}$  in 15% water/ $\text{DMSO-}d_6$ .

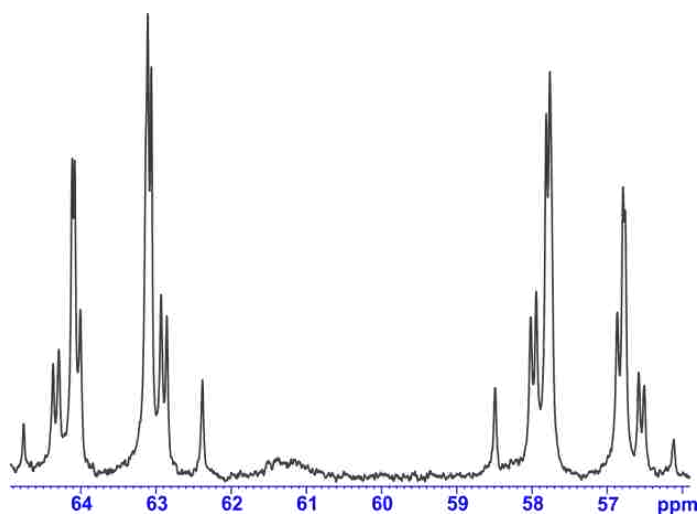


**Figure 4.7** Close-up of the complex multiplet that arises after  $\text{Ni}_21\text{M}$  is dissolved in 15% water/organic solvent and sits for at least 24 hours.

When acetone was used as the organic solvent, some variability occurred in the initial spectra. This was a result of how the samples were prepared for NMR analysis. Initially all samples made with water/acetone were heated to completely dissolve the complex then cooled completely to room temperature before prepared the NMR samples. This led to differences in the initial spectra that made comparison between experiments difficult. It was found that if the complex/acetone/water mixture was allowed to stir for 30 minutes to an hour at room temperature, the complex would completely dissolve and this variability was mostly removed. Figure 4.8 shows the difference between initial spectra heated (left) and not heated (right).

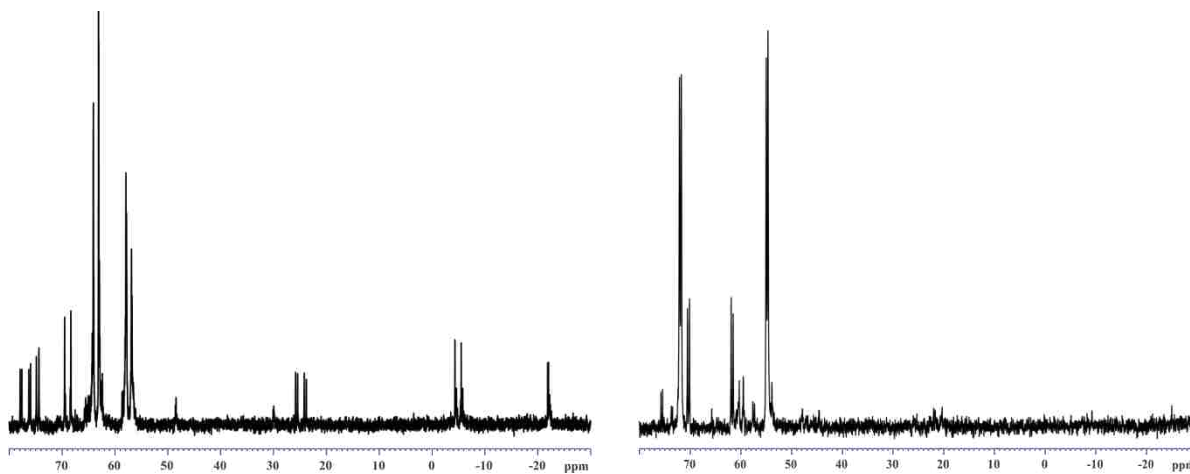


**Figure 4.8** Comparison between heating (left) the acetone/water mixture and not heating (right).

The initial spectra for both acetone and acetonitrile look very similar. These spectra clearly show significant broadening occurring on the signals for the initial complex (72 and 54 ppm for acetone and 77 and 59 ppm for acetonitrile). This broadening does not allow for any splitting to be observed for the initial complex. The broadening could result from a chloride ligand dissociating and then adding back to the complex rapidly. No new signals would be observed because of the speed with which this process occurs. It could also arise from a fast association/dissociation process between the complex and the added water. A water molecule could add to the Ni centers forming an 18 electron complex and then dissociate reforming the starting complex. Depending on the speed of this process, it could manifest itself as the broadening observed and new signals would not be observed. Inspection of the initial spectrum for DMSO does not reveal any broadened signals for the initial complex. In fact no signals are observed for the starting complex in the initial spectrum. These observations show that the reaction between the complex and water is accelerated when DMSO is the organic solvent.

Inspection of the spectra for all three solvent systems after 24 hours reveals the magnitude of the changes that occur during this reaction with water. For all three spectra, the only resonances that have increased in intensity are for **F**. All other resonances have reduced in

intensity except for two doublets (70.3 and 61.8 ppm in acetone and 73.5 and 64.7 in acetonitrile). These two doublets remain unchanged throughout the course of these experiments.  $^{31}\text{P}$ - $^{31}\text{P}$  COSY experiments conducted have shown very strong cross-peaks between these two sets of doublets proving they are one symmetrical complex, species **A**. The COSY experiments have helped in identifying other specific complexes present during the reaction, including **F**.

However, the changes that occur represent a problem for these experiments. Typically the COSY experiments required at least 20 hours of data collection to get satisfactory results. Because the changes are occurring as this data is recorded, some correlations were difficult to make with absolute certainty because of weak or missing cross-peaks. Another issue encountered during the COSY experiments is the overlapping signals that are present on all of the spectra. These overlapping signals again made it difficult to determine exact correlations between different resonances.

Despite the difficulties encountered during the COSY experiments, some very useful information has been gathered concerning the reactivity towards water. These experiments have shown that every major species present during the course of this reaction is a symmetrical complex with only one exception. Because of the structure of the tetrakisphosphine ligand, any unsymmetrical complex would give rise to 4 distinct resonances on the  $^{31}\text{P}$  NMR spectra. Only one species showed correlations to 4 distinct resonances, meaning this species is an unsymmetrical complex, species **C**. All other complexes, including the initial complex, **A** (Figure 4.9), **F** (Figure 4.7) and species **B** (Figure 4.10), show correlations between only two sets of resonances, meaning all of these complexes are symmetrical. Thus 5 major species have been identified via these COSY experiments (the initial complex, **A**, **B**, **C** and **F**). There are other

resonances observed during the course of these reactions. However, their intensities were always very low and in some cases were not observed.

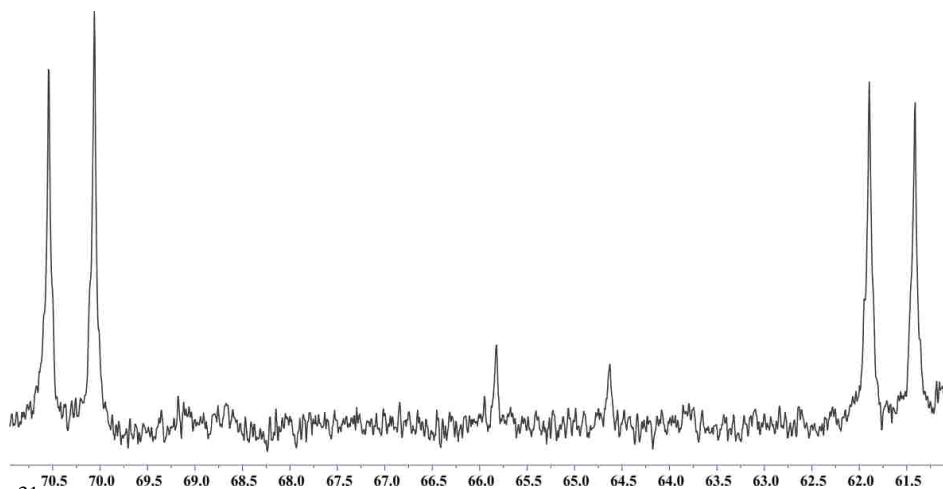


**Figure 4.9**  $^{31}\text{P}$  NMR spectrum showing the symmetrical doublets of **A** (70.3 ppm and 61.8 ppm in acetone/water). The small peaks in the center are for species **B**.

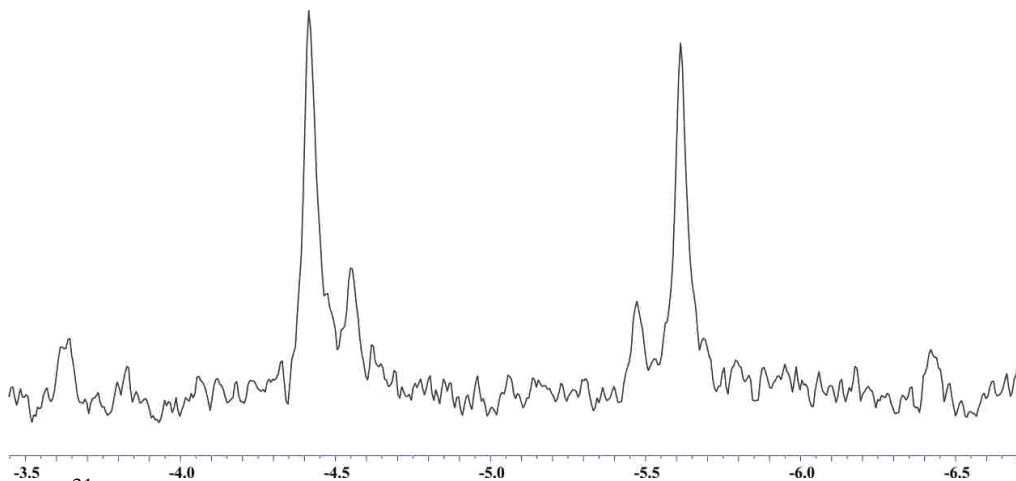


**Figure 4.10**  $^{31}\text{P}$  NMR spectrum showing one symmetrical multiplet assigned to species **B**. The other resonance appears at 65.2 ppm (small peaks in Figure 4.11).

Figure 4.11 shows the four distinct resonances that give rise to the one identifiable unsymmetrical species present in this reaction. There are two doublets of doublets (dd), one present downfield and the other present upfield. The downfield dd has coupling constants of 267 and 53 Hz. The upfield dd has coupling constants of 267 and 63 Hz. The large coupling constant of 267 Hz suggests *trans* coupling between two phosphines coordinated to a Ni center. The two smaller coupling constants of 53 and 64 Hz suggest two different *cis* couplings. The other

resonances give rise to a doublet at -22 ppm with a coupling constant of 26 Hz and a doublet of doublets of doublets (ddd) with coupling constants of 64, 53 and 26 Hz.

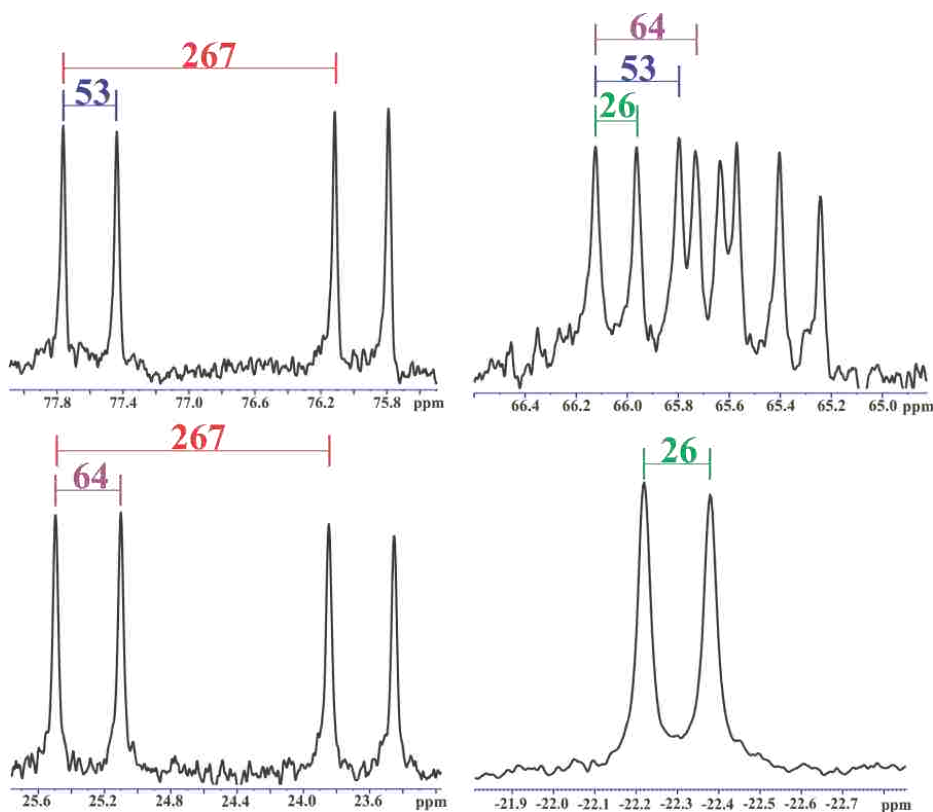


**Figure 4.11** The four distinct resonances observed for the unsymmetrical species **C** with measured coupling constants shown. This spectrum was recorded in DMSO- $d_6$  without any water present.

These coupling constants were measured on both the 250 MHz and 400 MHz spectrometers and did not change showing they are true coupling constants. Two possible unsymmetrical complexes are shown in Figure 4.12. The chemical shift differences observed for the 4 non-equivalent phosphines can be explained by two ideas. The one negative value versus the three positive values represents one phosphine not coordinated to the Ni (“dangling” phosphine) and three phosphines bound to the metal. The large differences between the three bound phosphines come about because of the different chelate rings being formed. It is known that different size chelate rings in transition metal/phosphine complexes can show downfield or upfield shifts in the chemical shift relative to non-chelating metal/phosphine complexes. 4-

membered chelates tend to show large upfield shifts while 5-membered chelates tend to show fairly large downfield shifts. 6 and 7-membered chelates show much smaller shifts upfield and downfield respectively.

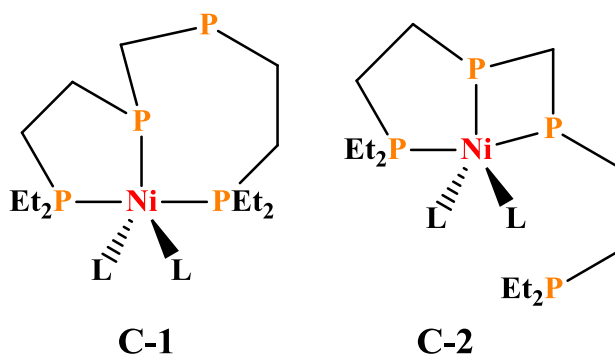


**Figure 4.12** Two possible unsymmetrical complexes for species **C**. The phenyl groups on the two internal phosphines have been omitted.

The downfield doublet of doublets centered near 77.7 ppm would be part of a 5-membered chelate ring and cause the downfield shift. The upfield dd centered near 24.5 ppm suggests this phosphorus is part of a 4-member chelate. These chelates show some of the largest shielding and results in large upfield shifts. A 7-membered chelate usually shows a small downfield shift which is not being observed in these resonances. The ddd resonance would be a part of both chelate rings and the affects would be nearly cancelled.

Thus, the chemical shift data suggests that **C-2** is the most likely structure. However, the coupling constants do not support this assignment. The ddd resonance shows two different *cis* couplings of 64 and 53 Hz. This is in line with the structure presented. However, this phosphine should not be coupled to the dangling phosphine. That would represent a 5-bond coupling and those typically are not observed. The coupling constants, therefore, point to **C-1** as being the most likely structure for this unsymmetrical species.

## 4.5 Varying the Concentration of Water

After observing the complete reaction in the 3 15% water/organic solvent systems, we next wanted to observe what effect varying the water concentration had on this reaction. These experiments were conducted in the same manner as the previous NMR experiments except that the amount of added water was varied from 5 to 30%. Acetone and acetonitrile were the two solvents investigated. When **Ni<sub>2</sub>1M** was dissolved in DMSO without any added water the <sup>31</sup>P NMR spectrum (Figure 4.13) showed the formation of new species.

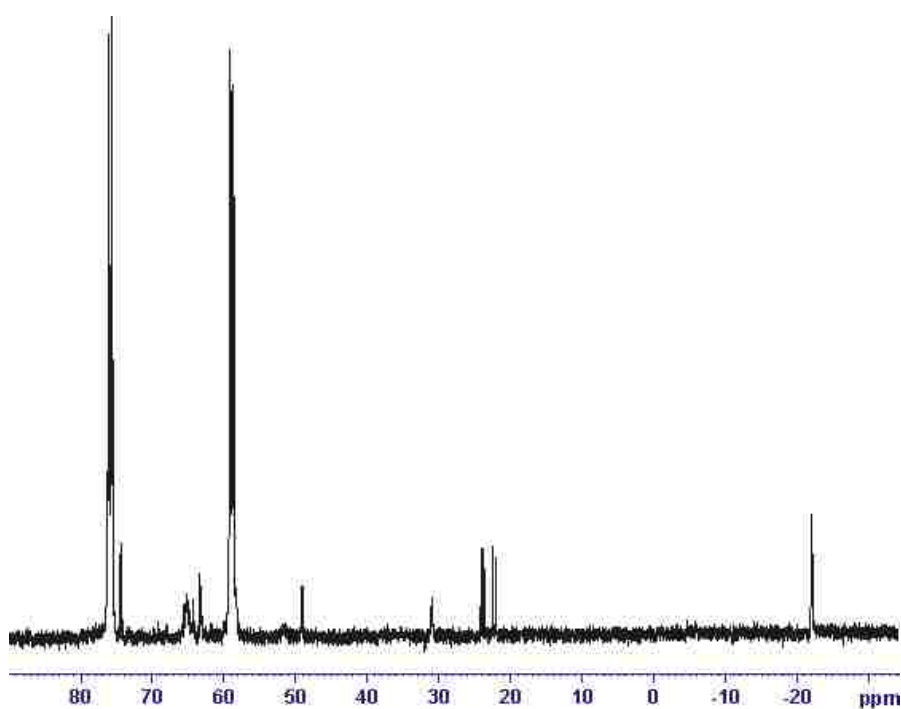


**Figure 4.13** <sup>31</sup>P NMR spectrum of **Ni<sub>2</sub>1M** dissolved in DMSO-*d*<sub>6</sub>.

This spectrum remained unchanged throughout the course of several days under an inert atmosphere or in air. The peaks for the initial complex are broadened like that observed in acetone/water and acetonitrile/water. The main species formed appears to be **C**, the unsymmetrical species. The downfield dd is overlapping with the initial complex resonances and is not completely seen but the upfield dd can be seen on the spectrum as can the doublet near -22 ppm. The ddd resonance is difficult to see but that is because of the small concentration of this

species. A closeup of the region between 66 and 64 ppm does reveal some small peaks that could be the ddd but they are not fully resolved. Upon the addition of any amount of water the changes begin to occur and lead to **F** becoming the dominant species within one day. It appears that **A** could also be formed because of the presence of the two doublets (74.5 ppm and 63 ppm) between the signals for the initial complex.

The acetone and acetonitrile solvent systems showed some interesting results when the concentration of water was varied. For both solvent systems, the addition of only 5% of water caused identical spectra for both solvent systems. An example of one is shown in Figure 4.14. There appears to be only one new species that is formed.

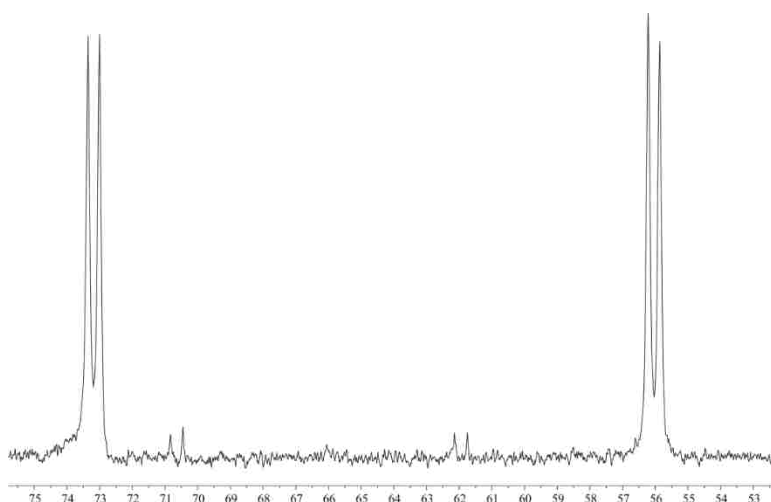


**Figure 4.14**  $^{31}\text{P}$  NMR spectrum observed in both acetone and acetonitrile with 5% water.

Based on the spectra, the species formed is **A**. Both the initial complex and **A** remain unchanged with 5% water in both solvent systems. Over long periods of time (a week or longer), there does appear to be other small symmetrical resonances that form. Some overlapping with the initial complex resonances occurs making it difficult to say for certain whether these are truly symmetrical. Based on these results, clearly the first reaction that occurs is the transformation of the initial complex to **A**. With only 5% water, the remaining reaction does not occur and **B**, **C** or **F** is not formed.



An increase to 10% water allows for the reaction to take place that leads to the formation of **F**. The reaction is slowed down in both solvent systems (Figures 4.15 and 4.16) but **F** still becomes the dominate species.

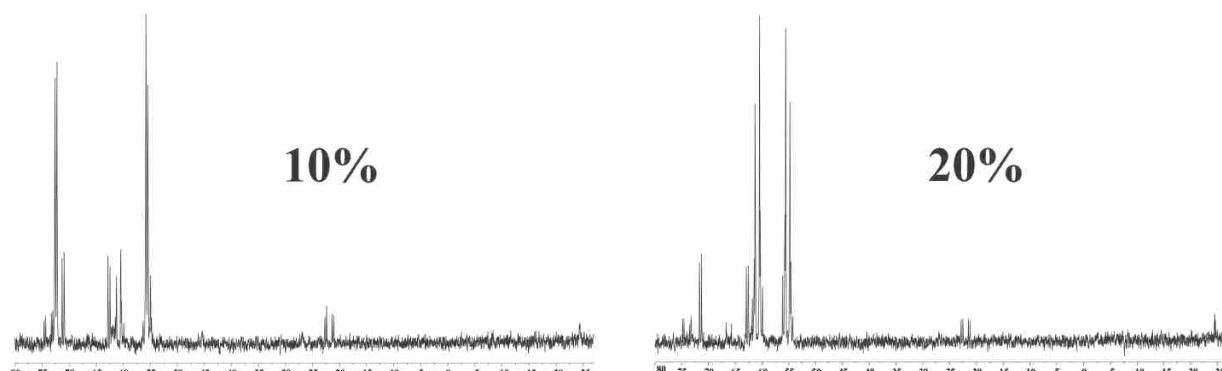


**Figure 4.15** <sup>31</sup>P NMR spectra of **Ni<sub>2</sub>1M** in 10% (left) and 20% (right) water/acetone. Both spectra were recorded after 24 hours.

With acetonitrile as the organic solvent, the effect of less water is not as pronounced as with acetone. **F** still becomes the major species in acetonitrile with 10% water after sitting for 24 hours. However, there are still large peaks present for the initial complex. These large peaks are not observed with 15% water after 24 hours. With acetone as the organic solvent, **F** is not observed after 24 hours with 10% water. After several days the resonances for **F** are observed and after more than a week they become the dominant species. Clearly, the reaction with water is slowed down in acetone much more than in acetonitrile.

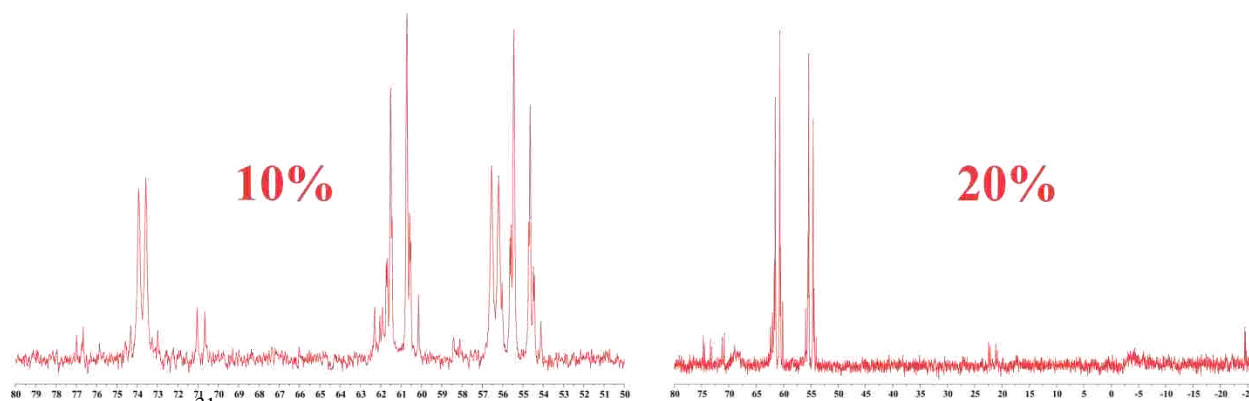


**Figure 4.16** <sup>31</sup>P NMR spectra of **Ni<sub>2</sub>1M** in 10% (left) and 20% (right) water/acetonitrile. Both spectra were recorded after 24 hours.

An increase to 20% water caused this reaction to speed up (Figures 4.15 and 4.16). In acetonitrile, the signals for the initial complex have completely disappeared after 24 hours and **F** has become the dominant species. With acetone, the initial signals are still present after 24 hours but their intensities have decreased significantly compared to the 15% water reactions. Again, **F** has become the dominant species. Increasing the water to 30% causes a dramatic change in the rate of the reaction. Figure 4.17 shows the initial spectrum for **Ni<sub>2</sub>1M** in 30% water/acetone.

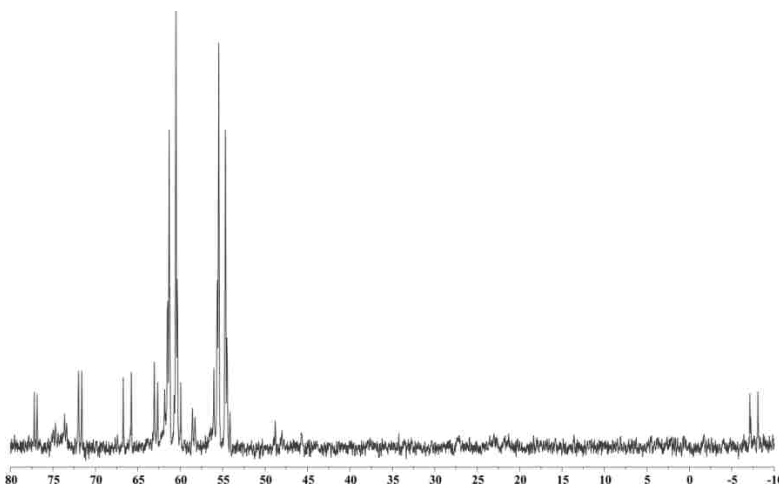


**Figure 4.17**  $^{31}\text{P}$  NMR spectra of **Ni<sub>2</sub>1M** in 30% water/acetone. The spectrum shown is for the initial spectrum.

The initial complex has almost completely disappeared and **F** is the largest complex present. There are small resonances present but they are nowhere near as large as with smaller amounts of water. With acetonitrile no other species are observed on the initial spectrum besides **F**.

#### **4.6 Identification of F and Attempts to Synthesize A, B and C**

After observing the reaction between **Ni<sub>2</sub>1M** and water under all of these conditions, many attempts were made to try and independently synthesize these newly-formed complexes. The first synthetic attempts were made towards identifying **F**. In every solvent system tested and with the addition of more than 5% water this species becomes the only species present via  $^{31}\text{P}$  NMR. The complex multiplet that arises for this complex is unlike any other observed during

the course of this reaction. It is a symmetrical pattern which points to this species being a symmetrical complex. The complex splitting pattern suggests that this complex is not composed of one molecule of **1M**. Our group has crystallographically characterized bimetallic Rh complexes containing two molecules of the tetraphosphine ligand (**1M** or **1R**). Detailed NMR analysis of these complexes was not conducted. However, the presence of two ligands in a bimetallic complex could lead to a very complex coupling pattern depending on the symmetry of the molecule and the conformation of the ligand within the molecule.

One experimental observation that points to the idea of a bimetallic Ni complex with two molecules of **1M** was observed during the reactions conducted in water/acetonitrile. It was observed that after 24 hours, a biphasic mixture was formed. A very small green layer is observed that separates out of the water/acetonitrile layer. The green color suggests that this tiny layer contains some NiCl<sub>2</sub> and because the layer settles to the bottom of the NMR tube (or flask when conducted on the bench-top) this suggests that the liquid is water. This tiny separation into two layers was observed for every reaction conducted with acetonitrile and more than 5% water. A double **1M**-bimetallic Ni complex would have a 1:1 ratio of **1M** to Ni. However, the starting bimetallic complex has a ratio of 1:2. This suggests that free NiCl<sub>2</sub> is present during this reaction and causes a small amount of water to separate from the water/acetonitrile layer leaving a 1:1 ratio in the water/acetonitrile layer. This separation is not observed in any other solvent system. However, because the same complex multiplet is observed in each solvent system, free NiCl<sub>2</sub> has to be present in all solvent systems.

To prove that this complex multiplet is caused by a double ligand complex formed in solution a simple experiment was conducted. Ni(BF<sub>4</sub>)<sub>2</sub> was dissolved in ethanol to form a light green solution. Next, 1 equivalent of **1M** was dissolved in ethanol and added drop-wise via

cannula to the rapidly stirring Ni solution under an inert atmosphere. The solution became yellow and then slightly yellow-orange as the addition proceeded. After the addition was complete, the flask was opened and 1 equivalent of NaCl was added. The solution immediately darkened to more of an orange-red color and as it stirred, a red powder precipitated.

The next day, the red powder was collected and NMR analysis revealed the  $^{31}\text{P}$  NMR spectrum in Figure 4.18. The spectrum shows a complex multiplet composed of 22 distinct lines exactly like what is observed during the water/organic solvent reactions.

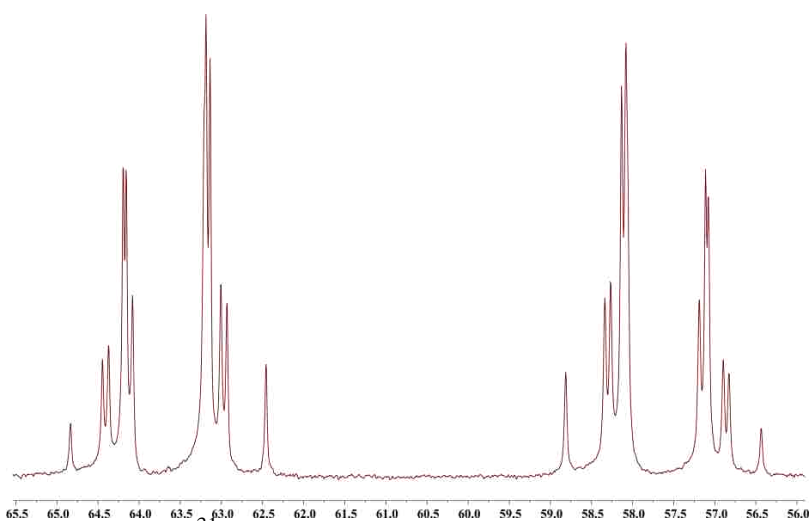


**Figure 4.18**  $^{31}\text{P}$  NMR spectrum of  $[\text{Ni}_2(\mu\text{-Cl})(\mathbf{1M})_2][\text{BF}_4]_3$

Slow evaporation of a concentrated dichloromethane solution in air produced crystals suitable for single-crystal X-ray diffraction. The crystal structure proved this complex multiplet is for a double ligand/bimetallic Ni complex,  $[\text{Ni}_2(\mu\text{-Cl})(\mathbf{1M})_2][\text{BF}_4]_3$  (**F**). An ORTEP plot of this complex is shown in Figure 4.19. The complex crystallizes in the  $\text{P}2_1/\text{c}$  space group with each Ni center possessing square pyramidal geometry with four of the phosphines occupying the basal plane and the bridging chloride ligand in the axial position for both square pyramids.

After the successful synthesis and characterization of **F**, many attempts were made to try and synthesize other complexes that could be present during the reaction with water. A lot of work focused on the addition of variable amounts of  $\text{AgBF}_4$  because chloride dissociation has to

play a role in the reaction between  $\text{Ni}_2\mathbf{1M}$  and water.  $\text{Ni}_2\mathbf{1M}$  was allowed to react with 1, 2 or 4 equivalents of  $\text{AgBF}_4$  in acetone. NMR analysis of these solutions after removing the precipitated  $\text{AgCl}$  revealed very broad peaks that did not resemble any stable species. Removal of the acetone under vacuum and redissolving the solid residue in another solvent did lead to the formation of well-resolved spectra.

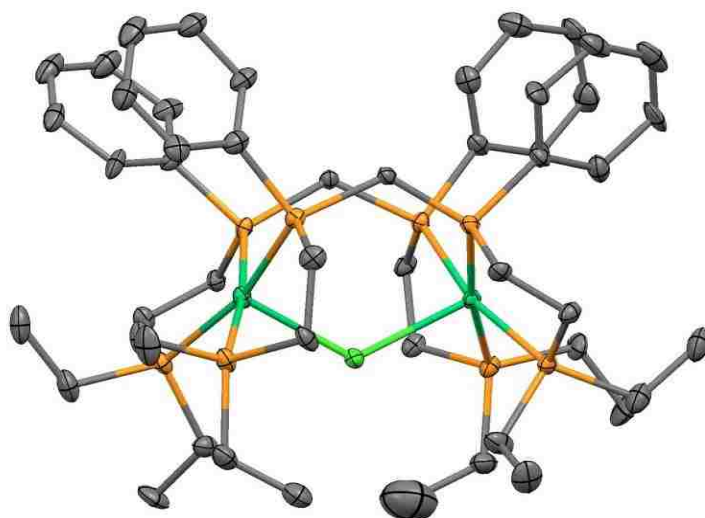


**Figure 4.19** ORTEP plot for  $[\text{Ni}_2(\mu\text{-Cl})(\mathbf{1M})_2][\text{BF}_4]_3$ . Hydrogen atoms have been omitted for clarity. The two Ni centers are shown in green. The Cl ligand is light green. The P atoms are orange and the C atoms are black.

The most important results were obtained with 4 equivalents of  $\text{AgBF}_4$ . When the residue is dissolved in acetonitrile, NMR analysis revealed the spectrum shown in Figure 4.20. The major species present corresponds to **B** with a minor amount of **F** present. As this sample sat **F** began to grow in intensity as **B** decreased in intensity. This indicates that **B** is a precursor to **F**. Also, because **F** is formed and continues to increase in concentration, the 4 equivalents of  $\text{AgBF}_4$  do not remove all four chlorides from the complex.

The addition of water to the acetonitrile solution actually stops the transformation of **B** to **F**. This was very surprising considering it was the addition of water to the Ni complexes that

causes the formation of **F**. Because of the symmetrical nature of the resonances, the complex has to be symmetrical. The extremely large difference in chemical shift (71.4 ppm and -0.9 ppm) suggests the two non-equivalent phosphines are in two very different chemical environments. One possibility to explain this could be different chelate ring sizes but complexes of that type are not expected to be symmetrical and would not give rise to the two symmetrical resonances observed. All attempts to crystallize this complex failed to give X-ray quality single crystals.

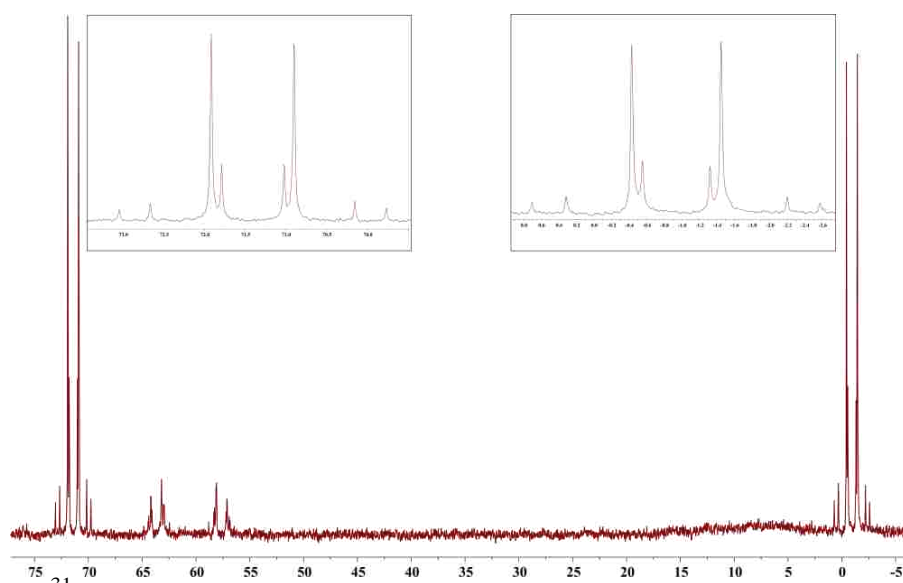


**Figure 4.20**  $^{31}\text{P}$  NMR spectrum of the solid residue dissolved in acetonitrile after reacting **Ni<sub>2</sub>1M** with 4 equivalents of  $\text{AgBF}_4$  in acetone.

Dissolving the residue in DMSO after removal of  $\text{AgCl}$  produces the spectrum shown in Figure 4.21. The spectrum clearly shows **C**, the unsymmetrical species, as being the dominant complex present. There is one other significant species present which gives rise to a resonance centered at -2.5 ppm. This resonance is significantly broadened and has not been identified. Unlike in acetonitrile, the spectrum remains unchanged after sitting for several days. **F** does not form during this time. Also, when water is added, **F** does not form. There are other resonances that begin to appear on the spectra over several days and grow in intensity but the resonances are

not those observed during the previous NMR experiments and remain unidentified. Again, all attempts to try and crystallize the unsymmetrical complex failed to give single crystals suitable for X-ray analysis.

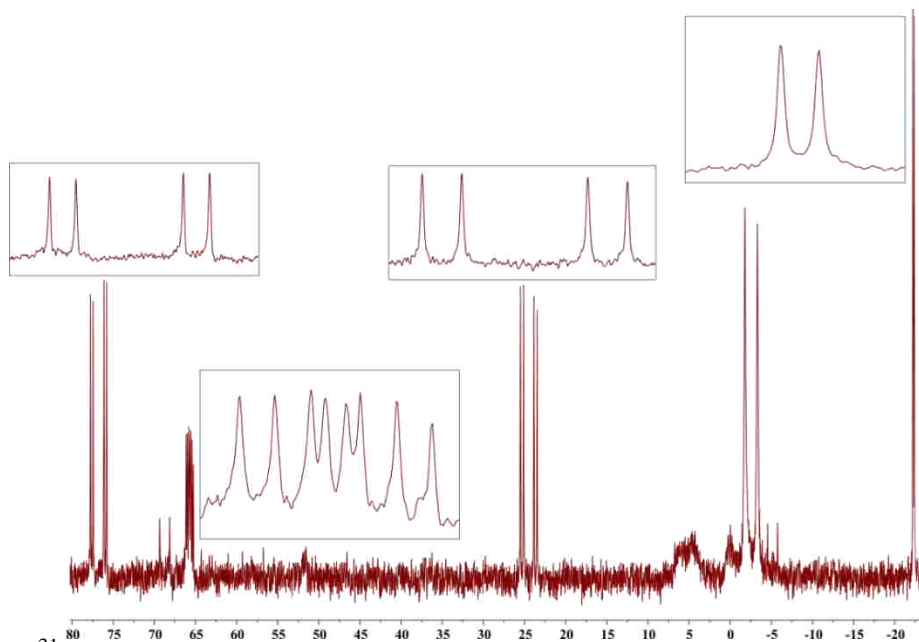


**Figure 4.21**  $^{31}\text{P}$  NMR spectrum of the solid residue dissolved in DMSO after reacting  $\text{Ni}_2\mathbf{1M}$  with 4 equivalents of  $\text{AgBF}_4$  in acetone.

#### 4.7 $\text{Ni}_2\mathbf{1R}$ and Water

All of the previous discussions have focused solely on the reaction between water and  $\text{Ni}_2\mathbf{1M}$ . Some of the same experiments were conducted with  $\text{Ni}_2\mathbf{1R}$  to determine how this complex reacts with water. These experiments were conducted in the same manner as the experiments with  $\text{Ni}_2\mathbf{1M}$ . Acetonitrile was the only organic solvent utilized for these experiments.  $\text{Ni}_2\mathbf{1R}$  has even worse solubility in acetone and a 10 mM concentration was not possible with any water/acetone solvent system. The previous experiments have shown that this concentration is the lowest concentration for obtaining high quality NMR spectra with satisfactory signal to noise ratios. Therefore, acetone could not be used as an organic solvent. Dissolving  $\text{Ni}_2\mathbf{1R}$  in DMSO with any amount of water produces the spectrum shown in Figure

4.22. This solvent system produces a complex that gives rise to two pseudo-triplets, one centered at 43.8 ppm and the other centered at 25.6 ppm. No other signals are present and the spectrum remains unchanged for several days. Therefore, the only solvent system investigated with **Ni<sub>2</sub>1R** was water/acetonitrile.

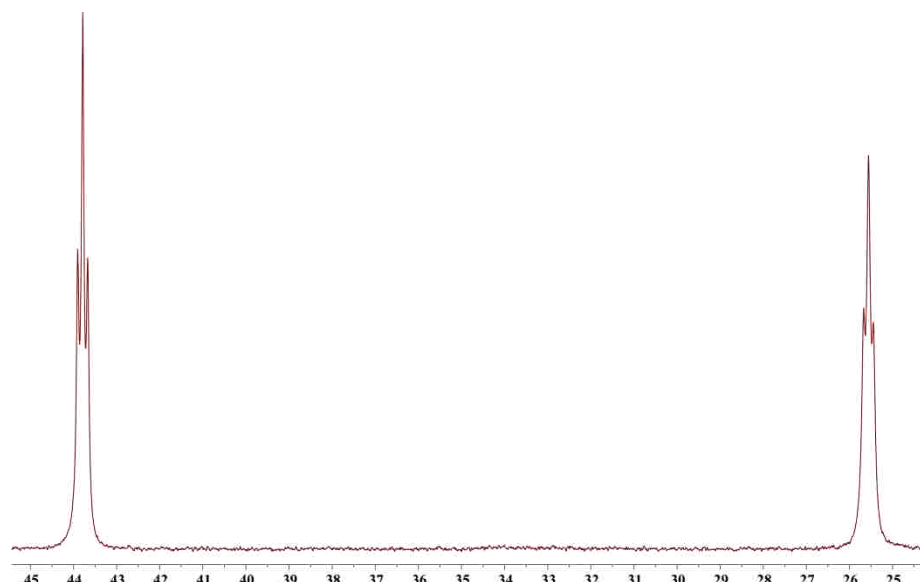


**Figure 4.22** <sup>31</sup>P NMR spectrum of **Ni<sub>2</sub>1R** dissolved in 15% water/DMSO

The *racemic* complex was investigated in 5, 10 and 15% water/acetonitrile. The results of these experiments are shown in Figures 4.23, 4.24 and 4.25. The spectra on the left are the initial spectra and the spectra on the right were recorded after sitting under N<sub>2</sub> for 24 hours. The initial resonances (73-75 ppm and 57-59 ppm) for **Ni<sub>2</sub>1R** are extremely broadened. This leads to very poor signal to noise ratios on the initial spectra. The broadening is exactly what is observed for **Ni<sub>2</sub>1M** and comes about from a rapid chloride dissociation/addition or a rapid addition-dissociation between the water molecules and the Ni centers. One major difference between **Ni<sub>2</sub>1R** and **Ni<sub>2</sub>1M** is observed in the experiment conducted with 5% water/acetonitrile (Figure 4.23).

With the *meso* complex, only one new complex was formed (**A**) and the reaction leading to **F** does not occur. This is not the case with the *racemic* complex. Initially there is only one



new complex that forms with 5% water. This new complex gives rise to two multiplets, one centered at 69.7 ppm and the other at 61.5 ppm and these resonances remain static for several days. The behavior of this complex is very similar to **A** and this complex will be labeled **A-1R**. Over time two new resonances begin to appear and slowly grow in intensity. These new resonances give rise to the two pseudo-triplets observed when **Ni<sub>2</sub>1R** is dissolved in water/DMSO. Over the course of several days these resonances grow in intensity and eventually become the major species observed on the spectrum.

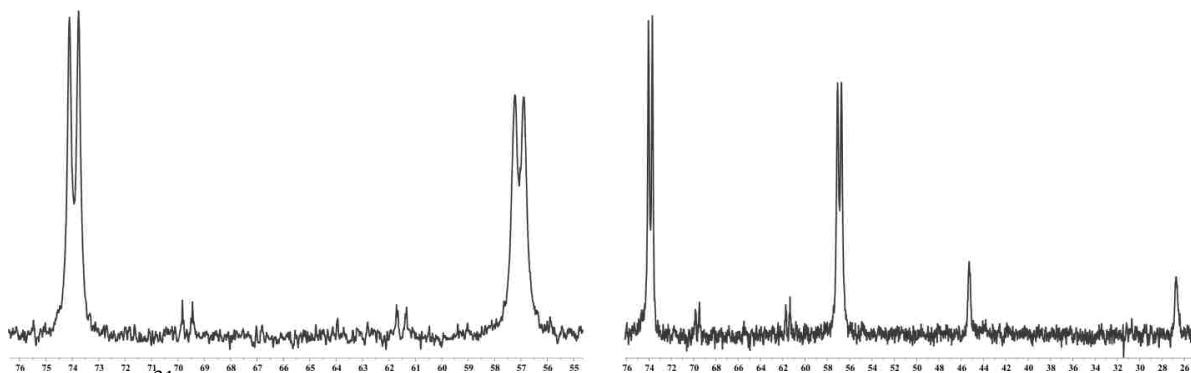


**Figure 4.23**  $^{31}\text{P}$  NMR spectra of **Ni<sub>2</sub>1R** in 5% water/acetonitrile. The spectrum on the left is the initial spectrum and the spectrum on the right was recorded after 24 hours.

This same behavior is observed in both 10% and 15% water/acetonitrile as seen in Figures 4.24 and 4.25. However, in the initial spectra the two pseudo-triplets have already formed. After 24 hours, these two new resonances have become the dominant signals present on the spectra. This behavior is analogous to the behavior of **F**,  $[\text{Ni}_2(\mu\text{-Cl})(\mathbf{1M})_2]^{+3}$ , from **Ni<sub>2</sub>1M**. This suggests that the *racemic* complex also reacts with water and this reaction leads to the formation of a bimetallic Ni/double ligand complex. The formation of this complex, **F-1R**, is accelerated as you increase the concentration of water just like with the *meso* complex. Based on these results, it appears that **Ni<sub>2</sub>1R** is more reactive towards water since only 5% water leads to the formation of **F-1R**, the proposed double ligand complex. No other resonances were

identified during the course of these experiments. All of the resonances observed are symmetrical which shows that the two new complexes formed, **A-1R** and **F-1R**, are symmetrical.

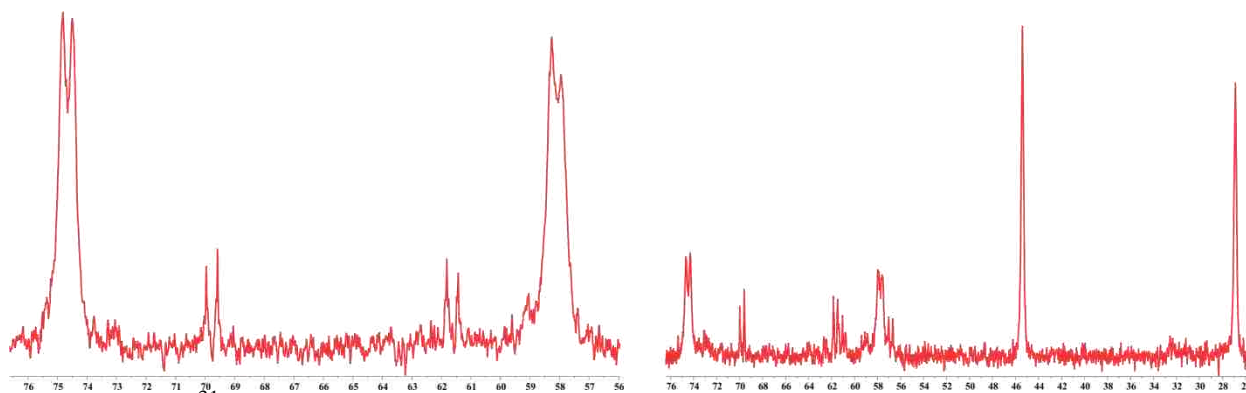


**Figure 4.24**  $^{31}\text{P}$  NMR spectra of  $\text{Ni}_2\mathbf{1R}$  in 10% water/acetonitrile. The spectrum on the left is the initial spectrum and the spectrum on the right was recorded after 24 hours.

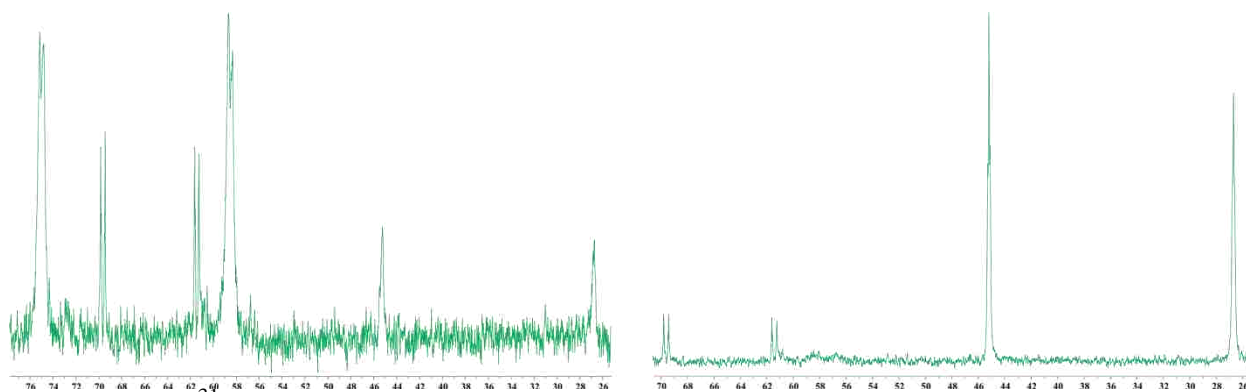


**Figure 4.25**  $^{31}\text{P}$  NMR spectra of  $\text{Ni}_2\mathbf{1R}$  in 15% water/acetonitrile. The spectrum on the left is the initial spectrum and the spectrum on the right was recorded after 24 hours.

As these solutions sit for longer periods of time, other resonances begin to form and grow in intensity over time. The two pseudo-triplets decrease in intensity as these new resonances increase which suggests that **F-1R** falls apart and leads to the formation of these resonances. Figure 4.26 shows a spectrum recorded after  $\text{Ni}_2\mathbf{1R}$  was dissolved in 15% water/acetonitrile and sat for 22 days under  $\text{N}_2$ . The four inserts show the splitting patterns for these four new signals. Analysis on both the 400 and 500 MHz spectrometers gives the same splittings proving that these are indeed coupling constants.

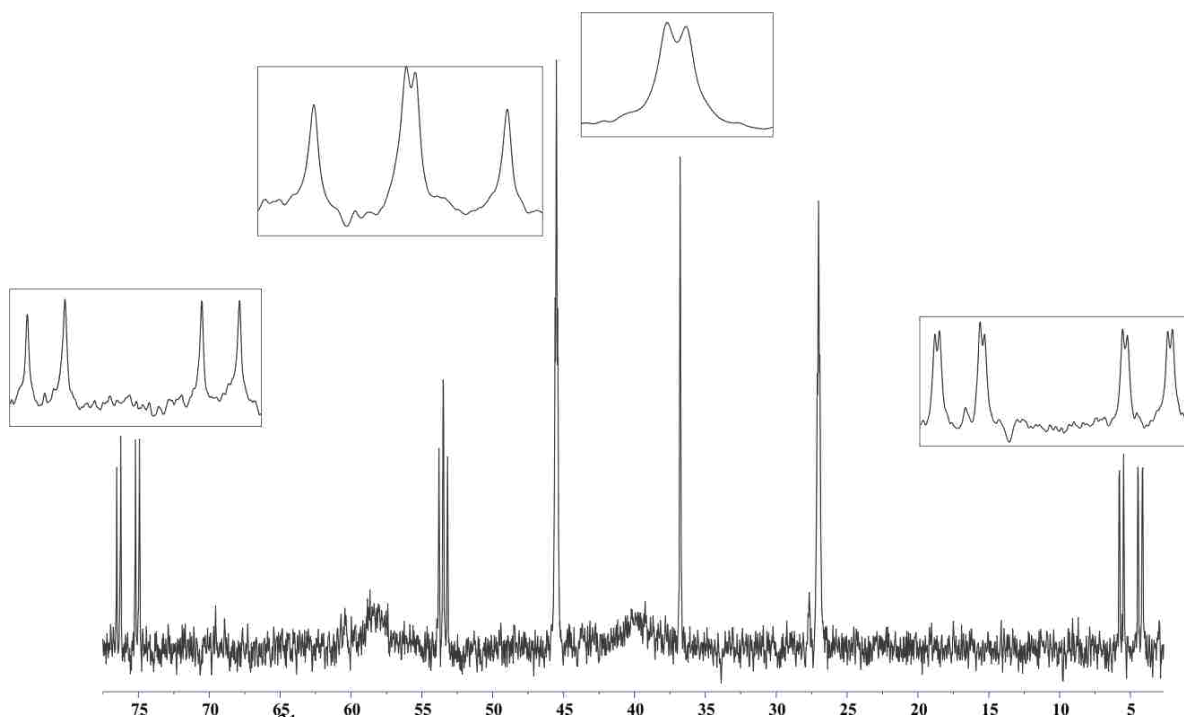


**Figure 4.26**  $^{31}\text{P}$  NMR spectrum of **Ni<sub>2</sub>1R** dissolved in 15% water/acetonitrile after sitting under  $\text{N}_2$  for 22 days.

A COSY experiment has shown that these four resonances are coupled to each other proving that these four resonances are caused by a new unsymmetrical species, **C-1R**. The downfield doublet of doublets centered at 76 ppm has coupling constants of 267 and 58 Hz. The doublet of doublets centered at 54 ppm has coupling constants of 64 and 58 Hz. The doublet centered at 37 ppm has a coupling constant of 7 Hz. The upfield doublet of doublets of doublets has coupling constants of 267, 64 and 7 Hz. The large coupling constant of 267 Hz suggests a *trans* coupling between two nonequivalent phosphines and the two different smaller coupling constants of 64 and 58 Hz suggests two different *cis* couplings. The coupling constant of 7 Hz suggests a long range coupling constant through the ligand backbone and not a coupling through a metal center. The downfield and upfield chemical shifts suggest two different size chelate rings, a 5 membered and a 4 membered chelate ring. Based on this analysis the most likely structure is a monometallic Ni complex with three bound phosphines and one dangling phosphine (Figure 4-12, complex **C-2**).

One problem with this assignment is the fact that the dangling phosphine resonance is centered at 37 ppm. We expect dangling phosphines to resonate much farther upfield and have a negative chemical shift. One explanation is that the dangling phosphine has become oxidized and leads to a chemical shift of 37 ppm (Figure 4.29). Another possibility is that this unsymmetrical species is not a monometallic complex but rather a bimetallic complex. One Ni center would have three phosphines coordinated and the other Ni center would have only one coordinated phosphine with the other coordination sites occupied by chloride anions and water or acetonitrile (Figure 4.27).

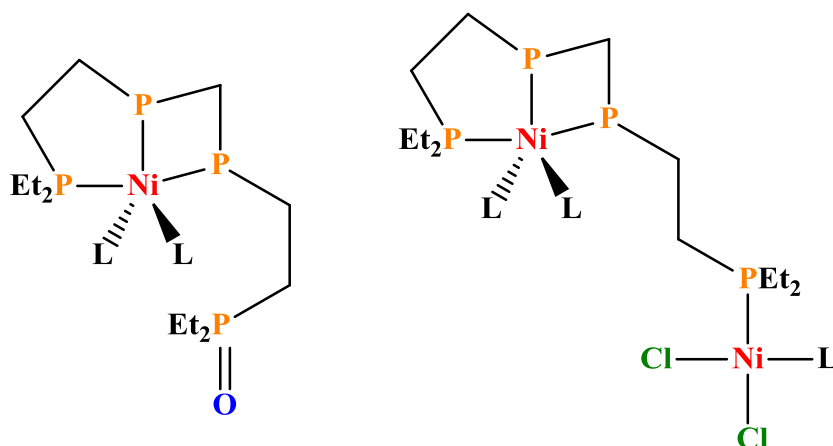


**Figure 4.27** Two possible structures of the unsymmetrical racemic complex observed via NMR. The L ligands could be  $\text{Cl}^-$ ,  $\text{OH}^-$ ,  $\text{H}_2\text{O}$  or  $\text{CD}_3\text{CN}$  and one or two L's could be bound to the metal.

Attempts were made to try and synthesis and crystallize the proposed double ligand bimetallic complex, **F-1R**. For this experiment, an 87% **1R**/13% **1M** mixture was dissolved in ethanol. 1 equivalent of  $\text{Ni}(\text{BF}_4)_2$  was dissolved in ethanol and the ligand solution was added drop-wise to the rapidly stirring Ni solution via cannula. After the addition was complete, 0.5 equivalents of NaCl were added. After the addition of the solid salt, a solid began to precipitate out of solution. This solution was allowed to stir overnight. The next day the solid was collected via filtration, washed with ethanol and dried under vacuum. NMR analysis of this solid

dissolved in acetone- $d_6$  revealed a mess of at least 30 resonances on the  $^{31}\text{P}$  spectrum. There appeared to be two pseudo-triplets but it was difficult to determine because of the abundance of other overlapping signals.

The remaining ethanol solution was concentrated under vacuum and analyzed via NMR. The spectrum (Figure 4.28) revealed the dominant species to be the two pseudo-triplets. The only other identifiable species was the unsymmetrical species. As the solution sat the unsymmetrical complex grew in intensity as the proposed double ligand complex decreased in intensity. Unfortunately, attempts to isolate and crystalize either of these complexes failed. However, this experiment clearly showed that **F-1R** converts to **C-1R**. Because this experiment was conducted with a 1:1 ratio of ligand to Ni, these two complexes should have the same stoichiometry. This suggests that the unsymmetrical species is a monometallic Ni complex and not a bimetallic complex (Figure 4.27). If it were a bimetallic complex then the conversion of **F-1R** to **C-1R** should liberate free phosphine and this was never observed via NMR.

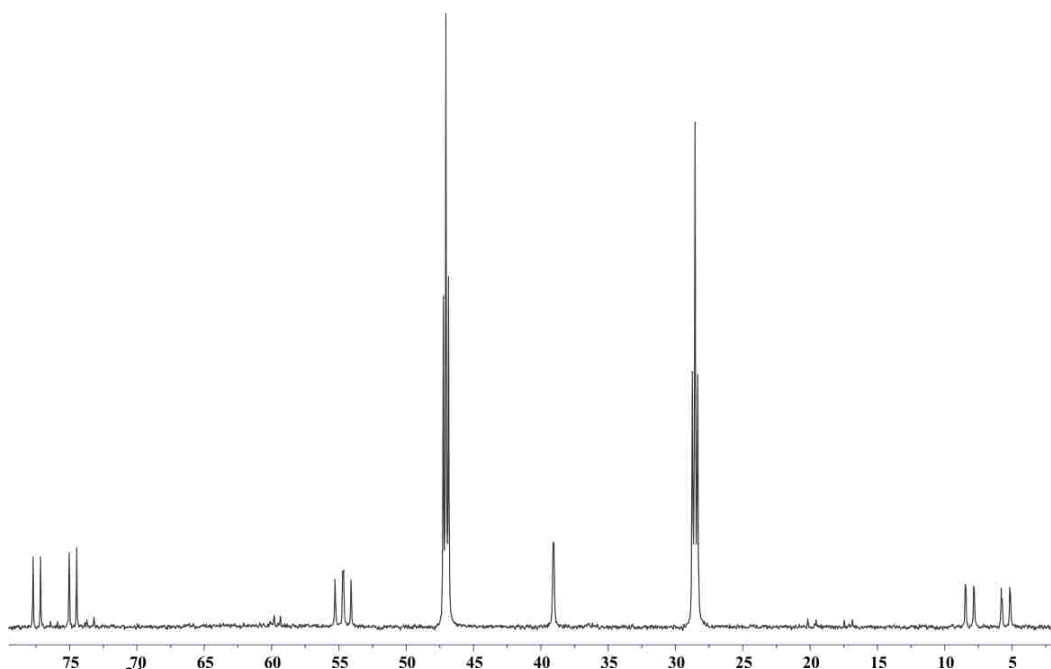


**Figure 4.28**  $^{31}\text{P}$  NMR spectrum of the concentrated ethanol solution during the attempted synthesis of the proposed *racemic* double ligand complex.

#### 4.8 Effect of Other Additives on the Reaction (NaCl, O<sub>2</sub>, Inhibitors, Heat)

Other NMR experiments were conducted to better understand the reactivity observed between the bimetallic complexes and water. Some of the most important experiments were conducted utilizing small amounts of added NaCl to observe what effect the chloride concentration had on this reaction. Figure 4.29 shows the major result from this set of experiments. The two spectra recorded were both in a 15% water/acetone solvent system under an inert atmosphere of N<sub>2</sub>. Both were recorded after the NMR tubes had sat for 24 hours. The top spectrum had 2 equivalents of NaCl added while the bottom spectrum contained only Ni<sub>2</sub>1M. The downfield resonance for the initial complex is highlighted in a black box on the spectrum. The resonance is almost 3 times more intense with 2 equivalents of NaCl! The experiment was repeated with the other 2 solvent systems and similar results were observed.

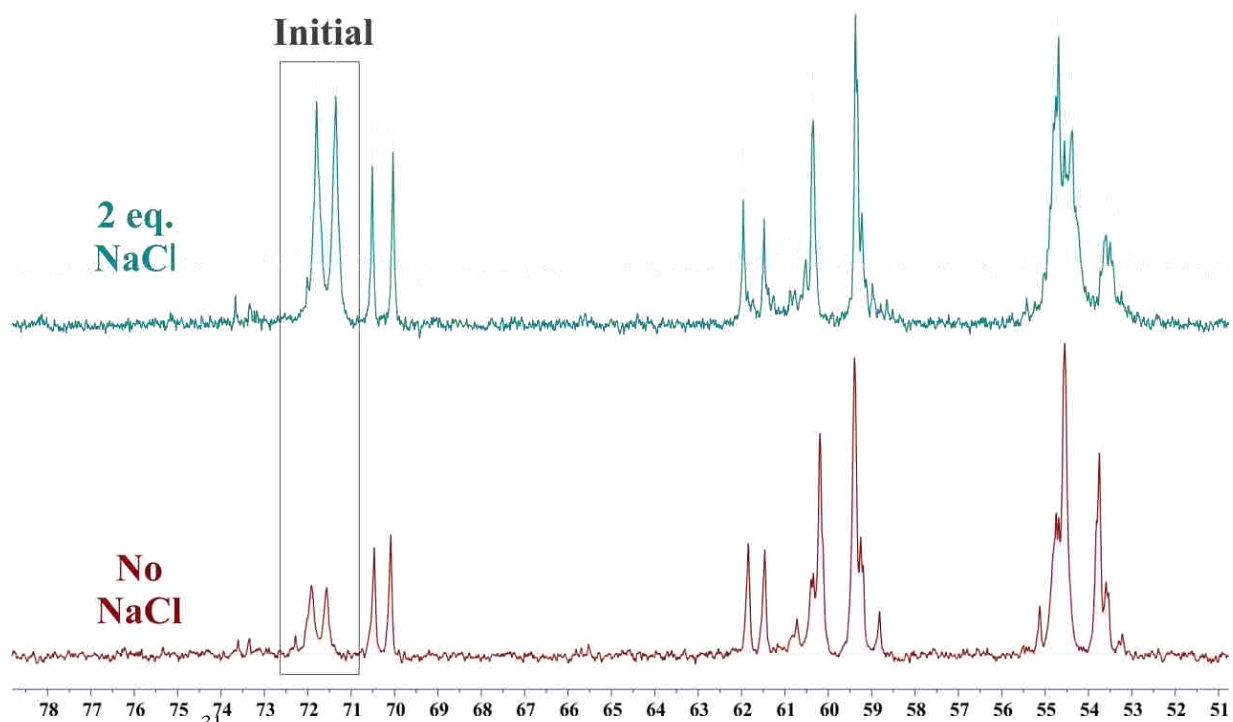


**Figure 4.29** <sup>31</sup>P NMR spectra showing the effect of added chloride on the reaction between Ni<sub>2</sub>Cl and water. The spectra were recorded in 15% water/acetone after 24 hours.

These experiments provided very convincing evidence that chloride dissociation was occurring during this reaction and helped support how important this process is important for the other reactions to occur (including the oxidative cleavage). Only 2 equivalents were required to see this dramatic of an effect on the transformation of the initial complex. The concentration added is not high enough to completely inhibit the reaction. The spectra have shown that the formation of **A** and **F** appear to be unaffected by the presence of the added chloride. Also, on some spectra there are very small resonances that could be for both **C** and **B** as was observed without the addition of NaCl. It seems that the addition of chloride only has an effect on the initial bimetallic complex.

These results indicate that chloride dissociation is the first step in this reaction. The addition of water to these bimetallic complexes causes chloride dissociation from the two initial bimetallic complexes. This dissociation leads to the formation of **A** (*meso*) or **A-1R**. With the *meso* complex and under low water concentrations, the reaction sequence which leads to the formation of **F** does not occur. More than 5 equivalents of NaCl were required to completely suppress the dissociation in 15% water/acetone. Under all other conditions observed, the formation of **F** does occur. The only difference is the time it takes for this transformation to occur.

All of the NMR experiments were conducted in conjunction with the oxidative cleavage reactions. Thus, many NMR tube reactions were exposed to air and had substrate present. As mentioned in Chapter 3, the addition of air leads to the oxidation of the tetraphosphine ligand with or without the substrate present. This oxidation is accelerated when substrate is present and under high pressure conditions. There are significant solvent effects that have been observed via

NMR. Both acetonitrile and DMSO inhibit the oxidation of the phosphine ligand when no substrate is present even under high pressure conditions.

The oxidation of the phosphine ligand leads to the formation of broad resonances on the  $^{31}\text{P}$  NMR spectra. They are caused by an interaction between the phosphine oxides and  $\text{NiCl}_2$ . The exact nature of this interaction is not known. The addition of air/ $\text{O}_2$  and substrate or just air/ $\text{O}_2$  does not have an effect on the reaction between the bimetallic complexes and water. All of the species that were identified during the NMR experiments under an inert atmosphere were also identified in these reactions. No other new species were observed in air/ $\text{O}_2$  besides the broad resonances. These results suggest that the complex formed upon the addition of  $\text{O}_2$  which is responsible for the oxidative processes is formed in such small concentrations that it cannot be observed during these experiments or it is such a short-lived species that we are unable to detect it via NMR.

To try and gain a better understanding of these oxidation processes, NMR experiments were conducted in the presence of air and substrate with and without the addition of between 2.5 and 3 equivalents of a radical inhibitor. Three different inhibitors (TEMPO, BHT and MEHQ) were investigated. The experiments were conducted in 15% water/acetone solvent systems. Figure 4.30 shows a comparison between two  $^{31}\text{P}$  NMR spectra. The top blue-green spectrum contained no added BHT and the bottom red spectrum contained almost 3 equivalents of BHT added. Both spectra were recorded after 2 days. The sample containing BHT shows no phosphine oxidation after 2 days while the sample without any added BHT clearly shows the phosphine oxidation via the presence of the broad resonances.

Similar results are also observed on the  $^1\text{H}$  spectra concerning the formation of the aldehyde. Figure 4.31 shows the difference in intensity between the aldehyde formed without



inhibitor present (top teal spectrum) and with BHT present (bottom red spectrum). The inhibitor causes about an order of magnitude decrease in the intensity of the aldehyde after 2 days. These experiments provide strong evidence for the idea that the two oxidative processes are linked. If phosphine oxidation does not occur then the oxidative cleavage will also not occur. Slowing down the oxidation of the phosphines slows down the oxidative cleavage of the substrate.

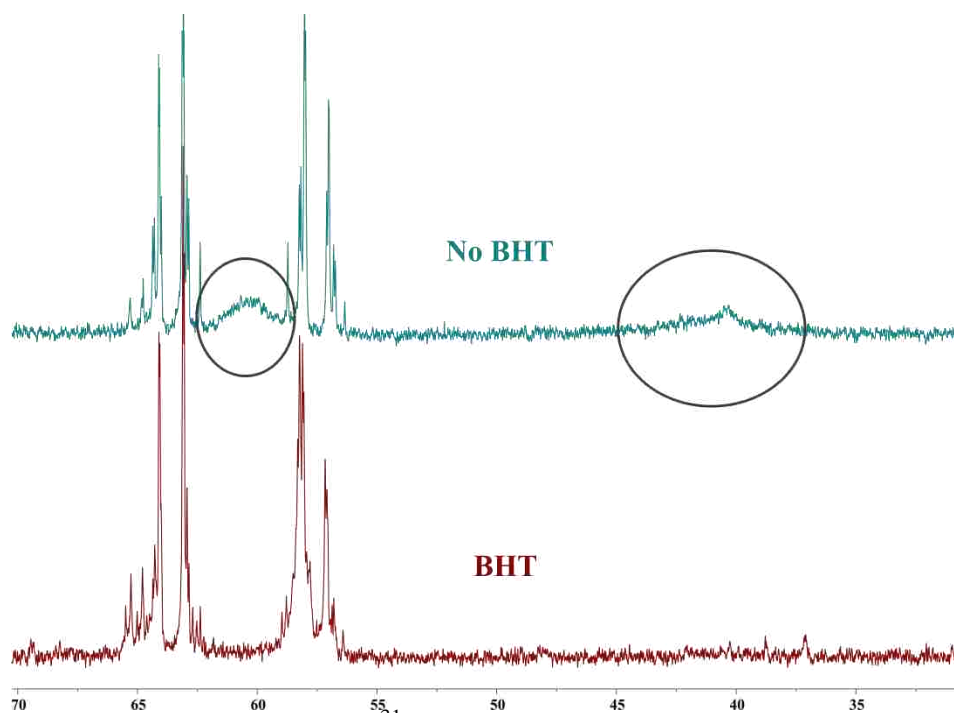


**Figure 4.30** Comparison between two  $^{31}\text{P}$  NMR in 15% water/acetone after the samples sat for 2 days. The top blue spectrum contains no added BHT and the bottom red spectrum contains almost 3 equivalents of BHT. The black circles highlight the broad resonances.

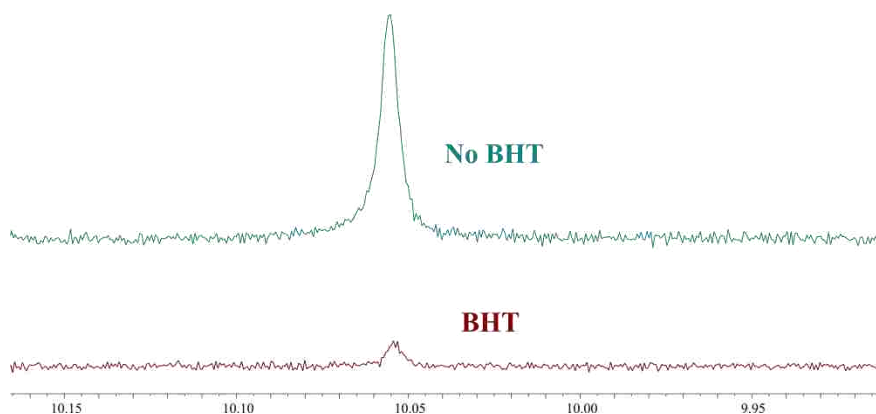


**Figure 4.31** Comparison between two  $^1\text{H}$  NMR spectra in 15% water/acetone after the samples sat for 2 days. The top teal spectrum contains no added BHT and the bottom red spectrum contains almost 3 equivalents of BHT.

The final variable that was tested during the NMR studies was the addition of heat to the samples. High-pressure NMR tubes were utilized for all of these experiments because of the heating involved. 15% water/acetonitrile was the solvent system utilized and 20 mM complex concentrations were utilized to ensure decent signal to noise ratios. These experiments produced some very surprising results. We initially proposed that heating the samples should accelerate the reaction between the complex and water and lead to the formation of **F** at a faster rate. What was actually observed was that heating these solutions completely inhibited the formation of **F** (Figure 4.32). Only a small amount of **A** is present during these experiments and both the initial complex resonances and the resonances for **A** remain unchanged after 24 hours of heating. Another broadened resonance is observed near 64 ppm. This resonance overlaps with one half of the signals for **A** and remains unchanged during 24 hours of heating. The identity of this broadened resonance is not known.

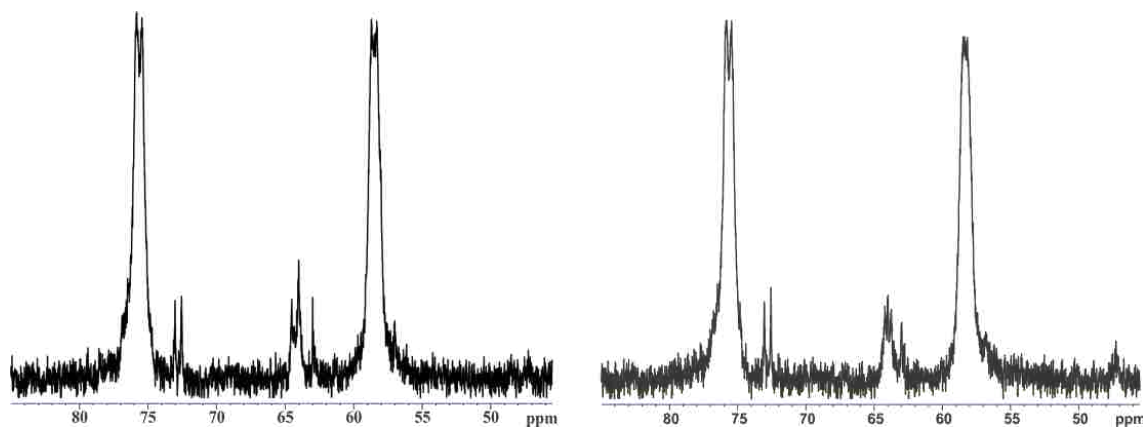


**Figure 4.32**  $^{31}\text{P}$  NMR spectra of  $\text{Ni}_2\mathbf{1M}$  dissolved in 15% water/acetonitrile and heated to  $90^\circ\text{C}$ . The spectrum on the left is the initial spectrum and the one on the right was recorded after 24 hours of heating.

The results observed while heating these samples have shown that the transformation of the initial complex to **F** or **F-1R** is temperature dependent. At room temperature the reactions leading to this transformation occur as long as enough water is present to facilitate the

transformation. At higher temperatures this transformation is completely inhibited and the only recognizable species present on the  $^{31}\text{P}$  spectra is **A** and the initial complex.

We then wanted to see if **F** was also sensitive to elevated temperatures. What we found was that heating **F** in 15% water/acetone causes the complex to fall apart and new species begin to appear on the NMR spectrum. Once the sample is cooled, **F** begins to be formed again and becomes the dominant species present (Figure 4.33). When 1 equivalent of  $\text{NiCl}_2$  is added to these reaction mixtures, **A**, **B** and **C** are all formed. When these solutions are exposed to air, the oxidative cleavage reaction and the phosphine oxidation occur. This leads to the presence of an aldehyde peak on the  $^1\text{H}$  spectrum and the broad resonances on the  $^{31}\text{P}$  spectrum. These experiments proved the importance of temperature on the reaction between the initial Ni complexes and water and they also proved the reversible nature of the reaction.

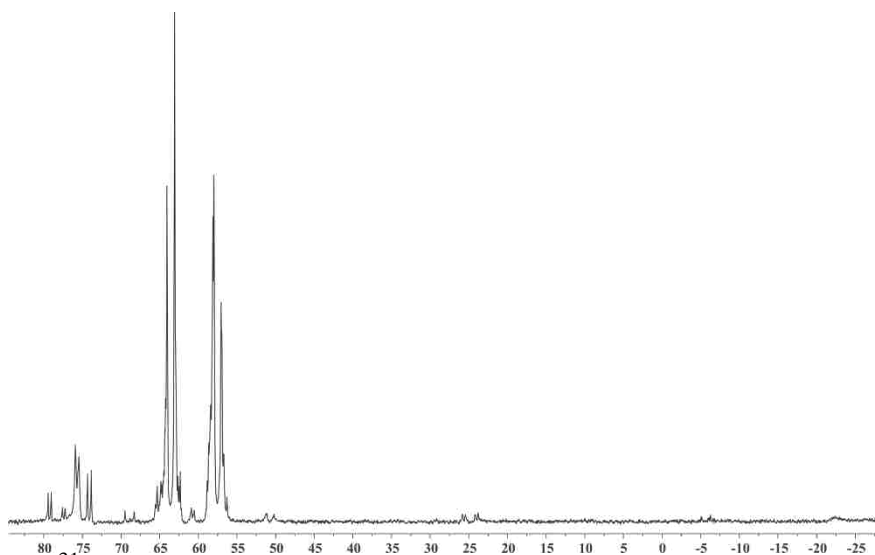


**Figure 4.33**  $^{31}\text{P}$  NMR spectrum of **F** dissolved in 15% water/acetone with 1 equivalent of  $\text{NiCl}_2$  added. The solution was heated for several hours and then allowed to sit at room temperature for one hour before recording the spectrum.

#### 4.9 Conclusions and Proposals

The solution-state chemistry of both **Ni<sub>2</sub>1M** and **Ni<sub>2</sub>1R** were investigated in a multitude of different solvents and solvent systems and under a host of different reaction conditions. All of

these results have provided some very important details concerning these two bimetallic complexes. The initial reports concerning the spin system of the *meso* complex is incorrect. This complex does not give rise to two doublets of triplets because the “triplet” splitting is not symmetrical. There is a 1.7 Hz difference in the two small splittings observed on both the 250 and 400 MHz spectrometers. The large splitting between the two pseudo-triplets corresponds to the *cis* coupling between the two inequivalent phosphines bound to the metal. The spectra observed suggest the observed resonances are a second-order pattern caused by an AA'XX' spin system. Because of CSA effects and smaller coupling constants between the other phosphines, the other splittings that should be observed cannot be resolved. Most likely this is also the case for **Ni<sub>2</sub>1R** but definitive proof has been difficult to obtain.

When water is added to either of these complexes a very complex reaction begins to take place. The results of these experiments have shown that this reaction is dependent on the water concentration, chloride concentration, temperature and organic solvent. For **Ni<sub>2</sub>1M** this reaction leads to the exclusive formation of **F**. This complex has been independently synthesized and characterized spectroscopically and via crystallography. The X-ray structure proved this species to be a bimetallic Ni complex containing a bridging chloride ligand and two molecules of **1M**,  $[\text{Ni}_2(\mu\text{-Cl})(\mathbf{1M})_2]^{3+}$ .

During the course of this reaction two other symmetrical complexes, **A** and **B**, and one unsymmetrical complex, **C**, were identified via NMR. When DMSO was the organic solvent, the addition of any amount of water led to the formation of **F**. When acetone and acetonitrile were utilized a clear dependence on the amount of water was observed. With 5% water added, only species **A** was observed. The remaining species, including **F**, were never observed during these reactions. Increasing the amount of water allowed for the reaction sequence to occur in

these two solvents. An increase in the amount of water causes the rate of this reaction to increase. In all reactions when the formation of **F** occurred, this complex became the only species present. The only difference observed was the amount of time it took for this to occur. This ranged from a few hours to more than a week depending on reaction conditions. When samples were kept at room temperature and under an inert atmosphere, **F** did not change.

Some similar reactivity was observed for **Ni<sub>2</sub>1R** when water was present, but there were some important differences. The initial reaction in water/acetonitrile leads to the formation of two symmetrical species, **A-1R** and **F-1R**. **F-1R** becomes the dominant species in solution and in some cases was the only observed species (in water/DMSO). Attempts to synthesize and characterize this complex via X-ray diffraction have failed. However, NMR analysis during these synthetic experiments showed that **F-1R** was synthesized but we were unable to isolate this complex. Based on these experiments we propose that this complex is a bimetallic Ni/double ligand complex similar to **F**. One difference between **Ni<sub>2</sub>1M** and **Ni<sub>2</sub>1R** concerns the amount of water that was required for this reaction to take place. When 5% water was added to **Ni<sub>2</sub>1R**, the transformation to **F-1R** did occur unlike with **Ni<sub>2</sub>1M**. Another difference between the two complexes concerns the proposed double ligand complexes formed during these reactions. **F-1R** is not stable at room temperature and falls apart to produce an unsymmetrical species, **C-1R**, which has been characterized via NMR. Complex **F**, on the other hand is stable at room temperature.

The addition of NaCl has several effects on this reaction. The addition of more than 5 equivalents stops the formation of any new species with 15% water. When only two equivalents are added, the transformation of the initial complex is slowed down in every solvent system tested. The formation of **F** and **F-1R** is unaffected by these additions. This addition only affects

the transformation of the initial complex. The intensity of the initial complex is about 3 times more intense after 24 hours with the addition NaCl. The resonances for the other identified species (**A**, **A-1R**, **B**, **C**, **F**, **F-1R** and **C-1R**) are all present with 2 equivalents of NaCl and no new resonances are observed.

When these solutions are exposed to air, over time broad resonances begin to form and can become the dominant species on the spectra. Experiments have proven that these broad resonances are caused by an interaction between the tetraphosphine oxide and NiCl<sub>2</sub>. The oxidation of the ligand is dependent on the organic solvent and the presence of substrate. The addition of radical inhibitors slows down the oxidation of the phosphine ligand but does not completely inhibit this process. This addition also slows down the oxidative cleavage when substrate is present. These experiments also showed that the phosphine oxidation and alkene oxidative cleavage are coupled together. If phosphine oxidation does not occur then the alkene oxidative cleavage will not occur. No evidence was found that the radical inhibitors affect the transformation of the initial complexes to **F** and **F-1R**.

The addition of heat also has a dramatic effect on this reaction. Heating these solutions does not allow for the transformation to **F** or **F-1R** to occur. These experiments have shown that only **A** or **A-1R** is formed while heating. Once the samples are cooled to room temperature, the transformation occurs and appears unaffected by the heating. When a solution of **F** is heated, this complex falls apart and begins to form new species. When NiCl<sub>2</sub> is added to **F** and heated, **A**, **B** and **C** are all observed via NMR. Cooling these solutions back to room temperature and allowing them to sit for an hour or more reforms **F**. When these experiments were conducted in the presence of air, the oxidative cleavage and phosphine oxidation were observed.

With all of these experiments and observations, a general picture for this reaction sequence can be devised. Starting with  $\text{Ni}_2\mathbf{1M}$  the first step in the reaction has to be the dissociation of at least one chloride ligand. This leads to the symmetrical complex **A**. Because this complex is symmetrical, the remaining three chloride ligands would have to rearrange to form a symmetrical complex. Three possible structures seem likely for this complex. The first would be a bridging chloride complex (Figure 4.34).

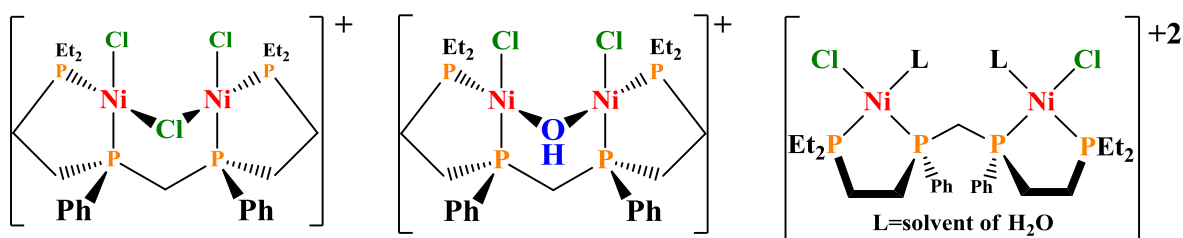


**Figure 4.34** Proposed structures for **A**.

If another chloride dissociates from the cationic complex, this could lead to the formation of an open-mode complex with two ligands (solvent or water) replacing the dissociated chlorides or to a bridging-hydroxide complex (Figure 4.34) similar to the structure characterized by Dr. Alex Monteil. The bridging complexes seem the most likely. The open mode structure would show some exchange between the solvent or water ligands which would broaden the resonances. These resonances were never broadened. Also different isomers could be formed depending on the placement of the chlorides and solvent or water on each Ni center. If the isomers were fairly static on the NMR time-scale, a large amount of signals would be observed from the different isomers and some would be unsymmetrical.

Complex **A** remains present in solution for the majority of the time during the transformation to **F** and the intensity of the resonances for **A** remain fairly constant. This suggests that the initial complex dissociates a chloride and leads to the formation of a certain

concentration of **A**, which remains present in the solution at this concentration until only **A** and **F** are observed. At this stage **A** begins to decrease in concentration until only **F** is present.

Under low water concentrations, the formation of **F** does not occur. These observations suggest the following reaction sequence. The addition of water causes **Ni<sub>2</sub>1M** to form a certain concentration of **A**, which then further reacts to form species **B** and **C** in small concentrations, leading to the formation of **F**. As **A** is converted to **B** and **C** and ultimately **F**, the concentration of the initial complex decreases to form more **A** to maintain the concentration of **A**. This sequence is continued until all of the initial complex disappears and **F** becomes the only species present.

The NMR data for **C** shows this complex to be an unsymmetrical complex with 4 nonequivalent phosphines. The most likely structure for this species based on the coupling constants and chemical shifts is shown in Figure 4.35. **C** is a monometallic complex with the tetraphosphine ligand wrapped around in a  $\kappa^3$ -coordination mode,  $[\text{NiCl}(\kappa^3\text{-}meso\text{-}et,ph\text{-}P_4)]^+$ .

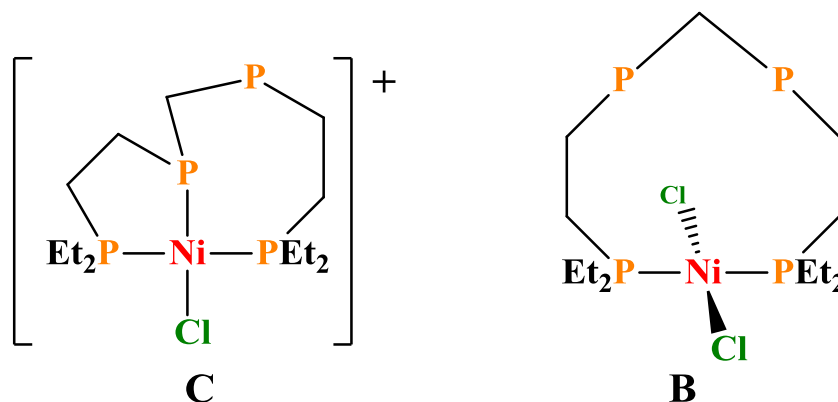


**Figure 4.35** Proposed structures of **C** and **B**

Complex **B** is a symmetrical complex but the two equivalent phosphines are in two very different chemical environments, which lead to the large difference in chemical shift between the two multiplets for this species. There are at least two possible scenarios which could cause this large chemical shift difference. The first scenario involves different chelate ring sizes but as



stated previously this is expected to give an unsymmetrical complex. The other possibility is shown in Figure 4.35. This complex is a square planar monometallic complex with the two external phosphines *trans* to each other. Two chloride ligands would occupy the other two coordination sites *trans* to each other. The other two phosphines are either not bound to the Ni center or only interacting weakly in a dynamic fashion. In solution this complex should behave as a symmetrical complex and give rise to two distinct multiplets. The two multiplets should have a large chemical shift difference because one set of phosphines is bound to the metal and the other is not. This is only a proposed structure and there are other possibilities as well.

Previous work from our group offers support for both of these monometallic structures. Booker Juma prepared the  $[\text{Ni}(\text{NCS})(\kappa^3\text{-meso-et,ph-P4})]^+$  complex ( $\text{SCN}^-$  counter anion) from the reaction of a 1:1 diastereomeric mixture of *rac,meso-et,ph-P4* ligand with one equivalent of  $\text{Ni}(\text{NCS})_2$  in EtOH.<sup>6</sup> Both the *rac* and *meso* monometallic complexes were isolated in high yields, but only crystals of the *meso*-diastereomer were grown and structurally characterized. The ORTEP of this complex is shown in Figure 4.36. An interesting aspect of this thiocyanate complex is that it has fluxional behavior in solution to produce a symmetrical  $^{31}\text{P}$  NMR spectrum. This was proposed to occur via dissociation of the one internal phosphine and coordination of the other to produce a symmetrical  $^{31}\text{P}$  NMR spectrum. The low solubility of this complex prevented Juma from doing variable temperature NMR experiments to probe the exchange rate. The lack of room temperature fluxionality in our chloride system is consistent with the weaker coordination of chloride versus thiocyanate and the  $\sigma\text{-trans}$  effect. The stronger coordinating  $\text{SCN}^-$  ligand in Juma's complex weakens the Ni-P bond making it easier to dissociate and exchange with the other internal phosphine. In our  $[\text{NiCl}(\kappa^3\text{-meso-et,ph-P4})]^+$

complex **C**, the  $\sigma$ -*trans* effect is reversed with the stronger coordinating phosphine weakening the Ni-Cl bond.

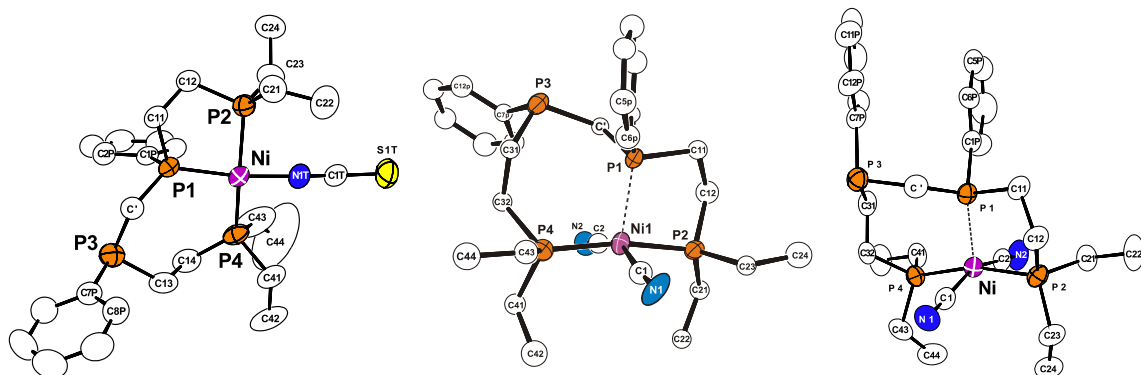


**Figure 4.36** ORTEP plots of  $[\text{Ni}(\text{NCS})(\kappa^3\text{-meso-et,ph-P4})]^+$ , *trans*- $\text{Ni}(\text{CN})_2(\kappa^{2.5}\text{-meso-et,ph-P4})$ , and *trans*- $\text{Ni}(\text{CN})_2(\kappa^{2.5}\text{-rac-et,ph-P4})$  prepared by Juma, Aubry, and Laneman, respectively.

Scott Laneman isolated the *trans*-spanning *rac*-et,ph-P4 complex *trans*- $\text{Ni}(\text{CN})_2(\kappa^{2.5}\text{-rac-et,ph-P4})$  while doing some of the initial cyanolysis experiments.<sup>7</sup> This has a long Ni-P1 axial bonding distance of 2.395(2) Å. The  $^{31}\text{P}$  NMR of this complex, however, is symmetrical demonstrating a rapid fluxionality and weak Ni-P interaction between the two internal phosphines. David Aubry isolated the less stable *meso* analog *trans*- $\text{Ni}(\text{CN})_2(\kappa^{2.5}\text{-meso-et,ph-P4})$ , which has a tendency to isomerize the *meso*-et,ph-P4 ligand into the *rac* diastereomer.<sup>8</sup> Unlike the *rac*-nickel complex, the *meso* complex is not fluxional at room temperature and shows four  $^{31}\text{P}$  NMR resonances consistent with the solid-state unsymmetrical structure. These previously identified complexes provide support for the proposed monometallic structures.

The final question to be addressed for this reaction sequence involves the transformation of **A** to **B** and **C**. This transformation would require the loss of one Ni center assuming both **C** and **B** are monometallic complexes. Experimental observations have shown that free  $\text{NiCl}_2$  is present in solution. One way for **A** to lose a Ni center would involve dissociation of one of the phosphine arms. We have used this same proposal to explain the fragmentation observed during

the hydroformylation studies using  $[\text{Rh}_2(\text{nbd})_2(\mathbf{1R})][\text{BF}_4]_2$  which leads to the formation of inactive mono- and bimetallic Rh complexes. If one phosphine arm dissociates, the exposed Ni center could become solvated by the water molecules present and release  $\text{NiCl}_2 \cdot \text{XH}_2\text{O}$ . The phosphine arm dissociation would be a very fast equilibrium and would not affect the resonances of **A**. The remaining fragment could then rearrange to form **C**. Addition of chloride to **C** could lead to the formation of **B**. **C** and **B** could then come together to form **F** or one of these complexes could react with another unidentified monometallic complex and form **F**. This would lead to the complete reaction sequence shown in Figure 4.37.

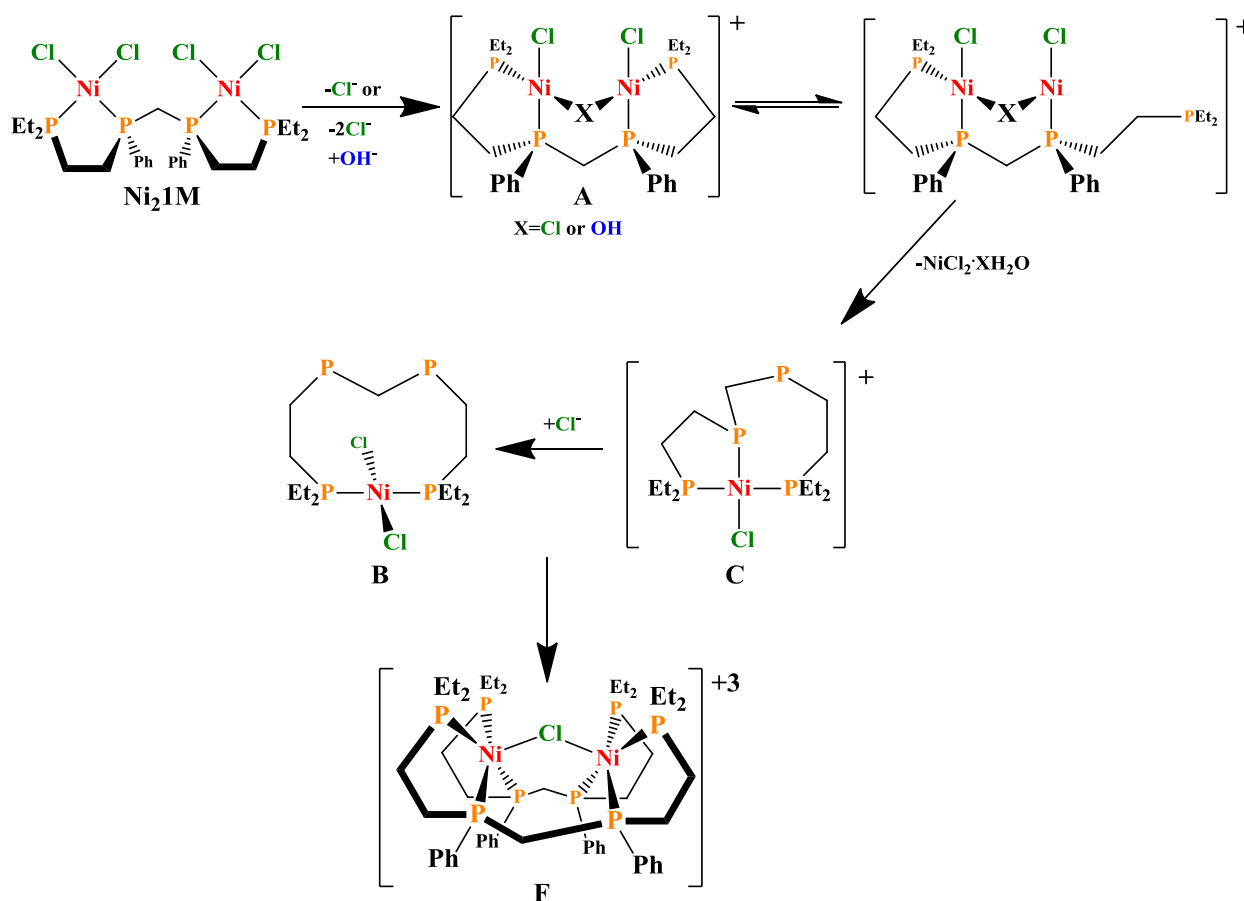


**Figure 4.37** Proposed reaction sequence for the transformation of  $\text{Ni}_2\mathbf{1M}$  to **F** in water/organic solvent systems.

The presence of cationic and multi-cationic metal complexes leads to an important conclusion about why water and the organic solvent are so important for this reaction sequence.

Two of the organic solvents, acetone and acetonitrile, have very similar polarities with acetonitrile being more polar. DMSO and water are the two most polar solvents typically used in chemistry. In acetone and acetonitrile, the addition of only 5% water leads to the formation of **A**. The reason the other species do not form in these solvent systems is because the total solvent polarity is not high enough to support multi-cationic complexes like **F**. As more water is added, the total solvent polarity increases and allows for these highly charged complexes to form. The formation of **F** occurs faster in acetonitrile because of its higher polarity compared to acetone. Because DMSO is already very polar, small amounts of cationic or multi-cationic species can be formed. However, **F** cannot form in the presence of DMSO only. The addition of water to DMSO increases the polarity and causes this transformation to occur. The addition of water could also help facilitate the loss of a metal center from **A** after phosphine arm dissociation.

A similar reaction scheme can be proposed for the reaction between water and **Ni<sub>2</sub>1R**. Initial chloride dissociation would lead to a bridging complex. Because of the structure of **1R**, a mono- or dibridging structure could be possible. The phosphine arm dissociation would occur but instead of leading to a monometallic complex, this dissociation would lead to the formation of a bimetallic Ni/double **1R** complex similar to **F**. This complex is not stable at room temperature and ultimately falls apart forming the unsymmetrical monometallic complex (**C-1R**) shown in Figure 4.38.

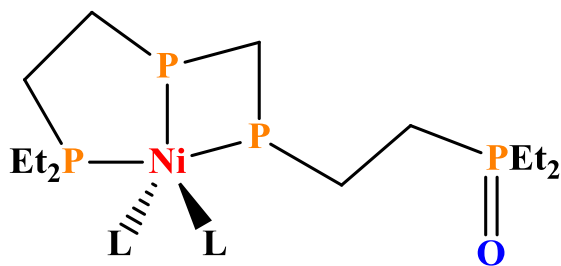


**Figure 4.38** Proposed structure for the unsymmetrical complex (**R-C**) formed from **Ni<sub>2</sub>1R**. The L's could be chloride, hydroxide or solvent and there could be one or two present.

The addition of O<sub>2</sub> to these systems leads to the oxidation of the phosphine ligand and the oxidative cleavage of an alkene. Once the phosphine has been completely oxidized, the oxidative cleavage reaction is stopped. The presence of non-coordinated phosphine moieties proposed in several of these structures could explain why we have observed this oxidation reactivity. The oxidation of these free phosphines would be coupled with the oxidative cleavage of the alkene. This reaction would be facilitated by the Ni centers because the complete oxidation of the phosphine does not occur with just O<sub>2</sub> nor does the oxidative cleavage reaction occur. This proposal is supported by almost all experimental evidence to date and provides the best explanation for the observed reactivity between the bimetallic complexes, water, O<sub>2</sub> and substrate.

#### 4.10 References

1. Crews, P.; Rodríguez, J.; Jaspars, M. *Organic Structure Analysis*, 2<sup>nd</sup> edition; Oxford University Press: London, 2010.
2. Silverstein, R. M.; Webster, F. X.; Kiemle, D. *Spectrometric Identification of Organic Compounds*, 7<sup>th</sup> edition; John Wiley & Sons: Hoboken, NJ, 2005.
3. Kühn, O. *Phosphorus-31 NMR Spectroscopy*; Springer: Berlin Heidelberg, Germany, 2008.
4. Garrou, P. E. *Chem. Rev.* **1981**, 81, 229-266.
5. Laneman, S. A.; Fronczek, F. R.; Stanley, G. G. *Inorg. Chem.* **1989**, 28, 1872-1878.
6. Juma, B., *Ph.D. Dissertation, Louisiana State University*, **1993**.
7. Aubry, D., *Ph.D. Dissertation, Louisiana State University*, **2003**.
8. Laneman, S., *Ph.D. Dissertation, Louisiana State University*, **1990**.

## CHAPTER 5: SYNTHESIS, SEPARATION AND CHARACTERIZATION OF 2R AND 2M AND Ni<sub>2</sub>2M AND Ni<sub>2</sub>2R.

### 5.1 Introduction

The NMR investigation into the solution-state chemistry of Ni<sub>2</sub>Cl<sub>4</sub>(*meso*-et,ph-P4), Ni<sub>2</sub>1M, and Ni<sub>2</sub>Cl<sub>4</sub>(*rac*-et,ph-P4), Ni<sub>2</sub>1R has reinforced a major problem with the complexes formed from these two tetraphosphine ligands. These complexes can readily fall apart under very mild conditions and give rise to several different mono- and bimetallic complexes. Based on the experimental evidence presented in this document, the major reason these complexes fall apart, besides being in the presence of water, is because of dissociation of one of the phosphine arms which ultimately leads to the formation of [Ni<sub>2</sub>(μ-Cl)(*meso*-et,ph-P4)<sub>2</sub>]<sup>+3</sup> from Ni<sub>2</sub>1M and a proposed double ligand bimetallic complex from Ni<sub>2</sub>1R. In the presence of O<sub>2</sub> and substrate, this dissociation can also lead to some oxidative cleavage of an alkene and complete oxidation of the phosphines.

The phosphine dissociation has also been identified as a major problem during the hydroformylation of alkenes using [Rh<sub>2</sub>(nbd)<sub>2</sub>(*rac*-et,ph-P4)][BF<sub>4</sub>] as the catalyst precursor. Spectroscopic studies have identified both mono- and bimetallic complexes that form upon exposing this complex to a mixture of H<sub>2</sub> and CO gas.<sup>1-4</sup> Utilizing a 30%/acetone solvent system limits some of these complexes from forming but fragmentation can still occur over time.<sup>5</sup> These mono- and bimetallic complexes are inactive for hydroformylation and represent the major deactivation pathway for this catalytic system.

These represent major issues when trying to investigate bimetallic complexes for bimetallic cooperativity during a catalytic reaction. We have shown that bimetallic cooperativity is occurring during hydroformylation with [Rh<sub>2</sub>(nbd)<sub>2</sub>(*rac*-et,ph-P4)][BF<sub>4</sub>]<sub>2</sub> and it still remains one of the best examples of bimetallic cooperativity today.<sup>6</sup> However, if the core bimetallic

structure would remain intact during the catalytic cycle, the Rh complex could show even higher turnover numbers and turnover frequencies than what we have observed.

A new tetratertiary phosphine ligand was designed by Dr. Stanley with the hope that this phosphine arm dissociation would be severely limited and thus lead to more active and longer living catalysts. The new ligands *rac,meso*-(Et<sub>2</sub>P-1,2-C<sub>6</sub>H<sub>4</sub>)PCH<sub>2</sub>P(1,2-C<sub>6</sub>H<sub>4</sub>-PEt<sub>2</sub>) (**2R** and **2M**, Figure 5.1) replace the ethylene linkage between the internal and external phosphines with a phenylene linkage. This will produce a far more rigid linkage between these two phosphines and should greatly increase the chelate effect with a metal center. This should severely limit the phosphine arm dissociation and give rise to more robust catalytic systems.

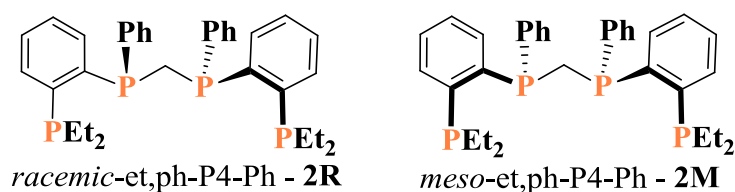
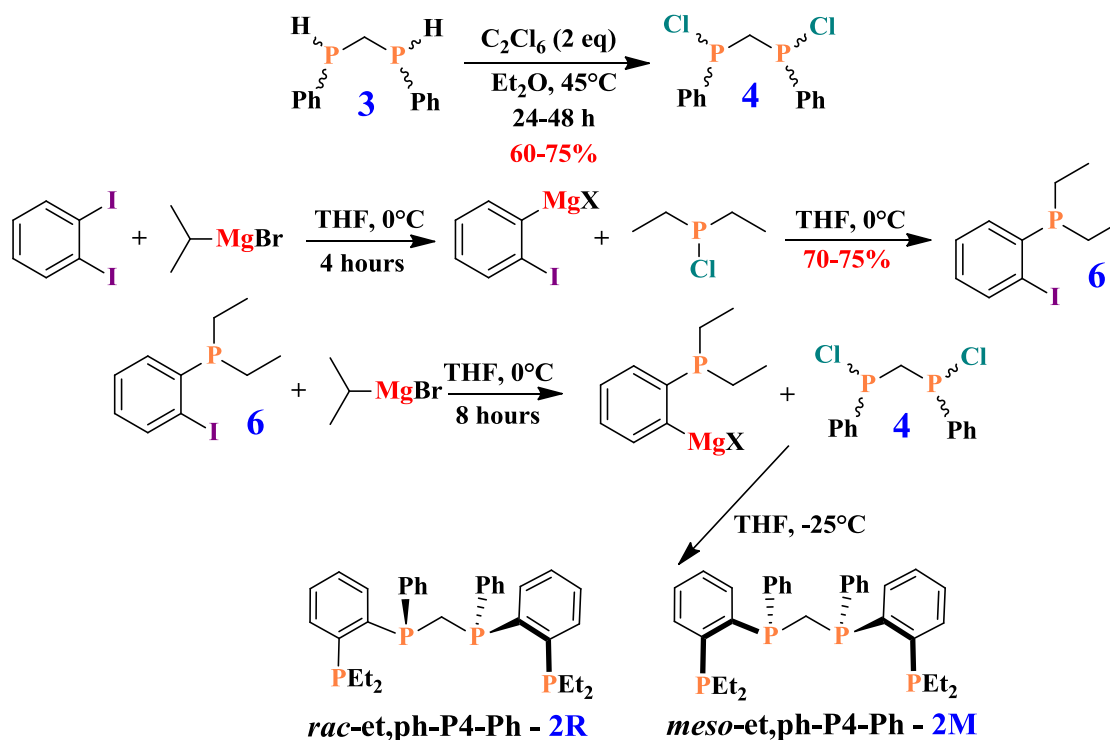


**Figure 5.1** The new, stronger chelating phosphine ligands **2R** and **2M**

## 5.2 Synthesis and Characterization of **2R** and **2M**

Dr. Alex Monteil was tasked with designing a synthetic route for the new phosphine ligands. This proved to be a very challenging endeavor but after several years and countless synthetic attempts he was able to successfully synthesis **2M** and **2R**.<sup>7</sup> The synthetic scheme is depicted in Scheme 5.1. In the first step, adapted from work by Weferling<sup>8</sup>, *bis*-(phenylphosphino)methane, **3**, is combined with 2 equivalents of hexachloroethane and heated to reflux in ether for 1 to 2 days to give, after workup, *bis*-(chlorophenylphosphino)methane, **4**, as a slightly pink air-, moisture- and heat-sensitive viscous liquid. The <sup>31</sup>P{<sup>1</sup>H} NMR spectrum of this species shows only a singlet at 81.7 ppm which indicates that only one diastereomer of **4** is formed. This is quite surprising considering that **3** is a roughly 50:50 mixture of both diastereomers. Other syntheses<sup>9,10</sup> of **4** are reported to give rise to both diastereomers.

**Scheme 5.1** Synthesis of **2R** and **2M**



The next stage of the reaction involves a two-step process, adapted from work by Boymond *et al.*,<sup>11</sup> leading to the formation of 1-(diethylphosphino)-2-iodobenzene (**6**). Diiodobenzene is reacted with isopropylmagnesium bromide and then treated with diethylchlorophosphine and allowed to stir overnight. After workup, **6** is isolated as an air-, moisture- and light-sensitive colorless liquid in high yield. This Grignard-mediated P-C coupling reaction allows for a facile synthesis of **6**. The final step of the synthesis involves another Grignard-mediated P-C coupling reaction. **6** is reacted with isopropylmagnesium bromide followed by the addition of **4** and allowed to stir overnight. Workup of this reaction mixture leads to the isolation of a white paste which was identified as a 50:50 mixture of **2R** and **2M** in modest yield. Figure 5.2 shows the <sup>31</sup>P NMR spectrum obtained for the white paste and the <sup>1</sup>H NMR spectrum of the central methylene protons.



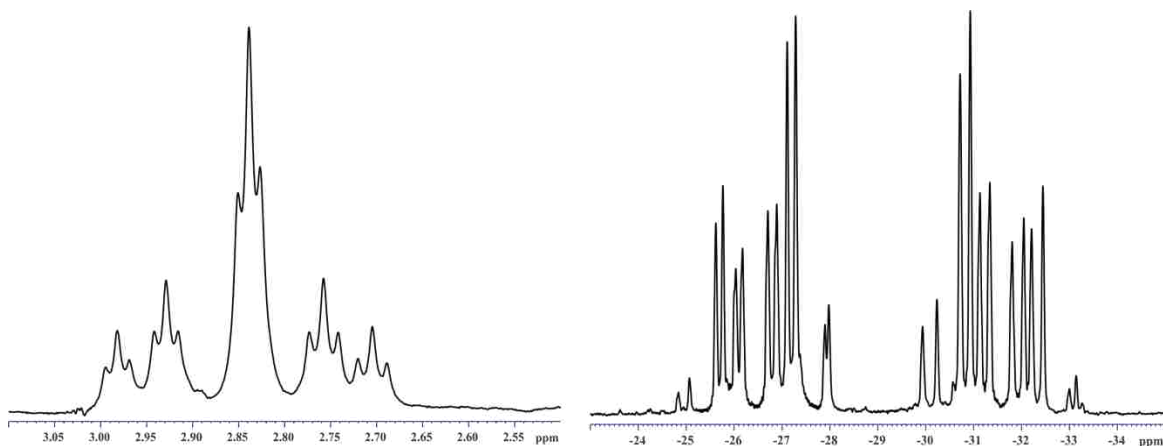


**Figure 5.2**  $^1\text{H}$  and  $^{31}\text{P}$  NMR spectra of a 50:50 mixture of **2M** and **2R**. The expanded  $^1\text{H}$  NMR shows the distinctive pattern of the methylene bridge region for the *rac* and *meso* diastereomers. **2R** is represented by the central triplet, while **2M** is the flanking set of four triplets. This set of peaks is the easiest way to identify the diastereomeric purity of the ligand.

### 5.3 Synthesis and Separation of $\text{Ni}_2\mathbf{2M}$ and $\text{Ni}_2\mathbf{2R}$

After the successful synthesis of **2M** and **2R**, the next goal was to synthesize the bimetallic Ni complexes,  $\text{Ni}_2\mathbf{2M}$  and  $\text{Ni}_2\mathbf{2R}$ , and then try to separate the two diastereomers. For the old bimetallic complexes  $\text{Ni}_2\text{Cl}_4(\textit{meso}\text{-et,ph-P4})$ ,  $\text{Ni}_2\mathbf{1M}$ , and  $\text{Ni}_2\text{Cl}_4(\textit{rac}\text{-et,ph-P4})$ ,  $\text{Ni}_2\mathbf{1R}$ , this was accomplished by utilizing ethanol as the solvent during the synthesis.<sup>12,13</sup>  $\text{Ni}_2\mathbf{1M}$  precipitates out of solution and can be collected via filtration. The remaining ethanol solution contains  $\text{Ni}_2\mathbf{1R}$ . This allows for a facile synthesis and separation most of the time.

Ethanol, therefore, was the first solvent utilized for the attempted synthesis of  $\text{Ni}_2\mathbf{2M}$  and  $\text{Ni}_2\mathbf{2R}$ . An orange powder did precipitate during the attempted synthesis with ethanol. NMR analysis revealed about a 50/50 mixture of the two complexes. After ethanol failed to give clean separation, methanol and 1-butanol were tested to see if clean separation would occur. These again produced orange solids as with the ethanol synthesis. NMR analysis revealed them to be enriched in  $\text{Ni}_2\mathbf{2M}$  (60-80%) with 1-butanol giving the highest amount of  $\text{Ni}_2\mathbf{2M}$ .

After these results, it was decided to attempt a mixed solvent system with 1-butanol. The first solvent utilized was dichloromethane. The mixed ligand was dissolved and added to the 1-

butanol solution containing  $\text{NiCl}_2$ . This solution was allowed to stir overnight during which another orange powder precipitated out of solution. NMR analysis of this powder revealed the  $^{31}\text{P}$  NMR spectrum shown in Figure 5.3 which shows two pseudo doublets of triplets, one centered at 70.1 ppm and the other centered at 50.5 ppm.

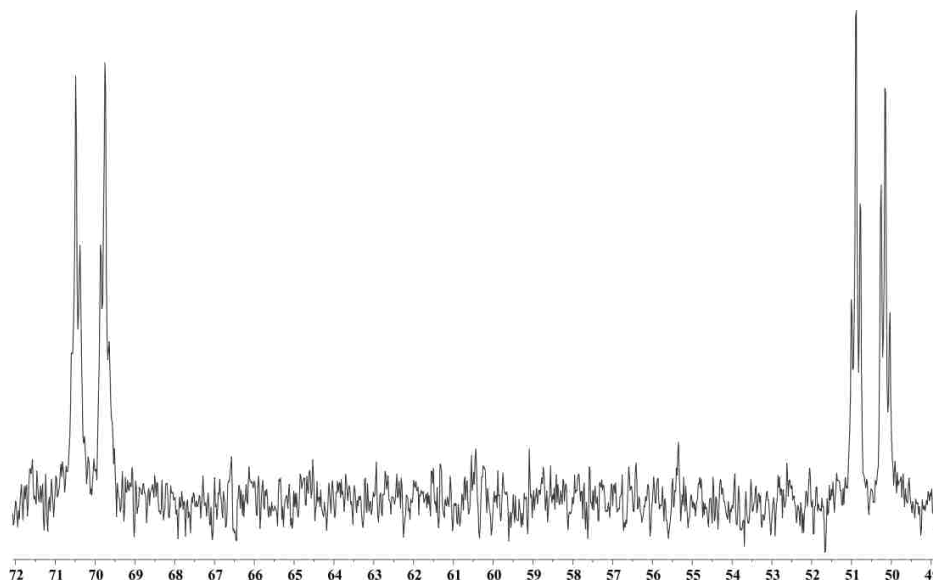


**Figure 5.3**  $^{31}\text{P}$  NMR spectrum of  $\text{Ni}_2\mathbf{2M}$  obtained from the 1-butanol/dichloromethane synthesis

$^1\text{H}$  analysis also revealed this to be a pure compound. Subsequent experiments have shown that this orange powder is  $\text{Ni}_2\mathbf{2M}$ . The remaining 1-butanol/dichloromethane solution was evaporated to dryness and redissolved in dichloromethane. A large excess of hexanes was added which precipitated out another orange powder. NMR analysis of this powder revealed it to be an 87:13 mixture of  $\text{Ni}_2\mathbf{2R}$  and  $\text{Ni}_2\mathbf{2M}$ . After a few more attempts it was found that dissolving the remaining solid in hot acetonitrile and allowing this to sit in air for a day or two will precipitate out pure  $\text{Ni}_2\mathbf{2R}$ . Thus, a clean and straightforward synthesis of the two complexes allows for clean separation of the two diastereomers. The  $^{31}\text{P}$  NMR spectrum of pure  $\text{Ni}_2\mathbf{2R}$  is shown in Figure 5.4.

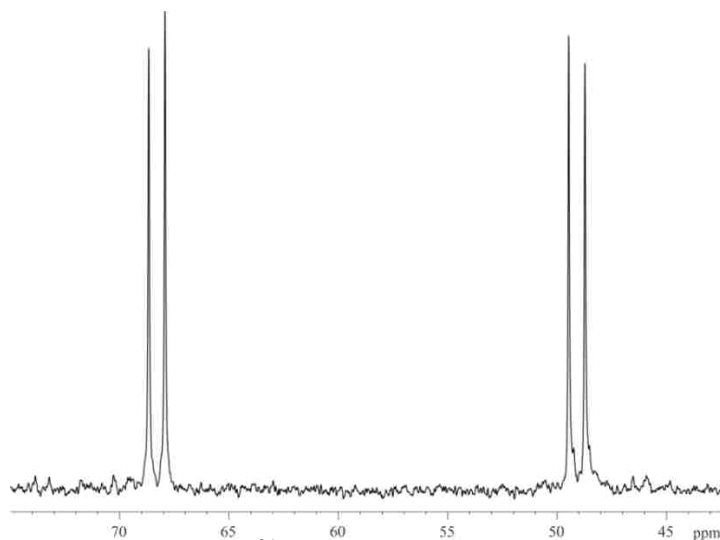


**Figure 5.4**  $^{31}\text{P}$  NMR spectrum of  $\text{Ni}_2\mathbf{2R}$ .

Definitive proof of these assignments for  $\text{Ni}_2\mathbf{2M}$  and  $\text{Ni}_2\mathbf{2R}$  came from single crystal X-ray analysis of two single crystals. The orange powders obtained from the synthesis can be recrystallized using acetonitrile or dichloromethane and afford crystals suitable for X-ray analysis. Figure 5.5 shows the ORTEP plots obtained from the X-ray analysis. The crystal structures revealed the expected square planar arrangement of two  $\text{Cl}^-$  ligands *cis* to each other along with two phosphine moieties chelated through the phenylene linkage for both metal centers. The bond lengths are very similar to the bond lengths of  $\text{Ni}_2\mathbf{1R}$  and  $\text{Ni}_2\mathbf{1M}$ <sup>12</sup> and also to each other.

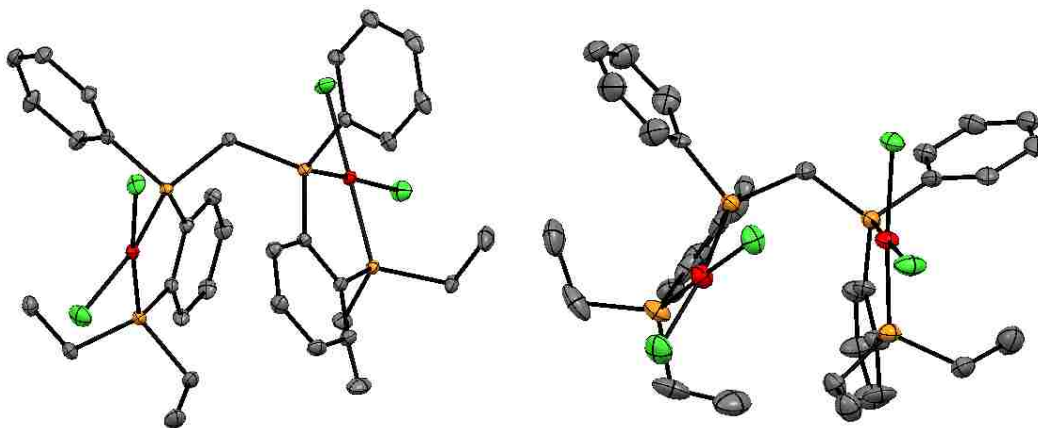


**Figure 5.5** ORTEP plots depicting  $\text{Ni}_2\mathbf{2R}$  (left) and  $\text{Ni}_2\mathbf{2M}$  (right). Hydrogen atoms have been omitted for clarity. Ni – red, Cl – green, P – orange, and C – gray.

The biggest difference between **Ni<sub>2</sub>2M** and **Ni<sub>2</sub>2R** is the rotational conformation adopted by each in the solid-state. For **Ni<sub>2</sub>2R**, the Ni centers are rotated away from one another adopting a completely open mode geometry in which the Ni centers are on opposite sides of the molecule with a Ni-Ni distance of 5.9027 Å and a Ni1-P2···P3-Ni2 torsional angle of 130°. This conformation is similar to the solid state structure of **Ni<sub>2</sub>1R** which also adopts an open mode conformation. However, the Ni-Ni distance (5.417 Å) and Ni1-P···P'-Ni2 torsional angle (106°) are both smaller for **Ni<sub>2</sub>1R**.<sup>12</sup>

**Ni<sub>2</sub>2M** adopts a partially closed mode geometry with a Ni-Ni distance of 4.404 Å and a Ni1-P2···P3-Ni2 torsional angle of -41°. This is facilitated by a weak interaction between Ni2 and C11 with a distance of 3.024 Å. This solid-state conformation is quite different compared to **Ni<sub>2</sub>1M** which adopts an open mode structure. **Ni<sub>2</sub>1M** has a considerable longer Ni-Ni distance (6.272 Å) and a much larger Ni1-P2···P3-Ni2 torsional angle (160°) compared to **Ni<sub>2</sub>2M**.<sup>12</sup> The solid-state structures of **Ni<sub>2</sub>2R** and **Ni<sub>2</sub>2R** are not solvent dependent. These rotational conformations have been observed regardless of the solvent (dichloromethane, acetonitrile or acetone) used for crystallization.

#### 5.4 Cyanolysis of **Ni<sub>2</sub>2M** and **Ni<sub>2</sub>2R** and Isolation of the Pure Diastereomers

After the successful synthesis and separation of the bimetallic Ni complexes, the next step was to try and isolate the pure ligand from the complexes. This was accomplished by reacting the individual complexes with a large excess of NaCN to liberate the ligand. The procedure tested was very similar to the one developed for the cyanolysis of **Ni<sub>2</sub>1M** and **Ni<sub>2</sub>1R**.<sup>13</sup>

The two new bimetallic complexes were separately suspended in methanol and an aqueous solution of NaCN was added. A two stage NaCN addition was utilized. The first addition involved 133 equivalents and the second addition involved 150 equivalents. The large

excess of  $\text{CN}^-$  was used in the hopes that the strong  $\sigma$ -donating ability of the  $\text{CN}^-$  ligand would completely displace the phosphine ligand from the metal complex. After stirring overnight the red methanol/water solutions were extracted with benzene. The red benzene extracts were concentrated under vacuum and then added to a neutral alumina column. The column was eluted with dichloromethane and allowed for the clean separation of the ligand from the red impurities.

The  $^1\text{H}$  and  $^{31}\text{P}$  spectra obtained for the isolated ligands are shown in Figures 5.6 and 5.7. These spectra were recorded in dichloromethane. Inspection of the methylene proton resonances reveals a small amount of the other diastereomer present in each sample but the purity of each major component is greater than 95%. The  $^1\text{H}$  spectrum for the methylene protons of **2M** reveals a complex splitting pattern which manifests itself as the four pseudo-triplets observed. The two protons will be inequivalent because of the symmetry of the ligand and this should give rise to two distant resonances for each proton with  $^1\text{H}$ - $^1\text{H}$  coupling and  $^1\text{H}$ - $^{31}\text{P}$  coupling which gives rise to the complex pattern observed. The  $^1\text{H}$  spectrum for **2R** reveals a broadened triplet centered at 2.8 ppm. These two protons should be equivalent and the triplet pattern is caused by equivalent coupling to the two internal phosphines with a measured coupling constant of 3.2 Hz. The broadening could be caused by long range  $^1\text{H}$  or  $^{31}\text{P}$  coupling. The  $^{31}\text{P}$  spectra reveal two 12-line patterns but the downfield half of the signals are significantly more broadened. This comes about because of the dichloromethane used as the solvent. Somehow this solvent causes this half of the spectrum to become broadened over time. We currently do not have an explanation for this broadening but these ligands should not remain dissolved in dichloromethane for more than a few hours.

These experiments have shown one surprising aspect of the new ligands **2M** and **2R**. During the cyanolysis of the old bimetallic Ni complexes, it was discovered that a significant

amount of isomerization of the ligands occurred. In fact it was shown that starting with pure  $\text{Ni}_2\mathbf{1M}$  you could obtain a mixture of  $\mathbf{1M}$  and  $\mathbf{1R}$  with more  $\mathbf{1R}$  than  $\mathbf{1M}$ . A small amount of isomerization does occur during the cyanolysis of  $\mathbf{2M}$  and  $\mathbf{2R}$ , but it is minuscule compared to the isomerization that could be observed with the old ligands.

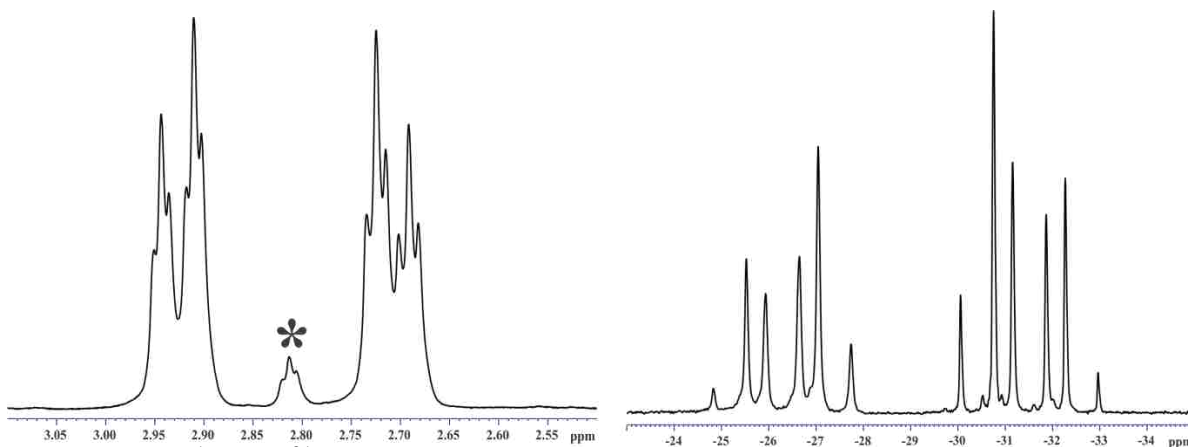


**Figure 5.6**  $^1\text{H}$  and  $^{31}\text{P}$  NMR spectra for  $\mathbf{2M}$ . The starred peak is a small amount of  $\mathbf{2R}$ .

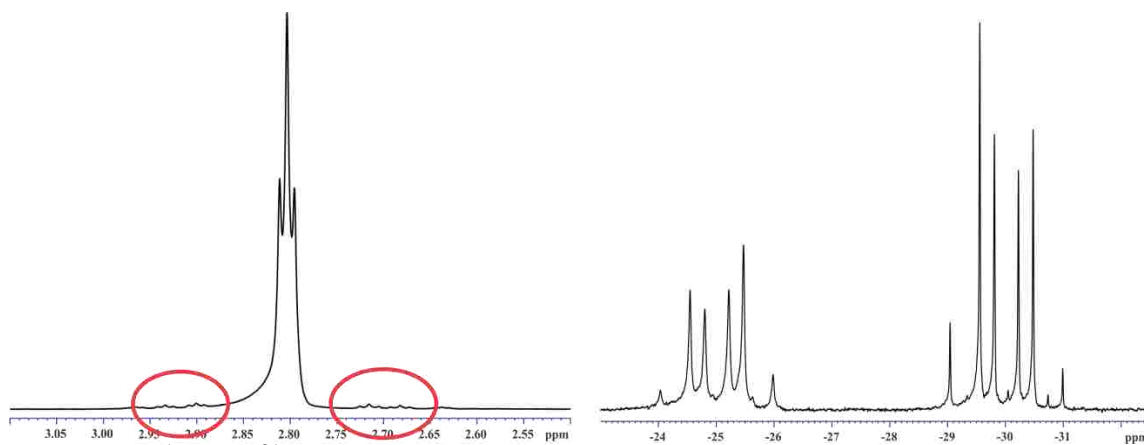


**Figure 5.7**  $^1\text{H}$  and  $^{31}\text{P}$  NMR spectra for  $\mathbf{2R}$ . The red circles mark a small amount of  $\mathbf{2M}$ .

Washing the column with methanol allowed us to collect the red impurities. NMR analysis of these extracts did not allow for identification of the red compounds. Dissolving the red compounds in benzene and allowing these solutions to sit for days at room temperature has afforded single crystals suitable for X-ray analysis. The structures of two of these crystals were solved and revealed them to be monometallic Ni-cyano complexes with the tetraphosphine (both

**2M** and **2R**) wrapped around a single metal center. ORTEP plots for the two crystal structures are shown in Figures 5.8 and 5.9.

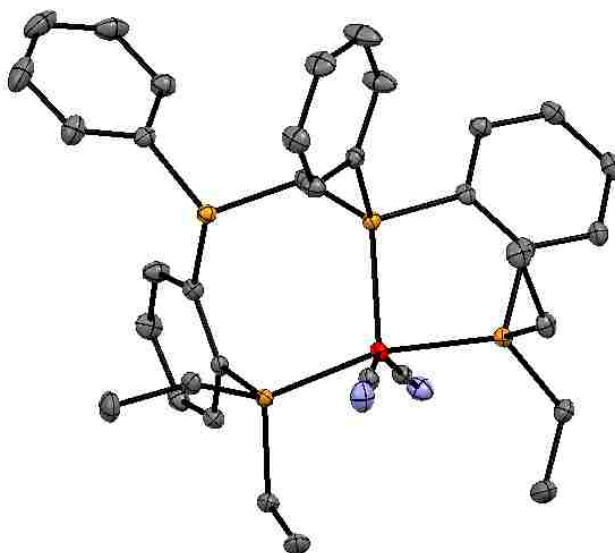


**Figure 5.8** ORTEP plot of  $\text{Ni}(\text{CN})_2(\kappa^3\text{-2M})$ . H atoms have been removed for clarity.  
Ni – red, P – orange, C – black, N - blue

Figure 5.8 shows the monometallic complex obtained with **2M**. The complex crystallized in the  $P2_1/c$  space group with distorted square pyramidal geometry. The two external phosphines and the two cyanide ligands occupy the square plane with one of the internal phosphines occupying the axial position. The other internal phosphine is not bound to the metal and has a Ni-P distance of 3.94 Å. The two Ni-P bond lengths in the square plane have bond lengths of 2.18 and 2.19 Å. The Ni-P distance for the apical internal phosphine occupying the axial position shows a longer bond length of 2.29 Å.

Figure 5.9 shows the structure of the  $[\text{Ni}(\text{CN})(\kappa^{3.5}\text{-2R})]\text{Cl}$  complex. The chloride counteranion is not shown in the ORTEP plot. The complex crystallizes in the  $P2_1/n$  space group with distorted square planar geometry. The distortion comes about from a weak interaction between one of the internal phosphines and the Ni center. The Ni-P distance is 2.82 Å which is

too large for a true Ni-P bond. The other three phosphines occupy three positions of the square plane with the final coordination site occupied by a cyanide ligand.

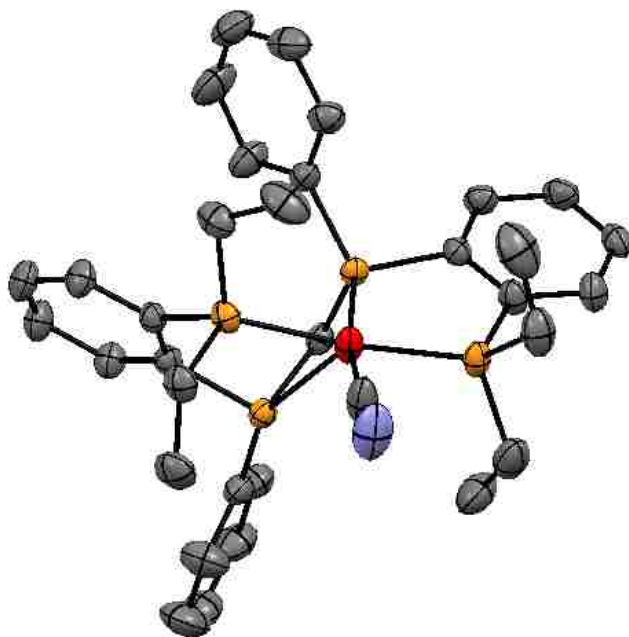


**Figure 5.9** ORTEP plot of  $[\text{Ni}(\text{CN})(\kappa^{3.5}\text{-2R})]^+$ . H atoms have been removed for clarity. Ni – red, P – orange, C – black, N – blue

The identification of these two monometallic complexes clearly demonstrates that 283 equivalents of  $\text{CN}^-$  are not enough to completely liberate the phosphine ligand from the metal complexes. These complexes remain in solution throughout the course of the cyanolysis and this considerable amount of cyanide is still not enough to liberate the stronger coordinating phosphine ligand.

The monometallic complexes have been further reacted with more NaCN (~150 equivalents) and another portion of free ligand is obtained. However, this is not a practical separation strategy to obtain the pure diastereomers because of the small percent yields and the excessively large amount of NaCN that is required to separate the ligand from the metal complexes especially if two or three separate cyanolysis experiments have to be conducted to remove the majority of the ligands from the Ni centers.



## 5.5 Preliminary Investigation into the Solution-State Chemistry and Reactivity of **Ni<sub>2</sub>2M** and **Ni<sub>2</sub>2R**

With the successful synthesis and separation of **Ni<sub>2</sub>2M** and **Ni<sub>2</sub>2R**, preliminary experiments were conducting concerning these complexes solution-state chemistry and reactivity. The first mode of reactivity investigated was alkene hydration. Several different reactions were conducted with **Ni<sub>2</sub>2M** and styrene as the substrate. All were conducted under an inert atmosphere inside glass pressure vessels. In the few reactions conducted no products were identified via GC/MS.

However, this complex did lead to the formation of polystyrene, which is a little unusual. After the solutions were heated and stirred overnight, a white clump was observed at the bottom of the reaction vessel. The clump was separated from the remaining solution via filtration and dried in air. NMR analysis of a piece of the clump revealed it to be polystyrene. This was never observed during any of the alkene hydration reactions discussed in Chapter 2. This observation suggests these new complexes could have some interesting catalytic reactivity.

Both complexes were also tested for the alkene oxidative cleavage reaction. The experiments were conducted under a balloon atmosphere of O<sub>2</sub> with styrene as the substrate. A small amount of benzaldehyde was observed after the solutions stirred overnight. The benzaldehyde was identified via GC/MS and NMR analysis. The amount of aldehyde was very similar to that observed with old ligand complexes, **Ni<sub>2</sub>1M** and **Ni<sub>2</sub>1R**. These results could suggest that the oxidative cleavage comes about from the oxidation of the phosphine ligands but more work needs to be done to validate this hypothesis. However, the fact that nearly identical amounts of aldehyde are produced for all 4 bimetallic complexes strongly points to the phosphine oxidation/oxidative cleavage pathway discussed in Chapter 3.

Some attempts were also made to investigate any reactivity between the new complexes and water via NMR analysis. Unfortunately it was discovered that these new complexes have very poor solubility in many solvents. In fact 10 mM solutions were not possible in any acetone/water or acetonitrile/water solvent systems. Thus it was not possible to obtain reasonable NMR spectra because of the low concentrations obtained in these solutions. A few spectra were obtained in water/acetone and water/acetonitrile. These spectra required over 1000 scans yet they still showed poor signal to noise ratios. There does appear to be at least one new symmetrical complex formed in the water/organic solvent systems suggesting these bimetallic complexes also react with water. More data is required in order to make any comparisons between the new and old complexes.

The reactivity between these new complexes and  $\text{Ag}^+$  was also investigated. A very surprising result was obtained during these experiments. **Ni<sub>2</sub>2M** was reacted with 4 equivalents of  $\text{AgBF}_4$  in acetone. After the precipitated  $\text{AgCl}$  was removed via centrifugation, a sample was collected for NMR analysis. The spectrum revealed two symmetrical multiplets, one centered at 65.8 ppm and the other centered at -10.7 ppm. The downfield multiplet is shown in Figure 5.10 next to the multiplet observed for complex **B** (Chapter 4). It is clear that these two species give rise to the same pattern with differences in the splittings between the resonances. This suggests that these complexes have the same structure. **B** has been proposed to be a monometallic Ni complex in which the two external phosphines are bound to the metal *trans* to one another and the two internal phosphines are not bound to the metal. It appears from this result that this structure is also possible with the new ligands.

One difference was that acetonitrile was not required to see the formation of this structure with the new ligand. During the reactions between **Ni<sub>2</sub>1M** and  $\text{Ag}$ , the only time **B** was observed

was when acetonitrile was the solvent. This complex did not form in acetone. Another difference observed was that over time the complex formed from **Ni<sub>2</sub>2M** did not convert to another complex unlike **B** which was found to convert to **F**.

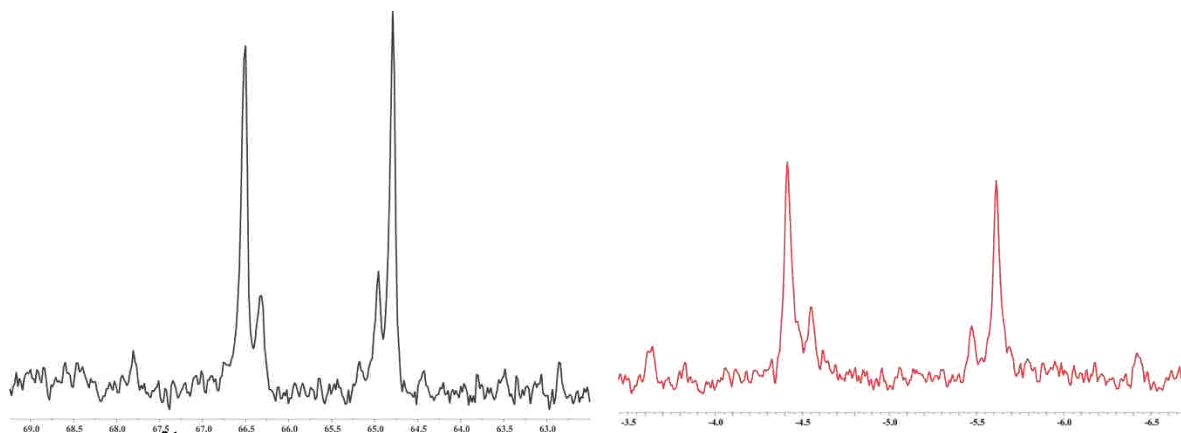


**Figure 5.10** <sup>31</sup>P NMR spectra showing the resonances observed when **Ni<sub>2</sub>2M** was reacted with 4 equivalents of AgBF<sub>4</sub> in acetone (black spectrum) and complex **B** (red spectrum) formed during the reaction between **Ni<sub>2</sub>1M** and water.

## 5.6 Conclusions

Dr. Alex Monteil developed and successfully synthesized the new linear tetratertiary phosphine ligands **2M** and **2R**. He developed a straightforward synthesis that allows for the isolation of a 50:50 mixture of **2M** and **2R** in modest yield. One important detail that has yet to be explained concerns the synthesis of **4**. This chlorinated phosphine should be formed as a mixture of two diastereomers. However, the NMR almost always reveals the presence of only one. We currently do not understand why this occurs and more work is continuing to figure out the mechanism for this chlorination process.

The synthesis of the bimetallic complexes has been developed. It was found that utilizing both dichloromethane and 1-butanol leads to very clean separation of **Ni<sub>2</sub>2M** and **Ni<sub>2</sub>2R**. The *meso* complex precipitates out of solution as an orange powder leaving behind mostly **Ni<sub>2</sub>2R**. Recrystallization of the mostly **Ni<sub>2</sub>2R** affords this complex in its pure form. Both complexes have been crystallized and their structures have been determined via single crystal X-ray

diffraction. This was the first time that **Ni<sub>2</sub>2R** was crystallized and allowed for irrefutable proof that both **2M** and **2R** are formed during the synthesis of the phosphine ligands.

Cyanolysis experiments have been conducted on both complexes to allow for the isolation of the pure ligand diastereomers. It has been found that during the course of the cyanolysis monometallic Ni/cyano complexes are formed which are stable towards the large excess of NaCN present in solution. Two of these complexes have been characterized via single crystal X-ray analysis. Both diastereomers are not susceptible to cyanide-induced isomerization, unlike **1M** which readily isomerizes to **1R**. This methodology, unfortunately, is currently not practical for isolating the pure diastereomers. Both diastereomers have been isolated and characterized in high purity (more than 95%) but the cyanolysis suffers from low yields of the free ligand (~40%) and the large amount of NaCN required to achieve these yields. Column chromatography seems to be a better suited separation technique for these ligands and work is currently underway to achieve clean separation of the diastereomers with some promising initial results obtained by Katerina Kalachnikova.

Preliminary investigations were begun into these two complexes reactivity and solution-state chemistry. Both complexes are capable of performing the oxidative cleavage of styrene. However, the results obtained so far suggest these complexes behave exactly like the old complexes **Ni<sub>2</sub>1M** and **Ni<sub>2</sub>1R**. More work will be required to prove this hypothesis. No alkene hydration reactivity was observed with the new bimetallic complexes but they did lead to the production of some polystyrene. This was never observed during all of the other alkene hydration experiments (Chapter 2) and this result suggests that these new complexes could show some interesting reactivity. Much more work will be required to determine whether any catalytic reactivity can be observed from these two complexes.

Attempts to investigate the reactivity between  $\text{Ni}_2\mathbf{2M}$  or  $\text{Ni}_2\mathbf{2R}$  and water have failed because of the complexes' poor solubility in all acetone/water and acetonitrile/water solvent systems attempted. Preliminary NMR spectra did show the formation of one symmetrical species but not enough data has been collected to make any comparisons with the old complexes. Other solvents, including DMSO and DMF, should be investigated to determine if any interesting reactivity between the complexes and water occur. Reactions with 4 equivalents of  $\text{AgBF}_4$  have allowed us to identify a new species which gives rise to a similar pattern as complex **B**, a proposed monometallic complex. These results coupled with the two crystal structures for the monometallic cyano complexes of  $\mathbf{2M}$  and  $\mathbf{2R}$  point to the possibility that the solution-state chemistry of these new ligands and complexes are, once again, very similar to the old complexes  $\text{Ni}_2\mathbf{1M}$  and  $\text{Ni}_2\mathbf{1R}$ . More research will be required to verify this hypothesis.

## 5.7 References

1. Matthews, R. C.; Howell, D. K.; Peng, W.-J.; Train, S. G.; Treleaven, W. D.; Stanley, G. G. *Angew. Chem., Int. Ed.* **1996**, 35, 2253-2256.
2. Matthews, R. C. *Ph. D. Dissertation, Louisiana State University, Baton Rouge, LA, 1999.*
3. Gueorguieva, P. G. *Ph. D. Dissertation, Louisiana State University, Baton Rouge, LA, 2004.*
4. Polakova, D. *Ph. D. Dissertation, Louisiana State University, Baton Rouge, LA, 2012.*
5. Aubry, D. A.; Bridges, N. N.; Ezell, K.; Stanley, G. G. *J. Am Chem. Soc.* **2003**, 125, 11180-11181.
6. Broussard, M. E.; Juma, B.; Train, S. G., Peng, W.-J.; Laneman, S. A.; Stanley, G. G. *Science* **1993**, 260, 1784-1788.
7. Monteil, A. *Ph. D. Dissertation, Louisiana State University, 2006.*
8. Weferling, N. *Z. Anorg. Allg. Chem.* **1987**, 548, 55-62.
9. Gol, F.; Hasselkuß, G.; Knüppel, P. C.; Stelzer, O. *Z. Naturforsch., B: Chem. Sci.* **1988**, 43, 31-44.

10. Schmidbaur, H.; Schnatterer, S. *Chem. Ber.* **1986**, 119, 2832-42.
11. Boymond, L.; Rottländer, M.; Cahiez, G.; Knochel, P. *Angew. Chem., Int. Ed.* **1998**, 37, 1701-1703.
12. Laneman, S. A.; Fronczek, F. R.; Stanley, G. G. *Inorg. Chem.* **1989**, 28, 1872-1878.
13. Aubry, D. A.; Laneman, S. A.; Fronczek, F. R.; Stanley, G. G. *Inorg. Chem.* **2001**, 40, 5036-5041.

## CHAPTER 6: EXPERIMENTAL PROCEDURES

### 6.1 General

All manipulations of air- and moisture-sensitive reagents were performed under an inert atmosphere of Nitrogen in either a Vacuum Atmospheres or MBraun Glovebox or using standard Schlenk techniques. All solvents were reagent grade or higher. When dealing with air-sensitive reagents, the solvents were degassed prior to use. The 1-hexene and 1-octene were stored under N<sub>2</sub> and passed through an alumina column prior to use. Styrene (99+% w/inhibitor present) was purified via removal of the inhibitor with aqueous NaOH and then passed through a neutral alumina column and stored under N<sub>2</sub> in the refrigerator in an Al foil-wrapped round bottom flask. All other alkenes were also passed through an alumina column prior to use. Triphenylphosphine (PPh<sub>3</sub>), tricyclohexylphosphine (PCy<sub>3</sub>), 1,2-bis(diphenylphosphino)ethane (dppe), 1,3-bis(diphenylphosphino)propane (dppp), 1,4-bis(diphenylphosphino)butane (dppb), 1,2-bis(dicyclohexylphosphino)ethane (dcpe), BISBI, NAPHOS, XANTPHOS, benzene-1,2-diamine (bzdiam), 1,10-phenanthroline (phen), tetramethylethylenediamine (TMEDA), dimethylglyoxime (dmgly) AgBF<sub>4</sub>, bis-(cylcooctadiene)Ni [Ni(COD)]<sub>2</sub>, PtCl<sub>2</sub>(PET<sub>3</sub>)<sub>2</sub>, PdCl<sub>2</sub>(PPh<sub>3</sub>)<sub>2</sub>, RhCl<sub>3</sub>, RhCl(PPh<sub>3</sub>)<sub>3</sub>, CoCl<sub>2</sub>, FeCl<sub>3</sub>, CuSO<sub>4</sub>, FeCl<sub>2</sub>, NiCl<sub>2</sub>, Ni(BF<sub>4</sub>)<sub>2</sub>, [IrCl(COD)]<sub>2</sub>, IrCl<sub>3</sub>, Rh(acac)(CO)<sub>2</sub>, PdCl<sub>2</sub>(benzonitrile)<sub>2</sub>, [RuCl<sub>2</sub>(benzene)]<sub>2</sub>, PtCl<sub>2</sub>(COD), Fe(BF<sub>4</sub>)<sub>2</sub>, CuCl<sub>2</sub>, ferrocenium tetrafluoroborate, NaCl, NH<sub>4</sub>Cl, I<sub>2</sub>, propanal, isobutyraldehyde, TEMPO, BHT, MEHQ, malonic acid, K<sub>2</sub>C<sub>2</sub>O<sub>4</sub>, CsOH, NaOH, KOH, concentrated HCl, concentrated H<sub>2</sub>SO<sub>4</sub>, 35% aqueous H<sub>2</sub>O<sub>2</sub> and 70% aqueous TBHP were purchased from commercial suppliers (Aldrich, Strem, Fischer) in their highest purity and used as received. NiCl<sub>2</sub>(PPh<sub>3</sub>)<sub>2</sub>, NiCl<sub>2</sub>(dppe), NiCl<sub>2</sub>(dcpe), NiCl<sub>2</sub>(dppp), NiCl<sub>2</sub>(dppb), mixed *meso*- and *racemic*-et,ph-P4 ligand, **1M** and **1R**, *meso*-Ni<sub>2</sub>Cl<sub>4</sub>(et,ph-P4), **Ni<sub>2</sub>1M**, and *racemic*-Ni<sub>2</sub>Cl<sub>4</sub>(et,ph-P4), **Ni<sub>2</sub>1R**, were synthesized using literature methods.<sup>1-8</sup> All

synthesized Ni complexes are air-stable in the solid-state and almost all of the complexes are air stable in the solution-state depending on solvents used.

$^{31}\text{P}$  and  $^1\text{H}$  NMR spectra were recorded on either a Bruker DPX-250, DPX-400, AV-400 or Varian-500 MHz spectrometer. All  $^1\text{H}$  NMR spectra were referenced internally to either added TMS (0.0 ppm) or to the residual solvent peak. All  $^{31}\text{P}$  NMR spectra were referenced externally to 85%  $\text{H}_3\text{PO}_4$  (0.0 ppm). Data processing was done using Topspin or Mestrenova software packages. FT-IR spectra were recorded on a Bruker Tensor 27 FT-IR. GC/MS data was recorded on an Agilent 6890N GC equipped with Autosample Loader and HP-5MS column (30m x 0.25 mm x 0.25  $\mu\text{m}$ ) connected to an Agilent 5975B MS. GPC data was obtained with a Phenogel 8  $\mu\text{m}$  x 7.8 mm x 30 cm column with a pore size of  $10^5$  angstroms eluted in THF at 1 mL/min. The detector was an Agilent DRI 1200.

For the X-ray crystallography suitable crystals were mounted on a glass fiber using epoxy. Data collection was performed on either a Nonius KappaCCD diffractometer using Mo  $\text{K}\alpha$  radiation and graphite crystal monochromators or a Bruker Kappa APEX-II DUO diffractometer using Mo  $\text{K}\alpha$  or Cu  $\text{K}\alpha$  radiation and graphite crystal monochromators.

## **6.2 Attempts at Alkene Hydration Catalysis**

### **6.2.1 General Comments**

All of the following reactions were conducted under an inert atmosphere of  $\text{N}_2$ . Two methods were used for the removal of precipitated  $\text{AgCl}$  when  $\text{AgBF}_4$  was utilized as an additive. Method A involved filtering the solution through a fine frit funnel before the addition of substrate and/or other additives. Method B involved transferring the mixture to a centrifuge tube and centrifuging the mixture for 5 to 10 minutes. The clear solution was then decanted into



a clean reaction flask before the addition of substrate and/or other additives. All solutions contained 10 mM concentrations of the complex or metal salt.

### 6.2.2 Reaction Types

**H1:** A Schlenk flask was charged with the appropriate amount of complex, organic solvent, water and any additives. If no  $\text{AgBF}_4$  was added, the substrate was also added at this time. When  $\text{AgBF}_4$  was utilized, the substrate and any other additive was added after the removal of the  $\text{AgCl}$ . The flask was attached to a condenser and this setup was placed onto a Schlenk line. The reaction mixture was then heated to  $80^\circ\text{C}$  overnight with rapid stirring. The next day the reaction mixture was cooled to room temperature. The flask was exposed to air and an aliquot was collected. The aliquot was diluted with acetone and analyzed via GC/MS to identify any products formed.

**H2:** A 3-neck flask was charged with the appropriate amount of complex, organic solvent and additive. If no  $\text{AgBF}_4$  was added, the substrate was also added at this time. When  $\text{AgBF}_4$  was added, the substrate and any other additive was added after removing the  $\text{AgCl}$ . The 3-neck flask was then connected to a condenser and attached to a Schlenk line. The flask was heated to  $80^\circ\text{C}$  with rapid stirring. As the flask was heated, the water was slowly added dropwise via cannula. In some cases an additive (KOH for example) was added with the water. After the addition, the flask was allowed to heat and stir overnight. The next day the reaction mixture was cooled to room temperature and an aliquot was collected. The aliquot was diluted with acetone and analyzed via GC/MS for the formation of any products.

**H3:** A 3-neck flask was charged with the appropriate amount of complex, organic solvent, water, additive and substrate. The flask was connected to a condenser and attached to a Schlenk line. The reaction mixture was heated to  $80^\circ\text{C}$  and allowed to heat and stir overnight.

The next day the flask was cooled to room temperature and an aliquot was collected. The aliquot was diluted with acetone and analyzed via GC/MS for the formation of any products.

### 6.2.3 Reaction Table

**Table 6.1** Alkene Hydration Reactions

Complex	Solvent System	Substrate	Additives	Temp.	Type
Ni <sub>2</sub> 1M	14 mL acetone/6 mL water	100 eq. 1-hex	4 eq. AgBF <sub>4</sub>	80°C	H1
Ni <sub>2</sub> 1M	14 mL acetone/6 mL water	100 eq. 1-hex	4 eq. AgBF <sub>4</sub>	80°C	H1
Ni <sub>2</sub> 1M	14 mL acetone/6 mL water	100 eq. 1-hex	4 eq. AgBF <sub>4</sub>	80°C	H1
Ni <sub>2</sub> 1M	14 mL acetone/6 mL water	100 eq. 1-hex	4 eq. AgBF <sub>4</sub> , 0.5 eq. KOH	80°C	H1
Ni <sub>2</sub> 1M	14 mL acetone/6 mL water	100 eq. 1-hex	4 eq. AgBF <sub>4</sub> , 2 eq. KOH	80°C	H1
Ni <sub>2</sub> 1M	14 mL acetone/6 mL water	50 eq. 1-hex	2 eq. AgBF <sub>4</sub>	80°C	H1
Ni <sub>2</sub> 1M	17 mL acetone/3 mL water	100 eq. 1-hex		80°C	H1
Ni <sub>2</sub> 1M	14 mL acetone/6 mL water	100 eq. 1-hex	2 eq. AgBF <sub>4</sub> , conc. H <sub>2</sub> SO <sub>4</sub>	80°C	H1
Ni <sub>2</sub> 1M	14 mL acetone/6 mL water	50 eq. 1-hex	2 eq. AgBF <sub>4</sub> , 1 eq. KOH	80°C	H1
Ni <sub>2</sub> 1M	14 mL acetone/6 mL water	50 eq. 1-hex	2 eq. AgBF <sub>4</sub> , 1 eq. KOH	80°C	H1
Ni <sub>2</sub> 1M	14 mL acetone/6 mL water	100 eq. 1-hex	4 eq. AgBF <sub>4</sub>	80°C	H1
Ni <sub>2</sub> 1M	14 mL acetone/6 mL water	100 eq. 1-hex	2 eq. AgBF <sub>4</sub> , 2 eq. CaCO <sub>3</sub>	80°C	H1
Ni <sub>2</sub> 1M	14 mL acetone/6 mL water	100 eq. 1-hex	2 eq. AgBF <sub>4</sub> , 2 eq. NaClO	80°C	H1
Ni <sub>2</sub> 1M	14 mL acetone/6 mL water	100 eq. 1-hex	4 eq. AgBF <sub>4</sub> , 1 eq. I <sub>2</sub>	80°C	H1
Ni <sub>2</sub> 1M	14 mL acetone/6 mL water	100 eq. 1-hex	1 eq. I <sub>2</sub>	80°C	H1
Ni <sub>2</sub> 1M	14 mL acetone/6 mL water	100 eq. 1-hex	4 eq. AgBF <sub>4</sub> , 1 eq. I <sub>2</sub>	80°C	H1
Ni <sub>2</sub> 1M	14 mL acetone/6 mL water	100 eq. 1-hex	4 eq. AgBF <sub>4</sub> , 2.2 eq. FeCl <sub>3</sub> , conc. HCl	80°C	H1
Ni <sub>2</sub> 1R	14 mL acetone/6 mL water	100 eq. 1-hex	2 eq. AgBF <sub>4</sub> , 2.2 eq. FeCl <sub>3</sub>	80°C	H1

Table 6.1 continued

Complex	Solvent System	Substrate	Additives	Temp.	Type
Ni <sub>2</sub> 1R	14 mL acetone/6 mL water	100 eq. 1-hex	2.2 eq. FeCl <sub>3</sub>	80°C	H1
Ni <sub>2</sub> 1R	14 mL acetone/6 mL water	100 eq. 1-hex	4 eq. AgBF <sub>4</sub>	80°C	H1
Ni <sub>2</sub> 1R	14 mL acetone/6 mL water	100 eq. 1-hex	2 eq. AgBF <sub>4</sub> , 18 eq. KOH	80°C	H1
Ni <sub>2</sub> 1R	14 mL acetone/6 mL water	100 eq. 1-hex	2 eq. AgBF <sub>4</sub> , 4 eq. KOH	80°C	H1
Ni <sub>2</sub> 1R	14 mL acetone/6 mL water	100 eq. 1-hex	4 eq. AgBF <sub>4</sub> , conc. HCl, 2.2 eq. FeCl <sub>3</sub>	80°C	H1
Ni <sub>2</sub> 1R	14 mL acetone/6 mL water	100 eq. 1-hex	4 eq. AgBF <sub>4</sub> , 4 eq. NaHCO <sub>3</sub> , 2.2 eq. FeCl <sub>3</sub>	80°C	H1
Ni <sub>2</sub> 1R	14 mL acetone/6 mL water	100 eq. 1-hex	4 eq. AgBF <sub>4</sub> , conc. HCl, 2.2 eq. FeCl <sub>3</sub>	80°C	H1
Ni <sub>2</sub> 1R	14 mL acetone/6 mL water	50 eq. 1-hex	4 eq. AgBF <sub>4</sub> , conc. HCl, 2 eq. I <sub>2</sub>	80°C	H1
Ni <sub>2</sub> 1R	14 mL acetone/6 mL water	100 eq. 1-hex	100 eq. NaOH	80°C	H2
Ni <sub>2</sub> 1R	14 mL acetone/6 mL water	200 eq. 1-hex	50 eq. NaOH	80°C	H2
Ni <sub>2</sub> 1M	14 mL acetone/6 mL water	100 eq. 1-hex	50 eq. NaOH	80°C	H2
Ni <sub>2</sub> 1R	14 mL acetone/6 mL water	100 eq. 1-hex	4 eq. AgBF <sub>4</sub> , 2 eq. NaOH, 2 eq. I <sub>2</sub>	80°C	H2
Ni <sub>2</sub> 1M	14 mL acetone/6 mL water	100 eq. 1-hex	8 eq. AgBF <sub>4</sub>	80°C	H2
Ni <sub>2</sub> 1R	14 mL acetone/6 mL water	100 eq. 1-hex	8 eq. AgBF <sub>4</sub> , conc. HCl	80°C	H2
Ni <sub>2</sub> 1M	14 mL methanol/6 mL water	100 eq. 1-hex	8 eq. AgBF <sub>4</sub>	80°C	H2
Ni <sub>2</sub> 1M	14 mL DMF/6 mL water	100 eq. 1-hex	8 eq. AgBF <sub>4</sub>	80°C	H1
Ni <sub>2</sub> 1M	14 mL THF/6 mL water	100 eq. 1-hex	8 eq. AgBF <sub>4</sub>	80°C	H1
Ni <sub>2</sub> 1M	14 mL acetone/6 mL water	100 eq. 1-hex	4 eq. AgBF <sub>4</sub>	80°C	H2

Table 6.1 continued

Complex	Solvent System	Substrate	Additives	Temp.	Type
Ni <sub>2</sub> 1M	14 mL acetone/6 mL water	100 eq. 1-hex	4 eq. AgBF <sub>4</sub> , 2 eq. I <sub>2</sub>	80°C	H2
Ni <sub>2</sub> 1M	14 mL acetone/6 mL water	100 eq. 1-hex	2 eq. AgBF <sub>4</sub> , 2 eq. I <sub>2</sub>	80°C	H2
Ni <sub>2</sub> 1M	14 mL acetone/6 mL water	100 eq. 1-hex	8 eq. AgBF <sub>4</sub> , conc. HCl	80°C	H2
Ni <sub>2</sub> 1R	14 mL acetone/6 mL water	100 eq. 1-hex	8 eq. AgBF <sub>4</sub>	80°C	H2
Ni <sub>2</sub> 1R	14 mL acetone/6 mL water	100 eq. 1-hex	2 eq. I <sub>2</sub>	80°C	H2
Ni <sub>2</sub> 1R	14 mL acetone/6 mL water	100 eq. 1-hex	8 eq. AgBF <sub>4</sub> , conc. HCl	80°C	H2
Ni <sub>2</sub> 1R	14 mL acetone/6 mL water	100 eq. 1-hex	2 eq. I <sub>2</sub>	80°C	H2
Ni <sub>2</sub> 1R	14 mL acetone/6 mL water	100 eq. 1-hex		80°C	H2
Ni <sub>2</sub> 1R	14 mL acetone/6 mL water	100 eq. 1-hex	2 eq. AgBF <sub>4</sub>	80°C	H2
Ni <sub>2</sub> 1R	14 mL acetone/6 mL water	100 eq. 1-hex		80°C	H2
Ni <sub>2</sub> 1M	14 mL acetone/6 mL water	100 eq. 1-hex	8 eq. AgBF <sub>4</sub>	80°C	H2
Ni <sub>2</sub> 1M	14 mL acetone/6 mL water	100 eq. 1-hex	8 eq. AgBF <sub>4</sub>	80°C	H2
NiCl <sub>2</sub> dppe	14 mL acetone/6 mL water	100 eq. 1-hex		80°C	H1
Ni <sub>2</sub> 1R	17 mL acetone/3 mL water	100 eq. 1-hex		80°C	H1
NiCl <sub>2</sub> dppe	14 mL acetone/6 mL water	100 eq. 1-hex		80°C	H1
NiCl <sub>2</sub> (PPh <sub>3</sub> ) <sub>2</sub>	14 mL acetone/6 mL water	100 eq. 1-hex		80°C	H1
NiCl <sub>2</sub> dppe	14 mL acetone/6 mL water	100 eq. 1-hex		80°C	H1
Ni <sub>2</sub> 1R	14 mL acetone/6 mL water	100 eq. 1-hex	2 eq. AgBF <sub>4</sub> , 1 eq. KOH	80°C	H2
Ni <sub>2</sub> 1R	14 mL acetone/6 mL water	100 eq. 1-hex	2 eq. AgBF <sub>4</sub> , 1 eq. KOH	80°C	H2
Ni <sub>2</sub> 1R	14 mL acetone/6 mL water	100 eq. 1-hex	4 eq. AgBF <sub>4</sub>	80°C	H2
Ni <sub>2</sub> 1R	14 mL acetone/6 mL water	100 eq. 1-hex	2 eq. AgBF <sub>4</sub> , 2 eq. CaCO <sub>3</sub>	80°C	H2

Table 6.1 continued

Complex	Solvent System	Substrate	Additives	Temp.	Type
Ni <sub>2</sub> 1R	14 mL acetone/6 mL water	100 eq. 1-hex	2 eq. AgBF <sub>4</sub> , 2 eq. NaClO	80°C	H2
Ni <sub>2</sub> 1R	14 mL acetone/6 mL water	100 eq. 1-hex	4 eq. AgBF <sub>4</sub> , 1 eq. I <sub>2</sub>	80°C	H2
Ni <sub>2</sub> 1R	14 mL acetone/6 mL water	100 eq. 1-hex	1 eq. I <sub>2</sub>	80°C	H2
Ni <sub>2</sub> 1R	14 mL acetone/6 mL water	100 eq. 1-octene		80°C	H2
Ni <sub>2</sub> 1R	14 mL acetone/6 mL water	100 eq. styrene		80°C	H2
Ni <sub>2</sub> 1R	14 mL acetone/6 mL water	100 eq. 1-hex		80°C	H2
Ni <sub>2</sub> 1R	14 mL acetone/6 mL water	100 eq. 1-hex	8 eq. AgBF <sub>4</sub>	80°C	H2
Ni <sub>2</sub> 1M	14 mL acetone/6 mL water	100 eq. 1-hex	4 eq. AgBF <sub>4</sub> , 2 mL HBF <sub>4</sub>	80°C	H2
Ni <sub>2</sub> 1M	14 mL acetone/6 mL water	100 eq. 1-hex	2 eq. ferrocenium BF <sub>4</sub>	80°C	H2
Ni <sub>2</sub> 1M	14 mL acetone/6 mL water	100 eq. 1-hex	4 eq. AgBF <sub>4</sub> , 2 eq. ferrocenium BF <sub>4</sub>	80°C	H2
Ni <sub>2</sub> 1M	14 mL acetone/6 mL water	100 eq. 1-hex	8 eq. AgBF <sub>4</sub>	80°C	H2
Ni <sub>2</sub> 1M	14 mL acetone/6 mL water	100 eq. 1-hex	2 eq. PPh <sub>3</sub>	80°C	H2
Ni <sub>2</sub> 1R	14 mL acetone/6 mL water	100 eq. 1-hex	2 eq. PPh <sub>3</sub>	80°C	H2
Ni <sub>2</sub> 1R	14 mL acetone/6 mL water	100 eq. 1-hex	2 eq. ferrocenium BF <sub>4</sub>	80°C	H2
Ni <sub>2</sub> 1R	14 mL acetone/6 mL water	100 eq. 1-hex	2 mL HBF <sub>4</sub> , 2 eq. PPh <sub>3</sub>	80°C	H2
Ni <sub>2</sub> 1R	14 mL acetone/6 mL water	1000 eq. 1-hex	4 eq. AgBF <sub>4</sub>	80°C	H2
Ni <sub>2</sub> 1R	14 mL acetone/6 mL water	100 eq. 1-hex	4 eq. AgBF <sub>4</sub> , 2 eq. ferrocenium BF <sub>4</sub>	80°C	H2
Ni <sub>2</sub> 1M	14 mL acetone/6 mL water	100 eq. 1-octene		80°C	H2
Ni <sub>2</sub> 1M	14 mL acetone/6 mL water	100 eq. styrene		80°C	H2
Ni <sub>2</sub> 1M	19 mL acetone/1 mL water	100 eq. 1-hex		80°C	H2

Table 6.1 continued

Complex	Solvent System	Substrate	Additives	Temp.	Type
Ni <sub>2</sub> 1M	14 mL acetone/6 mL water	100 eq. 1-hex	conc. HCl	80°C	H2
Ni <sub>2</sub> 1R	19 mL acetone/1 mL water	100 eq. 1-hex		80°C	H2
NiCl <sub>2</sub> dpppe	14 mL acetone/6 mL water	100 eq. 1-hex		80°C	H2
NiCl <sub>2</sub> (PPh <sub>3</sub> ) <sub>2</sub>	14 mL acetone/6 mL water	100 eq. 1-hex	conc. HCl	80°C	H2
Ni <sub>2</sub> 1M	14 mL THF/6 mL water	100 eq. 1-hex		80°C	H2
Ni <sub>2</sub> 1R	14 mL THF/6 mL water	100 eq. 1-hex		80°C	H2
Ni <sub>2</sub> 1M	14 mL acetone/6 mL water	100 eq. 1-hex	4 eq. AgBF <sub>4</sub>	80°C	H2
Ni <sub>2</sub> 1M	14 mL acetone/6 mL water	1000 eq. 1-hex	4 eq. AgBF <sub>4</sub>	80°C	H2
Ni <sub>2</sub> 1R	14 mL acetone/6 mL water	100 eq. 1-hex	4 eq. AgBF <sub>4</sub> , conc. HCl	80°C	H2
Ni <sub>2</sub> 1M	14 mL acetone/6 mL water	1 eq. 1-hex		80°C	H2
NiCl <sub>2</sub> (PPh <sub>3</sub> ) <sub>2</sub>	14 mL acetone/6 mL water	1 eq. 1-hex	2 eq. AgBF <sub>4</sub>	80°C	H2
NiCl <sub>2</sub> (PPh <sub>3</sub> ) <sub>2</sub>	14 mL acetone/6 mL water	2 eq. 1-hex		80°C	H2
Ni <sub>2</sub> 1M	14 mL acetone/6 mL water	100 eq. 1-hex	2 eq. PCy <sub>3</sub>	80°C	H2
NiCl <sub>2</sub> (PPh <sub>3</sub> ) <sub>2</sub>	14 mL acetone/6 mL water	2 eq. 1-hex		80°C	H2
Ni <sub>2</sub> 1M	14 mL methanol/6 mL water	100 eq. 1-hex	2 eq. AgBF <sub>4</sub>	80°C	H2
Ni <sub>2</sub> 1M	14 mL methanol/6 mL water	100 eq. 1-hex	4 eq. AgBF <sub>4</sub>	80°C	H2
Ni <sub>2</sub> 1M	14 mL CH <sub>3</sub> CN/6 mL water	100 eq. 1-hex	2 eq. AgBF <sub>4</sub>	80°C	H2
Ni <sub>2</sub> 1M	14 mL acetone/6 mL water	100 eq. 1-hex		80°C	H2
Ni <sub>2</sub> 1M	14 mL acetone/6 mL water	1000 eq. 1-hex		80°C	H2
Ni <sub>2</sub> 1R	14 mL acetone/6 mL water	1000 eq. 1-hex		80°C	H2

Table 6.1 continued

Complex	Solvent System	Substrate	Additives	Temp.	Type
Ni <sub>2</sub> 1M	14 mL acetone/6 mL water	100 eq. 1-hex	4 eq. KOH	80°C	H2
Ni <sub>2</sub> 1M	14 mL acetone/6 mL water	100 eq. 1-hex	2 eq. KOH	80°C	H2
Ni <sub>2</sub> 1M	14 mL acetone/6 mL water	100 eq. 1-hex		80°C	H2
Ni <sub>2</sub> 1M	14 mL acetone/6 mL water	100 eq. 1-hex	2 eq. KOH	80°C	H2
Ni <sub>2</sub> 1M	14 mL acetone/6 mL water	100 eq. 1-hex		80°C	H2
Ni <sub>2</sub> 1M	14 mL acetone/6 mL water	100 eq. 1-hex		80°C	H2
Ni <sub>2</sub> 1M	14 mL acetone/6 mL water	100 eq. 1-hex	3 eq. KOH	80°C	H2
Ni <sub>2</sub> 1M	14 mL acetone/6 mL water	1000 eq. 1-hex		80°C	H2
Ni <sub>2</sub> 1M	14 mL acetone/6 mL water	100 eq. 1-hex	1 eq. I <sub>2</sub>	80°C	H2
Ni <sub>2</sub> 1M	14 mL acetone/6 mL water	100 eq. 1-hex	100 eq. KOH	80°C	H2
Ni <sub>2</sub> 1M	14 mL acetone/6 mL water	100 eq. 1-hex	100 eq. KOH	80°C	H2
Ni <sub>2</sub> 1R	14 mL methanol/6 mL water	100 eq. 1-hex	2 eq. AgBF <sub>4</sub>	80°C	H2
Ni <sub>2</sub> 1R	14 mL methanol/6 mL water	100 eq. 1-hex	4 eq. AgBF <sub>4</sub>	80°C	H2
Ni <sub>2</sub> 1M	14 mL acetone/6 mL water	1000 eq. 1-hex		80°C	H2
Ni <sub>2</sub> 1M	14 mL acetone/6 mL water	100 eq. 1-hex	4 eq. KOH, conc. HCl	80°C	H2
PdCl <sub>2</sub> (PPh <sub>3</sub> ) <sub>2</sub>	14 mL acetone/6 mL water	100 eq. 1-hex		80°C	H2
CoCl <sub>2</sub> /PPh <sub>3</sub>	14 mL acetone/6 mL water	100 eq. 1-hex		80°C	H2
Ni <sub>2</sub> 1M	14 mL THF/6 mL water	100 eq. 1-hex	2 eq. AgBF <sub>4</sub>	80°C	H2
Ni <sub>2</sub> 1M	14 mL THF/6 mL water	100 eq. 1-hex	4 eq. AgBF <sub>4</sub>	80°C	H2
CoCl <sub>2</sub> /PCy <sub>3</sub>	14 mL acetone/6 mL water	100 eq. 1-hex		80°C	H2

**Table 6.1** continued

<b>Complex</b>	<b>Solvent System</b>	<b>Substrate</b>	<b>Additives</b>	<b>Temp.</b>	<b>Type</b>
<b>Ni<sub>2</sub>1M</b>	14 mL acetone/6 mL water	100 eq. styrene		80°C	H2
<b>Ni<sub>2</sub>1M</b>	14 mL acetone/6 mL water	100 eq. styrene	2 eq. AgBF <sub>4</sub>	80°C	H2
<b>Ni<sub>2</sub>1M</b>	14 mL acetone/6 mL water	100 eq. 1-octene		80°C	H2
PdCl <sub>2</sub> (PPh <sub>3</sub> ) <sub>2</sub>	14 mL acetone/6 mL water	100 eq. 1-hex	100 eq. KOH	80°C	H2
PtCl <sub>2</sub> (PEt <sub>3</sub> ) <sub>2</sub>	14 mL acetone/6 mL water	100 eq. 1-hex		80°C	H2
PdCl <sub>2</sub> (PPh <sub>3</sub> ) <sub>2</sub>	14 mL acetone/6 mL water	100 eq. 1-hex		80°C	H2
RhCl(PPh <sub>3</sub> ) <sub>3</sub>	14 mL acetone/6 mL water	100 eq. 1-hex	1 eq. AgBF <sub>4</sub>	80°C	H2
PdCl <sub>2</sub> (PPh <sub>3</sub> ) <sub>2</sub>	14 mL acetone/6 mL water	100 eq. 1-hex	2 eq. AgBF <sub>4</sub>	80°C	H2
PdCl <sub>2</sub> (PPh <sub>3</sub> ) <sub>2</sub>	14 mL acetone/6 mL water	100 eq. 1-hex	2 eq. AgBF <sub>4</sub>	80°C	H2
RhCl <sub>3</sub> /PPh <sub>3</sub>	14 mL acetone/6 mL water	100 eq. 1-hex	2 eq. AgBF <sub>4</sub> , conc. HCl	80°C	H2
PdCl <sub>2</sub> (PPh <sub>3</sub> ) <sub>2</sub>	14 mL acetone/6 mL water	100 eq. 1-hex	100 eq. KOH	80°C	H2
CuSO <sub>4</sub> /PPh <sub>3</sub>	14 mL acetone/6 mL water	100 eq. 1-hex		80°C	H2
RhCl <sub>3</sub> /PPh <sub>3</sub>	14 mL acetone/6 mL water	100 eq. 1-hex	100 eq. KOH	80°C	H2
NiCl <sub>2</sub> dppb	14 mL acetone/6 mL water	100 eq. 1-hex		80°C	H2
RhCl <sub>3</sub> /PPh <sub>3</sub>	14 mL acetone/6 mL water	100 eq. 1-hex	100 eq. KOH	80°C	H2
PtCl <sub>2</sub> (PEt <sub>3</sub> ) <sub>2</sub>	14 mL acetone/6 mL water	100 eq. 1-hex	2 eq. AgBF <sub>4</sub>	80°C	H2
RhCl <sub>3</sub> /PPh <sub>3</sub>	14 mL acetone/6 mL water	100 eq. 1-hex	100 eq. KOH	80°C	H2
NiCl <sub>2</sub> dppp	14 mL acetone/6 mL water	100 eq. 1-hex		80°C	H2
FeCl <sub>2</sub> /PPh <sub>3</sub>	14 mL acetone/6 mL water	100 eq. 1-hex		80°C	H2
PtCl <sub>2</sub> (PEt <sub>3</sub> ) <sub>2</sub>	14 mL acetone/6 mL water	100 eq. 1-hex	100 eq. KOH	80°C	H2
RhCl(PPh <sub>3</sub> ) <sub>3</sub>	14 mL acetone/6 mL water	100 eq. 1-hex	100 eq. KOH	80°C	H2



**Table 6.1** continued

<b>Complex</b>	<b>Solvent System</b>	<b>Substrate</b>	<b>Additives</b>	<b>Temp.</b>	<b>Type</b>
RhCl(PPh <sub>3</sub> ) <sub>3</sub>	14 mL acetone/6 mL water	100 eq. 1-hex	100 eq. KOH	80°C	H3
NiCl <sub>2</sub> dcpe	14 mL acetone/6 mL water	100 eq. 1-hex		80°C	H2
<b>Ni<sub>2</sub>1M</b>	14 mL acetone/6 mL water	100 eq. 1-hex		80°C	H2
PtCl <sub>2</sub> (PEt <sub>3</sub> ) <sub>2</sub>	14 mL acetone/6 mL water	100 eq. 1-hex	100 eq. KOH, conc. HCl	80°C	H2
NiCl <sub>2</sub> (PPh <sub>3</sub> ) <sub>2</sub>	14 mL acetone/6 mL water	100 eq. 1-hex		80°C	H2
RhCl(PPh <sub>3</sub> ) <sub>3</sub>	14 mL acetone/6 mL water	100 eq. 1-hex	100 eq. KOH, conc. HCl	80°C	H2
<b>Ni<sub>2</sub>1M</b>	14 mL acetone/6 mL water	100 eq. 1-hex		80°C	H2
Ni(COD)/PCy <sub>3</sub>	14 mL acetone/6 mL water	100 eq. 1-hex	conc. HCl	80°C	H2
PtCl <sub>2</sub> (PEt <sub>3</sub> ) <sub>2</sub>	14 mL acetone/6 mL water	100 eq. 1-hex	3 eq. AgBF <sub>4</sub> , conc. HCl	80°C	H2
RhCl(PPh <sub>3</sub> ) <sub>3</sub>	14 mL acetone/6 mL water	100 eq. 1-hex	1 eq. AgBF <sub>4</sub> , conc. HCl	80°C	H2
RhCl <sub>3</sub> /PPh <sub>3</sub>	14 mL acetone/6 mL water	100 eq. 1-hex	100 eq. KOH	80°C	H2
PdCl <sub>2</sub> (PPh <sub>3</sub> ) <sub>2</sub>	14 mL acetone/6 mL water	100 eq. 1-hex	conc. HCl	80°C	H2
<b>Ni<sub>2</sub>1M</b>	14 mL acetone/6 mL water	100 eq. 1-hex		80°C	H2
Ni/Rh/PPh <sub>3</sub>	14 mL acetone/6 mL water	100 eq. 1-hex		80°C	H2
CoCl <sub>2</sub> /PPh <sub>3</sub>	14 mL acetone/6 mL water	100 eq. 1-hex	100 eq. KOH	80°C	H2
RhCl <sub>3</sub> /PPh <sub>3</sub>	14 mL acetone/6 mL water	100 eq. 1-hex	20 eq. CaCO <sub>3</sub>	80°C	H2
RhCl <sub>3</sub> /PPh <sub>3</sub>	14 mL acetone/6 mL water	100 eq. 1-hex	20 eq. NH <sub>4</sub> Cl	80°C	H2
Ni/Co/PPh <sub>3</sub>	14 mL acetone/6 mL water	100 eq. 1-hex		80°C	H2
NiCl <sub>2</sub> (PPh <sub>3</sub> ) <sub>2</sub>	14 mL acetone/6 mL water	100 eq. 1-hex	20 eq. NH <sub>4</sub> Cl	80°C	H2
Ni/Zn/PPh <sub>3</sub>	14 mL acetone/6 mL water	100 eq. 1-hex	2 eq. AgBF <sub>4</sub>	80°C	H2
CoCl <sub>2</sub> /PPh <sub>3</sub>	14 mL acetone/6 mL water	100 eq. 1-hex	100 eq. KOH	80°C	H2

**Table 6.1** continued

<b>Complex</b>	<b>Solvent System</b>	<b>Substrate</b>	<b>Additives</b>	<b>Temp.</b>	<b>Type</b>
Ni(COD)/PCy <sub>3</sub>	14 mL acetone/6 mL water	100 eq. 1-hex	conc. HCl	80°C	H2
Ni/Pd/PPh <sub>3</sub>	14 mL acetone/6 mL water	100 eq. 1-hex		80°C	H2
Ni/Pt/PPh <sub>3</sub>	14 mL acetone/6 mL water	100 eq. 1-hex		80°C	H2
NiCl <sub>2</sub> (PCy <sub>3</sub> ) <sub>2</sub>	14 mL acetone/6 mL water	100 eq. 1-hex	3 eq. AgBF <sub>4</sub> , 4 eq. Et <sub>3</sub> N	80°C	H2
NiCl <sub>2</sub> (PCy <sub>3</sub> ) <sub>2</sub>	14 mL acetone/6 mL water	100 eq. 1-hex	3 eq. AgBF <sub>4</sub>	80°C	H2
<b>Ni<sub>2</sub>1M</b>	14 mL acetone/6 mL water	100 eq. 1-hex	5 eq. AgBF <sub>4</sub>	80°C	H2
NiCl <sub>2</sub> (PPh <sub>3</sub> ) <sub>2</sub>	14 mL acetone/6 mL water	100 eq. 1-hex	4 eq. AgBF <sub>4</sub>	80°C	H2
Ni/Cu/PPh <sub>3</sub>	14 mL acetone/6 mL water	100 eq. 1-hex	4 eq. AgBF <sub>4</sub>	80°C	H2
NiCl <sub>2</sub> (PPh <sub>3</sub> ) <sub>2</sub>	14 mL acetone/6 mL water	100 eq. 1-hex		80°C	H2
NiCl <sub>2</sub> dppp	14 mL acetone/6 mL water	100 eq. 1-hex	4 eq. AgBF <sub>4</sub>	80°C	H2
NiCl <sub>2</sub> dppe	14 mL acetone/6 mL water	100 eq. 1-hex	4 eq. AgBF <sub>4</sub>	80°C	H2
PtCl <sub>2</sub> (PEt <sub>3</sub> ) <sub>2</sub>	14 mL acetone/6 mL water	100 eq. 1-hex	4 eq. AgBF <sub>4</sub>	80°C	H2
<b>Ni<sub>2</sub>1M</b>	14 mL acetone/6 mL water	100 eq. 1-hex		80°C	H2
NiCl <sub>2</sub> (PPh <sub>3</sub> ) <sub>2</sub>	14 mL acetone/6 mL water	100 eq. 1-hex		80°C	H2
NiCl <sub>2</sub> dcpe	14 mL acetone/6 mL water	100 eq. 1-hex	4 eq. AgBF <sub>4</sub>	80°C	H2
FeCl <sub>2</sub> /PPh <sub>3</sub>	14 mL acetone/6 mL water	100 eq. 1-hex	2 eq. AgBF <sub>4</sub>	80°C	H2
<b>Ni<sub>2</sub>1M</b>	14 mL acetone/6 mL water	100 eq. 1-hex	5 eq. AgBF <sub>4</sub>	80°C	H3
NiCl <sub>2</sub> dppp	14 mL acetone/6 mL water	100 eq. 1-hex	2 eq. AgBF <sub>4</sub>	80°C	H3
NiCl <sub>2</sub> (PPh <sub>3</sub> ) <sub>2</sub>	14 mL acetone/6 mL water	100 eq. 1-hex	2 eq. AgBF <sub>4</sub>	80°C	H3
NiCl <sub>2</sub> (PPh <sub>3</sub> ) <sub>2</sub>	14 mL acetone/6 mL water	100 eq. 1-hex	2 eq. AgBF <sub>4</sub>	80°C	H3
<b>Ni<sub>2</sub>1M</b>	14 mL acetone/6 mL water	100 eq. 1-octene	4 eq. AgBF <sub>4</sub>	80°C	H3

Table 6.1 continued

Complex	Solvent System	Substrate	Additives	Temp.	Type
Ni <sub>2</sub> 1R	14 mL CH <sub>3</sub> CN/6 mL water	100 eq. 1-octene	4 eq. AgBF <sub>4</sub>	80°C	H3
Ni <sub>2</sub> 1M	14 mL THF/6 mL water	100 eq. 1-octene		80°C	H3
Ni <sub>2</sub> 1R	14 mL acetone/6 mL water	100 eq. 1-octene		80°C	H3
Ni <sub>2</sub> 1M	14 mL acetone/6 mL water	100 eq. 1-octene	4 eq. AgBF <sub>4</sub>	80°C	H3
Ni <sub>2</sub> 1R	14 mL acetone/6 mL water	100 eq. 1-octene	4 eq. AgBF <sub>4</sub>	80°C	H3
Ni <sub>2</sub> 1M	14 mL acetone/6 mL water	100 eq. 1-octene	8 eq. AgBF <sub>4</sub>	80°C	H3
Ni <sub>2</sub> 1R	14 mL acetone/6 mL water	100 eq. 1-octene	8 eq. AgBF <sub>4</sub>	80°C	H3
NiCl <sub>2</sub> (PPh <sub>3</sub> ) <sub>2</sub>	14 mL acetone/6 mL water	100 eq. 1-hex		80°C	H3
NiCl <sub>2</sub> (PCy <sub>3</sub> ) <sub>2</sub>	14 mL acetone/6 mL water	100 eq. 1-hex		80°C	H3
NiCl <sub>2</sub> dppe	14 mL acetone/6 mL water	100 eq. 1-hex	4 eq. AgBF <sub>4</sub>	80°C	H3
NiCl <sub>2</sub> dppp	14 mL acetone/6 mL water	100 eq. 1-hex	4 eq. AgBF <sub>4</sub>	80°C	H3
NiCl <sub>2</sub> dppe	14 mL acetone/6 mL water	100 eq. 1-hex	4 eq. AgBF <sub>4</sub>	80°C	H3
NiCl <sub>2</sub> dppp	14 mL acetone/6 mL water	100 eq. 1-hex	4 eq. AgBF <sub>4</sub>	80°C	H3
Ni <sub>2</sub> 1M	14 mL acetone/6 mL water	100 eq. 1-hex		80°C	H3
Ni <sub>2</sub> 1R	14 mL acetone/6 mL water	1000 eq. 1-hex		80°C	H3
Ni <sub>2</sub> 1M	14 mL acetone/6 mL water	100 eq. 1-hex		80°C	H3
Ni <sub>2</sub> 1M	14 mL acetone/6 mL water	100 eq. 1-hex	2 eq. AgBF <sub>4</sub>	80°C	H3
Ni <sub>2</sub> 1M	14 mL acetone/6 mL water	100 eq. 1-hex		80°C	H3
Ni <sub>2</sub> 1M	14 mL acetone/6 mL water	100 eq. 1-hex	2 eq. AgBF <sub>4</sub>	80°C	H3
Ni <sub>2</sub> 1M	14 mL acetone/6 mL water	100 eq. 1-hex		80°C	H3
NiCl <sub>2</sub> dppp	14 mL acetone/6 mL water	100 eq. 1-hex		80°C	H3

**Table 6.1** continued

<b>Complex</b>	<b>Solvent System</b>	<b>Substrate</b>	<b>Additives</b>	<b>Temp.</b>	<b>Type</b>
NiCl <sub>2</sub> dppp	14 mL acetone/6 mL water	2 eq. 1-hex		80°C	H3
<b>Ni<sub>2</sub>1M</b>	14 mL acetone/6 mL water	100 eq. 1-hex	8 eq. AgBF <sub>4</sub> , 100 eq. KOH	80°C	H3
<b>Ni<sub>2</sub>1M</b>	14 mL acetone/6 mL water	100 eq. 1-hex	4 eq. AgBF <sub>4</sub>	80°C	H3
<b>Ni<sub>2</sub>1R</b>	14 mL acetone/6 mL water	100 eq. 1-hex		80°C	H3
<b>Ni<sub>2</sub>1M</b>	14 mL acetone/6 mL water	100 eq. 1-hex		80°C	H3
NiCl <sub>2</sub> dppb	14 mL acetone/6 mL water	100 eq. 1-hex		80°C	H3
NiCl <sub>2</sub> dppb	14 mL acetone/6 mL water	100 eq. 1-hex	2 eq. AgBF <sub>4</sub>	80°C	H3
<b>Ni<sub>2</sub>1M</b>	14 mL acetone/6 mL water	100 eq. 1-hex	4 eq. AgBF <sub>4</sub>	80°C	H3
<b>Ni<sub>2</sub>1R</b>	14 mL acetone/6 mL water	1000 eq. 1-hex	4 eq. AgBF <sub>4</sub>	80°C	H3
<b>Ni<sub>2</sub>1M</b>	14 mL acetone/6 mL water	100 eq. 1-hex	4 eq. AgBF <sub>4</sub>	80°C	H3
NiCl <sub>2</sub> (PPh <sub>3</sub> ) <sub>2</sub>	14 mL acetone/6 mL water	100 eq. 1-hex		80°C	H3
<b>Ni<sub>2</sub>1R</b>	14 mL acetone/6 mL water	100 eq. 1-hex	4 eq. AgBF <sub>4</sub>	80°C	H3
<b>Ni<sub>2</sub>1M</b>	14 mL acetone/6 mL water	100 eq. 1-hex		80°C	H3
<b>Ni<sub>2</sub>1M</b>	14 mL acetone/6 mL water	100 eq. 1-hex	4 eq. AgBF <sub>4</sub>	80°C	H3
<b>Ni<sub>2</sub>1R</b>	14 mL acetone/6 mL water	100 eq. 1-hex	4 eq. AgBF <sub>4</sub>	80°C	H3
<b>Ni<sub>2</sub>1M</b>	14 mL acetone/6 mL water	2000 eq. 1-hex		80°C	H3
<b>Ni<sub>2</sub>1M</b>	14 mL acetone/6 mL water	1000 eq. 1-hex		80°C	H3
<b>Ni<sub>2</sub>1R</b>	14 mL acetone/6 mL water	10000 eq. 1-hex		80°C	H3
<b>Ni<sub>2</sub>1M</b>	14 mL acetone/6 mL water	100 eq. 1-hex		80°C	H3
<b>Ni<sub>2</sub>1M</b>	14 mL acetone/6 mL water	100 eq. 1-hex		80°C	H3
NiCl <sub>2</sub> (PPh <sub>3</sub> ) <sub>2</sub>	14 mL acetone/6 mL water	100 eq. 1-hex		80°C	H3

**Table 6.1** continued

<b>Complex</b>	<b>Solvent System</b>	<b>Substrate</b>	<b>Additives</b>	<b>Temp.</b>	<b>Type</b>
NiCl <sub>2</sub> dcpe	14 mL acetone/6 mL water	100 eq. 1-hex		80°C	H3
NiCl <sub>2</sub> /BISBI	14 mL acetone/6 mL water	100 eq. 1-hex		80°C	H3
NiCl <sub>2</sub> /NAPHOS	14 mL acetone/6 mL water	100 eq. 1-hex		80°C	H3
<b>Ni<sub>2</sub>1R</b>	14 mL acetone/6 mL water	100 eq. 1-hex	2 eq. AgBF <sub>4</sub>	80°C	H3
<b>Ni<sub>2</sub>1M</b>	14 mL acetone/6 mL water	100 eq. 1-hex	2 eq. AgBF <sub>4</sub>	80°C	H3
NiCl <sub>2</sub> (PPh <sub>3</sub> ) <sub>2</sub>	14 mL acetone/6 mL water	100 eq. 1-hex		80°C	H3
NiCl <sub>2</sub> (dppp)	14 mL acetone/6 mL water	100 eq. 1-hex		80°C	H3
<b>Ni<sub>2</sub>1M</b>	14 mL acetone/6 mL water	100 eq. 1-hex		80°C	H3
<b>Ni<sub>2</sub>1R</b>	14 mL acetone/6 mL water	100 eq. 1-hex		80°C	H3
NiCl <sub>2</sub> dcpe	14 mL acetone/6 mL water	100 eq. 1-hex		80°C	H3
NiCl <sub>2</sub> dppe	14 mL acetone/6 mL water	100 eq. 1-hex		80°C	H3
<b>Ni<sub>2</sub>1M</b>	14 mL acetone/6 mL water	100 eq. 1-hex		80°C	H3
<b>Ni<sub>2</sub>1R</b>	14 mL acetone/6 mL water	100 eq. 1-hex		80°C	H3
<b>Ni<sub>2</sub>1M</b>	14 mL acetone/6 mL water	100 eq. 1-hex		80°C	H3
<b>Ni<sub>2</sub>1M</b>	14 mL acetone/6 mL water	100 eq. 1-hex	8 eq. AgBF <sub>4</sub>	80°C	H3
<b>Ni<sub>2</sub>1M</b>	14 mL acetone/6 mL water	100 eq. 1-hex	4 eq. AgBF <sub>4</sub>	80°C	H3
NiCl <sub>2</sub> dppp	14 mL acetone/6 mL water	100 eq. 1-hex		80°C	H3
<b>Ni<sub>2</sub>1M</b>	14 mL acetone/6 mL water	10000 eq. 1-hex		80°C	H3
<b>Ni<sub>2</sub>1M</b>	14 mL acetone/6 mL water	1000 eq. 1-hex		80°C	H3
<b>Ni<sub>2</sub>1M</b>	14 mL acetone/6 mL water	100 eq. styrene	2 eq. AgBF <sub>4</sub>	80°C	H3
<b>Ni<sub>2</sub>1R</b>	14 mL acetone/6 mL water	100 eq. styrene	2 eq. AgBF <sub>4</sub>	80°C	H3

**Table 6.1** continued

<b>Complex</b>	<b>Solvent System</b>	<b>Substrate</b>	<b>Additives</b>	<b>Temp.</b>	<b>Type</b>
<b>Ni<sub>2</sub>1M</b>	14 mL acetone/6 mL water	100 eq. styrene	2 eq. AgBF <sub>4</sub> , 2 eq. KOH	80°C	H3
<b>Ni<sub>2</sub>1M</b>	14 mL acetone/6 mL water	100 eq. styrene	4 eq. AgBF <sub>4</sub> , 2 eq. KOH	80°C	H3
<b>Ni<sub>2</sub>1M</b>	14 mL acetone/6 mL water	100 eq. styrene		80°C	H3
<b>Ni<sub>2</sub>1R</b>	14 mL acetone/6 mL water	100 eq. styrene	2 eq. AgBF <sub>4</sub> , 2 eq. KOH	80°C	H3
NiCl <sub>2</sub> (PPh <sub>3</sub> ) <sub>2</sub>	14 mL acetone/6 mL water	100 eq. 1-hex		80°C	H3
<b>Ni<sub>2</sub>1M</b>	14 mL acetone/6 mL water	200 eq. 1-hex		80°C	H3
<b>Ni<sub>2</sub>1R</b>	14 mL acetone/6 mL water	100 eq. 1-hex		80°C	H3
NiCl <sub>2</sub> dppp	14 mL acetone/6 mL water	1000 eq. 1-hex		80°C	H3
<b>Ni<sub>2</sub>1R</b>	14 mL acetone/6 mL water	100 eq. 1-hex		80°C	H3
<b>Ni<sub>2</sub>1M</b>	14 mL acetone/6 mL water	100 eq. 1-hex		80°C	H3
<b>Ni<sub>2</sub>1M</b>	14 mL acetone/6 mL water	100 eq. 1-hex		80°C	H3
NiCl <sub>2</sub> (PPh <sub>3</sub> ) <sub>2</sub>	14 mL acetone/6 mL water	100 eq. 1-hex		80°C	H3
NiCl <sub>2</sub> (PPh <sub>3</sub> ) <sub>2</sub>	14 mL acetone/6 mL water	100 eq. 1-hex		80°C	H3
<b>Ni<sub>2</sub>1M</b>	14 mL acetone/6 mL water	4000 eq. 1-hex		80°C	H3
<b>Ni<sub>2</sub>1R</b>	14 mL acetone/6 mL water	100 eq. 1-hex	4 eq. KOH	80°C	H3
<b>Ni<sub>2</sub>1M</b>	14 mL acetone/6 mL water	4000 eq. 1-hex		80°C	H3
<b>Ni<sub>2</sub>1M</b>	14 mL acetone/6 mL water	100 eq. 1-hex	4 eq. CsOH	80°C	H3
<b>Ni<sub>2</sub>1R</b>	14 mL acetone/6 mL water	100 eq. 1-hex		80°C	H3
<b>Ni<sub>2</sub>1M</b>	14 mL acetone/6 mL water	4000 eq. 1-hex	4 eq. AgBF <sub>4</sub>	80°C	H3
<b>Ni<sub>2</sub>1M</b>	14 mL acetone/6 mL water	4000 eq. 1-hex		80°C	H3
<b>Ni<sub>2</sub>1R</b>	14 mL acetone/6 mL water	100 eq. 1-hex		80°C	H3

**Table 6.1** continued

<b>Complex</b>	<b>Solvent System</b>	<b>Substrate</b>	<b>Additives</b>	<b>Temp.</b>	<b>Type</b>
<b>Ni<sub>2</sub>1R</b>	14 mL acetone/6 mL water	100 eq. 1-hex		80°C	H3
<b>Ni<sub>2</sub>1M</b>	14 mL acetone/6 mL water	100 eq. 1-hex		80°C	H3
<b>Ni<sub>2</sub>1R</b>	14 mL acetone/6 mL water	2000 eq. 1-hex		80°C	H3
<b>Ni<sub>2</sub>1M</b>	14 mL acetone/6 mL water	1000 eq. 1-hex		80°C	H3
<b>Ni<sub>2</sub>1R</b>	14 mL acetone/6 mL water	100 eq. 1-hex		80°C	H3
NiCl <sub>2</sub> dcpe	14 mL acetone/6 mL water	100 eq. 1-hex		80°C	H3
NiCl <sub>2</sub> dcpe	14 mL acetone/6 mL water	100 eq. 1-hex	4 eq. AgBF <sub>4</sub>	80°C	H3
<b>Ni<sub>2</sub>1R</b>	14 mL acetone/6 mL water	1000 eq. 1-hex	4 eq. AgBF <sub>4</sub>	80°C	H3
<b>Ni<sub>2</sub>1M</b>	14 mL acetone/6 mL water	200 eq. 1-hex		80°C	H3
<b>Ni<sub>2</sub>1M</b>	14 mL acetone/6 mL water	2000 eq. 1-hex		80°C	H3
NiCl <sub>2</sub> dppp	14 mL acetone/6 mL water	100 eq. 1-hex		80°C	H3
<b>Ni<sub>2</sub>1R</b>	14 mL acetone/6 mL water	100 eq. 1-hex		80°C	H3
<b>Ni<sub>2</sub>1M</b>	14 mL acetone/6 mL water	100 eq. 1-hex	4 eq. AgBF <sub>4</sub>	80°C	H3
NiCl <sub>2</sub> dppp	14 mL acetone/6 mL water	100 eq. 1-hex		80°C	H3
<b>Ni<sub>2</sub>1R</b>	14 mL acetone/6 mL water	1000 eq. 1-hex		80°C	H3
<b>Ni<sub>2</sub>1R</b>	14 mL acetone/6 mL water	1000 eq. 1-hex		80°C	H3
NiCl <sub>2</sub> dppe	14 mL acetone/6 mL water	100 eq. 1-hex		80°C	H3
NiCl <sub>2</sub> dppp	14 mL acetone/6 mL water	100 eq. 1-hex		80°C	H3
<b>Ni<sub>2</sub>1M</b>	14 mL acetone/6 mL water	100 eq. 1-hex		80°C	H3
NiCl <sub>2</sub> dppp	14 mL acetone/6 mL water	100 eq. 1-hex	2 eq. AgBF <sub>4</sub>	80°C	H3
NiCl <sub>2</sub> dppp	14 mL acetone/6 mL water	100 eq. 1-hex	2 eq. AgBF <sub>4</sub>	80°C	H3

**Table 6.1** continued

<b>Complex</b>	<b>Solvent System</b>	<b>Substrate</b>	<b>Additives</b>	<b>Temp.</b>	<b>Type</b>
<b>Ni21M</b>	14 mL acetone/6 mL water	100 eq. 1-hex		80°C	H3
NiCl <sub>2</sub> dppe	14 mL acetone/6 mL water	100 eq. 1-hex		80°C	H3
NiCl <sub>2</sub> dppe	14 mL acetone/6 mL water	100 eq. 1-hex	2 eq. AgBF <sub>4</sub>	80°C	H3
NiCl <sub>2</sub> dcpe	14 mL acetone/6 mL water	200 eq. 1-hex		80°C	H3
<b>Ni<sub>2</sub>1M</b>	14 mL acetone/6 mL water	200 eq. 1-hex		80°C	H3
<b>Ni<sub>2</sub>1R</b>	14 mL acetone/6 mL water	2000 eq. 1-hex		80°C	H3
<b>Ni<sub>2</sub>1R</b>	14 mL acetone/6 mL water	10000 eq. 1-hex		80°C	H3
NiCl <sub>2</sub> dppp	14 mL acetone/6 mL water	100 eq. 1-hex		80°C	H3
<b>Ni<sub>2</sub>1R</b>	14 mL acetone/6 mL water	2000 eq. 1-hex		80°C	H3

### 6.3 Hydration Screening Experiments

#### 6.3.1 The Ligand Solution

A portion of a hexane solution containing 75% **1R** and 25% **1M** (based on <sup>31</sup>P integration) was transferred to a 25 mL Schlenk flask. The hexane was removed under vacuum with gentle heating leaving behind the ligand mixture as a highly viscous oil. The oil was kept under vacuum overnight to ensure all of the solvent was removed. The weight of the ligand mixture was obtained via the weighing by difference technique (3.64 g). The ligand mixture was then dissolved in 7.8 mL of diethyl ether to form a 1 M mixed ligand solution. This solution was sealed with a glass stopper and kept inside a freezer to limit the amount of solvent evaporation. 200 μL aliquots of this solution were added for each hydration screening experiment

#### 6.3.2 Reaction Setup

In the glovebox a heavy-walled glass pressure vessel was charged with the appropriate amount of metal salt or complex, the organic solvent and 200 μL of the mixed ligand solution.



This vessel was sealed and the reaction mixture was stirred and heated to dissolve all of the metal content. The solution was then cooled to room temperature and placed back inside the glovebox. The substrate and appropriate amount of water was then added to the solution. This solution was then heated and stirred typically overnight. The next day the solution was cooled and an aliquot was collected typically in air. The aliquot was diluted with acetone and analyzed via GC/MS. If decomposition of the starting material was observed (black solid and black solution) the reaction was stopped and analyzed via GC/MS.

For all reactions, the total metal content was  $4 \times 10^{-4}$  moles with  $2 \times 10^{-4}$  moles of ligand unless  $\text{CuCl}_2$  was added. The following metal salts/complexes were used:  $[\text{IrCl}(\text{COD})]_2$  – Ir1,  $\text{IrCl}_3$  – Ir3,  $\text{Rh}(\text{acac})(\text{CO})_2$  – Rh1,  $\text{RhCl}_3$  – Rh3,  $\text{PdCl}_2(\text{benzotrile})_2$  – Pd,  $\text{Ni}(\text{COD})_2$  – Ni0,  $\text{NiCl}_2$  – Ni2,  $[\text{RuCl}_2(\text{benzene})]_2$  – Ru,  $\text{PtCl}_2(\text{COD})$  – Pt,  $\text{CoCl}_2$  – Co,  $\text{CuCl}_2$  – Cu,  $\text{FeCl}_2$  – Fe.

### 6.3.3 Reaction Table

**Table 6.2** Hydration Screening Experiments

Metals	Solvent System	Temp.	Substrate	Additive
Ir1/Rh3	19 mL THF/1 mL water	90°C	100 eq. styrene	triethylamine
Ir1/Co	19 mL THF/1 mL water	90°C	100 eq. styrene	triethylamine
Ni0	19 mL THF/1 mL water	90°C	100 eq. styrene	none
Ir1/Pd	19 mL THF/1 mL water	90°C	100 eq. styrene	$\text{CuCl}_2$
Ni0	19 mL THF/1 mL water	room temp.	100 eq. styrene	none
Ir1/Cu	19 mL THF/1 mL water	90°C	100 eq. styrene	none
Ir1/Fe	19 mL THF/1 mL water	90°C	100 eq. styrene	none
Ir1/Ru	19 mL THF/1 mL water	90°C	100 eq. styrene	none
Ir1/Rh1	19 mL THF/1 mL water	90°C	100 eq. styrene	none
Ir1/Ni2F	19 mL acetone/1 mL water	90°C	100 eq. 1-hexene	none

**Table 6.2** continued

<b>Metals</b>	<b>Solvent System</b>	<b>Temp.</b>	<b>Substrate</b>	<b>Additive</b>
Cu/Fe	19 mL acetone/1 mL water	90°C	100 eq. 1-hexene	none
Cu/Co	19 mL acetone/1 mL water	90°C	100 eq. 1-hexene	none
Cu/Co	19 mL acetone/1 mL water	90°C	100 eq. 1-hexene	none
Cu/Rh1	19 mL acetone/1 mL water	90°C	100 eq. 1-hexene	none
Ir1/Pt	19 mL acetone/1 mL water	90°C	100 eq. 1-hexene	none
Ir1/Pt	19 mL THF/1 mL water	90°C	100 eq. styrene	none
Pt/Ir3	19 mL acetone/1 mL water	90°C	100 eq. 1-hexene	none
Pt/Rh1	19 mL THF/1 mL water	90°C	100 eq. styrene	none
Pt/Rh3	19 mL THF/1 mL water	90°C	100 eq. styrene	none
Pt/Cu	19 mL CH <sub>3</sub> CN/ 1 mL water	90°C	100 eq. styrene	none
Ir3	19 mL CH <sub>3</sub> CN/0.36 mL water	90°C	100 eq. styrene	none
Pt/Fe	19 mL THF/1 mL water	90°C	100 eq. styrene	none
Pt/Co	19 mL THF/1 mL water	90°C	100 eq. styrene	none
Pd/Ru	19 mL THF/0.36 mL water	90°C	100 eq. styrene	none
Pd/Ru	19 mL 3:1 tbutol:ipropol/0.36 mL water	90°C	100 eq. styrene	none
Pd/Ru	19 mL 3:1 tbutol:ipropol/0.5 mL water	90°C	100 eq. styrene	CuCl <sub>2</sub> , O <sub>2</sub> balloon
Pt	19 mL 3:1 tbutol:ipropol/1 mL water	90°C	100 eq. styrene	none
Pd	19 mL 3:1 tbutol:ipropol/1 mL water	90°C	100 eq. styrene	5 drops NEt <sub>3</sub>
Ir1	19 mL THF/1 mL water	90°C	100 eq. styrene	bromobenzene, 2 eq AgBF <sub>4</sub>

**Table 6.2** continued

<b>Metals</b>	<b>Solvent System</b>	<b>Temp.</b>	<b>Substrate</b>	<b>Additive</b>
Co	19 mL THF/1 mL water	90°C	100 eq. styrene	4 eq AgBF <sub>4</sub>
Rh3/Fe	19 mL THF/1 mL water	90°C	100 eq. styrene	none
Ir3/Fe	19 mL THF/1 mL water	90°C	100 eq. styrene	CuCl <sub>2</sub>
Ir3/Fe	19 mL THF/1 mL water	90°C	100 eq. styrene	none
Rh1/Fe	19 mL THF/1 mL water	90°C	100 eq. styrene	CuCl <sub>2</sub>
Pd/Ru	19 mL THF/1 mL water	90°C	100 eq. styrene	CuCl <sub>2</sub>
Ir1/Ru	19 mL THF/1 mL water	90°C	100 eq. styrene	none
Rh3	19 mL acetone/1 mL water	90°C	100 eq. 1-hexene	none
Rh1	19 mL acetone/1 mL water	90°C	100 eq. 1-hexene	none
Pd/Ru	19 mL THF/1 mL water	90°C	100 eq. styrene	CuCl <sub>2</sub> , in air
Pd/Ru	19 mL THF/1 mL water	90°C	100 eq. styrene	none
Pd/Fe	19 mL THF/1 mL water	90°C	100 eq. styrene	CuCl <sub>2</sub>
Rh1/Fe	19 mL THF/1 mL water	room temp.	100 eq. styrene	none
Rh3/Fe	19 mL THF/1 mL water	room temp.	100 eq. styrene	none
Ir1	19 mL methanol/1 mL water	90°C	100 eq. 1-hexene	none
Rh1	19 mL methanol/1 mL water	90°C	100 eq. 1-hexene	none
Cu	19 mL THF/1 mL water	90°C	100 eq. styrene	none
Pt/Fe	19 mL THF/1 mL water	90°C	100 eq. styrene	none
Ir1	19 mL THF/1 mL water	90°C	100 eq. styrene	none
Co	19 mL THF/1 mL water	90°C	100 eq. styrene	triethyl amine
Ir1	19 mL THF/1 mL water	90°C	100 eq. styrene	triethyl amine

## 6.4 Oxidative Cleavage Reactions

### 6.4.1 Reaction Types

**OC1:** A 50 mL round-bottom flask or Erlenmeyer flask was charged with the appropriate amount of metal complex, organic solvent, water, additive and substrate. A pipette was used to bubble air into the solution for 2-3 minutes. The flask was then sealed with a glass stopper fitter with a Glindemann PTFE sealing ring and allowed to rapidly stir at room temperature. Periodically, the stirring was stopped and an aliquot was collected. The aliquot was diluted with acetone and analyzed via GC/MS. More air was bubbled into the solution via pipette before the flask was sealed and allowed to stir. The reactions were allowed to stir for between 1 and 4 days.

**OC2:** A Schlenk flask was charged with the appropriate amount of metal complex, organic solvent and additive. The mixture was allowed to stir for 5-10 minutes to dissolve as much complex as possible. The substrate was then added followed by the appropriate amount of water. The flask was then sealed with a balloon which was secured using wire. The balloon was then pressurized with O<sub>2</sub> gas from a gas tank with the gas regulator set to 30 psig. The solution was allowed to stir rapidly overnight. The next day the stirring was stopped and the remaining pressure was vented from the balloon. An aliquot of the solution was collected, diluted with acetone and analyzed via GC/MS. In some cases NMR samples were also collected and analyzed.

### 6.4.2 Reaction Tables

The following four tables contain the majority of the oxidative cleavage and oxidation reactions conducted. The tables are divided up for the three organic solvents investigated (acetone, acetonitrile and DMSO). The final table contains the reactions conducted with TBHP

and H<sub>2</sub>O<sub>2</sub>. The following abbreviations appear in the tables: TMEDA – tetramethylethylenediamine, bzdiam – benzene-1,2-diamine or *o*-phenylenediamine, phen – 1,10-phenanthroline, dmgly – dimethylgloxime. All reactions contain 10 mM concentrations of complexes or metal salts.

**Table 6.3** Oxidative Cleavage Reactions with Acetone

<b>Complex</b>	<b>Acetone</b>	<b>Water</b>	<b>Additives</b>	<b>Substrate</b>	<b>Type</b>
Ni <sub>2</sub> 1M	17 mL	3 mL	100 eq. ethanol	100 eq. styrene	OC1
Ni <sub>2</sub> 1M	17 mL	3 mL	100 eq. 2-propanol	100 eq. styrene	OC1
Ni <sub>2</sub> 1M	17 mL	3 mL	100 eq. 2-propanol	100 eq. styrene	OC1
Ni <sub>2</sub> 1M	17 mL	3 mL	100 eq. 2-propanol	100 eq. styrene	OC2
Ni <sub>2</sub> 1M	17 mL	3 mL	100 eq. ethanol	100 eq. styrene	OC2
Ni <sub>2</sub> 1M	17 mL	3 mL	100 eq. propanal	100 eq. styrene	OC1
Ni <sub>2</sub> 1M	17 mL	3 mL	100 eq. propanal	100 eq. styrene	OC2
Ni <sub>2</sub> 1M	20 mL	0.36 mL	none	100 eq. styrene	OC1
Ni <sub>2</sub> 1M	17 mL	3 mL	10 eq. NH <sub>4</sub> Cl	100 eq. styrene	OC1
Ni <sub>2</sub> 1M	17 mL	3 mL	10 eq. acetic acid	100 eq. styrene	OC1
Ni <sub>2</sub> 1M	17 mL	3 mL	10 eq. NH <sub>4</sub> Cl	100 eq. styrene	OC2
Ni <sub>2</sub> 1M	17 mL	3 mL	10 eq. PPh <sub>3</sub>	100 eq. styrene	OC2
Ni <sub>2</sub> 1M	17 mL	3 mL	100 eq. isobutyraldehyde	100 eq. styrene	OC1
Ni <sub>2</sub> 1M	17 mL	3 mL	10 eq. FeCl <sub>3</sub>	100 eq. styrene	OC2
Ni <sub>2</sub> 1M	17 mL	3 mL	10 eq. ascorbic acid	100 eq. styrene	OC1
Ni <sub>2</sub> 1M	17 mL	3 mL	none	30 eq. styrene	OC1
Ni <sub>2</sub> 1M	17 mL	3 mL	2 eq. AgBF <sub>4</sub>	30 eq. styrene	OC1
Ni <sub>2</sub> 1M	17 mL	3 mL	2 eq. AgBF <sub>4</sub>	30 eq. styrene	OC1
Ni <sub>2</sub> 1M	17 mL	3 mL	4 eq. AgBF <sub>4</sub>	30 eq. styrene	OC1
Ni <sub>2</sub> 1M	17 mL	3 mL	4 eq. AgBF <sub>4</sub> , 30 eq. 2-propanol	30 eq. styrene	OC1
Ni <sub>2</sub> 1M	17 mL	3 mL	4 eq. AgBF <sub>4</sub>	30 eq. styrene	OC2
Ni <sub>2</sub> 1M	17 mL	3 mL	none	30 eq. styrene	OC1
Ni(BF <sub>4</sub> ) <sub>2</sub> /2 eq. phen.	17 mL	3 mL	none	30 eq. styrene	OC1
Ni <sub>2</sub> 1M	8.5 mL	1.5 mL	none	30 eq. styrene	OC2

**Table 6.3** continued

<b>Complex</b>	<b>Acetone</b>	<b>Water</b>	<b>Additives</b>	<b>Substrate</b>	<b>Type</b>
Ni(BF <sub>4</sub> ) <sub>2</sub> /2 eq. dppe	17 mL	3 mL	none	30 eq. styrene	OC2
<b>Ni<sub>2</sub>1M</b>	17 mL	3 mL	none	30 eq. styrene	OC2
<b>Ni<sub>2</sub>1M</b>	17 mL	3 mL	none	30 eq. styrene	OC2
NiCl <sub>2</sub> /2 eq. dppe	17 mL	3 mL	none	30 eq. styrene	OC1
Ni(BF <sub>4</sub> ) <sub>2</sub> /2 eq. bzdpm	17 mL	3 mL	none	30 eq. styrene	OC1
Ni(BF <sub>4</sub> ) <sub>2</sub> /2 eq. dmgly	17 mL	3 mL	none	30 eq. styrene	OC1
Ni(BF <sub>4</sub> ) <sub>2</sub> /2 eq. bzdpm	17 mL	3 mL	none	30 eq. styrene	OC2
Ni(BF <sub>4</sub> ) <sub>2</sub> /2 eq. phen.	17 mL	3 mL	none	30 eq. styrene	OC2
NiCl <sub>2</sub> /2 eq. bzdpm	20 mL	none	none	30 eq. styrene	OC2
NiCl <sub>2</sub> /2 eq. phen.	20 mL	none	none	30 eq. styrene	OC2
<b>Ni<sub>2</sub>1M</b>	19.5 mL	0.3 mL	none	30 eq. styrene	OC2
<b>Ni<sub>2</sub>1M</b>	18.8 mL	1.0 mL	none	30 eq. styrene	OC2
<b>Ni<sub>2</sub>1M</b>	17.8 mL	2.0 mL	none	30 eq. styrene	OC2
<b>Ni<sub>2</sub>1M</b>	17 mL	3 mL	10 eq. NaCl	30 eq. styrene	OC2
<b>Ni<sub>2</sub>1M</b>	17 mL	3 mL	10 eq. NaCl	30 eq. styrene	OC1
<b>Ni<sub>2</sub>1M</b>	17 mL	3 mL	2 eq. NaCl	30 eq. styrene	OC2
Ni(BF <sub>4</sub> ) <sub>2</sub> /2 eq. TMEDA	17 mL	3 mL	none	30 eq. styrene	OC1
NiCl <sub>2</sub> /2 eq. TMEDA	17 mL	3 mL	none	30 eq. styrene	OC1
Ni(BF <sub>4</sub> ) <sub>2</sub> /2 eq. TMEDA	17 mL	3 mL	none	30 eq. styrene	OC2
<b>Ni<sub>2</sub>1M</b>	17 mL	3 mL	60 eq. isobutyraldehyde	30 eq. styrene	OC2
<b>Ni<sub>2</sub>1M</b>	17 mL	3 mL	4 eq. NaCl	30 eq. styrene	OC2
<b>Ni<sub>2</sub>1M</b>	17 mL	3 mL	1 eq. NaCl	30 eq. styrene	OC2
<b>Ni<sub>2</sub>1M</b>	17 mL	3 mL	1 eq. NaCl	30 eq. styrene	OC2
<b>Ni<sub>2</sub>1M</b>	17 mL	3 mL	2 eq. NaCl	30 eq. styrene	OC1
<b>Ni<sub>2</sub>1M</b>	17 mL	3 mL	2 eq. NaCl	30 eq. styrene	OC2
<b>Ni<sub>2</sub>1M</b>	17 mL	3 mL	4 eq. NaCl	30 eq. styrene	OC2
<b>Ni<sub>2</sub>1M</b>	8.5 mL	1.5 mL	none	30 eq. 1-hexene	OC2
<b>Ni<sub>2</sub>1M</b>	16 mL	1 mL	3 mL propanal	30 eq. styrene	OC1
<b>Ni<sub>2</sub>1M</b>	17 mL	none	3 mL propanal	30 eq. styrene	OC2

**Table 6.3** continued

<b>Complex</b>	<b>Acetone</b>	<b>Water</b>	<b>Additives</b>	<b>Substrate</b>	<b>Type</b>
<b>Ni<sub>2</sub>1M</b>	17 mL	none	3 mL isobutyraldehyde	30 eq. styrene	OC2
<b>Ni<sub>2</sub>1M</b>	~25 mL	none	3 mL propanal, 4 eq. AgBF <sub>4</sub>	30 eq. styrene	OC2
Ni(BF <sub>4</sub> ) <sub>2</sub> /1 eq. dppe	20 mL	none	1 eq. 1,2-benzenediamine	30 eq. styrene	OC2
Ni(BF <sub>4</sub> ) <sub>2</sub> /1 eq. dppp	20 mL	none	1 eq. 1,2-benzenediamine	30 eq. styrene	OC2
Ni(BF <sub>4</sub> ) <sub>2</sub> /1 eq. dppe	17 mL	3 mL	1 eq. 1,2-benzenediamine	30 eq. styrene	OC2
Ni(BF <sub>4</sub> ) <sub>2</sub> /1 eq. dppp	17 mL	3 mL	1 eq. 1,2-benzenediamine	30 eq. styrene	OC2
RhCl(PPh <sub>3</sub> ) <sub>3</sub>	17 mL	3 mL	none	30 eq. 1-hexene	OC2
NiCl <sub>2</sub> /2 eq. bzdiam	17 mL	none	3 mL propanal	30 eq. styrene	OC2
NiCl <sub>2</sub> /2 eq. phen.	17 mL	none	3 mL propanal	30 eq. styrene	OC2
NiCl <sub>2</sub> /2 eq. dmgly	17 mL	none	3 mL propanal	30 eq. styrene	OC2
Ni(BF <sub>4</sub> ) <sub>2</sub> /2 eq. dcpe	20 mL	none	none	40 eq. 1-hexene	OC2
<b>Ni<sub>2</sub>1M</b>	4.2 mL	0.8 mL	none	30 eq. cis-4-nonene	OC2
<b>Ni<sub>2</sub>1M</b>	4.2 mL	0.8 mL	none	30 eq. trans-4-nonene	OC2
<b>Ni<sub>2</sub>1M</b>	2.5 mL	2.5 mL	none	50 eq. styrene	OC2
<b>Ni<sub>2</sub>1M</b>	2.5 mL	2.5 mL	1 eq. NH <sub>4</sub> Cl	50 eq. styrene	OC2
<b>Ni<sub>2</sub>1R</b>	17 mL	3 mL	1 eq. NaCl	30 eq. styrene	OC2
<b>Ni<sub>2</sub>1R</b>	17 mL	3 mL	2 eq. NaCl	30 eq. styrene	OC1
<b>Ni<sub>2</sub>1R</b>	17 mL	3 mL	4 eq. NaCl	30 eq. styrene	OC2
<b>Ni<sub>2</sub>1R</b>	8.5 mL	1.5 mL	none	30 eq. 1-hexene	OC2
<b>Ni<sub>2</sub>1R</b>	16 mL	1 mL	3 mL propanal	30 eq. styrene	OC1
<b>Ni<sub>2</sub>1R</b>	17 mL	none	3 mL propanal	30 eq. styrene	OC2
<b>Ni<sub>2</sub>1R</b>	17 mL	none	3 mL isobutyraldehyde	30 eq. styrene	OC2
<b>Ni<sub>2</sub>1R</b>	19.5 mL	0.3 mL	none	30 eq. styrene	OC2
<b>Ni<sub>2</sub>1R</b>	18.8 mL	1.0 mL	none	30 eq. styrene	OC2
<b>Ni<sub>2</sub>1R</b>	17.8 mL	2.0 mL	none	30 eq. styrene	OC2
<b>Ni<sub>2</sub>1R</b>	17 mL	3 mL	10 eq. NaCl	30 eq. styrene	OC2

**Table 6.4** Oxidative Cleavage Reactions with Acetonitrile

<b>Complex</b>	<b>CH<sub>3</sub>CN</b>	<b>Water</b>	<b>Additives</b>	<b>Substrate</b>	<b>Type</b>
Ni <sub>2</sub> 1M	17 mL	3 mL	none	100 eq. styrene	OC2
Ni <sub>2</sub> 1M	17 mL	3 mL	none	100 eq. styrene	OC2
Ni <sub>2</sub> 1M	17 mL	3 mL	100 eq. 2-propanol	100 eq. styrene	OC2
Ni <sub>2</sub> 1M	17 mL	3 mL	100 eq. ethanol	100 eq. styrene	OC2
Ni <sub>2</sub> 1M	17 mL	3 mL	none	100 eq. styrene	OC1
Ni <sub>2</sub> 1M	17 mL	3 mL	none	10 eq. styrene	OC1
Ni <sub>2</sub> 1M	17 mL	3 mL	10 eq. propanal	10 eq. styrene	OC2
Ni <sub>2</sub> 1M	17 mL	3 mL	none	5 eq. styrene	OC2
Ni <sub>2</sub> 1M	17 mL	3 mL	none	1 eq. styrene	OC1
Ni <sub>2</sub> 1M	17 mL	3 mL	none	10 eq. stilbene	OC1
Ni <sub>2</sub> 1M	17 mL	3 mL	10 eq. malonic acid	10 eq. styrene	OC2
Ni <sub>2</sub> 1M	17 mL	3 mL	none	30 eq. styrene	OC1
Ni <sub>2</sub> 1M	17 mL	3 mL	none	30 eq. styrene	OC1
Ni <sub>2</sub> 1M	17 mL	3 mL	2 eq. AgBF <sub>4</sub>	30 eq. styrene	OC2
Ni <sub>2</sub> 1M	19.8 mL	none	2 eq. CsOH	30 eq. styrene	OC1
Ni <sub>2</sub> 1M	19.8 mL	none	4 eq. CsOH	30 eq. styrene	OC1
Ni <sub>2</sub> 1M	17 mL	3 mL	2 eq. BHT	30 eq. styrene	OC2
Ni <sub>2</sub> 1M	17 mL	3 mL	2 eq. ferrocenium BF <sub>4</sub>	30 eq. styrene	OC2
Ni <sub>2</sub> 1M	17 mL	3 mL	none	30 eq. styrene	OC1
Ni <sub>2</sub> 1M	17 mL	3 mL	none	50 eq. 1-hexene	OC2
Ni <sub>2</sub> 1M	17 mL	3 mL	30 eq. 1-butanol	30 eq. styrene	OC2
Ni <sub>2</sub> 1M	17 mL	3 mL	none	30 eq. cyclopentene	OC1
Ni <sub>2</sub> 1M	17 mL	3 mL	10 eq. NH <sub>4</sub> Cl	30 eq. styrene	OC1
Ni <sub>2</sub> 1M	8.5 mL	1.5 mL	none	1 eq. styrene	OC1
Ni <sub>2</sub> 1M	7 mL	3 mL	none	30 eq. styrene	OC1
Ni(BF <sub>4</sub> ) <sub>2</sub> /2 eq. dppe	17 mL	3 mL	none	30 eq. styrene	OC1
Ni(BF <sub>4</sub> ) <sub>2</sub> /2 eq. dppe	17 mL	3 mL	none	30 eq. styrene	OC2
Ni <sub>2</sub> 1M	17 mL	3 mL	3 eq. BHT	30 eq. styrene	OC2
Ni <sub>2</sub> 1M	17 mL	3 mL	none	30 eq. styrene	OC2
Ni(BF <sub>4</sub> ) <sub>2</sub> /1 eq. dppe	17 mL	3 mL	none	30 eq. styrene	OC1
Ni(BF <sub>4</sub> ) <sub>2</sub> /2 eq. dppe	20 mL	none	none	30 eq. styrene	OC1
NiCl <sub>2</sub> /2 eq. dppe	20 mL	none	none	30 eq. styrene	OC1
NiCl <sub>2</sub> /2 eq. dppe	20 mL	none	none	30 eq. styrene	OC1



Table 6.4 continued

Complex	CH <sub>3</sub> CN	Water	Additives	Substrate	Type
Ni(BF <sub>4</sub> ) <sub>2</sub> /2 eq. dppp	17 mL	3 mL	none	30 eq. styrene	OC1
NiCl <sub>2</sub> /2 eq. dppp	17 mL	3 mL	none	30 eq. styrene	OC1
Ni(BF <sub>4</sub> ) <sub>2</sub> /2 eq. dppp	17 mL	3 mL	none	30 eq. styrene	OC2
NiCl <sub>2</sub> /2 eq. dppp	17 mL	3 mL	none	30 eq. styrene	OC2
Ni <sub>2</sub> 1M	17 mL	3 mL	none	30 eq. styrene	OC2
Ni <sub>2</sub> 1M	17 mL	3 mL	1 eq. NaCl	30 eq. styrene	OC2
Ni <sub>2</sub> 1M	17 mL	3 mL	2 eq. dppe	30 eq. styrene	OC2
Ni <sub>2</sub> 1M	17 mL	3 mL	2 eq. NaCl	30 eq. styrene	OC2
Ni <sub>2</sub> 1M	17 mL	3 mL	2 eq. NaCl	30 eq. styrene	OC1
Ni <sub>2</sub> 1M	17 mL	3 mL	1 eq. NaCl	30 eq. styrene	OC2
Ni <sub>2</sub> 1M	17 mL	3 mL	2 eq. NaCl	30 eq. styrene	OC2
Ni <sub>2</sub> 1M	19.8 mL	none	2 eq. dppe	30 eq. styrene	OC2
Ni <sub>2</sub> 1M	17 mL	3 mL	2 eq. NaCl	10 eq. styrene	OC2
Ni <sub>2</sub> 1M	17 mL	3 mL	2 eq. dppe, 1 eq. NaCl	10 eq. styrene	OC2
Ni <sub>2</sub> 1M	17 mL	3 mL	none	50 eq. norbornene	OC2
Ni <sub>2</sub> 1M	19.5 mL	0.3 mL	none	30 eq. styrene	OC2
Ni <sub>2</sub> 1M	18.8 mL	1.0 mL	none	30 eq. styrene	OC2
Ni <sub>2</sub> 1M	17 mL	3 mL	none	30 eq. norbornene	OC1
Ni <sub>2</sub> 1M	17 mL	3 mL	none	30 eq. styrene	OC2
Ni <sub>2</sub> 1M	17 mL	3 mL	1 eq. Fe(BF <sub>4</sub> ) <sub>2</sub>	30 eq. styrene	OC2
Ni <sub>2</sub> 1M	17 mL	3 mL	1 eq. CoCl <sub>2</sub>	30 eq. styrene	OC2
Fe(BF <sub>4</sub> ) <sub>2</sub> /2 eq. dppe	20 mL	none	none	30 eq. styrene	OC2
CoCl <sub>2</sub> /2 eq. dppe	20 mL	none	none	30 eq. styrene	OC2
Fe(BF <sub>4</sub> ) <sub>2</sub> /2 eq. dppe	17 mL	3 mL	none	30 eq. styrene	OC2
CoCl <sub>2</sub> /2 eq. dppe	17 mL	3 mL	none	30 eq. styrene	OC2
CuSO <sub>4</sub> /2 eq. dppe	17 mL	3 mL	none	30 eq. styrene	OC2
RhCl <sub>3</sub> /3 eq. dppe	17 mL	3 mL	none	30 eq. styrene	OC2
RhCl <sub>3</sub> /3 eq. dppe	20 mL	none	none	30 eq. styrene	OC2
PtCl <sub>2</sub> (PEt <sub>3</sub> ) <sub>2</sub>	17 mL	3 mL	none	30 eq. styrene	OC2
PdCl <sub>2</sub> (PPh <sub>3</sub> ) <sub>2</sub>	17 mL	3 mL	none	30 eq. styrene	OC2
Ni <sub>2</sub> 1M	16 mL	1 mL	3 mL propanal	30 eq. styrene	OC2
Ni <sub>2</sub> 1M	3.4 mL	0.6 mL	none	30 eq. trans-5-decene	OC2
Ni <sub>2</sub> 1M	17 mL	none	3 mL propanal	30 eq. styrene	OC2

Table 6.4 continued

Complex	CH <sub>3</sub> CN	Water	Additives	Substrate	Type
<b>Ni<sub>2</sub>1M</b>	17 mL	none	3 mL isobutyraldehyde	30 eq. styrene	OC2
NiCl <sub>2</sub> (dppe)	17 mL	none	3 mL propanal	30 eq. styrene	OC2
NiCl <sub>2</sub> (dppp)	17 mL	none	3 mL propanal	30 eq. styrene	OC2
NiCl <sub>2</sub> (PPh <sub>3</sub> ) <sub>2</sub>	17 mL	none	3 mL propanal	30 eq. styrene	OC2
<b>Ni<sub>2</sub>1M</b>	8.5 mL	1.5 mL	none	30 eq. cyclohexene	OC2
NiCl <sub>2</sub> (dcpe)	17 mL	none	3 mL propanal	30 eq. styrene	OC2
NiCl <sub>2</sub> (dppp)	16 mL	1 mL	3 mL propanal	30 eq. styrene	OC2
NiCl <sub>2</sub> (dppp)	16 mL	1 mL	3 mL propanal	30 eq. cyclohexene	OC2
NiCl <sub>2</sub> (PPh <sub>3</sub> ) <sub>2</sub>	16 mL	1 mL	3 mL propanal	30 eq. styrene	OC2
NiCl <sub>2</sub> (dppe)	16 mL	1 mL	3 mL propanal	30 eq. styrene	OC2
NiCl <sub>2</sub> /1 eq. BISBI	20 mL	none	none	30 eq. styrene	OC2
<b>Ni<sub>2</sub>1M</b>	17 mL	3 mL	none	40 eq. cyclopentene	OC2
NiCl <sub>2</sub>	17 mL	none	3 mL isobutyraldehyde	50 eq. 1-octene	OC2
Ni(BF <sub>4</sub> ) <sub>2</sub>	17 mL	none	3 mL isobutyraldehyde	50 eq. 1-octene	OC2
<b>Ni<sub>2</sub>1M</b>	8.5 mL	1.5 mL	none	100 eq. 1-octene	OC2
NiCl <sub>2</sub> (dppe)	5 mL	none	100 eq. isobutyraldehyde	50 eq. styrene	OC2
NiCl <sub>2</sub> (dppp)	5 mL	none	100 eq. isobutyraldehyde	50 eq. styrene	OC2
NiCl <sub>2</sub> (dcpe)	5 mL	none	100 eq. isobutyraldehyde	50 eq. styrene	OC2
<b>Ni<sub>2</sub>1R</b>	4.2 mL	0.8 mL	none	50 eq. styrene	OC2
<b>Ni<sub>2</sub>1R</b>	4.2 mL	0.8 mL	2 eq. NH <sub>4</sub> Cl	50 eq. styrene	OC2
<b>Ni<sub>2</sub>1R</b>	4.2 mL	0.8 mL	2 eq. NaCl	50 eq. styrene	OC2
<b>Ni<sub>2</sub>1R</b>	17 mL	3 mL	none	30 eq. styrene	OC2
<b>Ni<sub>2</sub>1R</b>	17 mL	3 mL	1 eq. NaCl	30 eq. styrene	OC2
<b>Ni<sub>2</sub>1R</b>	17 mL	3 mL	2 eq. dppe	30 eq. styrene	OC2
<b>Ni<sub>2</sub>1R</b>	17 mL	3 mL	2 eq. NaCl	30 eq. styrene	OC2
<b>Ni<sub>2</sub>1R</b>	17 mL	3 mL	2 eq. NaCl	30 eq. styrene	OC1
<b>Ni<sub>2</sub>1R</b>	17 mL	3 mL	1 eq. NaCl	30 eq. styrene	OC2
<b>Ni<sub>2</sub>1R</b>	17 mL	3 mL	2 eq. NaCl	30 eq. styrene	OC2
<b>Ni<sub>2</sub>1R</b>	19.8 mL	none	2 eq. dppe	30 eq. styrene	OC2
<b>Ni<sub>2</sub>1R</b>	19.5 mL	0.3 mL	none	30 eq. styrene	OC2
<b>Ni<sub>2</sub>1R</b>	18.8 mL	1.0 mL	none	30 eq. styrene	OC2
<b>Ni<sub>2</sub>1R</b>	5 mL	none	100 eq. isobutyraldehyde	50 eq. styrene	OC2

Table 6.4 continued

Complex	CH <sub>3</sub> CN	Water	Additives	Substrate	Type
Ni <sub>2</sub> 1R	17 mL	3 mL	none	10 eq. stilbene	OC1
Ni <sub>2</sub> 1R	17 mL	3 mL	10 eq. malonic acid	10 eq. styrene	OC2
Ni <sub>2</sub> 1R	17 mL	3 mL	2 eq. AgBF <sub>4</sub>	30 eq. styrene	OC2
Ni <sub>2</sub> 1R	19.8 mL	none	2 eq. CsOH	30 eq. styrene	OC1
Ni <sub>2</sub> 1R	19.8 mL	none	4 eq. CsOH	30 eq. styrene	OC1
Ni <sub>2</sub> 1R	17 mL	3 mL	2 eq. BHT	30 eq. styrene	OC2
Ni <sub>2</sub> 1R	17 mL	3 mL	2 eq. ferrocenium BF <sub>4</sub>	30 eq. styrene	OC2

Table 6.5 Oxidative Cleavage Reactions with DMSO

Complex	DMSO	Water	Additives	Substrate	Type
Ni <sub>2</sub> 1M	17 mL	3 mL	100 eq. ethanol	100 eq. styrene	OC1
Ni <sub>2</sub> 1M	17 mL	3 mL	none	30 eq. styrene	OC2
Ni <sub>2</sub> 1M	19 mL	1 mL	none	30 eq. styrene	OC2
Ni <sub>2</sub> 1M	17 mL	3 mL	1 eq. NaCl	30 eq. styrene	OC2
Ni <sub>2</sub> 1M	8.5 mL	1.5 mL	none	30 eq. styrene	OC2
Ni <sub>2</sub> 1M	8.5 mL	1.5 mL	none	30 eq. styrene	OC2
Ni <sub>2</sub> 1M	17 mL	3 mL	2 eq. NH <sub>4</sub> Cl	30 eq. styrene	OC2
Ni <sub>2</sub> 1M	17 mL	3 mL	2 eq. NaCl	30 eq. styrene	OC2
Ni <sub>2</sub> 1M	17 mL	3 mL	None	30 eq. styrene	OC2
Ni <sub>2</sub> 1M	17 mL	3 mL	2 eq. BHT	30 eq. styrene	OC2
Ni <sub>2</sub> 1M	19.8 mL	none	None	30 eq. styrene	OC2
Ni <sub>2</sub> 1M	20 mL	none	None	30 eq. styrene	OC2
Ni <sub>2</sub> 1M	20 mL	none	None	30 eq. styrene	OC1
Ni <sub>2</sub> 1M	20 mL	none	2 eq. AgBF <sub>4</sub>	30 eq. styrene	OC2
Ni <sub>2</sub> 1M	20 mL	none	4 eq. AgBF <sub>4</sub>	30 eq. styrene	OC2
Ni(BF <sub>4</sub> ) <sub>2</sub> /2 eq. dppe	20 mL	none	None	30 eq. styrene	OC2
NiCl <sub>2</sub> /2 eq. dppe	20 mL	none	None	30 eq. styrene	OC2
CoCl <sub>2</sub> /2 eq. dppe	20 mL	none	None	30 eq. styrene	OC2
CoCl <sub>2</sub> /2 eq. dppe	17 mL	3 mL	None	30 eq. styrene	OC2
Ni <sub>2</sub> 1M	17 mL	none	3 mL ethanol	30 eq. styrene	OC2
Ni <sub>2</sub> 1M	17 mL	none	3 mL 2-propanol	30 eq. styrene	OC2
NiCl <sub>2</sub> (PPh <sub>3</sub> ) <sub>2</sub>	20 mL	none	None	30 eq. styrene	OC2
NiCl <sub>2</sub> (dcpe)	20 mL	none	None	30 eq. styrene	OC2
NiCl <sub>2</sub> (dppe)	20 mL	none	None	30 eq. styrene	OC2
NiCl <sub>2</sub> (dppp)	20 mL	none	None	30 eq. styrene	OC2
Ni(BF <sub>4</sub> ) <sub>2</sub> /2 eq. dppe	20 mL	none	None	30 eq. styrene	OC2

**Table 6.5** continued

<b>Complex</b>	<b>DMSO</b>	<b>Water</b>	<b>Additives</b>	<b>Substrate</b>	<b>Type</b>
Ni(BF <sub>4</sub> ) <sub>2</sub> /2 eq. dppp	20 mL	none	None	30 eq. styrene	OC2
NiCl <sub>2</sub> /2 eq. dppe	20 mL	none	None	30 eq. styrene	OC2
NiCl <sub>2</sub> /2 eq. dppp	20 mL	none	None	30 eq. styrene	OC2
Ni(BF <sub>4</sub> ) <sub>2</sub> /2 eq. bzdam.	20 mL	none	None	30 eq. styrene	OC2
NiCl <sub>2</sub> /2 eq. bzdam.	20 mL	none	None	30 eq. styrene	OC2
Ni(BF <sub>4</sub> ) <sub>2</sub> /2 eq. phen.	20 mL	none	None	30 eq. styrene	OC2
NiCl <sub>2</sub> /2 eq. phen.	20 mL	none	None	30 eq. styrene	OC2
<b>Ni<sub>2</sub>1M</b>	20 mL	none	2 eq. NH <sub>4</sub> Cl	30 eq. styrene	OC2
<b>Ni<sub>2</sub>1M</b>	20 mL	none	2 eq. NaCl	30 eq. styrene	OC2
Ni(BF <sub>4</sub> ) <sub>2</sub> /2 eq. dmgly	20 mL	none	none	30 eq. styrene	OC2
NiCl <sub>2</sub> /2 eq. dmgly	20 mL	none	none	30 eq. styrene	OC2
Fe(BF <sub>4</sub> ) <sub>2</sub> /2 eq. dppe	20 mL	none	none	30 eq. styrene	OC2
CoCl <sub>2</sub> /2 eq. dppe	20 mL	none	none	30 eq. styrene	OC2
CuSO <sub>4</sub> /2 eq. dppe	20 mL	none	none	30 eq. styrene	OC2
<b>Ni<sub>2</sub>1M</b>	18 mL	none	2 mL propanal	30 eq. styrene	OC2
<b>Ni<sub>2</sub>1M</b>	18 mL	none	2 mL isobutyraldehyde	30 eq. styrene	OC2
<b>Ni<sub>2</sub>1M</b>	17 mL	none	3 mL propanal	30 eq. styrene	OC2
<b>Ni<sub>2</sub>1M</b>	17 mL	none	3 mL isobutyraldehyde	30 eq. styrene	OC2
<b>Ni<sub>2</sub>1M</b>	17 mL	none	3 mL isobutyraldehyde, 2 eq. BHT	30 eq. styrene	OC2
<b>Ni<sub>2</sub>1M</b>	17 mL	none	3 mL isobutyraldehyde, ex. BHT	30 eq. styrene	OC2
<b>Ni<sub>2</sub>1M</b>	20 mL	none	none	30 eq. styrene	OC2
NiCl <sub>2</sub> (dppe)	17 mL	none	3 mL propanal	30 eq. styrene	OC2
NiCl <sub>2</sub> (dppp)	17 mL	none	3 mL propanal	30 eq. styrene	OC2
NiCl <sub>2</sub> (PPh <sub>3</sub> ) <sub>2</sub>	17 mL	none	3 mL propanal	30 eq. styrene	OC2
Ni(BF <sub>4</sub> ) <sub>2</sub> /2 eq. dppe	17 mL	none	3 mL propanal	30 eq. styrene	OC2
Ni(BF <sub>4</sub> ) <sub>2</sub> /2 eq. dppp	17 mL	none	3 mL propanal	30 eq. styrene	OC2
Ni(BF <sub>4</sub> ) <sub>2</sub> /3 eq. PPh <sub>3</sub>	17 mL	none	3 mL propanal	30 eq. styrene	OC2
<b>Ni<sub>2</sub>1M</b>	17 mL	none	3 mL propanal	30 eq. styrene	OC2
NiCl <sub>2</sub> /2 eq. dppe	17 mL	none	3 mL propanal	30 eq. styrene	OC2

**Table 6.5** continued

Complex	DMSO	Water	Additives	Substrate	Type
NiCl <sub>2</sub> /2 eq. dppp	17 mL	none	3 mL propanal	30 eq. styrene	OC2
NiCl <sub>2</sub> (dcpe)	17 mL	none	3 mL propanal	30 eq. styrene	OC2
Ni(BF <sub>4</sub> ) <sub>2</sub> /2 eq. dppe	17 mL	none	3 mL propanal	30 eq. cyclohexene	OC2
Ni(BF <sub>4</sub> ) <sub>2</sub> /2 eq. dppp	17 mL	none	3 mL propanal	30 eq. cyclohexene	OC2
NiCl <sub>2</sub> (dppe)	16 mL	1 mL	3 mL propanal	30 eq. styrene	OC2
NiCl <sub>2</sub> (dppp)	16 mL	1 mL	3 mL propanal	30 eq. styrene	OC2
NiCl <sub>2</sub> /2 eq. dppe	16 mL	1 mL	3 mL propanal	30 eq. styrene	OC2
NiCl <sub>2</sub> /2 eq. dppp	16 mL	1 mL	3 mL propanal	30 eq. styrene	OC2
Ni(BF <sub>4</sub> ) <sub>2</sub> /2 eq. dppe	17 mL	none	3 mL propanal	50 eq. styrene	OC2

**Table 6.6** Oxidation Reactions with H<sub>2</sub>O<sub>2</sub> and TBHP

Complex	Solvent	Oxidant	Atm.	Substrate
NiCl <sub>2</sub> (dppe)	9 mL DCM	30 eq. 70% aq. TBHP	air	30 eq. styrene
NiCl <sub>2</sub> (dppe)	9 mL DCM	30 eq. 35% aq. H <sub>2</sub> O <sub>2</sub>	air	30 eq. styrene
NiCl <sub>2</sub> (dppp)	9 mL DCM	30 eq. 70% aq. TBHP	air	30 eq. styrene
NiCl <sub>2</sub> (dppp)	9 mL DCM	30 eq. 35% aq. H <sub>2</sub> O <sub>2</sub>	air	30 eq. styrene
NiCl <sub>2</sub> (dppe)	9 mL DCM	30 eq. 70% aq. TBHP	N <sub>2</sub>	30 eq. styrene
NiCl <sub>2</sub> (dppp)	9 mL DCM	30 eq. 70% aq. TBHP	N <sub>2</sub>	30 eq. styrene
<b>Ni<sub>2</sub>1M</b>	9 mL DCM	30 eq. 70% aq. TBHP	N <sub>2</sub>	30 eq. styrene
NiCl <sub>2</sub> (dppe)	9 mL DCM	30 eq. 70% aq. TBHP	N <sub>2</sub>	30 eq. styrene
<b>Ni<sub>2</sub>1M</b>	9 mL DCM	30 eq. 35% aq. H <sub>2</sub> O <sub>2</sub>	N <sub>2</sub>	30 eq. styrene
<b>Ni<sub>2</sub>1R</b>	9 mL DCM	30 eq. 35% aq. H <sub>2</sub> O <sub>2</sub>	N <sub>2</sub>	30 eq. styrene
<b>Ni<sub>2</sub>1M</b>	9 mL DCM	30 eq. 35% aq. H <sub>2</sub> O <sub>2</sub>	air	30 eq. styrene
<b>Ni<sub>2</sub>1R</b>	9 mL DCM	30 eq. 35% aq. H <sub>2</sub> O <sub>2</sub>	air	30 eq. styrene
<b>Ni<sub>2</sub>1M</b>	9 mL CH <sub>3</sub> CN	60 eq. 70% aq. TBHP	air	60 eq. styrene
<b>Ni<sub>2</sub>1R</b>	9 mL CH <sub>3</sub> CN	60 eq. 70% aq. TBHP	N <sub>2</sub>	60 eq. styrene
<b>Ni<sub>2</sub>1R</b>	9 mL CH <sub>3</sub> CN	60 eq. 70% aq. TBHP	air	60 eq. styrene
NiCl <sub>2</sub> (dppe)	9 mL CH <sub>3</sub> CN	30 eq. 70% aq. TBHP	air	30 eq. styrene
NiCl <sub>2</sub> (dppe)	9 mL CH <sub>3</sub> CN	30 eq. 35% aq. H <sub>2</sub> O <sub>2</sub>	air	30 eq. styrene
NiCl <sub>2</sub> (dppp)	9 mL CH <sub>3</sub> CN	30 eq. 70% aq. TBHP	air	30 eq. styrene
NiCl <sub>2</sub> (dppp)	9 mL CH <sub>3</sub> CN	30 eq. 35% aq. H <sub>2</sub> O <sub>2</sub>	air	30 eq. styrene
NiCl <sub>2</sub> (dppe)	9 mL CH <sub>3</sub> CN	30 eq. 70% aq. TBHP	N <sub>2</sub>	30 eq. styrene
NiCl <sub>2</sub> (dppp)	9 mL CH <sub>3</sub> CN	30 eq. 70% aq. TBHP	N <sub>2</sub>	30 eq. styrene
NiCl <sub>2</sub> (dppe)	9 mL CH <sub>3</sub> CN	30 eq. 35% aq. H <sub>2</sub> O <sub>2</sub>	N <sub>2</sub>	30 eq. styrene
NiCl <sub>2</sub> (dppp)	9 mL CH <sub>3</sub> CN	30 eq. 35% aq. H <sub>2</sub> O <sub>2</sub>	N <sub>2</sub>	30 eq. styrene
NiCl <sub>2</sub> (dcpe)	9 mL CH <sub>3</sub> CN	30 eq. 35% aq. H <sub>2</sub> O <sub>2</sub>	N <sub>2</sub>	30 eq. styrene

**Table 6.6** continued

Complex	Solvent	Oxidant	Atm.	Substrate
Ni(BF <sub>4</sub> ) <sub>2</sub> /1 eq. dppe	9 mL CH <sub>3</sub> CN	30 eq. 35% aq. H <sub>2</sub> O <sub>2</sub>	N <sub>2</sub>	30 eq. styrene
Ni(BF <sub>4</sub> ) <sub>2</sub> /1 eq. dppp	9 mL CH <sub>3</sub> CN	30 eq. 35% aq. H <sub>2</sub> O <sub>2</sub>	N <sub>2</sub>	30 eq. styrene
NiCl <sub>2</sub> (dppe)	9 mL CH <sub>3</sub> CN	30 eq. 70% aq. TBHP	N <sub>2</sub>	30 eq. styrene
NiCl <sub>2</sub> (dppe)	9 mL CH <sub>3</sub> CN	30 eq. 70% aq. TBHP	air	30 eq. styrene
NiCl <sub>2</sub> (dppe)	9 mL CH <sub>3</sub> CN	30 eq. 35% aq. H <sub>2</sub> O <sub>2</sub>	N <sub>2</sub>	30 eq. styrene
NiCl <sub>2</sub> (dppe)	9 mL CH <sub>3</sub> CN	30 eq. 35% aq. H <sub>2</sub> O <sub>2</sub>	air	30 eq. styrene
<b>Ni<sub>2</sub>1M</b>	9 mL CH <sub>3</sub> CN	50 eq. 70% aq. TBHP	N <sub>2</sub>	50 eq. styrene
<b>Ni<sub>2</sub>1M</b>	9 mL CH <sub>3</sub> CN	50 eq. 35% aq. H <sub>2</sub> O <sub>2</sub>	N <sub>2</sub>	50 eq. styrene
<b>Ni<sub>2</sub>1M</b>	9 mL CH <sub>3</sub> CN	50 eq. 70% aq. TBHP	air	50 eq. styrene
<b>Ni<sub>2</sub>1M</b>	9 mL CH <sub>3</sub> CN	50 eq. 35% aq. H <sub>2</sub> O <sub>2</sub>	air	50 eq. styrene
<b>Ni<sub>2</sub>1R</b>	9 mL CH <sub>3</sub> CN	50 eq. 70% aq. TBHP	N <sub>2</sub>	50 eq. styrene
<b>Ni<sub>2</sub>1R</b>	9 mL CH <sub>3</sub> CN	50 eq. 35% aq. H <sub>2</sub> O <sub>2</sub>	N <sub>2</sub>	50 eq. styrene
<b>Ni<sub>2</sub>1R</b>	9 mL CH <sub>3</sub> CN	50 eq. 70% aq. TBHP	air	50 eq. styrene
<b>Ni<sub>2</sub>1R</b>	9 mL CH <sub>3</sub> CN	50 eq. 35% aq. H <sub>2</sub> O <sub>2</sub>	air	50 eq. styrene

## 6.5 NMR Reactions

### 6.5.1 Reaction Conditions When Acetone-*d*<sub>6</sub> was Utilized

In the glovebox a vial was charged with the appropriate amount of Ni complex, acetone and D<sub>2</sub>O. The vial was sealed and either heated to completely dissolve the complex or stirred for between 30 minutes and 1 hour to completely dissolve the complex. The vial was then transferred to the glovebox and the NMR tubes were prepared and monitored via <sup>1</sup>H and <sup>31</sup>P NMR.

### 6.5.2 Reaction Conditions when CD<sub>3</sub>CN or DMSO-*d*<sub>6</sub> was Utilized

In the glovebox a vial was charged with the appropriate amount of Ni complex and deuterated organic solvent. The vial was sealed and swirled to completely dissolve the complex. The appropriate amount of water was then added and the NMR tubes were prepared. The tubes were then monitored via <sup>1</sup>H and <sup>31</sup>P NMR.

### 6.5.3 Reaction Table

**Table 6.7** NMR Scale Reactions

Complex	Solvent System	Additives	Substrate	Tubes (conditions)
Ni <sub>2</sub> 1M	1.7 mL acetone/ 0.3 mL D <sub>2</sub> O	none	100 eq. 1-hexene	1-air
Ni <sub>2</sub> 1M	1.7 mL acetone/ 0.3 mL D <sub>2</sub> O	none	50 eq. 1-hexene	1-N <sub>2</sub> , 2-air
Ni <sub>2</sub> 1M	1.7 mL acetone/ 0.3 mL D <sub>2</sub> O	none	50 eq. 1-hexene	1-air
Ni <sub>2</sub> 1M	1.7 mL acetone/ 0.3 mL D <sub>2</sub> O	none	50 eq. 1-hexene	1-air
Ni <sub>2</sub> 1M	1.7 mL acetone/ 0.3 mL D <sub>2</sub> O	none	50 eq. 1-hexene	1 & 2-air
Ni <sub>2</sub> 1M	1.7 mL acetone/ 0.3 mL D <sub>2</sub> O	none	50 eq. 1-hexene	1-50 psig
Ni <sub>2</sub> 1M	1.7 mL acetone/ 0.3 mL D <sub>2</sub> O	3 eq. TEMPO	50 eq. 1-hexene	1 & 2-air, 1-Al foil, 2-TEMPO
Ni <sub>2</sub> 1M	1.8 mL acetone/ 0.2 mL D <sub>2</sub> O	none	5 eq. 1-hexene	1-100 psig
Ni <sub>2</sub> 1M	1.0 mL acetone/ D <sub>2</sub> O added	none	none	1-N <sub>2</sub> then water added
Ni <sub>2</sub> 1M	1.8 mL acetone/ 0.2 mL D <sub>2</sub> O	none	10 eq. styrene	1-air
Ni <sub>2</sub> 1M	0.85 mL acetone/ 0.15 mL D <sub>2</sub> O	10 eq. ethanol	10 eq. styrene	1-air
Ni <sub>2</sub> 1M	0.8 mL THF/0.2 mL D <sub>2</sub> O	10 eq. ethanol	10 eq. styrene	1 & 2-air, 2-ethanol
Ni <sub>2</sub> 1M	0.85 mL THF/ 0.15 mL D <sub>2</sub> O	none	10 eq. styrene	1-50 psig
Ni <sub>2</sub> 1M	1.7 mL acetone/ 0.3 mL D <sub>2</sub> O	3 eq. BHT	5 eq. styrene	1-air, 2-air, BHT
Ni <sub>2</sub> 1M	1.0 mL CD <sub>3</sub> CN/ D <sub>2</sub> O added	none	5 eq. styrene	1-air, water added after 3 days
Ni <sub>2</sub> 1M	0.8 mL CD <sub>3</sub> CN/ 0.2 mL D <sub>2</sub> O	none	5 eq. styrene	1-air
Ni <sub>2</sub> 1M	1.7 mL acetone/ 0.3 mL D <sub>2</sub> O	3 eq. MEHQ	5 eq. styrene	1-air, 2-air, MEHQ
Ni <sub>2</sub> 1M	0.85 mL acetone/ 0.15 mL D <sub>2</sub> O	none	none added	1-N <sub>2</sub>
Ni <sub>2</sub> 1M	0.85 mL acetone/ 0.15 mL D <sub>2</sub> O	2 eq. BHT	none added	1-N <sub>2</sub> with BHT
Ni <sub>2</sub> 1M	0.8 mL CD <sub>3</sub> CN/ 0.2 mL D <sub>2</sub> O	none	5 eq. 1-hexene	1-N <sub>2</sub> , no subs., 2-air, substrate

Table 6.7 continued

Complex	Solvent System	Additives	Substrate	Tubes (conditions)
Ni <sub>2</sub> 1M	0.8 mL CD <sub>3</sub> CN/ 0.2 mL D <sub>2</sub> O	none	none	1-N <sub>2</sub>
Ni <sub>2</sub> 1M	1 mL DMSO	none	none	1-air
Ni <sub>2</sub> 1M	0.7 mL DMSO/ 0.3 mL D <sub>2</sub> O	none	none	1-air
Ni <sub>2</sub> 1M	1.7 mL CD <sub>3</sub> CN/ 0.3 mL D <sub>2</sub> O	2 eq. NaCl	1-hexene	1-N <sub>2</sub> , NaCl, 2-air, substrate, NaCl
Ni <sub>2</sub> 1M	0.85 mL CD <sub>3</sub> CN/ 0.15 mL D <sub>2</sub> O	none	none	1-80 psig
Ni <sub>2</sub> 1M	0.85 mL DMSO/ 0.15 mL D <sub>2</sub> O	none	none	1-80 psig
Ni <sub>2</sub> 1M	1.7 mL acetone/ 0.3 mL D <sub>2</sub> O	2 eq. NaCl	two drops of 1-hexene	1-N <sub>2</sub> , NaCl, 2-air, substrate, NaCl
Ni <sub>2</sub> 1M	1.7 mL DMSO/ 0.3 mL D <sub>2</sub> O	2 eq. NaCl	two drops of 1-hexene	1-N <sub>2</sub> , NaCl, 2-air, substrate, NaCl
Ni <sub>2</sub> 1M	2 mL DMSO	none	two drops of 1-hexene	1-N <sub>2</sub> , 2-air, 3-80 psig, heated to 60 C
Ni <sub>2</sub> 1M	1.7 mL CD <sub>3</sub> CN/ 0.3 mL D <sub>2</sub> O	none	two drops of 1-hexene	1-N <sub>2</sub> , 2-air, 3-95 psig
Ni <sub>2</sub> 1M	0.8 mL CD <sub>3</sub> CN/ 0.2 mL D <sub>2</sub> O	none	<i>trans</i> -β-methylstyrene	1-air
Ni <sub>2</sub> 1M	0.8 mL CD <sub>3</sub> CN/ 0.2 mL D <sub>2</sub> O	none	<i>trans</i> -β-methylstyrene	1-air
Ni <sub>2</sub> 1M	0.8 mL DMF/0.2 mL D <sub>2</sub> O	none	none	1-air
Ni <sub>2</sub> 1M	0.95 mL acetone/ 0.05 mL D <sub>2</sub> O	none	none	1-N <sub>2</sub> , 2-air
Ni <sub>2</sub> 1M	0.90 mL acetone/ 0.1 mL D <sub>2</sub> O	none	none	1-N <sub>2</sub> , 2-air
Ni <sub>2</sub> 1M	0.85 mL acetone/ 0.15 mL D <sub>2</sub> O	none	none	1-N <sub>2</sub> , 2-air
Ni <sub>2</sub> 1M	0.80 mL acetone/ 0.2 mL D <sub>2</sub> O	none	none	1-N <sub>2</sub> , 2-air
Ni <sub>2</sub> 1M	0.70 mL acetone/ 0.3 mL D <sub>2</sub> O	none	none	1-N <sub>2</sub> , 2-air
Ni <sub>2</sub> 1M	0.95 mL CD <sub>3</sub> CN/ 0.05 mL D <sub>2</sub> O	none	none	1-N <sub>2</sub> , 2-air
Ni <sub>2</sub> 1M	0.90 mL CD <sub>3</sub> CN/ 0.1 mL D <sub>2</sub> O	none	none	1-N <sub>2</sub> , 2-air
Ni <sub>2</sub> 1M	0.85 mL CD <sub>3</sub> CN/ 0.15 mL D <sub>2</sub> O	none	none	1-N <sub>2</sub> , 2-air
Ni <sub>2</sub> 1M	0.80 mL CD <sub>3</sub> CN/ 0.2 mL D <sub>2</sub> O	none	none	1-N <sub>2</sub> , 2-air



Table 6.7 continued

Complex	Solvent System	Additives	Substrate	Tubes (conditions)
<b>Ni<sub>2</sub>1M</b>	0.70 mL CD <sub>3</sub> CN/ 0.3 mL D <sub>2</sub> O	none	none	1-N <sub>2</sub> , 2-air
<b>Ni<sub>2</sub>1M</b>	0.95 mL DMSO/ 0.05 mL D <sub>2</sub> O	none	none	1-N <sub>2</sub> , 2-air
<b>Ni<sub>2</sub>1M</b>	0.85 mL DMSO/ 0.15 mL D <sub>2</sub> O	none	none	1-N <sub>2</sub> , 2-air
<b>Ni<sub>2</sub>1M</b>	0.85 mL acetone/ 0.15 mL D <sub>2</sub> O	2 eq. NaCl	none	1-N <sub>2</sub> , 2-air
<b>Ni<sub>2</sub>1M</b>	0.85 mL CD <sub>3</sub> CN/ 0.15 mL D <sub>2</sub> O	2 eq. NaCl	none	1-N <sub>2</sub> , 2-air
<b>Ni<sub>2</sub>1M</b>	0.85 mL DMSO/ 0.15 mL D <sub>2</sub> O	2 eq. NaCl	none	1-N <sub>2</sub> , 2-air
<b>Ni<sub>2</sub>1M</b>	0.85 mL acetone/ 0.15 mL D <sub>2</sub> O	10 eq. NaCl	none	1-N <sub>2</sub> , 2-air
<b>Ni<sub>2</sub>1M</b>	0.85 mL CD <sub>3</sub> CN/ 0.15 mL D <sub>2</sub> O	10 eq. NaCl	none	1-N <sub>2</sub> , 2-air
<b>Ni<sub>2</sub>1R</b>	0.95 mL CD <sub>3</sub> CN/ 0.05 mL D <sub>2</sub> O	none	none	1-N <sub>2</sub> , 2-air
<b>Ni<sub>2</sub>1R</b>	0.90 mL CD <sub>3</sub> CN/ 0.1 mL D <sub>2</sub> O	none	none	1-N <sub>2</sub> , 2-air
<b>Ni<sub>2</sub>1R</b>	0.85 mL CD <sub>3</sub> CN/ 0.15 mL D <sub>2</sub> O	none	none	1-N <sub>2</sub> , 2-air
<b>Ni<sub>2</sub>1R</b>	0.80 mL CD <sub>3</sub> CN/ 0.2 mL D <sub>2</sub> O	none	none	1-N <sub>2</sub> , 2-air
<b>Ni<sub>2</sub>1R</b>	0.70 mL CD <sub>3</sub> CN/ 0.3 mL D <sub>2</sub> O	none	none	1-N <sub>2</sub> , 2-air
<b>Ni<sub>2</sub>1R</b>	0.85 mL CD <sub>3</sub> CN/ 0.15 mL D <sub>2</sub> O	2 eq. NaCl	none	1-N <sub>2</sub> , 2-air
<b>Ni<sub>2</sub>1R</b>	0.85 mL CD <sub>3</sub> CN/ 0.15 mL D <sub>2</sub> O	10 eq. NaCl	none	1-N <sub>2</sub> , 2-air
<b>Ni<sub>2</sub>1R</b>	1.7 mL CD <sub>3</sub> CN/ 0.3 mL D <sub>2</sub> O	3 eq. BHT	5 eq. styrene	1-air, 2-air, BHT
<b>Ni<sub>2</sub>1R</b>	0.8 mL CD <sub>3</sub> CN/ 0.2 mL D <sub>2</sub> O	none	5 eq. 1-hexene	1-N <sub>2</sub> , no subs., 2-air, substrate
<b>Ni<sub>2</sub>1R</b>	1.7 mL CD <sub>3</sub> CN/ 0.3 mL D <sub>2</sub> O	2 eq. NaCl	1-hexene	1-N <sub>2</sub> , NaCl, 2-air, substrate, NaCl
<b>Ni<sub>2</sub>1R</b>	0.8 mL CD <sub>3</sub> CN/ 0.2 mL D <sub>2</sub> O	none	<i>trans</i> -β-methylstyrene	1-air
<b>Ni<sub>2</sub>1R</b>	1 mL DMSO	none	none	1-air
<b>Ni<sub>2</sub>1R</b>	1.7 mL CD <sub>3</sub> CN/ 0.3 mL D <sub>2</sub> O	none	two drops of 1-hexene	1-N <sub>2</sub> , 2-air, 3-95 psig
<b>Ni<sub>2</sub>1R</b>	1.7 mL DMSO/ 0.3 mL D <sub>2</sub> O	none	two drops of 1-hexene	1-N <sub>2</sub> , 2-air, substrate

## 6.6 Ni<sub>2</sub>1M under Balloon Pressure O<sub>2</sub>

### 6.6.1 Acetone and Water

A Schlenk flask was charged with 0.145 g Ni<sub>2</sub>1M, 17 mL acetone and 3 mL water. The flask was sealed with a balloon secured with a wire. The balloon was pressured with O<sub>2</sub> gas and the solution was allowed to stir overnight. The next day an aliquot of the light yellow solution was collected and analyzed via NMR. The remaining solution was evaporated to dryness under vacuum and heat. The green solid residue was dissolved in water and aliquot was collected and analyzed via NMR.

### 6.6.2 Acetonitrile and Water

The same procedure for acetone and water was utilized for this experiment. The solid that remained did not completely dissolve in water.

### 6.6.3 DMSO and Water

The same procedure was followed for this experiment except the solvents were not removed under vacuum.

### 6.6.4 Added Substrate

The three experiments were repeated except that 50 equivalents of styrene were added. The NMR spectrum for DMSO/water remained the same. The spectra obtained from water/acetone and water/acetonitrile were the same.

## 6.7 Identification of the Broad Resonances

### 6.7.1 Oxidation of 1M and 1R and the Interaction with Added NiCl<sub>2</sub>

A portion (~ 0.20 g) of mixed ligand (63% 1M/37% 1R) was dissolved in 17 mL acetone-*d*<sub>6</sub> and 3 mL D<sub>2</sub>O. An aliquot of this solution was collected and analyzed via NMR. Several drops of 35% aqueous H<sub>2</sub>O<sub>2</sub> was added to the remaining solution in air and the solution

was stirred for 30 minutes. An aliquot of this solution was collected and analyzed via NMR. The remaining solution was evaporated to dryness under vacuum with heating. 30 mg of  $\text{NiCl}_2 \cdot 6\text{H}_2\text{O}$  was added to the white residue that remained and this solid material was dissolved in a 50/50 acetone- $d_6$ / $\text{D}_2\text{O}$  solvent mixture. An aliquot of this solution was collected and analyzed via NMR. This solution was then evaporated to dryness under vacuum with heating. The solid residue that remained was dissolved in  $\text{D}_2\text{O}$ . An aliquot was collected and analyzed via NMR.

### 6.7.2 $\text{Ni}_2\mathbf{1M}$ and $\text{O}_2$

A Schlenk flask was charged with 0.145 g  $\text{Ni}_2\mathbf{1M}$ , 17 mL acetone and 3 mL water. The Schlenk flask was then sealed with a balloon secured with wire. The balloon was pressurized with  $\text{O}_2$  gas and the remaining mixture was allowed to stir overnight. During this time the complex completely dissolved and overnight the solution became light yellow in color. The next day the pressure was vented and the solvents were evaporated to dryness under vacuum and heat leaving behind a green residue. The green residue was dissolved in ~ 2 mL of  $\text{D}_2\text{O}$ . An aliquot of this solution was collected for NMR analysis. Comparison between this spectrum and the final spectrum obtained from 6.6.1 revealed the same species were present proving both contained the tetraphosphine oxide.

### 6.8 Synthesis of $[\text{Ni}_2(\mu\text{-Cl})(\mathbf{1M})_2][\text{BF}_4]_3, \mathbf{F}$

1.2 g (2.6 mmol)  $\mathbf{1M}$  were dissolved in 50 mL of ethanol and transferred to a Schlenk flask. Another Schlenk flask was charged with 0.88 g (2.6 mmol)  $\text{Ni}(\text{BF}_4)_2 \cdot 6\text{H}_2\text{O}$ . 50 mL of ethanol were added to the flask and the light green solution was degassed with a stream of  $\text{N}_2$ . The ligand solution was then added drop-wise to the rapidly stirring Ni solution. After the addition was complete, the flask was opened and 0.15 g (2.6 mmol) NaCl was added. The

solution was allowed to stir and a red/orange solid precipitated out of solution. After stirring overnight the red/orange solid was collected via filtration and rinsed with ethanol and dried in air. A small portion of the solid was dissolved in dichloromethane and the solution was allowed to slowly evaporate. This produced crystals suitable for single crystal X-ray diffraction.  $^1\text{H}$  NMR: see below, peaks marked with red stars are solvent,  $^{31}\text{P}$  NMR: 64.96-62.30 ppm (m), 58.90-56.40 ppm (m).

### 6.9 Attempted Synthesis of **F-1R**

The same procedure for the synthesis of the synthesis of **F** was used for the synthesis of **F-1R**. The only differences was that 1.09 g ~90% **1R**, 0.80 g  $\text{Ni}(\text{BF}_4)_2 \cdot 6\text{H}_2\text{O}$  and 0.069 g  $\text{NaCl}$  were utilized. A solid precipitated out of solution. NMR analysis revealed it was not the desired product. NMR analysis of the ethanol solution revealed the major species present to be **F-1R**. Attempts to isolate this species failed because it is not stable at room temperature and converts to an unsymmetrical monometallic complex.

### 6.10 Reactions Between $\text{Ni}_2\text{1M}$ and $\text{AgBF}_4$

A Schlenk flask was charged with 0.10 g  $\text{Ni}_2\text{1M}$ , a specific amount of  $\text{AgBF}_4$  (1, 2 or 4 equivalents) and 20 mL of acetone. The flask was wrapped with Al foil and the resulting orange/yellow to yellow mixture was allowed to stir for several hours to overnight. The mixture was transferred to a 50 mL glass centrifuge tube and centrifuged for 5 to 10 minutes. The clear solution was decanted into a clean Schlenk flask and an aliquot was collected for NMR analysis. The remaining solution was evaporated to dryness under vacuum and heat. The resulting yellow to yellow/orange solid was then dissolved in a specific solvent (acetonitrile or DMSO) and an aliquot was collected for NMR analysis. All attempts at recrystallizing the solids failed.

## 6.11 Synthesis of *racemic-,meso-et,ph-P4-Ph*, 2R and 2M

### 6.11.1 Synthesis of bis-(chlorophenylphosphino)methane, 4.

A Schlenk flask was charged with 6.0 g (25.8 mmoles) of bis-(phenylphosphino)methane, 12.23 g (51.7 mmoles) of hexachloroethane and 50 mL of diethyl ether. The flask was attached to a reflux condenser and heated to 45°C for between 24-72 hours. Completion of the reaction was indicated by the solution becoming light pink in color and a white solid precipitating out of solution. The flask was then removed from the condenser and concentrated under vacuum. As it was concentrated more white solid precipitated. The concentrated solution was then filtered over a plug of celite using a coarse frit funnel. The remaining solvent was removed under vacuum leaving behind a light pink, slightly viscous oil. Yields are typically between 60-75% and purity is 98% or higher based on <sup>31</sup>P NMR.

<sup>31</sup>P NMR (101.2 MHz, CDCl<sub>3</sub>): δ 81.7 (s). <sup>1</sup>H NMR (250 MHz, C<sub>6</sub>D<sub>6</sub>): δ 7.5 (m, 4H), 7.2 (m, 6H), and 2.9 (br s, 2H). <sup>13</sup>C NMR (62.8 MHz, CDCl<sub>3</sub>): δ 134.4 (m), 127.7, 125.5 (m), 73.9 (m), 42.2 (t, *J* = 42.3 Hz).

### 6.11.2 Synthesis of 1-(diethylphosphino)-2-iodobenzene, 6.

The following procedure was conducted in aluminum foil-wrapped glassware to exclude light. A Schlenk flask was charged with 25.00 g (75.77 mmoles) of 1,2-diiodobenzene and 80 mL of THF. A second Schlenk flask was charged with 26.13 mL (75.77 mmoles) of a 2.9 M THF solution of isopropylmagnesium bromide. The Grignard solution was added to the cooled flask via cannula. It is important that the Grignard flask is kept in a room temperature water bath to ensure that the Grignard does not precipitate out of solution. The cooled reaction flask was stirred at 0°C for 4 hours. Then a solution of diethylchlorophosphine (9.72 g, 78 mmoles) dissolved in 90 mL of THF and cooled to 0°C was added dropwise via cannula. The yellow

solution was then allowed to warm to room temperature and stirred overnight. The next day 80 mL of water was added and the organic layer was separated. The aqueous layer was extracted with 3 50 mL portions of diethyl ether. The extracts and organic layer were combined and dried over sodium sulfate. Solvents were removed under vacuum leaving a yellow oil. The product was isolated via short-path distillation to yield 16.0 g of an air- and light-sensitive colorless liquid. Yields are usually between 70-75% and purity is usually greater than 99% via  $^{31}\text{P}$  NMR.  $^{31}\text{P}$  NMR (101.2 MHz,  $\text{C}_6\text{D}_6$ ):  $\delta$  0.3 (s).  $^1\text{H}$  NMR (250 MHz,  $\text{C}_6\text{D}_6$ ):  $\delta$  7.7 (br m, 1H), 7.2 (sharp m,  $J = 7.3$  Hz, 2H), 6.8 (sharp m,  $J = 7.3$  Hz, 1H), 1.5 (m, 4H), and 0.9 (m,  $J = 7.3$  Hz,  $J_{\text{P,H}} = 7.7$  Hz, 6H).  $^{13}\text{C}$  NMR (62.8MHz,  $\text{C}_6\text{D}_6$ ):  $\delta$  142.3 (d,  $J = 15.3$  Hz), 139.5 (s), 139.4 (d,  $J = 15.3$  Hz), 108.5 (d,  $J = 40.3\text{Hz}$ ), 77.4 (d,  $J = 30.7$  Hz), 76.6 (s), 19.3, and 9.5 (d,  $J = 13.4$  Hz).

### 6.11.3 Synthesis of *racemic-meso-et,ph-P4-Ph*, 2R and 2M.

A Schlenk flask was charged with 12.00 g 1-(diethylphosphino)-2-iodobenzene (41.1 mmoles) and 50 mL THF and wrapped with Al foil to exclude light. The solution was cooled to  $0^\circ\text{C}$  and treated with 14.17 mL (41.1 mmoles) of a 2.9 M THF solution of isopropylmagnesium bromide via cannula. The solution was allowed to stir for 8 hours at  $0^\circ\text{C}$ . It was then cooled to  $-25^\circ\text{C}$  using a dry ice/acetone bath and 6.18 g (20.5 mmoles) of bis-(chlorophenylphosphino)methane dissolved in 20 mL THF was added dropwise via cannula. The solution was then allowed to warm to room temperature and stirred overnight. The next day 30 mL of water were added and the organic layer was separated from the aqueous layer. The aqueous layer was extracted with 3 30 mL portions of diethyl ether. The organic layer and extracts were combined and dried over sodium sulfate. The solution was concentrated under vacuum and then passed through a short alumina column. Short-part vacuum distillation gave unreacted 1-(diethylphosphino)-2-iodobenzene as the only fraction. 200 mL of 1-butanol was

added to the remaining yellow paste and heated with a heat gun. As it heated a small amount of white solid precipitated out of solution. The solution was filtered to remove this inorganic impurity (soluble only in water) and the 1-butanol was removed under vacuum leaving behind *racemic*-,*meso*-*et*,*ph*-P4-*ph* in greater than 96% purity. An alternative to the alumina column is dissolving the slightly yellow paste in ethanol and placing it in a -20°C freezer. The P4 ligand precipitates out of solution and adheres to the sides of the flask. The remaining ethanol solution is poured out of the flask leaving behind *racemic*-,*meso*-*et*,*ph*-P4-*ph* in greater than 95% purity. This step is done after removing the inorganic impurity.

$^{31}\text{P}$  NMR (101.2 MHz,  $\text{CD}_2\text{Cl}_2$ ):  $\delta$  -24.83 to -33.14 (m, 22 lines)

### 6.12 Synthesis of *rac*- and *meso*- $\text{Ni}_2\text{Cl}_4(\text{et},\text{ph}\text{-P4-Ph})$ , $\text{Ni}_2\text{2R}$ and $\text{Ni}_2\text{2M}$

2.21 g (394  $\mu\text{moles}$ ) of mixed *rac*-,*meso*-*et*,*ph*-P4-*Ph* were dissolved in 100 mL of dichloromethane and placed into a Schlenk flask creating a clear, colorless solution. Another Schlenk flask was charged with 1.87 g (787  $\mu\text{moles}$ )  $\text{NiCl}_2\cdot 6\text{H}_2\text{O}$  and 100 mL of 1-butanol and heated with a heat gun to dissolve all of the Ni, creating a clear, green solution. The ligand solution was added dropwise via cannula to the rapidly stirring  $\text{NiCl}_2$  solution. As the addition proceeded the solution became orange in color and slowly darkened. After the addition the solution was a very dark red color. The solution was allowed to stir overnight during which an orange powder precipitated out of solution. The powder was collected via filtration, washed with 1-butanol and dried in air. NMR analysis revealed this to be pure  $\text{Ni}_2\text{2M}$ . The remaining 1-butanol/dichloromethane solution was evaporated to dryness leaving behind a red/black residue. The residue was dissolved in dichloromethane and then filtered to remove any unreacted  $\text{NiCl}_2$ . The dichloromethane was concentrated under vacuum. NMR analysis of this solution revealed it to be composed mostly (~85% based on  $^{31}\text{P}$ ) of the *racemic* Ni complex with a small amount of

*meso* and one other unidentified compound. A large excess of hexanes was added to the concentrated DCM solution and an orange powder precipitated. The powder was collected via filtration, washed with hexanes and dried under vacuum. NMR analysis of this powder revealed it to be an 87/13 mixture of *racemic/meso* bimetallic complexes. Dissolving this powder in hot acetonitrile and allowing it to sit in air for 1 to 2 days affords the *racemic* complex in its pure form.

**Ni<sub>2</sub>2M:** <sup>31</sup>P NMR (162 MHz, CD<sub>2</sub>Cl<sub>2</sub>) δ 71.2 (pseudo-dt, J=75 Hz), 51.7 (pseudo-dt, J=75 Hz), <sup>1</sup>H NMR (400 MHz, CD<sub>2</sub>Cl<sub>2</sub>) δ 8.61-8.50 (m, 2H), 7.80-7.71 (m, 4H), 7.65-7.60 (m, 6H), 7.44-7.38 (m, 2H), 7.29-7.22 (m, 4H), 4.44-4.31 (m, 1H), 4.25-4.14 (m, 1H), 2.51-2.37 (m, 2H), 2.21-1.99 (m, 4H), 1.91-1.76 (m, 2H), 1.18 (dt, 6H, J<sub>HP</sub>=18.6 Hz, J<sub>HH</sub>=7.6 Hz), 1.03 (dt, 6H, J<sub>HP</sub>=20.3 Hz, J<sub>HH</sub>=7.5 Hz)

**Ni<sub>2</sub>2R:** <sup>31</sup>P NMR (162 MHz, CD<sub>2</sub>Cl<sub>2</sub>) δ 69.1 (pseudo-d, J=75 Hz), 50.3 (pseudo-d, J=75 Hz), <sup>1</sup>H NMR (400 MHz, CD<sub>2</sub>Cl<sub>2</sub>) δ 9.59-9.53 (m, 2H), 8.14-8.06 (m, 2H), 8.02-7.95 (m, 4H), 7.83-7.76 (m, 2H), 7.55-7.40 (m, 8H), 4.57 (t, 2H), 2.39-2.26 (m, 2H), 1.88-1.72 (m, 2H), 1.57-1.42 (m, 4H), 1.02 (dt, 6H, J<sub>HP</sub>=20 Hz, J<sub>HH</sub>=7.5 Hz), 0.70 (dt, 6H, J<sub>HP</sub>=17.9 Hz, J<sub>HH</sub>=7.6 Hz)

## 6.13 Cyanolysis of Ni<sub>2</sub>2R and Ni<sub>2</sub>2M

### 6.13.1 Cyanolysis of Ni<sub>2</sub>2M

A Schlenk flask was charged with 0.20 g *meso*-Ni<sub>2</sub>Cl<sub>4</sub>(*et,ph-P4-ph*) and 75 mL methanol creating an orange suspension. Another Schlenk flask was charged with 1.59 g (133 equivalents) NaCN and 20 mL water. The NaCN solution was added to the methanol suspension via cannula. Almost immediately the slurry changed from orange to red and became clear. This red solution was allowed to stir for 3 hours. Then, 1.79 g (150 equivalents) of NaCN was added and the mixture was allowed to stir for another hour. The very red solution was extracted with 3 50 mL



portions of benzene. The red benzene extracts were concentrated under vacuum. The concentrated extract was then passed through a short alumina column to remove the colored impurities. The clear, colorless benzene solution was then evaporated to dryness leaving behind a white paste. Analysis of the white paste revealed it to be the *meso* diastereomer (>95%) with a small amount of the *racemic* diastereomer.

$^{31}\text{P}$  NMR (162 MHz,  $\text{CD}_2\text{Cl}_2$ ):  $\delta$  -24.1 to -26.2 (m), -29.2 to -31.2 (m),  $^1\text{H}$  NMR (400 MHz,  $\text{CD}_2\text{Cl}_2$ ):  $\delta$  7.63-7.55 (m, 4H), 7.50-7.23 (overlapping ms, 14H), 2.96-2.89 (m, 1H), 2.74-2.66 (m, 1H), 1.74-1.59 (m, 4H), 1.58-1.36 (m, 4H), 0.97 (dt, 6H,  $J_{\text{HP}}=14.8$  Hz,  $J_{\text{HH}}=7.6$  Hz), 0.77 (dt, 6H,  $J_{\text{HP}}=14.8$  Hz,  $J_{\text{HH}}=7.5$  Hz)

### 6.13.2 Cyanolysis of $\text{Ni}_2\text{2R}$

The same procedure was followed for the *racemic* complex as was used for the *meso* complex. Analysis of the white paste showed the *racemic* diastereomer (~97%) with just a trace of the *meso*.

$^{31}\text{P}$  NMR (162 MHz,  $\text{CD}_2\text{Cl}_2$ ):  $\delta$  -24.3 to -27.6 (m), -29.7 to -32.9 (m),  $^1\text{H}$  NMR (400 MHz,  $\text{CD}_2\text{Cl}_2$ ):  $\delta$  7.55-7.39 (overlapping ms, 8H), 7.37-7.24 (overlapping ms, 10H), 2.80 (t, 2H,  $J_{\text{HP}}=3.3$  Hz) 1.70-1.35 (overlapping ms, 8H), 0.93 (dt, 6H,  $J_{\text{HP}}=15.1$  Hz,  $J_{\text{HH}}=7.6$  Hz), 0.78 (dt, 6H,  $J_{\text{HP}}=14.9$  Hz,  $J_{\text{HH}}=7.6$  Hz)

### 6.13.3 Cyanolysis of mixed $\text{Ni}_2\text{2M}/\text{Ni}_2\text{2R}$

A very similar procedure was used for the mixed complexes except that 0.50 g of the mixed complex was suspended in 100 mL methanol and 3.98 g (133 equivalents) NaCN in 40 mL water was added first. Then 4.48 g (150 equivalents) NaCN was added second. The concentrated benzene extract was allowed to stand at room temperature for several days and several different crystal morphologies slowly precipitated out of solution. Two different

structures were determined from these crystals: orange blades which were determined to be  $\text{Ni}(\text{CN})_2(\kappa^{2.5}\text{-meso-et,ph-P4-ph})$  and orange plates which were determined to be  $[\text{NiCN}(\kappa^{3.5}\text{-racemic-et,ph-P4-ph})]\text{Cl}\cdot\text{benzene}$ . There were also very small needles which have not been solved yet.

#### 6.14 References

1. Van Hecke, G. R.; Horrocks, Jr., W. D. *Inorg. Chem.* **1966**, 5, 1968-1974.
2. Venanzi, L. M. *J. Chem. Soc.* **1958**, 719-724.
3. Browning, M. C.; Davies, R. F. B.; Morgan, D. J.; Sutton, L. E.; Venanzi, L. M. *J. Chem. Soc.* **1961**, 4816-4823.
4. Booth, G.; Chatt, J. *J. Chem. Soc.* **1965**, 3238-3241.
5. Angulo, I. M.; Bouwman, E.; van Gorkum, R.; Lok, S. M.; Lutz, M.; Spek, A. L. *J. Mol. Catal. A: Chem.* **2003**, 202, 97-106.
6. Laneman, S. A.; Fronczek, F. R.; Stanley, G. G. *Inorg. Chem.* 1989, 28, 1872-1878.
7. Aubry, D. A.; Laneman, S. A.; Fronczek, F. R.; Stanley, G. G. *Inorg. Chem.* 2001, 40, 5036-5041.
8. Monteil, A. *Ph.D. Dissertation, Louisiana State University*, **2006**.

## APPENDIX

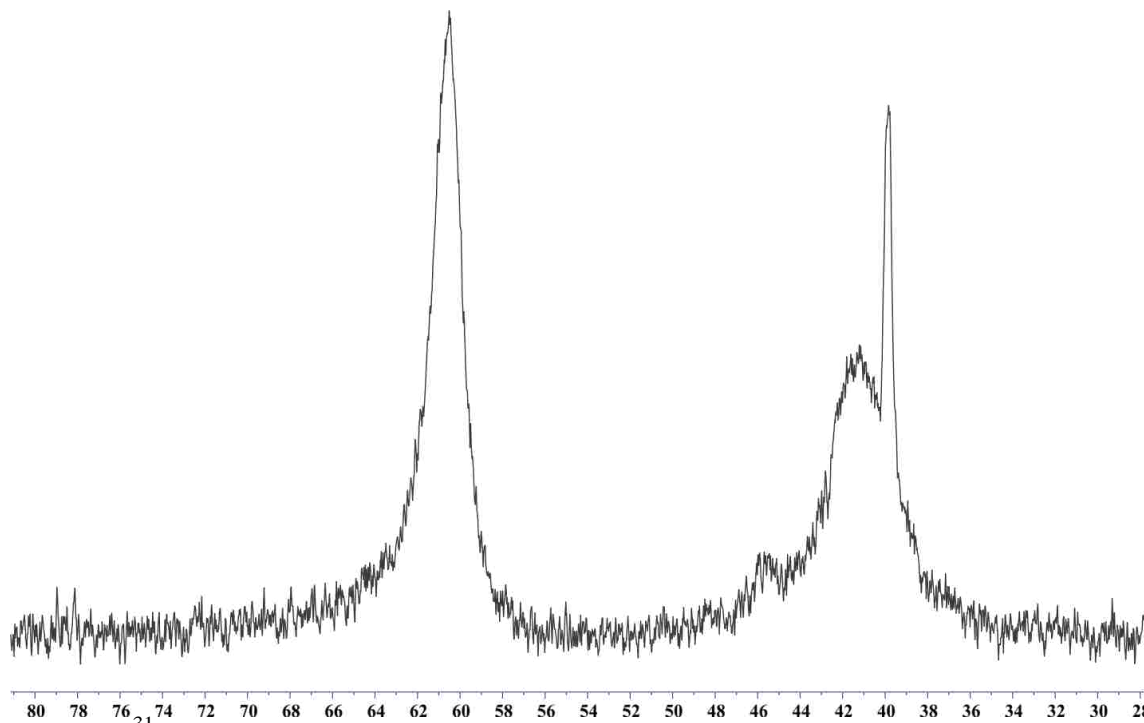


**Figure A.1**  $^{31}\text{P}$  NMR spectrum of  $\text{Ni}_2\text{IM}$  after stirring under an  $\text{O}_2$  atmosphere for 24 hours in acetone/water.

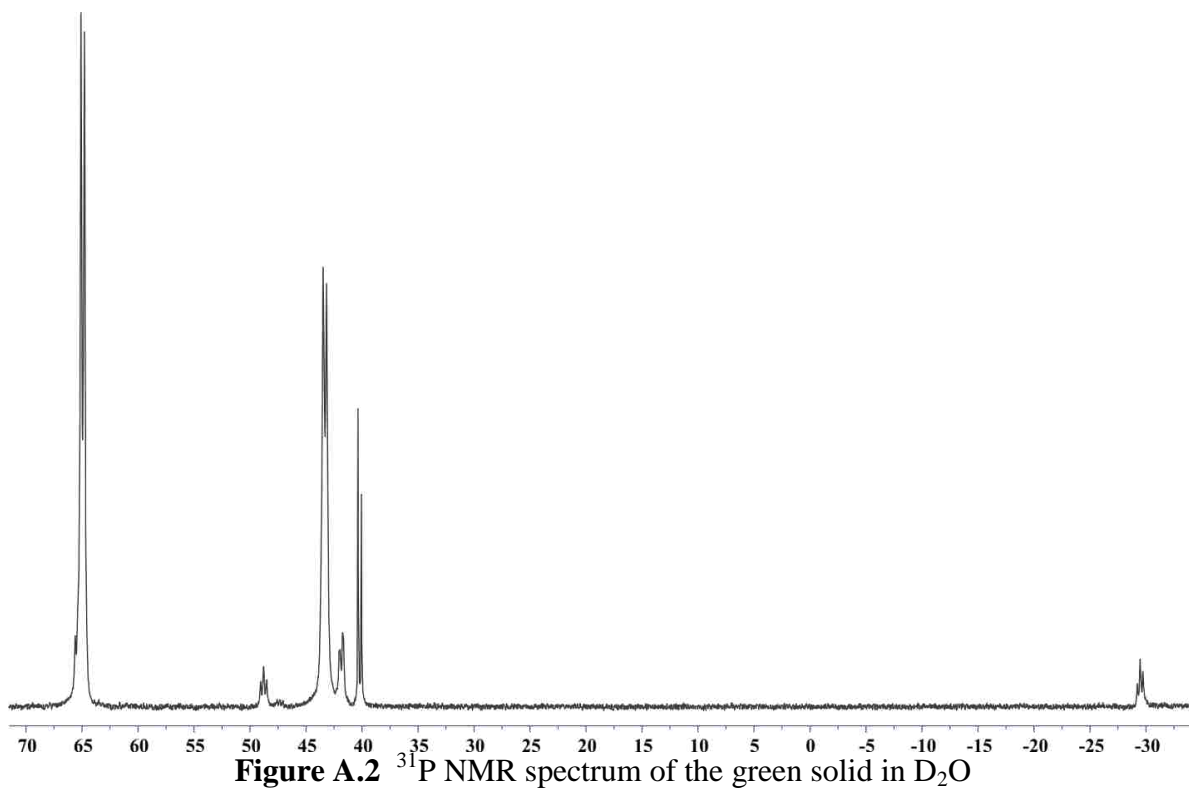


**Figure A.2**  $^{31}\text{P}$  NMR spectrum of the green solid in  $\text{D}_2\text{O}$

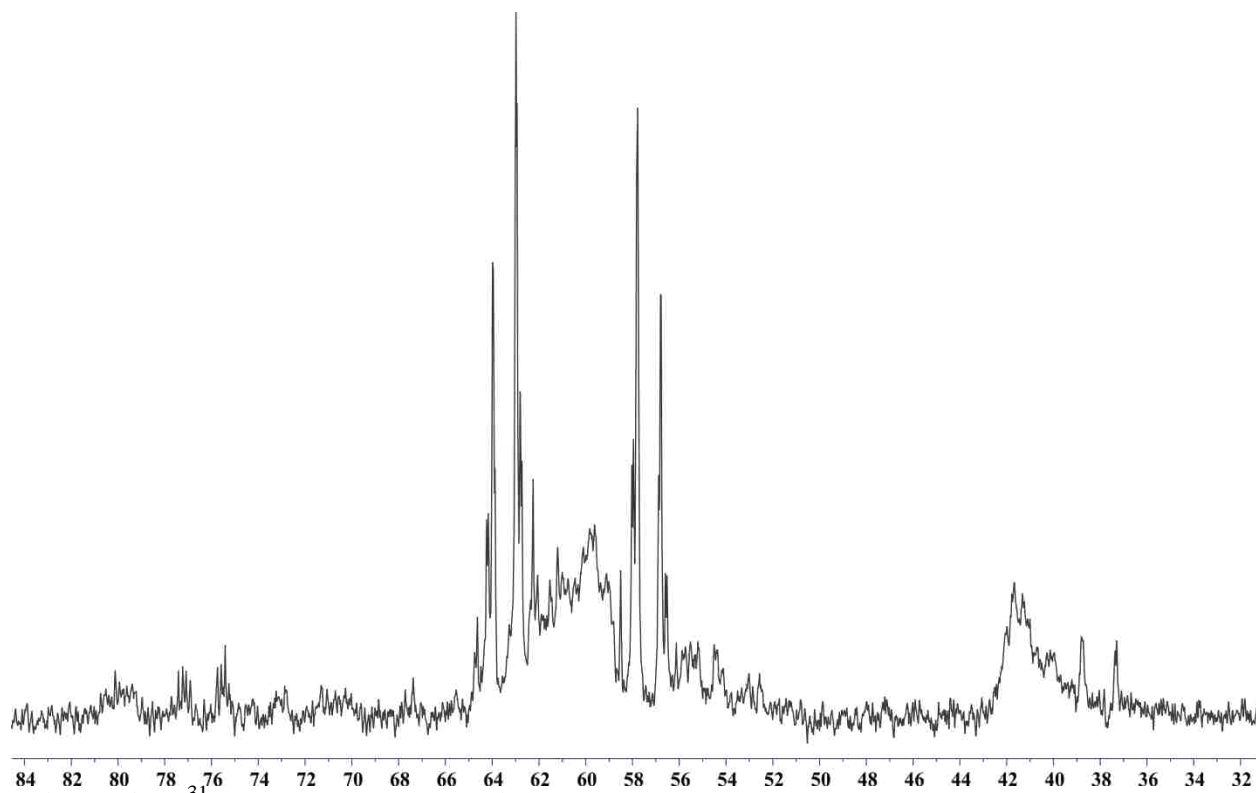


**Figure A.3**  $^{31}\text{P}$  NMR spectrum of  $\text{Ni}_2\mathbf{1M}$  after stirring under an  $\text{O}_2$  atmosphere for 24 hours in acetonitrile/water.

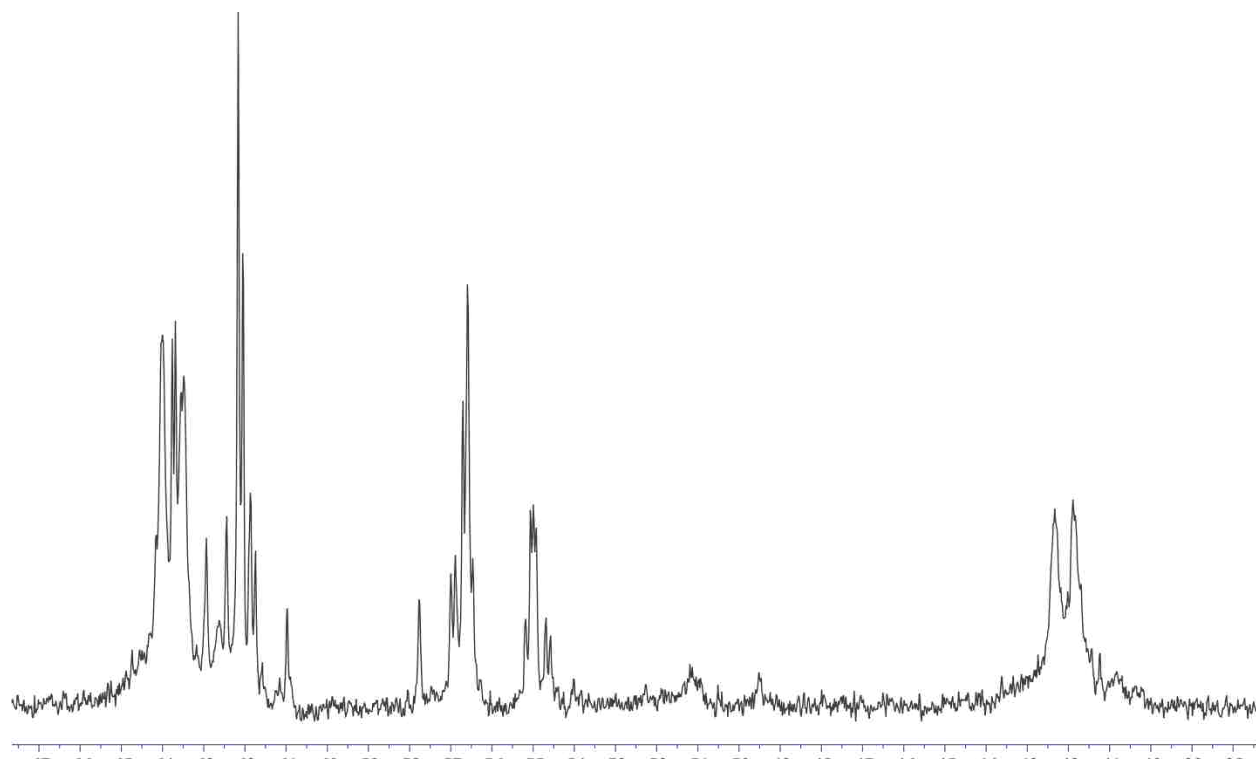


**Figure A.4**  $^{31}\text{P}$  NMR spectrum of the solid obtained from Figure 6.3 after removal of all volatile materials and dissolving in  $\text{D}_2\text{O}$

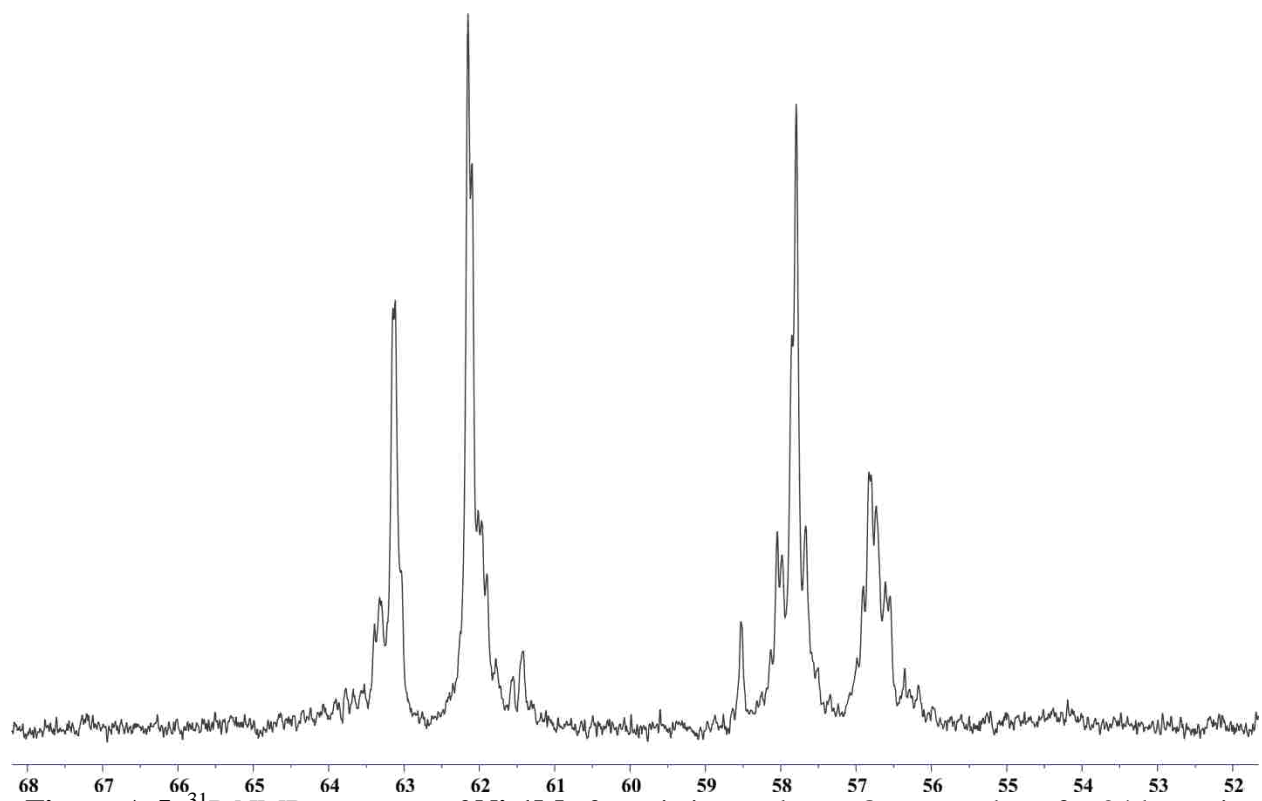


**Figure A.5**  $^{31}\text{P}$  NMR spectrum of  $\text{Ni}_2\text{1M}$  after stirring under an  $\text{O}_2$  atmosphere for 24 hours in DMSO/water.

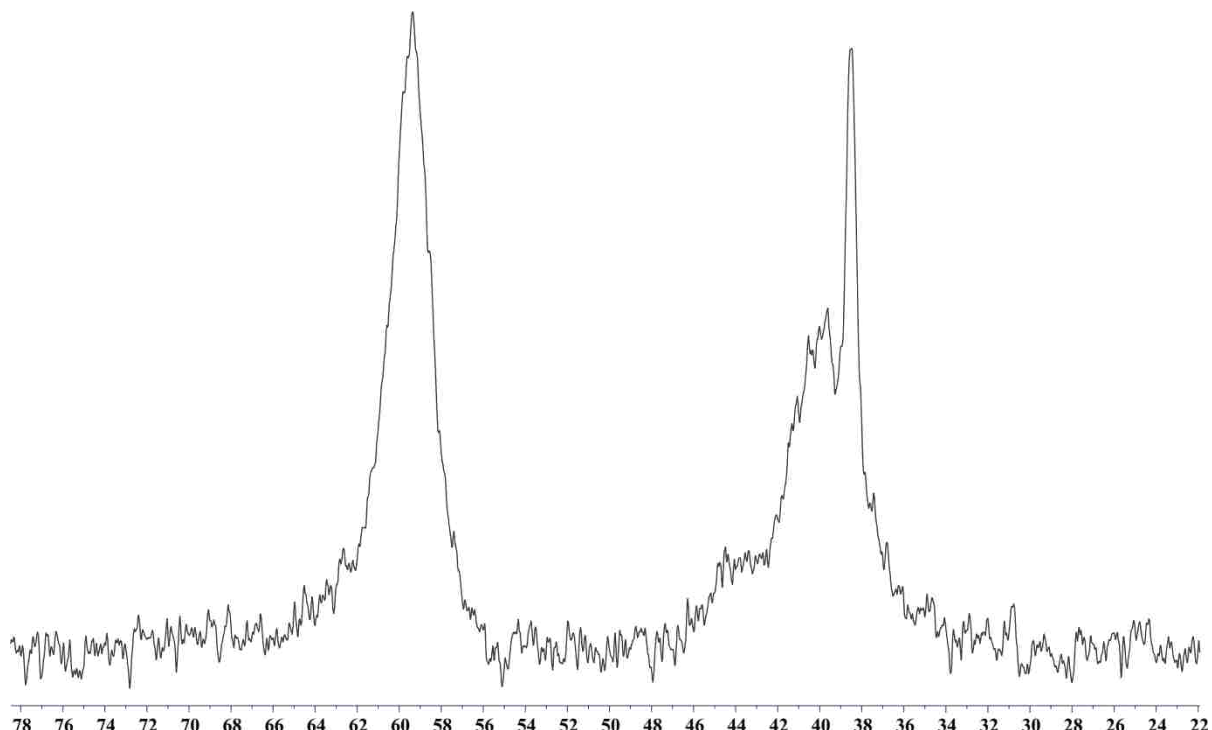


**Figure A.6**  $^{31}\text{P}$  NMR spectrum obtained with substrate in acetone/water or acetonitrile/water.

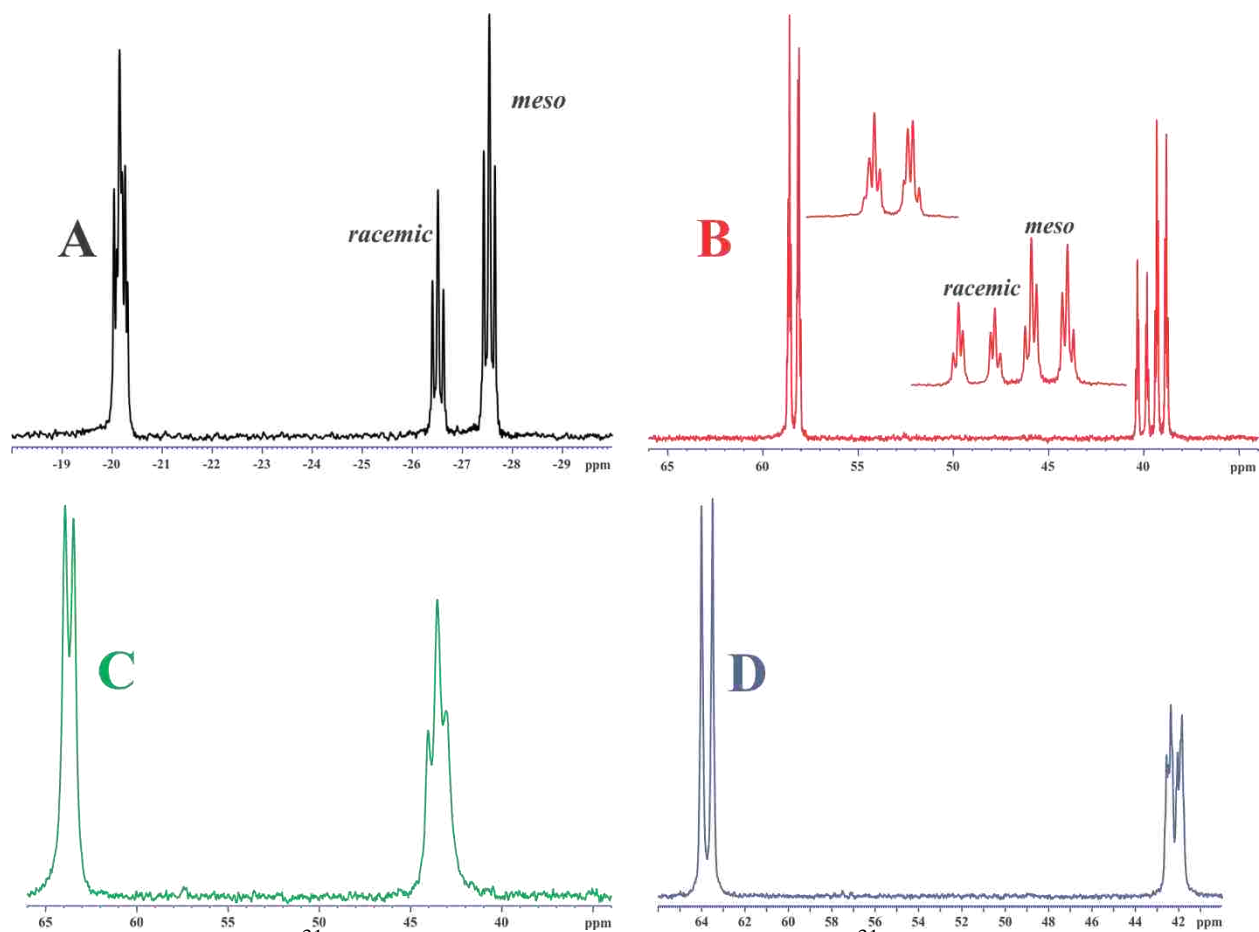


**Figure A.7** A –  $^{31}\text{P}$  NMR of the tetraphosphine ligand, B –  $^{31}\text{P}$  NMR spectrum of the tetraphosphine oxide, C –  $^{31}\text{P}$  NMR of the interaction between the tetraphosphine oxide and  $\text{NiCl}_2$ , D –  $^{31}\text{P}$  NMR of the phosphine oxide/ $\text{NiCl}_2$  in  $\text{D}_2\text{O}$

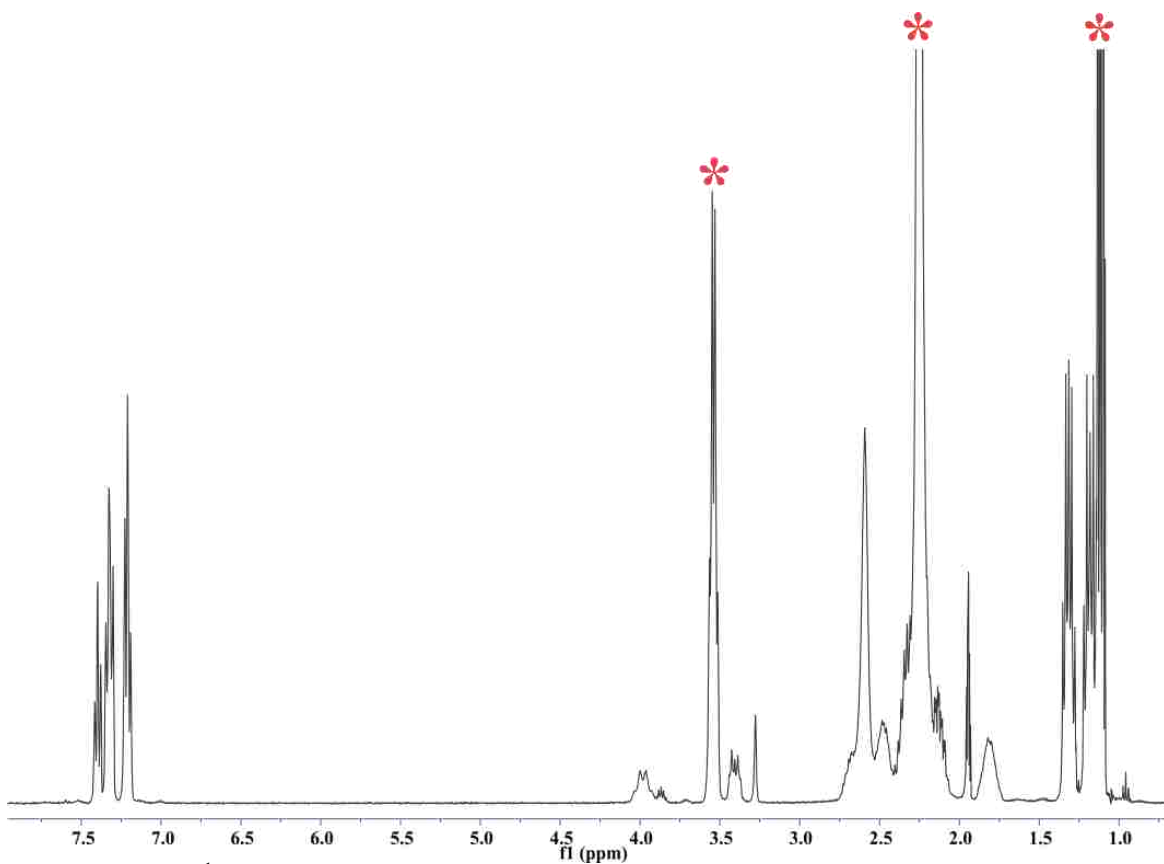


**Figure A.8**  $^1\text{H}$  NMR spectrum of  $[\text{Ni}_2(\mu\text{-Cl})(\mathbf{1M})_2][\text{BF}_4]_3$ . Starred peaks are solvent.

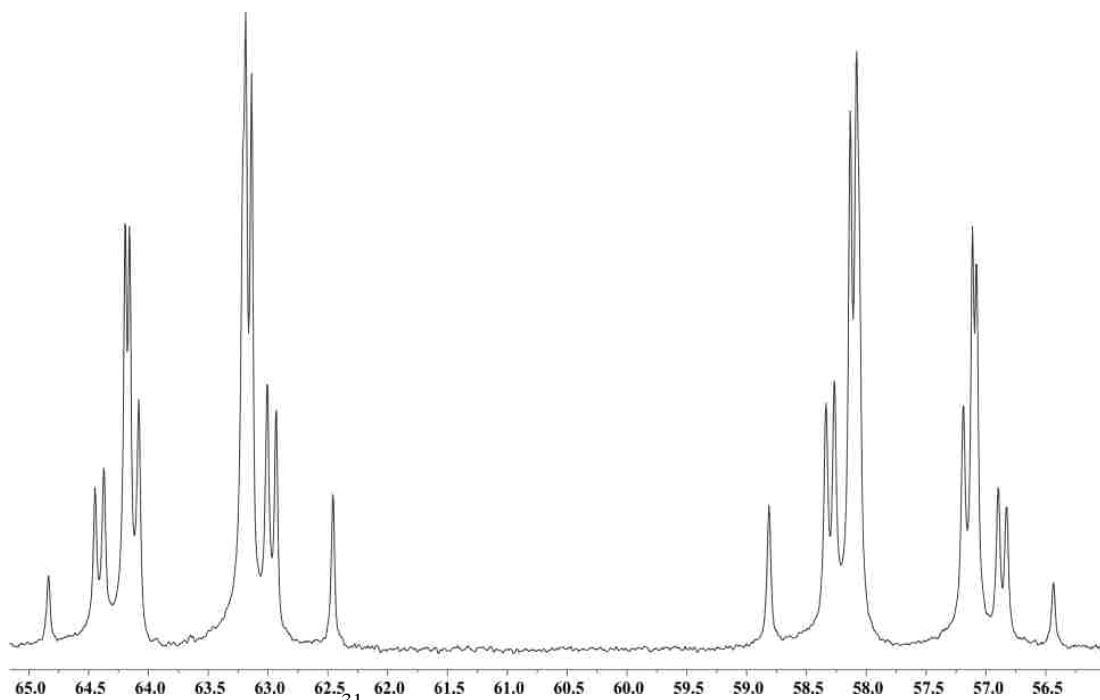


**Figure A.9**  $^{31}\text{P}$  NMR spectrum of  $[\text{Ni}_2(\mu\text{-Cl})(\mathbf{1M})_2][\text{BF}_4]_3$

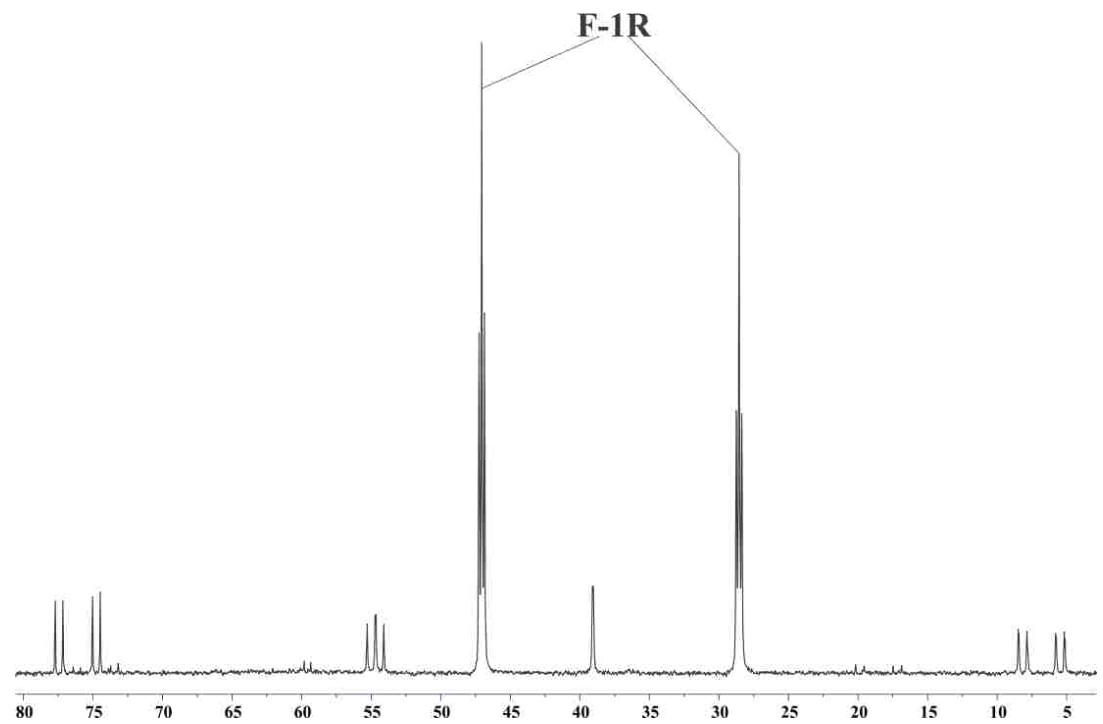
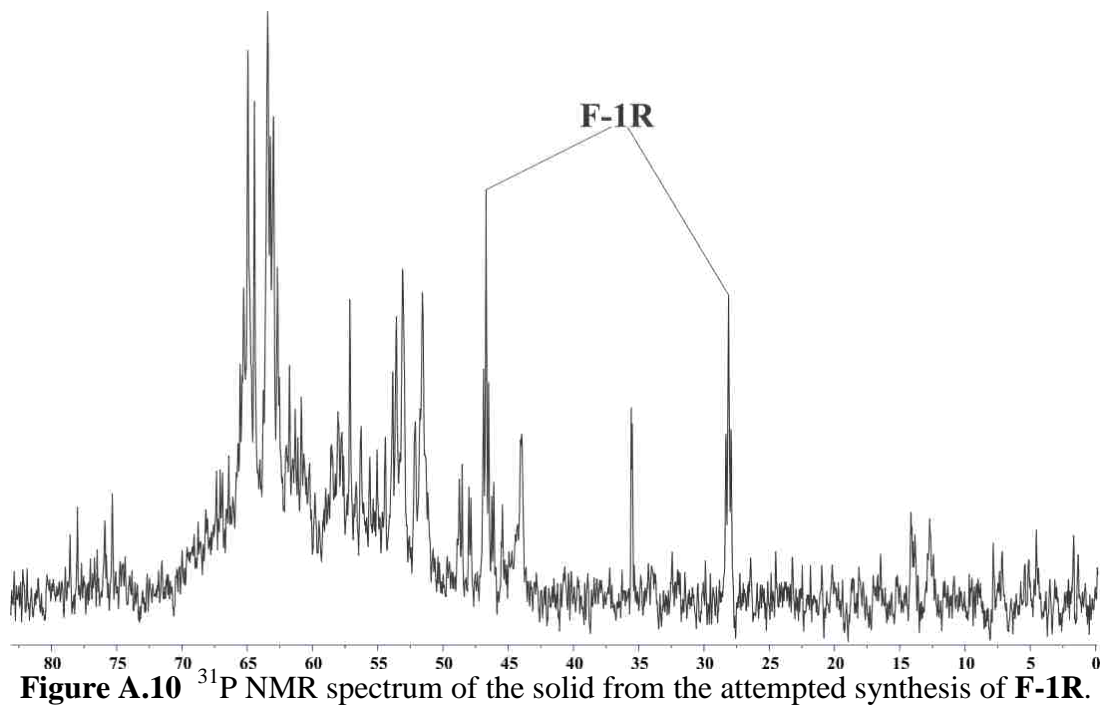


**Figure A.11**  $^{31}\text{P}$  NMR spectrum of the ethanol solution from the attempted synthesis of **F-1R**.



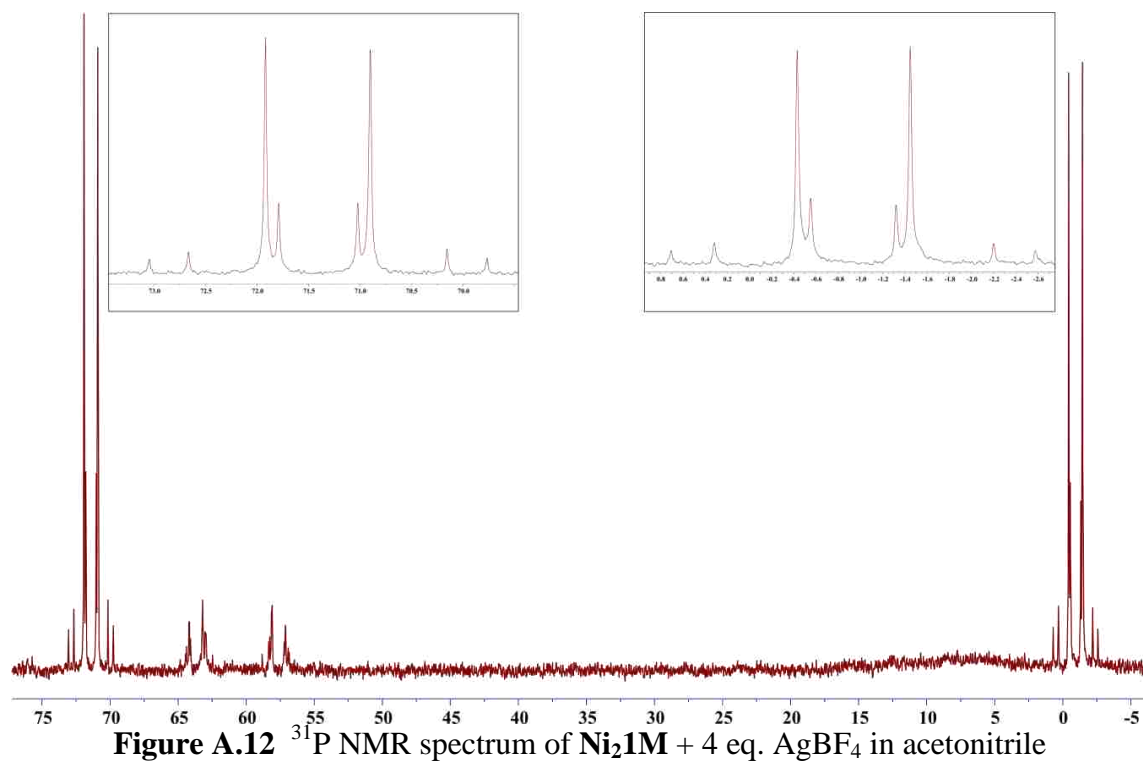


**Figure A.12**  $^{31}\text{P}$  NMR spectrum of  $\text{Ni}_2\mathbf{1M}$  + 4 eq.  $\text{AgBF}_4$  in acetonitrile

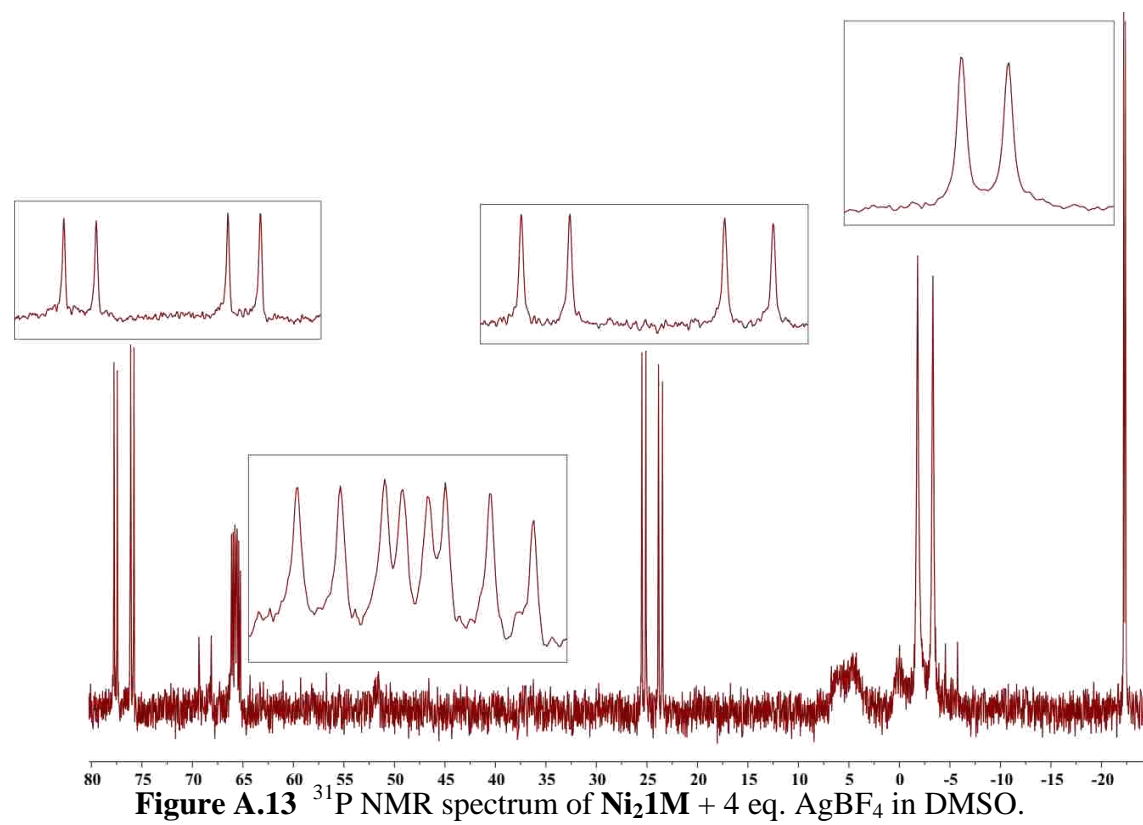


**Figure A.13**  $^{31}\text{P}$  NMR spectrum of  $\text{Ni}_2\mathbf{1M}$  + 4 eq.  $\text{AgBF}_4$  in DMSO.

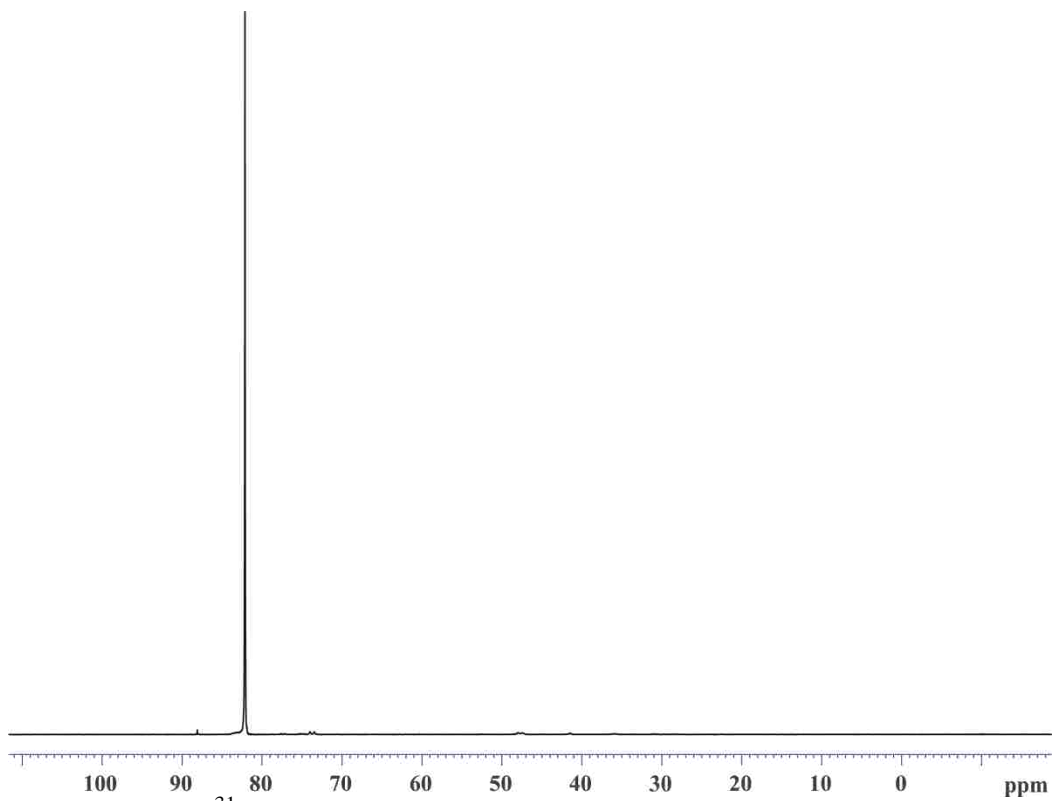


**Figure A.14**  $^{31}\text{P}$  NMR spectrum of bis-(chlorophenylphosphino)methane, **4**.

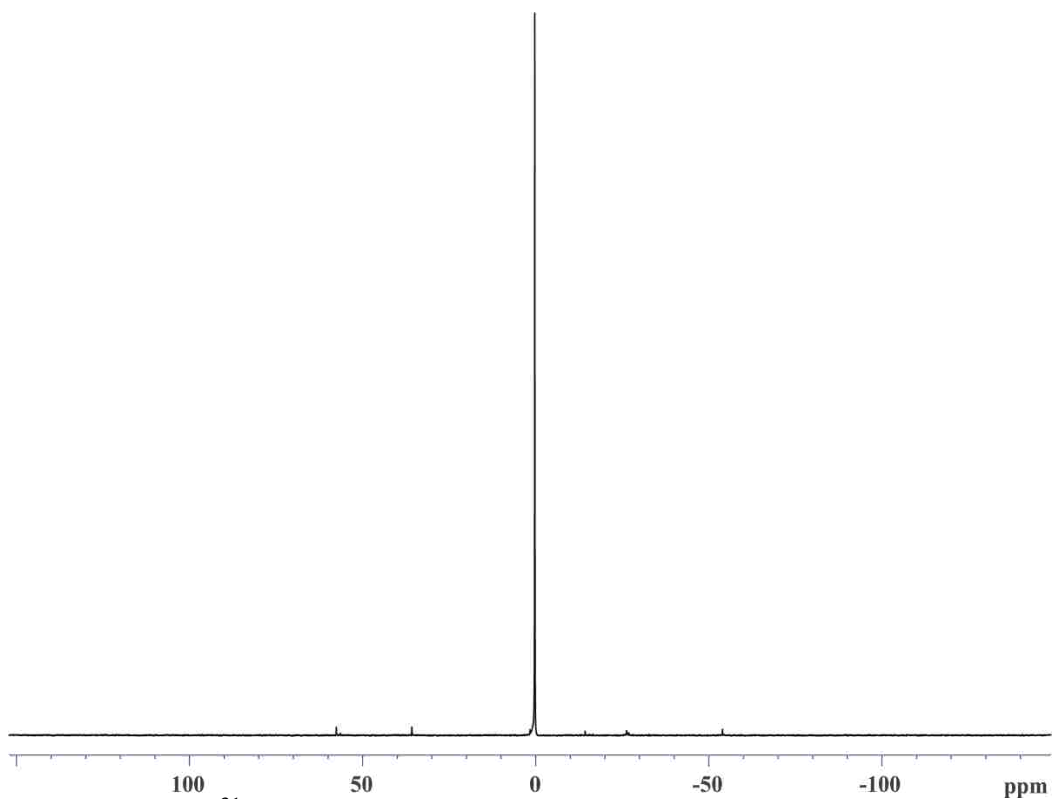


**Figure A.15**  $^{31}\text{P}$  NMR spectrum of 1-(diethylphosphino)-2-iodobenzene, **6**.

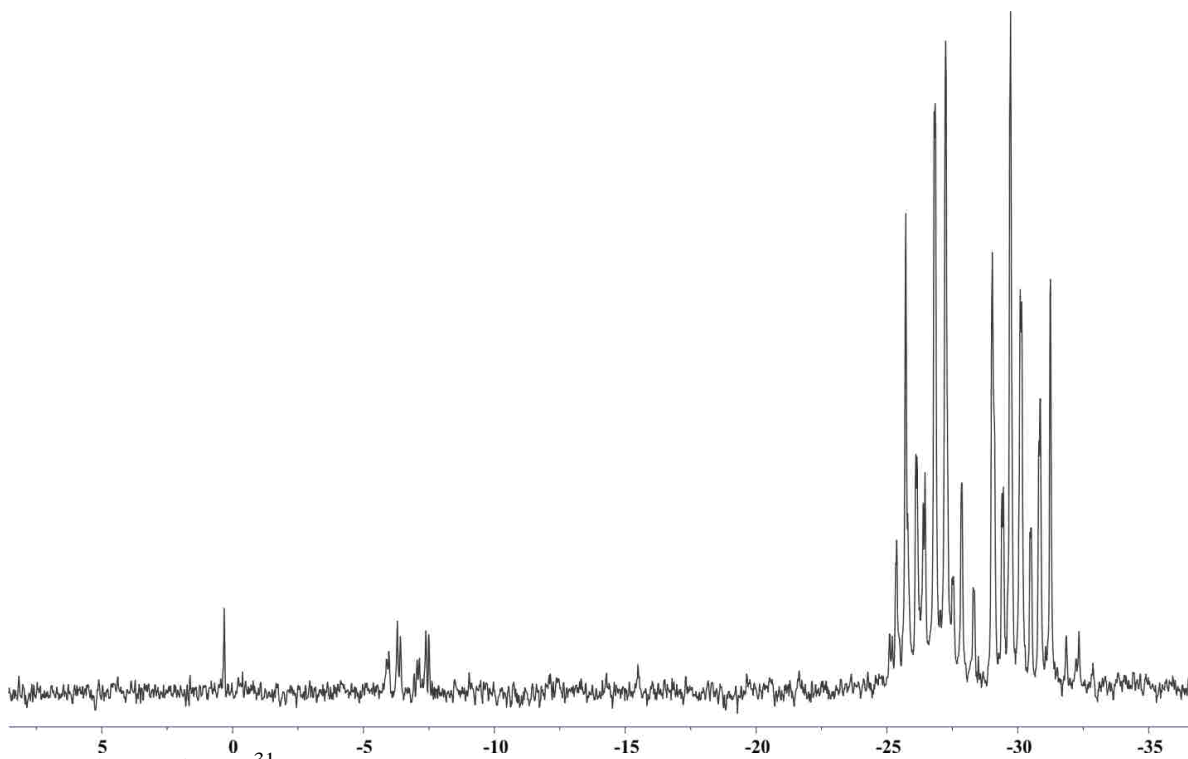


**Figure A.16**  $^{31}\text{P}$  NMR spectrum of mixed **2M** and **2R** using the alumina column.

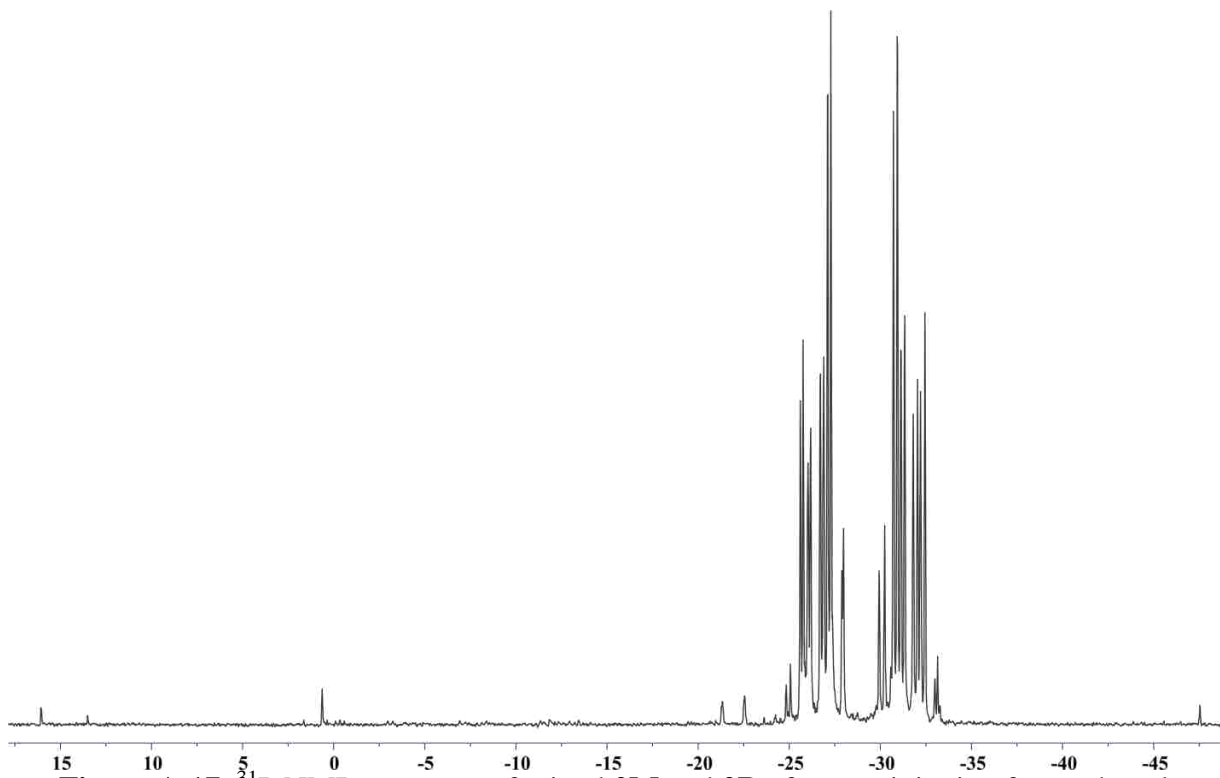


**Figure A.17**  $^{31}\text{P}$  NMR spectrum of mixed **2M** and **2R** after precipitating from ethanol.

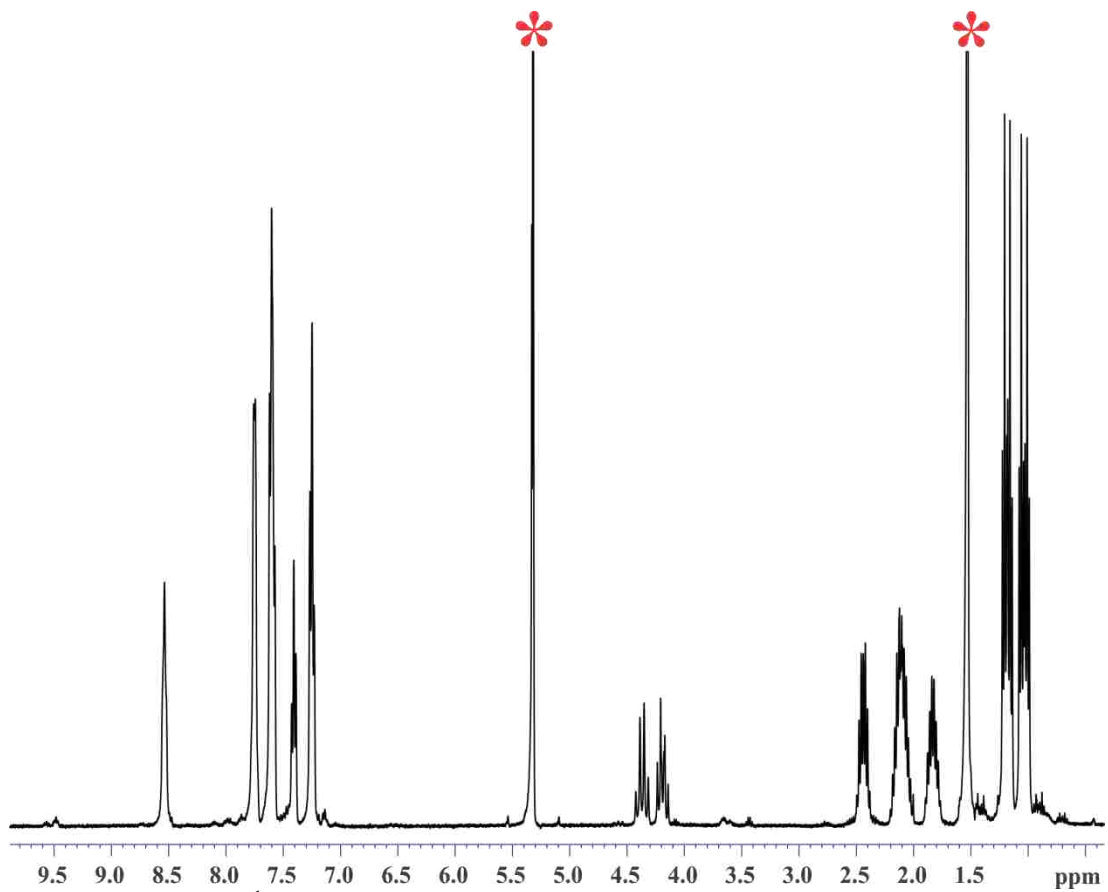


**Figure A.18**  $^1\text{H}$  NMR spectrum of  $\text{Ni}_2\text{2M}$ . Starred peaks are from solvent.

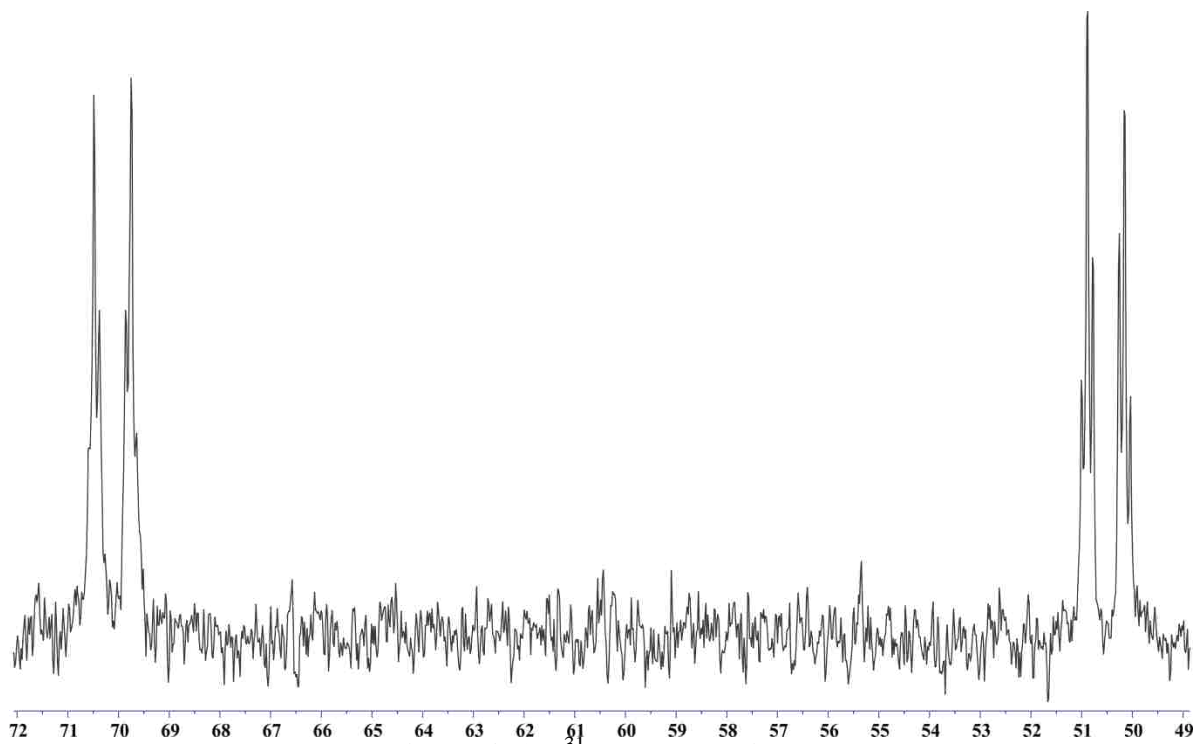


**Figure A.19**  $^{31}\text{P}$  NMR of  $\text{Ni}_2\text{2M}$

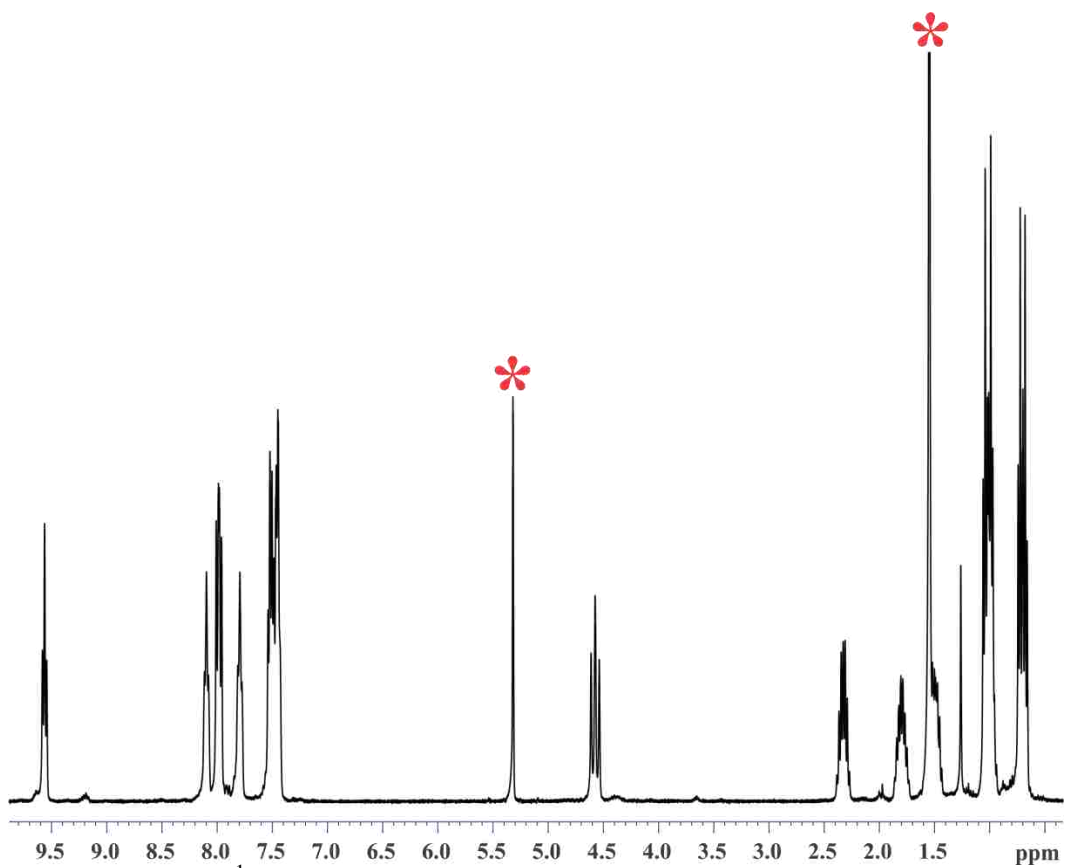


**Figure A.20**  $^1\text{H}$  NMR spectrum of  $\text{Ni}_2\text{2R}$ . Starred peaks are from solvent.

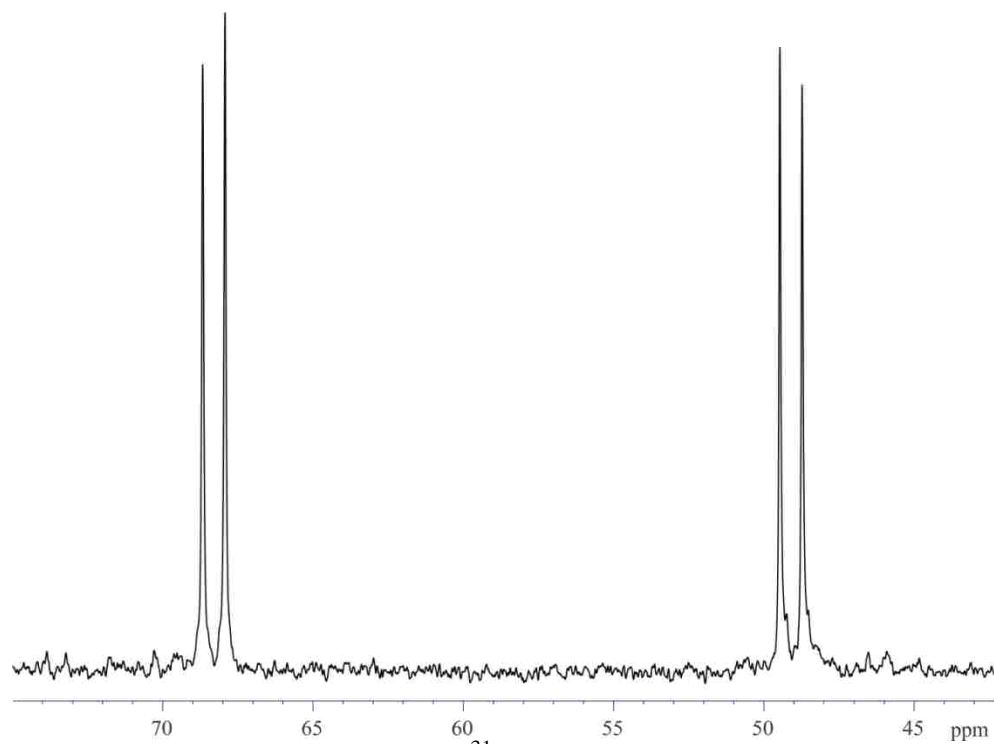


**Figure A.21**  $^{31}\text{P}$  NMR of  $\text{Ni}_2\text{2R}$

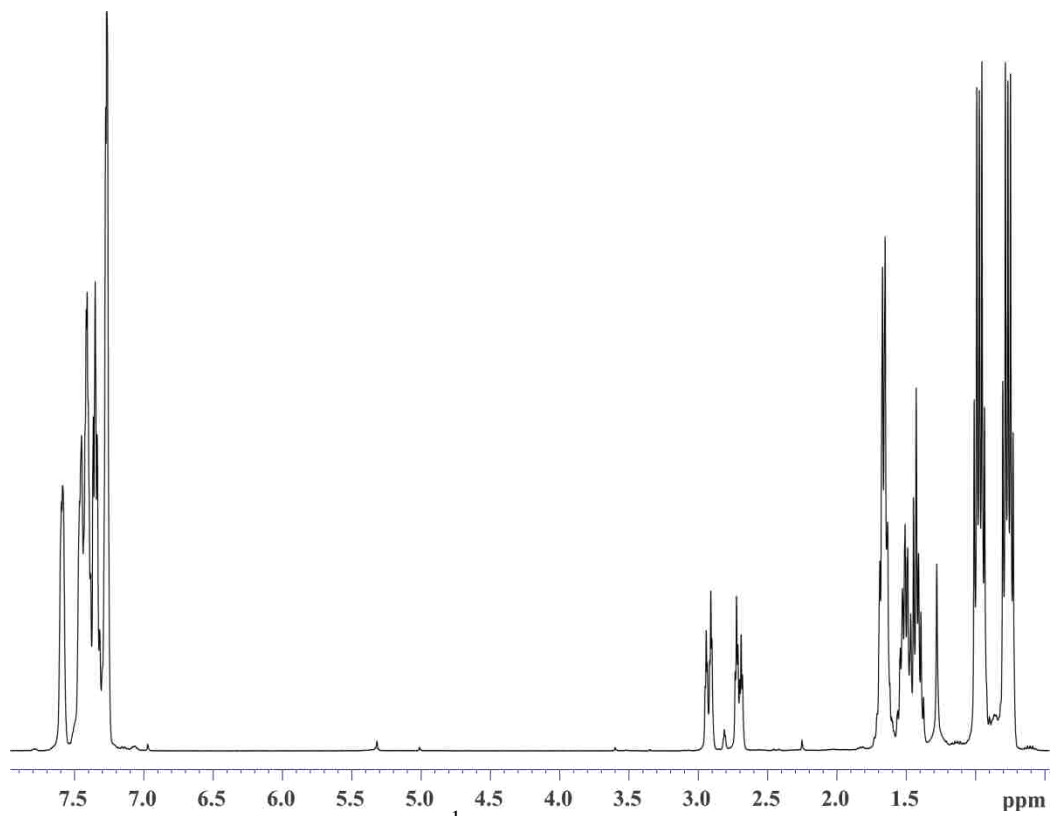


**Figure A.22**  $^1\text{H}$  NMR spectrum of 2M.

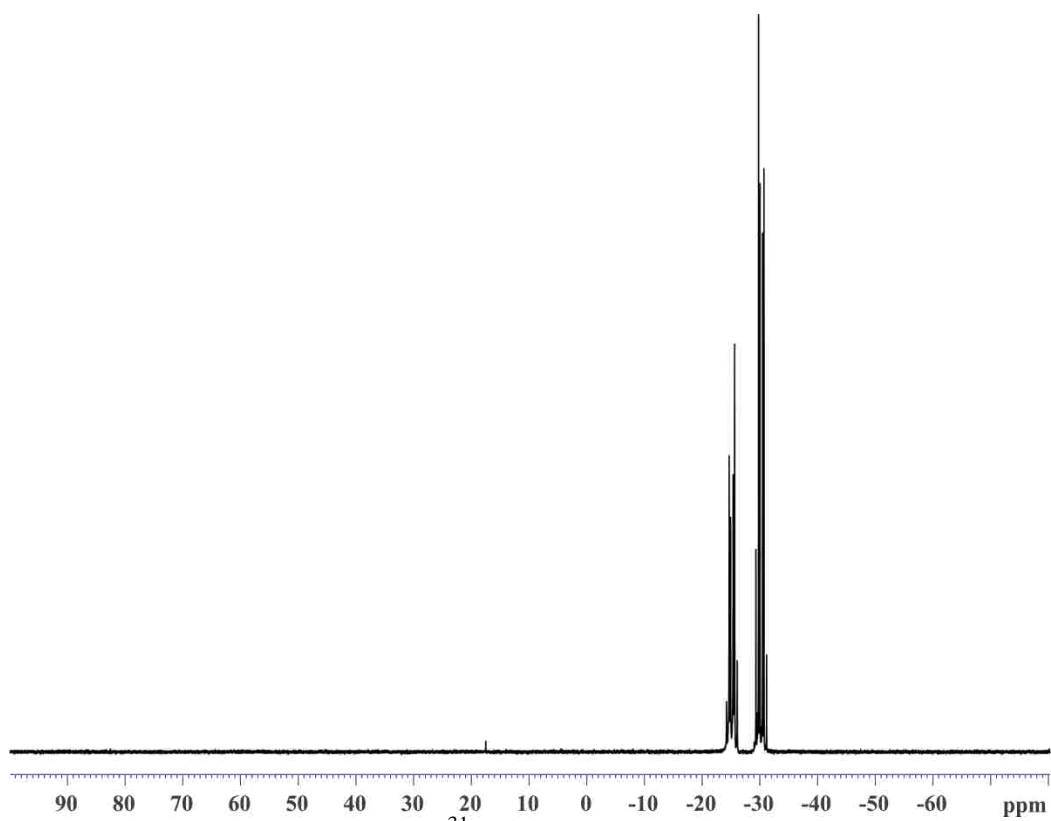


**Figure A.23**  $^{31}\text{P}$  NMR spectrum of 2M.

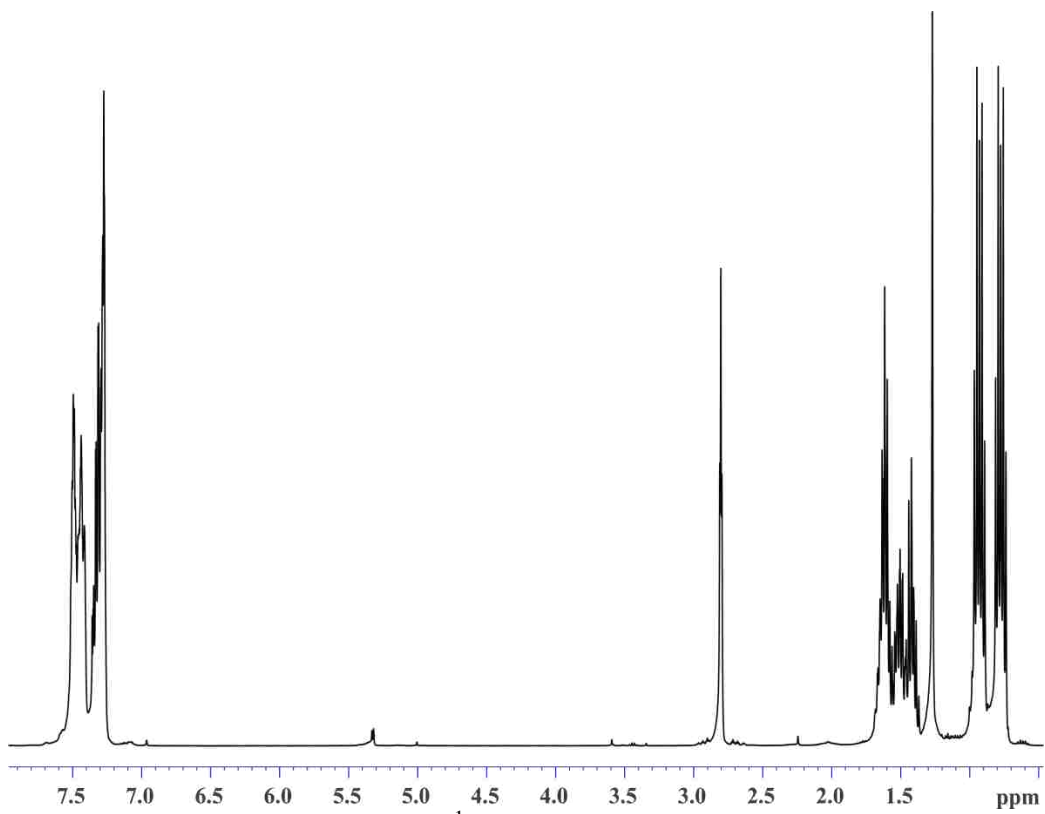


**Figure A.24**  $^1\text{H}$  NMR spectrum of **2R**

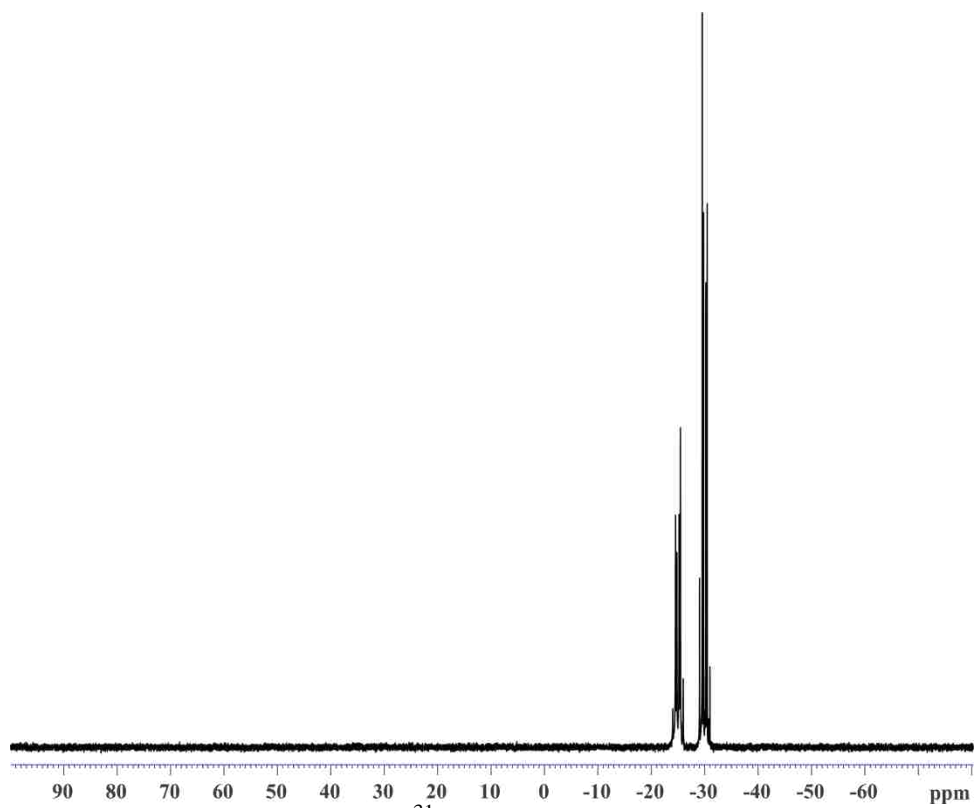


**Figure A.25**  $^{31}\text{P}$  NMR spectrum of **2R**.

## **VITA**

William Schreiter was born in May 1982 in Appleton, WI. At the age of 12 he moved with his family to Lockport, Louisiana where he graduated high school in 2000. After high school, he enrolled at Lawrence University. In June 2004 he graduated with a Bachelor of Arts degree in Chemistry with honors in independent study. After taking a year off, he enrolled in the graduate program of Louisiana State University. He currently is a doctoral candidate in the Department of Chemistry and plans to graduate in May 2013.